Australia's National
Science Agency

# Georges River Aquatic Health Monitoring Program: Report 1. 2022

Sarah Stephenson, Monique Binet, Nai Tran-Dinh and Merrin Adams

EP2022-1328

14th April 2022

Prepared for: Illawarra Coal Metallurgical/South32

Chris Schultz

Polly Barlow

Commercial-in-confidence

Oceans and Atmosphere

Land and Water

Energy

## Citation

Stephenson SA, Binet MT, Tran-Dinh N, Adams MS (2022) Georges River Aquatic Health Monitoring Program report 1. CSIRO, Australia. EP2022-1328

## Copyright



## Important disclaimer

# Contents

# Figures

# Tables

# Acknowledgments

We thank Paul Greenfield for his assistance with bioinformatics and data processing.

We thank Dr Anthony Chariton for the initial experimental design of the GRAHMP and reviewing results for this report.

We thank Dr David Midgley for statistical guidance, graphical data visualisation support, and CSIRO internal review.

We thank Dr Sharon Hook for CSIRO internal report review.

We thank Dr Lisa Golding for her assistance with ecotoxicity test reviews.

We acknowledge the Traditional Custodians whose ancestral lands we live and work upon and we pay our respects to their Elders past and present. We acknowledge and respect the deep spiritual connection and the relationship that Aboriginal and Torres Strait Islander people have to Country.

We also pay our respects to the Dharawal People and the cultural authority of Aboriginal and Torres Strait Islander people and their nations in the Georges River area, as well as those across Australia.

# Executive summary

This is the first of three scientific reports for the Georges River Aquatic Health Monitoring Program (GRAHMP). The Environmental Protection Authority (EPA) and the Georges River catchment community have concerns over the water quality and ecological values of the upper Georges River. The GRAHMP was developed in 2020 to investigate the ecological health and condition of the Georges River.

The GRAHMP follows a multiple lines of evidence approach to assess the water quality and ecological condition of the upper Georges River. Multiple lines of evidence approaches are regarded as robust scientific monitoring programs used by environmental regulators to identify the key environmental disturbance drivers and ecological responses in an ecosystem. Several lines of evidence were used in this study to describe the health of the Georges River catchment downstream of South 32 Illawarra Metallurgical Coal's (IMC) discharge into Brennans Creek at license point 10 (LDP10). Lines of evidence included those to assess for likelihood of impact (ecotoxicology and water chemistry on the discharge waters) and those to assess for observed ecological impact, i.e., changes in community structure and biodiversity (using macrobenthic/macroinvertebrate and gene loci DNA metabarcoding). These lines of evidence have been used yearly in previous programs (Environment Improvement Programs), since 2013, to assess for environmental impact of South 32/IMCs discharge from LDP10 and to identify any changes/improvements to water quality and ecology of the ecosystem over time, as South 32/IMC take steps to improve the quality of the discharge into Brennans Creek.

The current GRAHMP study was initially developed to investigate water quality and ecological changes to the Georges River pre and post installation of a long term water treatment plant (WTP) at licence discharge point 40 (LDP40). However, the long term Appin North WTP (ANWTP) is still under construction, and instead, a temporary WTP, which does not capture Brennans Creek Dam discharge was installed in May 2021. Therefore, this report presents an assessment of ecosystem health pre-installation of the long term WTP implementation, but also includes assessments of toxicity and chemistry of the discharge from the temporary WTP as a means to forecast water quality improvements once the long term WTP is complete. The input from the temporary WTP constitutes <3% of the total discharge at Brennans Creek, therefore, the effects of discharge from LDP40 would be minimal to the overall results reported here. Once the long term ANWTP is

commissioned, the discharge from the plant will be more significant than the current temporary WTP, with a reduced discharge expected from LDP10.

Flow and water level data was included in this program which were used to interpret some of the changes to water quality at each site during the sampling occasions. For example, linking rainfall and flow to occasions when improvements to water quality were observed (reduction in metals) when high rainfall caused increased flow through the system. Water flow and pool levels fluctuated over the program period.

Water discharged from LDP40 is of higher quality than LDP10 due to the reverse osmosis (RO) treatment processes with lower conductivity and reduced metal concentrations. However, LDP40 discharge samples were low in alkalinity, which could pose an ecological risk, and was the likely cause of toxicity in these samples. The importance of ionic balances for freshwater systems are discussed in the report.

In this study it is evident that the reference sites GRQ1 and GRUFS have geographical, structural habitat, riparian vegetation, light conditions, and physical features that differ to those at the discharge monitoring sites. The very upper reaches of the Georges River (upstream of the Brennans Creek confluence) contain only a small number of permanent pools, limiting the number of suitable sites available as reference sites. Subsequently, GRUFS, GRQ1 and Point 11 are the only options for reference sites. We acknowledge that this limits the experimental design and that these geographical, and physical substrate differences also contribute to biological variation, however, these are the best pool sites available upstream of the discharge. Point 11 may be confounded by licenced mine discharge from Appin East (Point 19) (as it is located between the Appin East discharge point and the confluence of Brennans Creek with the Georges River). This report can only describe the biological interactions with the water quality variables measured at the time of sampling.

In general, based on the parameters measured, water quality was poorer at the discharge monitoring sites than at reference sites. Water quality parameters measured at reference sites were mostly within the ANZG (2018) guideline value (GV) ranges, with some exceptions for one or two sites at each sampling occasion. The pH (7.6-8.9) of waters from Point 10 and all downstream sites were higher than those at reference sites (4.9-7.2). Conductivity, pH, alkalinity, aluminium, copper, and to a lesser extent, nickel, as well as all measures of nitrogen decreased with increasing distance from the discharge source at LDP10 and LDP40.

Aluminium continues to be a metal detected in sites across the survey. Aluminium was high and above GV for all discharge monitoring sites in 2020 and was also detected in the reference sites in Autumn 2021. Zinc concentrations were erratic across the program and did not follow any trend with respect to distance from discharge. Indeed, on one occasion (Autumn 2021), zinc was not detected at Point 10 but was 5-fold higher than the GV at the next closest site, Point 12. It is recommended that field blanks be introduced into the program to rule out sample contamination during handling.

Conductivity and the concentrations of aluminium, nickel and total nitrogen have generally declined over time since the first aquatic health monitoring program in 2013. Zinc concentrations at the reference sites have been above the GV over time. The long-term trend assessment also found that zinc concentrations have been erratic and fluctuated over time, but that most other detected metals remained high at most discharge monitoring sites and were appreciably lower at the downstream site GRQ18. While pH also generally followed a decreasing trend with increasing distance downstream from LDP10, there was no observed change in pH over time, i.e., pH was high, and more alkaline in 2020 and 2021 (pH 7.6-8.9) at the upper discharge monitoring sites and low and more acidic (pH 4.9-6.8) at the reference sites GRQ1 and GRUFS.

All macrobenthic surveys found marked differences in community structure between reference and discharge monitoring sites, with water chemistry explaining a vast majority of the total variation in the ecological data. In particular, pH was shown to be a key correlate of macrobenthic, prokaryote, eukaryote and diatom micro-eukaryote communities. This suggests that the discharge waters may be altering the catchment's aquatic biotic communities, with this effect being more pronounced at the upstream discharge monitoring sites (Points 10, 12 and Jutts). The use of SIGNAL, a program designed to focus the analysis on the sensitivity of macrobenthic taxa to varying ecological conditions, was also examined. SIGNAL scores overall were low, however there were differences in SIGNAL scores between the reference and discharge monitoring sites, indicating a lower level of ecological integrity at the discharge monitoring sites.

The metabarcoding survey captured a broad component of the ecosystems biodiversity and showed similar ecological trends to the macrobenthic patterns at a broader scale of Operational Taxonomic Units (OTUs) for prokaryotes, eukaryotes and diatoms. The metabarcoding for the sampling occasions Spring 2019, Spring 2020 and Spring 2021 all showed that at the OTU level, community composition differed between reference sites and discharge monitoring sites for

prokaryotes, eukaryotes and diatoms. These observations were supported by statistical analyses which presented evidence of the differences between reference and discharge treatment community structure and showed a correlation with water quality changes. The main driving water quality factors which contributed most to the variation in all the metabarcoded communities were pH, conductivity and on occasion, total nitrogen and metals such as aluminium, copper, nickel and zinc. The metabarcoding analysis assisted in identifying potential key biological indicators which were representative of the treatments i.e., more abundant in either reference or discharge monitoring sites. Indicator taxa that were responding positively and negatively were identified.

Initial analyses of water from the temporary WTP indicated an improvement in water quality, particularly reduced metal concentrations. However, pH and conductivity of LDP40 waters, on occasion were outside of the GV range. Furthermore, the ecotox results using LDP40, on occasion, indicated toxicity for *C. dubia*, most likely due to ionic imbalances and low conductivity. Based on these water quality analyses from the temporary WTP (LDP40), it suggests that improvement to water quality is expected when the long term ANWTP is implemented in 2022, and if the water from the WTP is comparable to the receiving water, improvements to ecological health may likely be recorded at downstream discharge monitoring sites.

# 1 Introduction

## 1.1 Program requirements

The aim of the Georges River Aquatic Health Monitoring Program (GRAHMP) is to investigate changes in water quality in the upper Georges River via an ecological and chemical evidence-based approach, specifically investigating changes with implementation of a reverse osmosis (RO) Water Treatment Plant (WTP).

In April 2019, the EPA issued Illawarra Metallurgical Coal (IMC) with a Notification of Intention (NoI) to make licence changes to provide greater certainty in the achievement of water quality outcomes, address the ongoing delays in environmental improvements and to provide data for greater public involvement in the regulatory decision-making process. IMC reviewed measures that could be undertaken to meet the proposed water quality concentration limits in the NoI and made a commitment to the EPA to progress the proposed improvements.

The EPA issued a Notice of Variation to Environmental Protection Licence (EPL) 2504 in March 2020. The EPA revoked the Georges River Environment Improvement Program (EIP2) and attached Special Condition E1.1 to the EPL requiring the installation and operation of a Water Treatment Plant (WTP) at Appin North by 31 March 2021 to meet revised water quality concentration limits (detailed in Condition E1.1). A further Notice of Variation was issued on 20 March 2021 extending the date for the operation of the Appin North WTP (ANWTP) to 30 November 2021, now July 2022. The EPA specified concentration limits that the WTP must be designed to meet and they required the development of an aquatic health monitoring program to verify improvements to the aquatic health of the Georges River. The Notice of Variation issued in March 2021 also included the new Point 40 (LDP40), that will be used to monitor compliance with the water quality concentration limits associated with the discharge from the new long term ANWTP.

## 1.2 EPL Requirements

The Georges River Aquatic Health Monitoring Program (GRAHMP) is a requirement of EPL 2504, Special Condition E3 which states: E3.1 The licensee must prepare an aquatic health monitoring

program to verify improvements to the aquatic health of the Georges River following commissioning of the reverse osmosis water treatment plant required by condition E1.1.

The monitoring must include:

• quantitative sampling of macroinvertebrates;

• ecological assessment processed using DNA extracted from sediment (as appropriate);

• in-stream water quality assessment;

• laboratory ecotoxicology and chemistry water testing; and

• pool level and flow monitoring.

The Appin North Water Treatment Plant (ANWTP) was due to be commissioned in November 2021 but due to COVID-19 impacts and delays the ANWTP is now due to be installed in July 2022. A temporary WTP was commissioned in May 2021 which discharges via LDP40 into the Brennans creek adjacent to LDP10. It is expected that the long term ANWTP will treat an average of 1.5 ML of water per day as opposed to the current temporary WTP plant being less than 1 ML/day. The pool that both LDP40 and LDP10 discharge into is referred to as Point 10 when referring to the macro-invertebrate and eDNA monitoring within this report.

## 1.3 Objectives of this report

The main aim of the Program is to summarize the changes in biotic (macrobenthic, DNA metabarcoding) and abiotic measurements (chemistry, physicochemical and flow) over time. The Program aims to examine the water quality in the Georges River pre-installation (2020, 2021, Autumn 2022) and post-installation (Spring 2022, 2023) of the long term ANWTP. This 2022 initial report includes data for nine sites within the Georges River catchment prior to installation of the long term ANWTP, and also examines the quality of water from a temporary reverse osmosis WTP at Point 40 (LDP40), which mixes with water from LDP10 in the pool immediately below LDP10, at Point 10. The 2022 report examines the abiotic and biotic data obtained for the Georges River Aquatic Health Monitoring Program (GRAHMP) in two parts. Firstly, it provides focussed detail on the water level (Section 3.1), water chemistry (Section 3.2),ecotoxicology (Section 3.4) and

macrobenthic surveys (Section 3.6) from Autumn and Spring 2020 and 2021, and the Spring 2021 eDNA and Spring 2020-2021 DNA metabarcoding surveys (Section 3.8). Secondly it provides an overview of the long term trends (2013-2021) in these parameters, chemistry long term patterns (Section 3.3), long term ecotoxicology (Section 3.5) and macrobenthic long term patterns (Section 3.7) In addition, the report aims to summarise the long term information within a weight of evidence framework, drawing upon the collective results of the water chemistry, physical properties, water flow, community ecology and ecotoxicological data.

The metabarcoding (DNA-profiling broad eukaryote, prokaryote communities and diatom micro-eukaryotes) survey was included in the weight of evidence program as a component of the biological community structure line of evidence. The metabarcoding data provides a comprehensive representation of the biological community and hence compliments the other traditional macrobenthic microscopy biological lines of evidence approaches in the GRAHMP.

To aid comparisons, in accordance with the experimental design previously used for EIP2 (Chariton and Stephenson 2018 and 2020), the macrobenthic and metabarcoding data were examined as two statistical treatments, reference and discharge monitoring:

(i) Reference sites – 3 sites prior to the mine's influence; and

(ii) Discharge monitoring sites – 6 sites which capture the gradient from the mine.

The entire 4-year program aims to test the hypothesis:

> *There will be an improvement to water quality and ecotoxicity in pools downstream of the discharge into Brennans Creek, following the commencement of operation of the ANWTP. There will be a gradual increase in the abundance of contaminant-sensitive taxa within pools downstream of the discharge into Brennans Creek.*

The aim of the GRAHMP is to verify changes in water quality by:

a) comparing water chemistry in the Georges River before and after commencement of the ANWTP;

b) assessing the ecotoxicity of discharge waters from LDP10 and LDP40;

c) comparing the in-stream and sediment biota of pools downstream of the discharge with reference sites (located upstream of the Brennans Creek confluence);

d) calculating changes over time in the composition of in-stream and sediment biota, particularly downstream of the discharge; and

e) assessing the downstream gradient changes in composition of the in-stream and sediment biota.

### 1.3.1 2020-2021 surveys

These were examined by:

1. Summarising the water chemistry, water flow and water level measurements obtained in Autumn and Spring for both 2020 and 2021;

2. Interpreting the 2020 and 2021 ecotoxicological tests data performed on waters obtained from the discharge pipes (end of pipe sampling) at LDP10 and LDP40.

3. Exploring trends in macrobenthic invertebrate abundance and richness from samples obtained in Autumn and Spring;

4. Analysis of SIGNAL scores;

5. Exploring compositional patterns (community structure) of in-stream macrobenthic invertebrate communities sampled in Autumn and Spring;

6. Exploring correlative relationships between water chemistry and macrobenthic communities;

7. Exploring compositional patterns in the metabarcoding data for prokaryotes and eukaryotes communities;

8. Exploring correlative relationships between the water chemistry, environmental parameters and metabarcoding data; and

9. Exploring eDNA detection of platypus and Macquarie perch.

### 1.3.2 Long-term trends (2013-2021)

These were assessed by:

1. Examining long-term patterns in key water quality parameters;

2. Summarising the overall trends in macrobenthic invertebrate abundance and family richness;

3. Analysing and interpreting long-term patterns in SIGNAL scores. This approach is used to score macrobenthic samples from Australian rivers based on the known sensitivities of specific macrobenthic taxa. SIGNAL predicts that macrobenthic communities with high scores tend to be from sites with low levels of contamination (e.g., increased nutrients and changes in conductivity) and high dissolved oxygen;

4. Analysing the abundance and occurrences of three Leptophlebiidae genera (*Atelophlebia*, *Ulmerophlebia* and *Koornonga*) (2016-2021); and

5. Interpreting the ecotoxicological tests data performed on waters obtained from the discharge pipes at Point 10 (LDP10) (2013-2021).

# 2 Methods

## 2.1 Site locations

The study area is located within the upper Georges River Catchment. The study area commences at site GRQ1 and flows down to GRQ18 (Figure 1) a distance gradient of approximately 9.3km. The catchment of the Georges River drains a landmass of nearly 1000 square kilometres, including parts of 14 local government areas (LGAs) (NSW DPE 2022). The land use in the upper reaches includes a mixture of protected areas including the Dharawal National Park, industrial land use and rural agricultural land use. The South32 Illawarra Metallurgical Coal (IMC) Appin East colliery and West Cliff Coal Preparation Plant/Appin North colliery are located within the upper catchment of the Georges River. Water from the Appin North and West Cliff Coal Preparation Plant sites currently discharge site water into Brennans Creek Dam, which flows into Brennans Creek, before reaching the Georges River. The water that is discharged from Brennans Creek Dam consists of flows from Brennans Creek (diverted around the coal wash emplacement area), clean runoff from northern areas of the site, water from IMC site stormwater ponds, diverted water from the water treatment plant, rainfall falling on the Brennans Creek Dam surface, water entrained in coal wash emplaced or water resulting from rainfall infiltration through the coal wash emplacement area. The Georges River catchment land use becomes progressively more urbanised and industrial, moving downstream to Campbelltown and Liverpool LGAs. The entire Georges River catchment is one of Australia's most urbanised catchments.

In total the experimental design consisted of nine sampling sites divided into two statistical treatments, reference and discharge monitoring (Table 1 and Figure 1). These sites are:

**Reference sites (3 sites)** – GRQ1, GRUFS and Point 11; and

**Discharge monitoring sites (6 sites)**, which capture the gradient from Brennans Creek discharge - Point 10, Point 12, Jutts Crossing (here on referred to as Jutts), Pool 16, Pool 32 and GRQ18.

This report will refer to the three reference sites collectively as the reference treatment and the six discharge monitoring sites collectively as the discharge monitoring treatment.

In addition, sampling was also carried out at end of pipe at LDP40, a recent addition to the study, which was not initially factored into the experimental design. A temporary WTP was installed in

May 2021 to treat water from underground operations at Appin North using reverse osmosis (RO) and discharged via a pipe that sits beside the current LDP10 discharge pipe (Figure 2), such that both discharges enter and mix in the pool at site Point 10 in Brennans Creek. Discharge from both LDP40 and LDP10 during the sampling period have fluctuated over time, however, a large proportion of the flow in Brennans Creek, is water from LDP10. The discharge volumes from LDP10 being typically 30-300-fold higher than that from LDP40 (based on data provided in this report). In July 2022, the long term WTP will process both waters from Appin North underground operations together with water from the emplacement underdrainage, which is currently being discharged into Brennans Creek Dam.

It should also be noted that the Point 11 reference site may be confounded by licenced mine discharge from Appin East (Point 19) (as it is located between the Appin East discharge point and the confluence of Brennans Creek with the Georges River).

**Table 1. Location of sampling sites, treatment allocation and sampling type that occurred at each location**

| Site code | Stream | Location | Distance from LDP10/ LDP40 (km) | Easting | Northing | Treatment/ Statistical group | Sampling activities |
|---|---|---|---|---|---|---|---|
| GRQ1 | Georges R. | U/S of confluence | 1.3 | 297082 | 6211446 | Reference | Water chemistry, macrobenthos, metabarcoding, eDNA and water flow/level of the pool ecosystem |
| GRUFS | Georges R. | U/S of confluence | 1 | 297082 | 6211771 | Reference | Water chemistry, macrobenthos, metabarcoding, eDNA and water flow/level of the pool ecosystem |
| Point 11 | Brennans Ck | U/S of Brennans and Georges confluence | 0.4 | 297207 | 6212940 | Reference | Water chemistry, macrobenthos, metabarcoding, eDNA and water flow/level of the pool ecosystem |
| Point 10 (LDP10) | Brennans Ck | Discharge point (LDP10) | 0 | 297558 | 6212772 | Discharge monitoring | Ecotoxicity and associated water chemistry from water from end of pipe; Water chemistry, macrobenthos, metabarcoding, eDNA and water flow/level of the pool ecosystem |
| Point 40 (LDP40) | Brennans Ck | ANWTP discharge point, adjacent to LDP10 | 0 | 297558 | 6212772 | Additional monitoring | Ecotoxicity testing and associated water chemistry from water from end of pipe, water flow |
| Point 12 | Georges R. | D/S of Brennans and Georges confluence | 0.5 | 297157 | 6213016 | Discharge monitoring | Water chemistry, macrobenthos, metabarcoding, eDNA and water flow/level of the pool ecosystem |
| Jutts | Georges R. | D/S of Jutts Crossings | 1 | 296844 | 6213232 | Discharge monitoring | Water chemistry, macrobenthos, metabarcoding, eDNA and water flow/level of the pool ecosystem |
| Pool 16 | Georges R. | D/S of Kennedy Ck | 2 | 296890 | 6213908 | Discharge monitoring | Water chemistry, macrobenthos, metabarcoding, eDNA and water flow/level of the pool ecosystem |
| Pool 32 | Georges R. | D/S of Sawpit Gully | 4 | 297192 | 6215029 | Discharge monitoring | Water chemistry, macrobenthos, metabarcoding, eDNA and water flow/level of the pool ecosystem |
| GRQ18 | Georges R. | U/S of O'Hares confluence | 8 | 296748 | 6217637 | Discharge monitoring | Water chemistry, macrobenthos, metabarcoding, eDNA and water flow/level of the pool ecosystem |

U/S - upstream; D/S - downstream

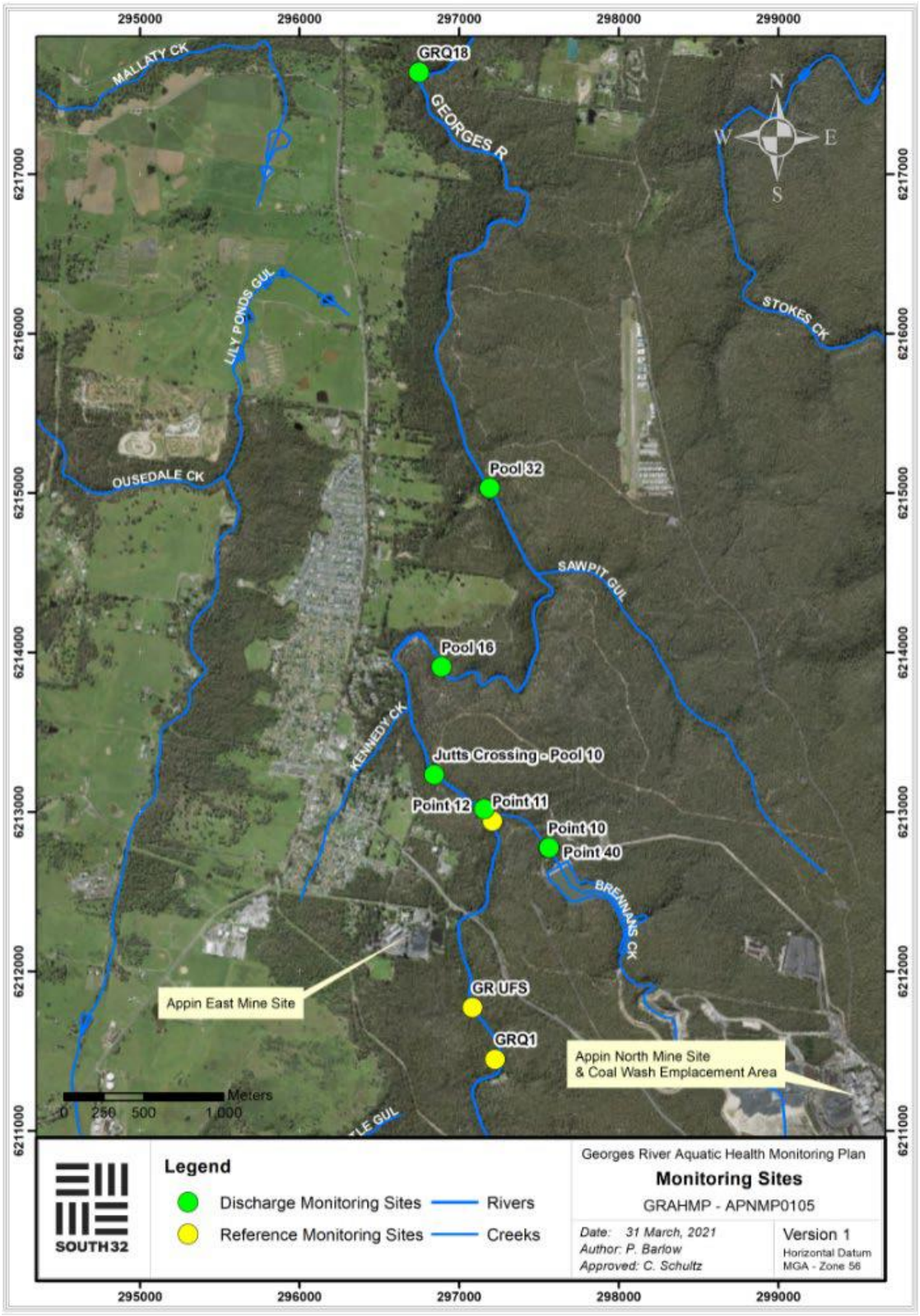


**Figure 1. Location of sampling sites.**

Reference sites = GRQ1, GRUFS (Georges River) and Point 11 (Upstream of Brennans Ck and Georges River confluence);
Discharge monitoring sites = Jutts-pool 10, Point 10, Point 12, Pool 16, Pool 32 and GRQ18

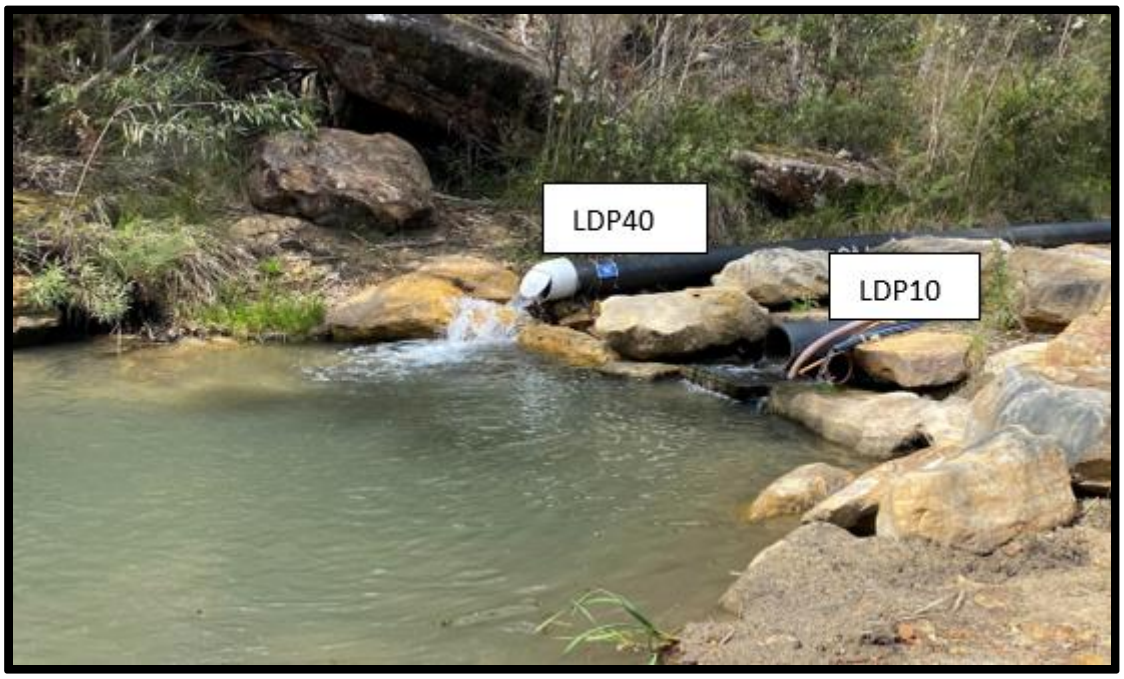


**Figure 2. LDP10 and LDP40 discharge pipes flowing into Point 10 site at Brennans Creek.**

LDP10 and LDP40 samples for ecotox analysis and associated water chemistry were collected at end of pipes. Water chemistry samples for macrobenthic analysis were sampled from the pool.


**Figure 3. Georges River reference sites.**

a) GRQ1 the most upstream site of the survey b) GRUFS Upper flow station of the Georges River, upstream of Appin North and Brennans Creek confluence. c) Point 11 reference site upstream of the Brennans Creek and Georges River confluence but downstream of GRQ1 and GRUFS. Photos taken during Spring 2021 sampling.


**Figure 4. Georges River discharge monitoring sites.**

a) Point 10: Pool at the discharge point LDP10 b) Point 12: downstream of Brennans Creek and Georges River confluence c) Jutts: downstream of Jutts Crossing d) Pool 16: downstream of Kennedy Creek e) Pool 32: downstream of Sawpit Gully f) GRQ18: furthest downstream site, upstream of O'Hares confluence.

Photos taken during Spring 2021 sampling except for Pool32 taken in Spring 2020.

## 2.2 Pool water levels and flow monitoring

At the completion of the 2018/2019 study on the Georges River (Chariton and Stephenson 2020), it was recommended that flow and level monitoring be included in future programs at some sites to help interpret ecological, chemical and ecotoxicological findings at each site. Therefore, in the current study, the following measurements were included: monitoring of pool levels at each site; discharge rates at LDP10 and flow rates at the reference site, upper flow station, GRUFS, which was frequently dry during sampling in previous years. The water flow at GRUFS is highly variable which makes it challenging as a reference site.

Pool water levels were monitored at each site by South 32 staff using installed pressure sensors and loggers at each of the pool monitoring sites (refer to Figure 1). Water level data were calibrated to an installed benchmark (in this case a nail), typically a single bolt inserted to the rock-bar or bedrock step (Figure 5). Loggers were housed in PVC pipes bolted to the pool's rock-bar or step (Figure 5). Logging was set to 1-hour intervals to adequately capture fluctuating water levels across the duration of the monitoring program.


**Figure 5. Water level field sampling equipment.**

Example of equipment at Point 10 showing nail with pink flag tape and logger casing clamped against sandstone pool banks.

Surface flows were monitored by South 32 staff using spot flow gauging at GRUFS (Figure 1). A Pygmy flow meter was used to calculate the discharge during inspections at the site, on a biannual basis. This flow discharge was obtained by measuring the velocity of the water at different points across a known cross-sectional area at GRUFS.

Discharge flows from the two discharge points at Point 10, from LDP10 and LDP40 were recorded over the sampling period. Total discharge including spillway values were measured for Brennans Creek Dam LDP10. Daily rainfall (mm) data was also downloaded from Wedderburn, NSW weather station for 2021 (Bureau of Meteorology 2021), to help interpret the pool level data.

## 2.3 Water chemistry methods

Samples were collected from the pools of water at each location immediately prior to macrobenthos sampling for a range of water quality parameters that were measured either in-situ or preserved and sent to Australian Laboratory Services (ALS) for analyses or both (Table 2).
It should be noted that the sample locations are slightly different here than those collected for ecotoxicity testing and analysed for the same analytes listed in (Table 2), which were collected at end of pipe for the LDP10 and LDP40 pipes. Therefore, once the WTP started discharging at LDP40 in May 2021, water collected for water chemistry alongside the macrobenthic sampling (described in this section) contained contributions from both LDP10 and LDP40. To differentiate the sample locations (end of pipe or pool sampled), herein, Point 10 refers to the pool following LDP10 and LDP40, whereas LDP10 refers to the discharge at end of pipe. At LDP40, water was only ever collected from end of pipe and is referred to throughout this report as LDP40. Sampling and analysis of these waters was co-ordinated by South 32 staff and results were provided to CSIRO for interpretation. Samples for metal analyses were filtered to 0.45 µm in the field by South 32 staff. In-situ measurements of temperature, conductivity, pH, dissolved oxygen, and turbidity (Table 2) were also obtained by South 32 staff using a Horiba U51 water quality device. For all analyses examining the relationships between the benthic biota and water chemistry, and for trend analysis of water chemistry, measurements provided by ALS were used in preference to the in-situ measurements, with the exceptions being dissolved oxygen, temperature, conductivity and pH, for which the in-situ measurements were used when available. In Autumn, 2020, in-situ data was not available, therefore measured values reported by ALS were used instead. Given the large number of water quality variables historically measured, analysis of long-term patterns in water quality (2013-2021) were restricted to a selection of key variables which are included in the current

GRAHMP and have historically been shown to be elevated in the discharge waters. These were: conductivity, pH, aluminium, cobalt, copper, nickel, zinc and total nitrogen.

**Table 2. Water chemistry parameters analysed as part of EPL 2540**

| Contaminant/analyte | Unit of Measure | Analysis | |
|---|---|---|---|
| | | In-situ | ALS |
| **pH** | pH units | X | X |
| **Dissolved Oxygen** | mg/L | X | |
| **Temperature** | °C | X | |
| **Electrical Conductivity** | µS/cm | X | X |
| **Bicarbonate Alkalinity (as $CaCO_3$)** | mg/L | | X |
| **Dissolved Aluminium** | µg/L | | X |
| **Dissolved Cobalt** | µg/L | | X |
| **Dissolved Copper** | µg/L | | X |
| **Dissolved Nickel** | µg/L | | X |
| **Dissolved Zinc** | µg/L | | X |
| **Total Nitrogen (as N)** | mg/L | | X |
| **Nitrite + Nitrate (as N)** | mg/L | | X |
| **Total Kjeldahl Nitrogen (as N)** | mg/L | | X |

Water samples were filtered in the field with 0.45µm filter. Dissolved is <0.45µm.

## 2.4 Ecotoxicological testing

Samples were collected for both ecotoxicity testing and water chemistry on four quarterly occasions in 2021.

### 2.4.1 Ecotoxicity tests in 2021

Ecotoxicity tests were carried out by Ecotox Services Australia (ESA), Sydney on four quarterly samples (February, May, August and November) collected from end of pipe at LDP10, discharge water from Brennans Creek Dam that flows into Brennans Creek and into the Georges River. Following installation of a temporary RO WTP at Appin North, quarterly testing was also carried out on three samples (May, August and November) collected from LDP40, at the pipe from the temporary WTP. Two ecotoxicity tests were carried out with each sample to compare the

ecotoxicity of the current licence discharge point waters (LDP10) to the assessment criteria in EPL 2504 (Table 3). LDP40 was included in the study following commissioning of the temporary WTP and will ultimately become the licence discharge point following commissioning of the long term WTP at Appin North.

Toxicity tests included the chronic 7-d reproductive impairment test using the cladoceran *Ceriodaphnia* cf *dubia* and the acute 4-d larval imbalance test with *Melenotaenia splendida* (Rainbowfish). In addition, the chronic 7-d survival using *C. dubia* was also measured as an additional test endpoint calculated from the 7-d reproductive test data. The *C. dubia* toxicity tests followed the methods of ESA Standard Operating Procedure (SOP) 102 (ESA, 2016a), based on USEPA (2020b) and Bailey et al., (2000). The fish ecotoxicity tests followed the methods described in ESA SOP 117 (ESA, 2016b) and was based on USEPA (2002b) with adaptations for use with the native rainbowfish. A brief summary is provided below.

Samples were diluted to 6.3, 13, 25, 50 and 100% with diluted mineral water (DMW, pH 8.1-8.2, conductivity of 172-176 μS/cm) where 100% sample is undiluted. The samples were not filtered or adjusted in any way prior to ecotoxicity testing. For the *C. dubia* tests, ten replicates per concentration of sample were prepared and one neonate (<24h old) added to each replicate. For the fish tests, four replicates per concentration of sample were prepared and five larval fish added to each replicate. Controls consisting of DMW were also prepared. The pH, conductivity and dissolved oxygen were measured in each dilution and control throughout each test. The test vessels were incubated at 25°C. The number of surviving (unaffected) inoculated *C. dubia* and the number of offspring (newly hatched neonates) per surviving *C. dubia* were counted daily for 7 days (allowing enough time for three broods). The number of unaffected larval fish were counted daily for 96 h. Affected fish were removed and euthanised. The fish test was carried out in compliance with the animal ethics licence (Animal Research Authority CSB V20/10359(3)[1]).

The *C. dubia* tests were renewed daily, however fish larval imbalance test solutions were not renewed, following advice from the ecotoxicity testing laboratory (ESA) that this species is particularly sensitive to handling, and that mortality in controls would occur if renewals were done. This was in line with the EPA requirements that stated fish tests could be done with or

[1] Issued by the Animal Care and Ethics Committee of The Secretary, Department of Regional NSW, NSW Department of Primary Industries, valid from 11 May 2021 to 11 May 2022.

without renewals (Table 3). If renewals in this test are desired for future samplings to avoid potential degassing occurring during tests, preliminary experiments would be required to determine the acceptable renewal test conditions for this species. In addition, routine reporting of physico-chemical properties throughout the test period in test reports will be helpful to determine if extensive degassing has occurred. This was requested by CSIRO post-hoc and was provided by the testing lab for one sampling only (November 2021).

The concentration to cause 10% effect (decrease) (EC10) on *C. dubia* 7-d reproduction and 7-d survival, and *M. splendida* 96-h larval imbalance were calculated by linear interpolation or log-logit interpolation, while the 50% effect concentrations (EC50s) were calculated using linear interpolation, log-logit interpolation or trimmed Spearman Karber methods. Hypothesis tests were also used to determine the highest concentration (lowest dilution) of sample water tested to have no significant ($p \leq 0.05$) effect (NOEC) on the test species and endpoints. While hypothesis testing to derive NOEC values is no longer recommended (Fox, 2008; Warne and van Dam, 2008), it was included here for comparison to EC10 values that could not be calculated or were unreliable.

**Table 3. Ecotoxicity tests and assessment criteria from EPL 2504**

| Species | Sampling Frequency | Sampling Method | Assessment Criteria |
|---|---|---|---|
| *Ceriodaphnia dubia* | Quarterly (minimum of 80-day intervals) | Chronic toxicity<br>US EPA Short-term Methods for Estimating the Chronic Toxicity of Effluents and Receiving Waters to Freshwater Organisms, 4th Edition (2002), EPA-821-R-02-013. | $EC10^5$ reproduction ≥ 100% sample |
| *Melenotaenia duboulayi or Melenotaenia splendida* | Quarterly (minimum of 80-day intervals) | 96-hour larval imbalance test with or without water renewal (if with renewal – daily or once at 48 hours).<br>US EPA (2002). Methods for Measuring the Acute Toxicity of Effluents and Receiving Waters to Freshwater and Marine Organisms. 5 ed.<br>EPA-821-R-02-012. Washington DC, USA. | EC10 reproduction ≥ 100% sample |

### 2.4.2 Ecotoxicity tests: long term assessment (2013-2021)

All ecotoxicity tests were performed by ESA. Between 2013 and 2021 a range of ecotoxicity tests using fish, shrimp, duckweed, cladocerans and microalgae (Table 4) were performed on discharge waters collected from LDP10. However, for the current GRAHMP (EPL 2504), ecotoxicological testing was reduced to two freshwater ecotoxicity tests: a 7-d chronic survival and reproduction test using the cladoceran *C. dubia* and an acute 96-h larval imbalance test with rainbowfish *M. splendida.*

Long term ecotoxicity comparisons were made with LDP10 samples only because LDP40 was only tested in 2021. The EC10 values, the assessment criteria of EPL 2504, were compared. Toxicity was also expressed as toxic units (TUs) for each ecotoxicity test (100 ÷ EC10) to enable direct comparisons between the ecotoxicity data and for presentations in figures. A TU of 1 indicates that the sample is not toxic (EC10 ≥ 100%) and a TU >1 indicates that the sample is toxic (EC10 <100%).

**Table 4. Ecotoxicity tests performed on LDP10 waters between 2013-2017**

| Test organism | Test |
|---|---|
| *Melanotaenia duboulayi* (fish) | 96-h acute fish imbalance test |
| *Paratya australiensis* (shrimp) | 10-day acute survival test |
| *Lemna disperma* (duckweed) | 7-day acute growth inhibition |
| *Ceriodaphnia* cf *dubia* (cladoceran) | Partial life-cycle 7-day survival |
| *Ceriodaphnia* cf *dubia* (cladoceran | Partial life-cycle 7-day reproduction |
| *Ceriodaphnia* cf *dubia* (cladoceran) | 48-h acute survival test |
| *Selenastrum capricornutum* (microalga) | 72-h chronic algal growth inhibition |

## 2.5 Macrobenthos sampling

On all occasions (Spring 2013 - Spring 2021) at each site, macroinvertebrates were sampled from three to five random pool edges, then combined giving one sample at each site (Downs et al., 2002). The number of replicates for each site was increased from three to five in 2018. Pool-edge samples were collected from depths of 0.2-0.5 m within 2 m of the bank. A suction sampler described by Brooks (1994) was placed over the substrate and operated for one minute at each

sampling location. The sample was washed thoroughly over a 500-µm mesh sieve. All material retained on the 500-µm mesh sieve was preserved in 70% ethanol for laboratory sorting.

Macrobenthic sorting and identification was performed by Niche Environment and South32 and provided to CSIRO in a tabulated format. The data were presented at the taxonomic level of Family. In addition, abundances of three potential indicator taxa from *Leptophlebiidae* (*Atelophlebia*, *Ulmerophlebia* and *Koornonga*) were analysed from the data obtained between 2016 and 2021.

For the current GRAHMP report 1, sampling for the macrobenthic surveys was performed in Autumn 2020 (24th March 2020), Spring 2020 (14th October 2020), Autumn 2021 (11th May 2021) and Spring 2021 (19th - 21st October 2021). Water chemistry samples were collected at the same time as the macrobenthic samples. The Spring 2020 sample Point 11 replicate sample 2 was removed from the analysis due to no macroinvertebrates being observed in the sample.

## 2.6 Collection and analysis of DNA samples for metabarcoding

### 2.6.1 DNA sample collection and processing

The collection of samples for the DNA-based survey (metabarcoding) was performed concurrent to the Spring 2020 and Spring 2021 macrobenthic survey. At each site, five sediment samples were collected from the soft sediment located approximately 1 m from the edge of the water bodies where the water column was approximately 30 to 40 cm deep. Areas of high aquatic vegetation biomass or areas with shading over the underlying aquatic system were excluded from sampling. All materials used for the collection and storage of DNA samples were soaked for at least 24 h in 1% sodium hypochlorite and rinsed thoroughly five times with Milli-Q water (Millipore, Academic Water Systems, Australia). Surficial sediment samples (top 2 cm) were obtained using a clean shallow polycarbonate corer (diameter 10 cm). All samples were transferred into DNA-free sterile 50 mL Greiner tubes and placed on ice immediately, then frozen at -80°C within 8 h of collection. Samples were thawed just prior to DNA extraction. Using 10 g of homogenised sediment, DNA was extracted and purified from each using Qiagen DNeasy PowerMax® Soil isolation kits (QIAGEN® Germany) following the manufacturer's protocols.

Three primer sets from two conserved gene regions were targeted to capture the system's biodiversity. 18S V7 rDNA gene (Hardy et al., 2010) was amplified for broad eukaryotes monitoring; and the 18S V4 (Zimmerman et al., 2011) region was amplified for diatom

(Bacillariophyceae) specific eukaryotes. Diatoms were included in the design because many of the potential indicator OTUs from previous reports associated with differences between reference and discharge monitoring sites were diatoms (Chariton and Stephenson, 2018 and 2020).

For bacteria communities, the V4 region of the 16SrDNA gene for prokaryotes was amplified (Caporaso et al., 2012). For all 2020 samples and 2021 samples, three identical polymerase chain reaction (PCR) plates were amplified for each primer set (18S V7, 18S V4, 16S V4) and the amplicons for the three PCRs were pooled into one library per target primer set. For 18S V7 PCRs, in addition to the sediment DNA samples, reference samples containing sequences of the saltwater crocodile (*Crocodylus porosus)* and a tropical marine cnidarian (*Carukia barnesi*) were also processed in three sample replicates as positive controls. For 16S V4 a synthetic chimeric bacterial control (containing fungal mycorrhizal species, *Cairneyella variabilis*), was processed alongside DNA and for 18S V4 diatoms two marine micro-eukaryote species, *Dunaliella sp*. and *Ulkenia sp*. were processed as PCR positive controls. Negative water controls were included in all PCR experiments to test for biological contamination during amplification. Amplification and purification success were interrogated on a MultiNA gel, MultiNA© (Shimadzhu, Oceania). The three pooled final amplicon library concentrations were measured on the Nanodrop® spectrophotometer (Thermo Fisher Scientific, Waltham, MA USA). Target gene libraries of DNA samples from 2020 and 2021 were then prepared with the Illumina Tru-Seq PCR-free library preparation kit and libraries were sequenced over one MiSeq run at 2x 250bp. The Illumina MiSeq sequencing was performed by the Ramaciotti Centre for Genomics, UNSW. The Spring 2020 samples were sequenced in February 2021 and the Spring 2021 samples were sequenced in January 2022.

### 2.6.2 Bioinformatics 18S and 16S rDNA

Sequenced data were processed using a custom pipeline (Greenfield Hybrid Amplicon Pipeline (GHAP) which is based around USEARCH tools V11 (Edgar, 2013). The pipeline is available at https://data.csiro.au/dap/landingpage?pid=csiro:26534. GHAP first demultiplexes the sequence reads to produce a pair of files for each sample. These paired reads were then merged, trimmed, de-replicated, and clustered at 97% similarity to generate a set of representative OTU (Operational Taxonomic Units) sequences which were classified after clustering at 97% similarity in sequences. USearch V11 tools (fastq_mergepairs, derep_fulllength and cluster_otus) (Edgar, 2013) were used for the merging, de-replicating and clustering steps.

For 18S, the 2020 and 2021 sequencing data was processed with the previous EIP2 OTU sequencing data from 2019 to ensure consistent OTU assignments and temporal comparisons. For 18S each OTU sequence was classified in two different ways: first, by using the RDP Classifier (v2.10.2) to determine a taxonomic classification for each sequence, down at best to the level of genus; and second, by using ublast to match a representative sequence from each OTU against a curated set of 18S reference sequences derived from the SILVA v128 SSU reference set for the broad eukaryotes V7 dataset (Cole et al., 2014; Quast et al., 2013). This 18S reference set was built by taking all the eukaryote sequences from the SILVA v128 SSU dataset, and removing those sequences found to contain bacterial or chloroplast regions. PR2 taxonomic reference set (Guillou et al., 2013) was used to assign taxonomy to the V4 diatoms 18S dataset. The pipeline then used usearchglobal to map the merged reads from each sample back onto the OTU sequences to obtain accurate read counts for each OTU/sample pairing. The classified OTUs and the counts for each sample were finally used to generate OTU tables in both text and BIOM (v1) file formats, complete with taxonomic classifications, species assignments and counts for each sample. All OTUs with a maximum read abundance of 50 reads, or that were only observed in less than four biological replicates were removed.

Diatom OTUs were assigned taxonomy using the PR2 database and it should be noted diatom taxonomy is classified predominantly based on the shapes and morphological features of the cells (Guillou et al., 2013). For example, taxa are split based on the presence of a raphe, the raphe is a cell structure that allows diatom cells to move over surfaces.

For 16S, the latest 2020 and 2021 sequencing data was processed with the previous EIP2 OTU sequencing data from 2019 to ensure consistent OTU assignments. For 16S representative sequences from each OTU were classified both by finding their closest match in a set of reference 16S sequences, and by using the RDP Naïve Bayesian Classifier. The pipeline used both the RDP 16S Training Set and the RefSeq 16S reference sequence collection for the purposes of species-level classification. The pipeline then mapped the merged reads back onto the classified OTU sequences to obtain accurate read counts for each OTU/sample pairing and generate OTU tables in both text and .biom (v1) formats, complete with taxonomic classifications and species assignments. The OTU tables were then summarised over all taxonomic levels, combining the counts for identified taxa across all OTUs. The pipeline finally classifies all the merged reads using the RDP Classifier, regardless of whether they were assigned to an OTU. This last step is done to

provide confidence in the clustering and OTU formation steps by providing an independent view of the community structure.

After processing, and prior to statistical analyses, the data sets were filtered to remove potentially erroneous sequences. For all data sets, the proportion of contamination OTU reads in the positive controls (the max read count that is not the positive control divided by the positive control read count) was determined. The proportion of read counts for each OTU in each sample (the read count for each OTU divided by the total read count for that sample) was determined to identify sequencing leakage. The proportion of contamination was relatively low in all data sets (between 0.0007 18S V7 and 0.001 18S V4 diatoms) and this value was set as the cut-off for filtering the dataset. If the proportion of read counts for each OTU per sample was less than the proportion of contamination then those reads were removed from the dataset. After quality control checks were complete, controls were removed from the dataset. Any OTUs that had a match percent of <80 or appeared in less than two samples were all removed. Processed data has been archived in CSIRO's Data Access Portal (DAP) http://data.csiro.au.

## 2.7 eDNA detecting platypus and Macquarie perch DNA in the Georges River

South32 requested an eDNA analysis of *Ornithorhynchus anatinus* (platypus) and *Macquaria australasica* (Macquarie perch) after earlier research studies (Griffiths et al., 2021) in the middle reaches of the Georges River had found positive detection of Macquarie Perch and an equivocal (one of the six qPCR assays were positive) result for platypus in the middle reaches of the Georges River. Previous eDNA surveys in the upper Georges River during September 2020 and Feb 2021 detected both species in the middle reaches, downstream of Wedderburn (Griffiths et al., 2021). South32 contracted enviroDNA (Melbourne, Australia) to process the environmental samples and run the eDNA analysis in 2021. In September 2021, water samples were collected from the 9 sites in the Georges River by South32 following sampling protocols developed by EnviroDNA. At each site, three samples were collected by passing 600-1250 ml water (average 992 ml) through a 1.2 µm syringe filter. Filtration was undertaken on-site to reduce DNA degradation during transport of whole water samples (Yamanaka et al*.,* 2016). Clean sampling protocols were employed to minimise contamination between sites including new sampling equipment at each site, not entering water, and taking care not to transfer soil, water, or vegetation between sites. A preservative (0.5 ml 10xTris-EDTA) was added to the filters after filtering to minimise DNA

degradation. Filters were stored out of sunlight and at ambient temperature before being transported to the laboratory for processing.

DNA was extracted from the filters using a commercially available DNA extraction kit (Qiagen DNeasy Blood and Tissue Kit). Real-time quantitative Polymerase Chain Reaction (qPCR) assays were used to amplify the target DNA, using a species-specific probe targeting a small region of the mitochondrial DNA of each target species (Macquarie perch and platypus). The platypus qPCR assay was completed with forward primer OAcr_F CAGCAATACCCTAGACAAGG, reverse primer OAcr_R CGCTTCAATGGCTGCGC, and MGB probe OAcr_MGB CGAACCCCATGAGTAGAAAAT (Lugg et al., 2018). Primer specificity was checked using a Blast search of the NCBI nucleotide database, with no close matches found outside of *O. anatinus* (Lugg et al., 2018). The Macquarie perch qPCR assay details could not be shared due to this information being the Intellectual Property of EnviroDNA. Available gene sequences were compared between related taxa (including humans) and a probe sequence selected to detect the target species. Where possible, further in-vitro (tissue samples) testing was undertaken on the target species and closely related co-occurring species to check for cross-amplification of non-target DNA. Assays were performed in triplicate on each sample. Positive and negative controls were included for all assays as well as an Internal Positive Control (IPC) to detect inhibition (Goldberg et al., 2016). At least three positive PCRs (out of nine assays undertaken for each site) were required to classify the site as positive for the presence of the target species. To minimise false positives, sites were considered unreliable if only 1 or 2 assays returned a positive result, indicating very low levels of target DNA. While trace amounts of DNA may indicate the target species is present in low abundance, it may also arise from sample contamination through the sampling or laboratory screening process (minimised through strict protocols and negative controls), facilitated movement of DNA between waterbodies (i.e., water birds, recreational anglers, water transfers, predator scats), or dispersal from further upstream. If greater confidence is required, further sampling is recommended at multiple sites to confirm the presence or absence of the target species. Repeat sampling is also recommended to help determine the tenure of the species at a site (i.e., resident or transient).

## 2.8 Statistical analysis

### 2.8.1 Macrobenthos data (2020 and 2021)

Multivariate statistics on community structure were undertaken using the statistical software package Primer 7+ (Plymouth Marine Laboratory, UK). Prior to multivariate analysis, the macrobenthos data were log10 transformed. Ordinations of the data were performed by non-metric multidimensional scaling (nMDS) using the Bray-Curtis similarity coefficient. Statistical differences between sites were tested by permutational multivariate analysis of variance (PERMANOVA), with differences between sites identified by pairwise a posteriori tests based on 9999 random permutations. The key taxa contributing to significant differences between sites were identified using Primer's SIMPER function, Primer 7+ (Plymouth Marine Laboratory, UK).

The relationships between macrobenthic communities and environmental variables were examined using distance-based linear models (DISTLM) (Legendre and Anderson, 1999). In order to match the number of biological and environmental (physico-chemical) samples, i.e., one sample per site, the similarity matrix for the biological data was recalculated using the distance between centroids for each site derived from the replicate samples. The environmental variables obtained from the monitoring program were both numerous and often strongly correlated, and consequently all highly correlated variables ($r>0.95$) were removed. To reduce over-fitting and to conform to the assumptions of the analysis (number of biological samples > environmental variables), DISTLM was performed using only a limited number of environmental variables, with the variables selected a priori using Primer's BIOENV function. The final variables used in the DISTLM were pH, conductivity, alkalinity, dissolved aluminium, dissolved copper, dissolved nickel, dissolved zinc and total nitrogen. It is emphasised that these variables provide a summary of the discharge water, and it is not possible to robustly quantify the contribution of each measured variable in isolation. The dbRDA option was selected to provide an ordination of the fitted values from the model.

### 2.8.2 Long-term patterns in macrobenthos

Univariate attributes of the macrobenthos data were obtained using Primer 7's 'Diverse' function. As part of the GRAHMP requirement to enable a balanced comparison between the reference and discharge monitoring sites, differences in total abundance and richness between the three reference sites and three of the six discharge monitoring sites (Point 12, Pool 32 and GRQ18) were

examined using a one-way ANOVA. Because of the change in replicates, three prior to 2018 and five subsequent, all univariate metrics are based on site means. Residuals were assessed for skewness, kurtosis, and normality, with homogeneity of variances examined using a modified Levene equal variance test. All univariate analyses were performed using NCSS v12 (Utah, USA).

### 2.8.3 SIGNAL

SIGNAL stands for Stream Invertebrate Grade Number – Average Level, and is simple approach used to score macrobenthic samples from Australian rivers based on the known sensitivities of specific macrobenthic taxa (Chessman, 1995). SIGNAL predicts that macrobenthic communities with high scores tend to be from sites with low levels of contamination (e.g., nutrients and conductivity) and high dissolved oxygen. In this report, scores were calculated using the SIGNAL 2.0 procedure described by Chessman (2003). As the total abundances of the sample varied greatly over time and within sites, here we used unweighted SIGNAL scores, i.e., derived from presence/absence data. SIGNAL scores are then used to putatively classify sites, with a SIGNAL value >6 suggesting clean water; 5-6, doubtful quality, possible mild contamination; 4-5 probable moderate contamination; and less than 4, probable severe contamination.

Comparisons in mean SIGNAL scores between the three reference sites and three of the six discharge monitoring sites (Point 12, Pool 32 and GRQ18) were examined using a one-way ANOVA. Based on the recommendations of Chariton and Stephenson (2018), the macroinvertebrate index EPT % (The sum of Ephemeroptera, Plecoptera and Trichoptera divided by the number of Chironomids) has been removed as a metric for the monitoring program. This is because the EPT index was designed for fast-moving rivers, and furthermore, plecopterans have never been sampled in this particular system.

### 2.8.4 Metabarcoding statistics (Spring 2019, 2020 and 2021)

Statistics were undertaken using the statistical software package Primer 7+ (Plymouth Marine Laboratory, UK). Univariate attributes of the metabarcoded data for each primer set were obtained using Primer 7's 'Diverse' function. To investigate patterns in community composition (beta diversity) subsampled OTU abundance tables were standardised and transformed to presence and absence for broad 18S V7rDNA and 18S V4rDNA diatoms OTUs and for 16S rDNA data was normalised prior to analysis.

OTUs were assigned to Family for the 16S rDNA dataset, Genus for the diatom 18S V4 rDNA dataset and Family for the broad 18S rDNA dataset. For the 18S and 16S rDNA data, ordination of the OTU data was performed by non-metric multidimensional scaling (nMDS) using the Bray-Curtis similarity coefficient, as was the PERMANOVA analysis. Statistical differences between reference and discharge monitoring sites, and individual sites were tested by a PERMANOVA. The relationships between metabarcoded communities and environmental variables were examined using distance-based linear models (DISTLM) on centroids for sites, as previously described for macroinvertebrate statistical methods. For metabarcoding, DistLMs were undertaken on the survey years combined datasets as well as on individual yearly datasets. The key OTUs contributing to significant differences between sites and community composition were identified using Primer's SIMPER function for all datasets. The alpha cut-off value for statistically significant results was $p<0.05$ throughout the study. For temporal analysis, 2019 OTU data was included for eukaryotes and bacteria data to compare OTU communities over time. OTU data from 2019 V7 18S rDNA and 16S rDNA was included in analysis of richness and PERMANOVA.

# 3 Results and Discussion

## 3.1 Pool water levels and flow

The average flow rate at GRUFS (Figure 6), confirms earlier findings that there were significant periods of time when this site had low or no flow since 2018. In the period from 2020 to 2021, higher flow rates were observed than in previous years, however, dryer spells were observed during January 2021 and November 2021, with very low water flow detected during Autumn 2020, Spring 2020, Summer 2020/21 and Winter to Spring 2021. Both Spring sampling events in 2020 and 2021 coincided with very low flow rates at GRUFS.

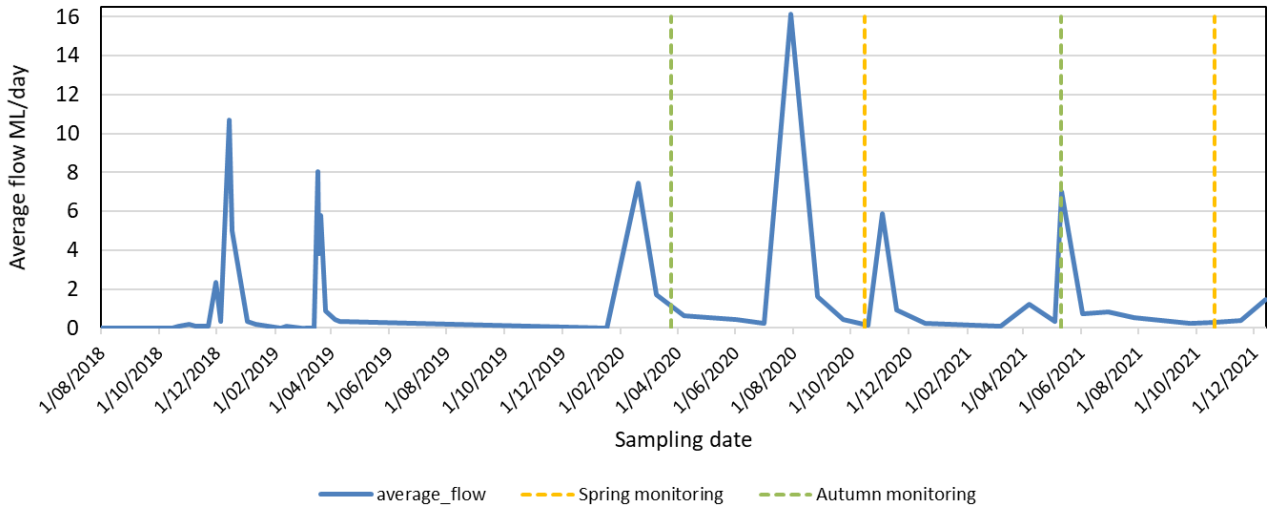


**Figure 6. Average flow (ML/day) at reference site GRUFS over sampling time period July 2018 – November 2021**

Pool water level data for each site are shown in Figure 7. In addition, rainfall data from Wedderburn station were overlayed onto the pool water level data. It should be noted that there were no suitable positions for water level monitoring at Pool 32, due to substrate type at this location. Pool 28a was used as a proxy for Pool 32 since these two pools were deemed to have similar characteristics and were geographically close. However, there was very little data provided for Pool 28a, with data available for only 5 of the 12 months in 2021. Therefore, this site is of little value for comparison to Pool 32. Data were also not available at all sites due to a faulty barometer that provided incorrect readings between 16$^{th}$ September to 24$^{th}$ October 2021. At Jutts an erratic high pool level was recorded in October, which is unlikely a correct reading, and more likely an error in measurement or was recorded at a time that the sensor was removed from the pool.

Despite these limitations, significant rainfall events and subsequent higher water levels were observed in March and May 2021. A smaller rainfall event in late August also caused a momentary increase in pool levels for most sites. All pools (except Pool 28a) were at a higher level when sampled in Autumn 2021, than in Spring 2021. Of note, is that discharge volumes from LDP10 were also 6-fold higher in Autumn 2021 than in Spring 2021 (Figure 8 and Figure 9) most probably due to the increased rainfall.

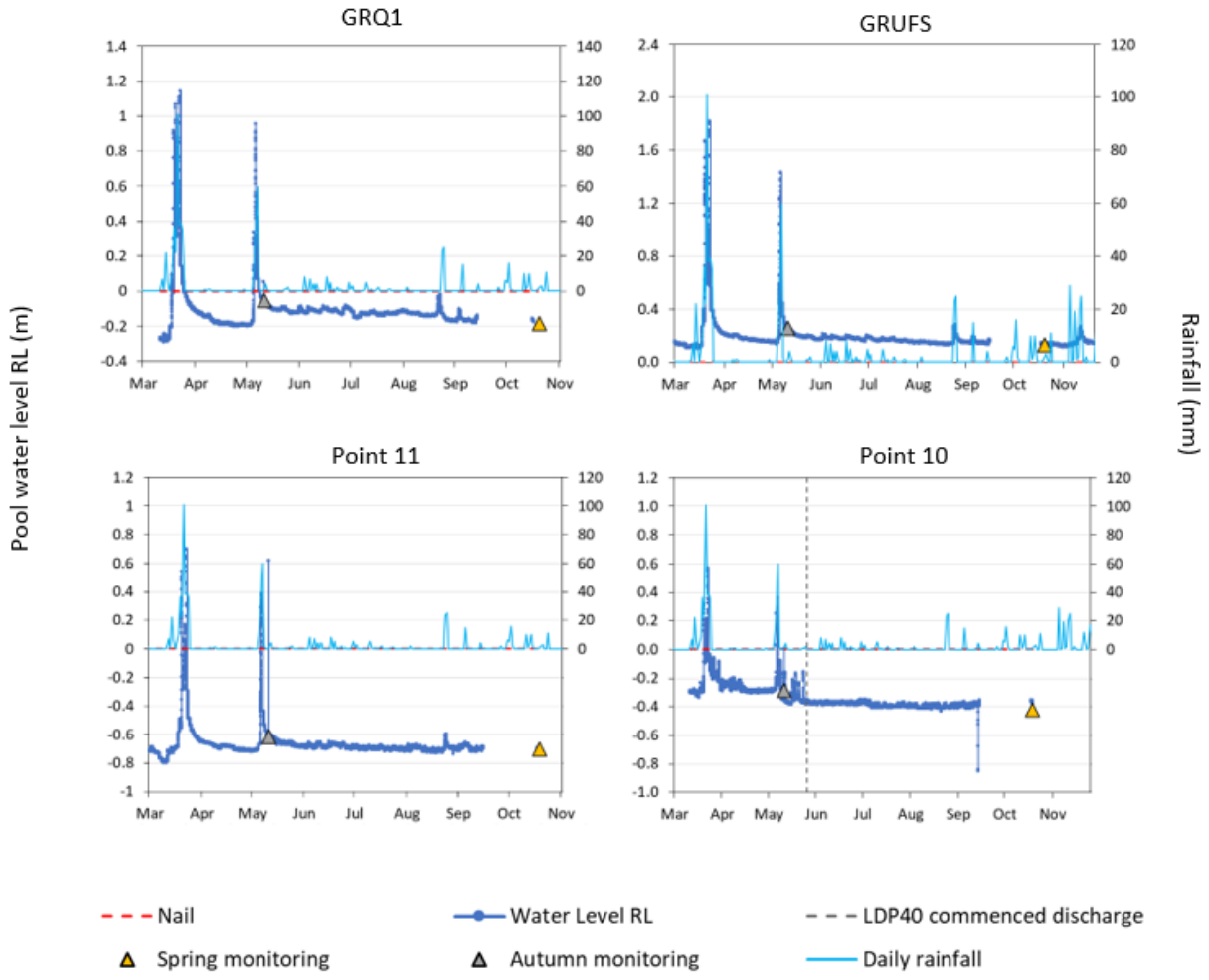


**Figure 7. Rainfall and relative (RL) water levels at each site during 2021.**

Water levels are relative since they are based on differences in distance from a set point (nail) installed above the water line at each site in March 2021. Pool 10 was drained in September for maintenance work.

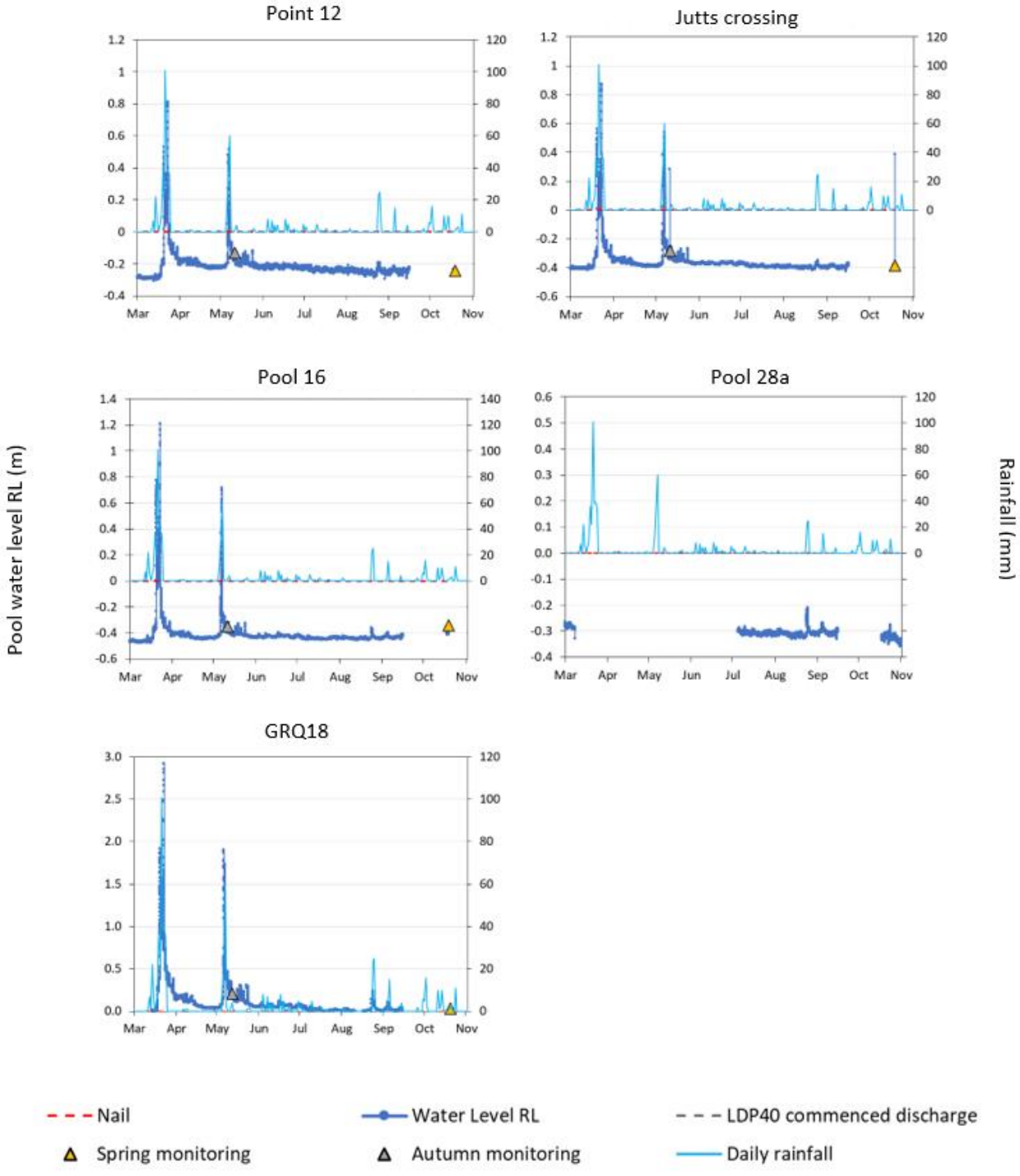


**Figure 7 (continued). Rainfall and relative (RL) water levels at each site during 2021.**

Water levels are relative since they are based on differences in distance from a set point (nail) installed above the water line at each site in March 2021. Pool 28a has been used a proxy for Pool 32.

The volumes of the discharges from LDP10 and LDP40 to the environment are shown in Figure 8 and Figure 9. The proportion of LDP40 water in overall discharge to the pool at Point 10 per month was very low, ranging from 0.20-3.3% (Figure 8). The WTP commenced discharging on 26 May 2021, after the Autumn sampling for 2021 was already completed. Therefore, only one sampling occasion for ecological and water monitoring in Spring 2021 included inputs from the WTP discharge at LDP40. The contribution from LDP40 to overall discharge to the environment was very low on that sampling occasion (Spring 2021) ranging from 0.8-2.1% (Figure 9).

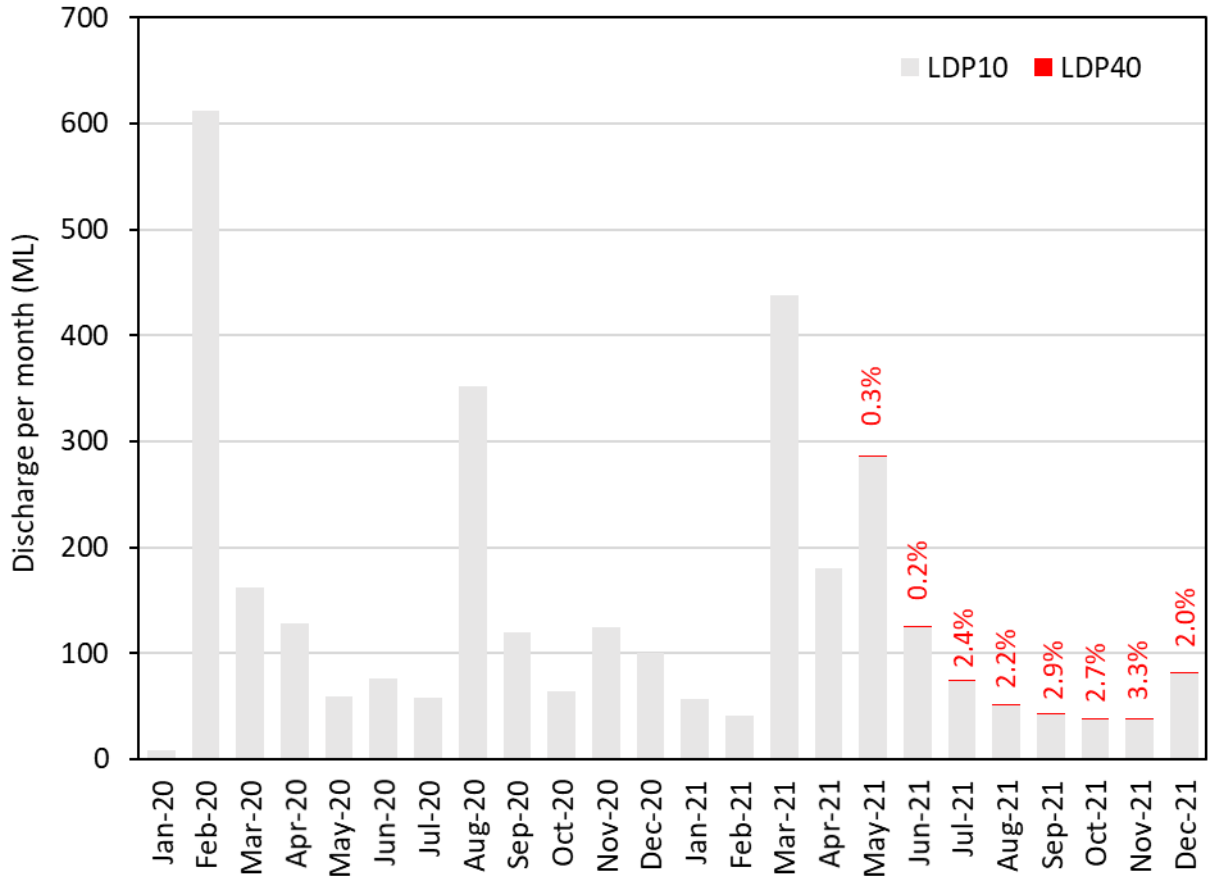


**Figure 8. Total monthly discharge volumes (ML) from LDP10 and LDP40 during 2020 and 2021**

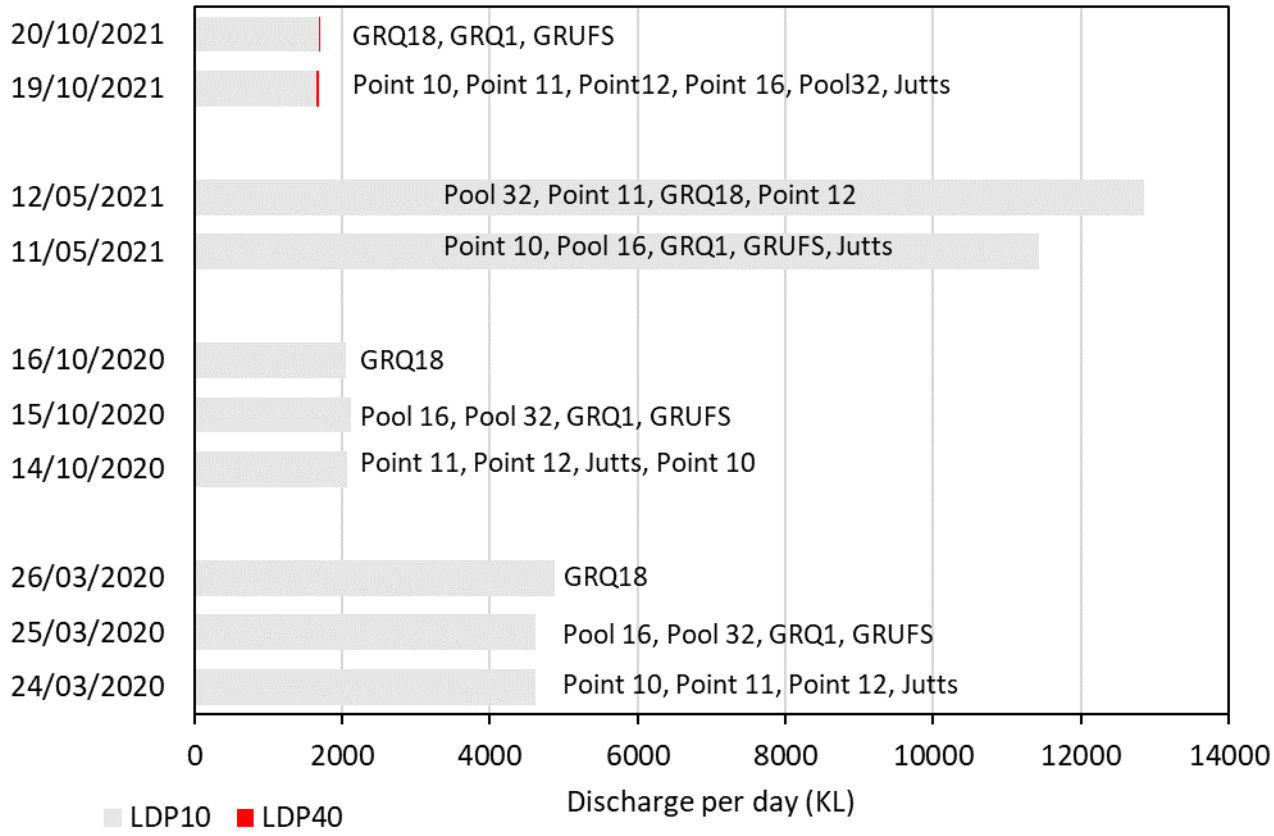


**Figure 9. Discharge to the environment from LDP10 and LDP40 during sampling from each site for monitoring of water chemistry, macroinvertebrates and metabarcoding.**

Site names beside each bar indicate the sites sampled on those dates.

## 3.2 Water chemistry (2020-2021)

Analyses for water chemistry, presented in Table 5 and Table 6, and Figure 10 and Figure 11, were carried out on samples from each location alongside the macroinvertebrate surveys. Additional analyses for water chemistry were undertaken on samples collected from the end of pipe alongside those for ecotoxicity testing and are reported separately in Section 3.4.

In general, based on the parameters measured, water quality relative to GV was poorer during 2020 and 2021 at the downstream discharge monitoring sites than at reference sites.

Water quality parameters measured at reference sites were mostly within the ANZG (2018) GV ranges, with some exceptions for one or two sites on each sampling occasion. Notably, waters from Point 11 were typically lower in zinc than the other reference sites, but higher in alkalinity,

pH and aluminium, with aluminium usually exceeding the GV. This nonuniformity at Point 11 may be due to the inputs from mine discharge at Appin East. In autumn 2021, however, aluminium concentrations were similarly elevated by almost 3-fold above the GV at all three reference sites, but these were still 2 to 4-fold lower than those measured at discharge monitoring sites.

The pH of waters from Point 10 and all downstream sites (7.6-8.9) were higher than those at reference sites (4.9-7.2). The pH for seven of the 12 samples collected at reference sites were within the acceptable range for lowland rivers (6.5-8.0). In contrast, the pH in waters collected from discharge and downstream sites except those at the most downstream site GRQ18 (on three of the four sampling occasions) were higher than the upper pH guideline limit of 8, with a range of 8.2 to 8.9. The pH was low for waters at reference sites which is similar to previous years. The reasons for the low pH in the reference sites is unknown but these sites may be naturally low due to riverbank vegetation-derived organic acids (Holland et al., 2012).

Conductivity (431-1860 µS/cm) was also higher at Point 10 and all downstream sites than those at reference sites (116-229 µS/cm), by up to 16-fold, however, the values always fell within the acceptable range for conductivity for lowland rivers (125-2200 µS/cm; ANZG, 2018). Across the four samplings in 2020 and 2021 from discharge monitoring sites, conductivity was highest in Autumn 2020, followed by Spring 2020, Spring 2021, then Autumn 2021.

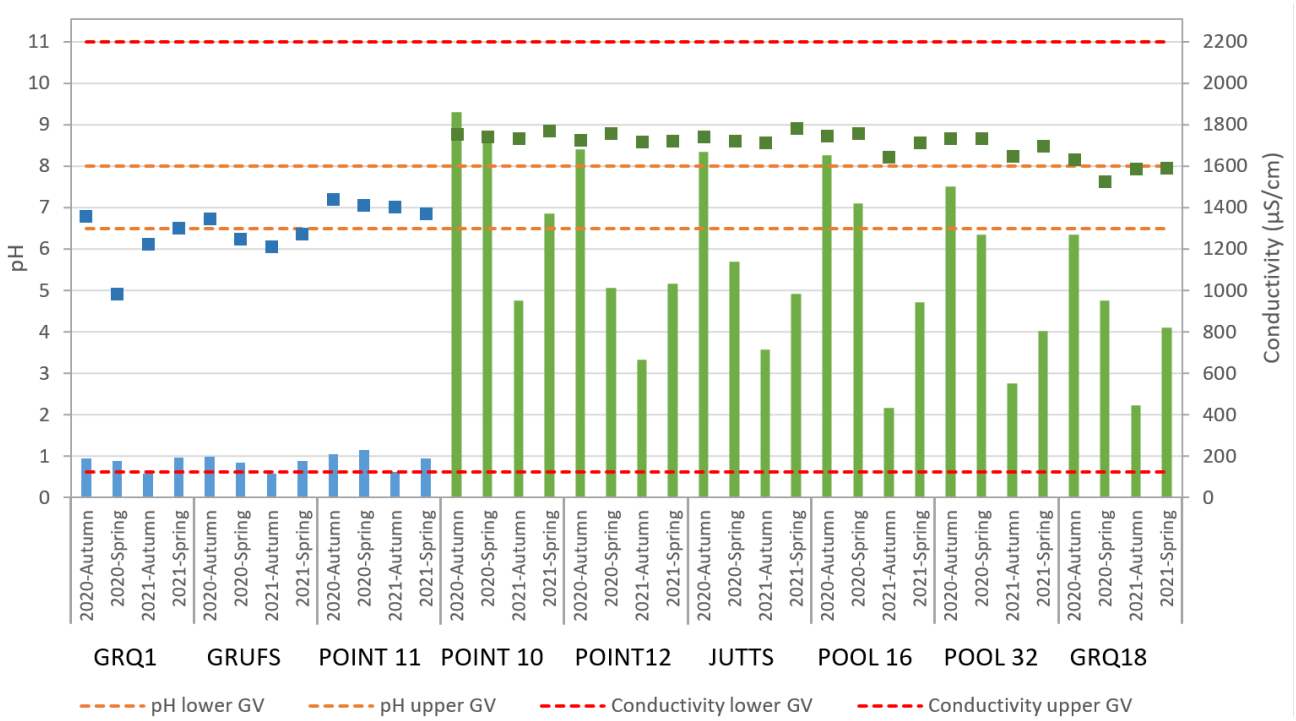


**Figure 10. Field measured pH and conductivity at nine study sites**

Note that field data were unavailable for Autumn 2020 samples so lab measurements are presented instead. Reference sites (blue) and discharge monitoring sites (green). Columns are conductivity and squares are pH. Dashed lines indicate upper and lower ANZG (2018) guideline values for pH and conductivity in lowland rivers.

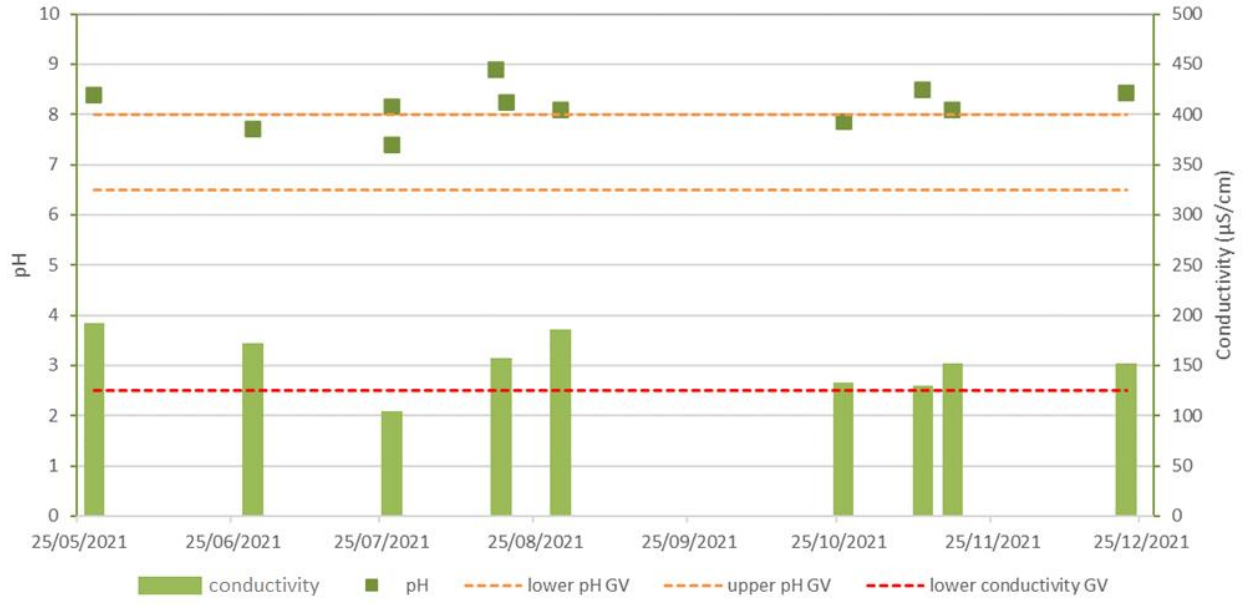


**Figure 11. Field measured pH and conductivity LDP40, end of pipe for temporary WTP plant.**

Dashed lines indicate upper and lower ANZG (2018) guideline values for pH and lower guideline value for conductivity in lowland rivers.

Aluminium concentrations were generally higher in Autumn than Spring for both years, but highest overall in Autumn 2021, when waters from all sites exceeded the GV (55 µg/L) by between 4 to 8-fold. In Autumn of 2020 and 2021, aluminium was elevated above the GV in all discharge monitoring sites, however in Spring of 2020 and 2021, concentrations of aluminium at sites further from LDP10 (GRQ18 in Spring 2020 and both Pool 32 and GRQ18 in Spring 2021) were below the GV.

Nitrogen (including NOx) was also usually higher in Autumn than Spring, being highest in waters collected in Autumn 2020, with total nitrogen exceeding the GV at four of the six monitoring sites. Alkalinity was generally higher at each site in 2020 than in 2021, and only at two downstream sites in Autumn 2021 (Pool 16 and GRQ18) did alkalinity fall below a bicarbonate trigger value previously derived by the Office for Environmental Heritage (OEH, 2012) of 225 mg/L for 95% species protection (noting this was based on North American acute ecotoxicity data with an applied acute-to-chronic ratio (ACR), and applicability for lowland rivers is not known).

For copper analyses, the concentration exceeded the GV at all discharge monitoring sites except at GRQ18 in Autumn and Spring 2020. In 2021, however, copper concentrations exceeded GV in Spring (with the exception of GRQ18) but not at any sites in Autumn.

Similarly, the GV for nickel was also usually exceeded at all discharge monitoring sites, in both 2020 and 2021 with the exception of Autumn 2021.

Conductivity, pH, alkalinity, aluminium, copper, and to a lesser extent, nickel, as well as all measures of nitrogen decreased with increasing distance from the discharge source at LDP10. The results for nitrogen, nickel and copper can partly be explained by rainfall variations, particularly the elevated rainfall that occurred during Autumn 2021. For aluminium, however, the results cannot be explained by the increased rainfall in Autumn 2021 and the reason for the elevated levels is unclear. Aluminium is relatively insoluble at pH 6 to 8, with the solubility of aluminium increasing under more acidic and more alkaline conditions, in the presence of complexing ligands, and at lower temperatures (Driscoll and Postek, 1996). The uptake and toxicity of aluminium in freshwater species also generally decreased with increasing water hardness (ANZG, 2018). This is recognised in different GVs for aluminium in freshwaters with a pH >6.5 (55 µg/L) and waters with a pH <6.5 (interim GV of 0.8 µg/L, although this is of low reliability) (ANZG, 2018).

Zinc concentrations were erratic across sites, with GV exceedances observed in both reference sites and discharge monitoring sites, with no relation to sampling occasion, or distance from discharge. Zinc concentrations were consistently above the GV (8 µg/L) in GRQ1 (17- 11µg/L) and

mostly above the GV for GRUFS (14 -<5µg/L). Zinc concentrations were higher in the references sites than some discharge monitoring sites. The source of zinc at the reference sites is unknown. The highest concentration of zinc was detected in Autumn 2021 at Point 12 when it was five times higher than the GV, but on that same sampling occasion no zinc was detected at the discharge site Point 10. These erratic zinc concentrations may be due to sample handling in the field, and it is recommended that field and trip blanks be used in future samplings to rule out the possibility of sample contamination during sampling and handling (e.g., field filtration).

The quality of the waters discharged from the new temporary WTP at LDP40 was similar to that measured at the reference sites, with the exception of pH and alkalinity, which were generally higher in water from LDP40. In comparison to all discharge and downstream sites, water from LDP40 was of higher quality, however, the pH was above the upper GV on all except three occasions, and conductivity fell below the lower GV on three occasions.

While the water collected at Point 10 includes discharges from both LDP10 and LDP40, the contribution from LDP40 was 0.8-2.2% of the total discharge volume (Figure 9). LDP40 came online on 26$^{th}$ May 2021 (Figure 8) after the Autumn sampling for 2021 was already completed. The reason for improved water quality (reduction in some metals) at all sites in Autumn 2021 was most likely due to increased rainfall that was flushing the system at the time, indicated by the increase in pool levels, water flow and rainfall during the Autumn 2021 sampling period, compared to those in Spring 2021 (Figure 6 and Figure 7).

**Table 5. Summary of water quality measurements taken alongside macrobenthic surveys in 2020**

| | | | Autumn 2020[a] | | | | | | | | | Spring 2020 | | | | | | | | |
|---|---|---|---|---|---|---|---|---|---|---|---|---|---|---|---|---|---|---|---|---|
| | | ANZG (2018) | Reference | | | Discharge monitoring | | | | | | Reference | | | Discharge monitoring | | | | | |
| Analyte | Units | Guideline | GRQ1 | GRUFS | Point 11 | Point 10 | Point 12 | Jutts | Pool 16 | Pool 32 | GRQ18 | GRQ1 | GRUFS | Point 11 | Point 10 | Point 12 | Jutts | Pool 16 | Pool 32 | GRQ18 |
| pH | pH Unit | 6.5-8 | 6.79 | 6.72 | 7.19 | **8.77** | **8.63** | **8.71** | **8.73** | **8.68** | **8.16** | **4.9** | **6.23** | 7.05 | **8.72** | **8.79** | **8.61** | **8.79** | **8.67** | 7.63 |
| Conductivity | µS/cm | 125-2200 | 190 | 196 | 211 | 1860 | 1680 | 1670 | 1650 | 1500 | 1270 | 177 | 167 | 229 | 1750 | 1010 | 1140 | 1420 | 1270 | 951 |
| Bicarbonate Alkalinity | mg/L | NV[bc] | 2 | <1 | 21 | 790 | 628 | 661 | 589 | 613 | 521 | 5 | 2 | 21 | 791 | 274 | 586 | 723 | 636 | 504 |
| Aluminium | µg/L | 55 | 10 | <10 | 50 | **310** | **280** | **290** | **210** | **100** | **80** | 10 | 10 | **70** | **340** | **100** | **160** | **140** | **60** | <10 |
| Cobalt | µg/L | 1 | <1 | <1 | <1 | <1 | <1 | <1 | <1 | <1 | 1 | 1 | <1 | <1 | **2** | <1 | <1 | 1 | <1 | <1 |
| Copper | µg/L | 1.3 | <1 | <1 | <1 | **3** | **3** | **2** | **3** | **2** | 1 | <1 | <1 | <1 | **6** | **2** | **3** | **3** | **2** | <1 |
| Nickel | µg/L | 11 | 2 | 2 | <1 | **26** | **23** | **23** | **26** | **24** | **21** | 2 | 1 | <1 | **25** | 7 | **16** | **19** | **18** | **16** |
| Zinc | µg/L | 8 | **17** | **12** | <5 | <5 | 7 | <5 | <5 | <5 | <5 | **17** | **10** | <5 | 8 | <5 | <5 | **11** | 8 | <5 |
| Nitrite + Nitrate (NOx) | µg/L | 40 | 7 | <2 | 3 | 605 | 501 | 508 | 369 | 197 | 63 | <10 | <10 | 30 | 60 | 20 | 30 | 10 | <10 | 40 |
| Total Kjeldahl Nitrogen | µg/L | NV | <50 | <50 | 90 | 360 | 140 | 120 | 180 | 200 | 140 | 100 | 100 | 100 | 200 | 200 | 200 | 100 | 100 | 200 |
| Total Nitrogen | µg/L | 500 | <10 | <10 | 90 | **960** | **640** | **630** | **550** | 400 | 200 | 100 | 100 | 100 | 300 | 200 | 200 | 100 | 100 | 200 |

[a] In Autumn 2020, no field data was available from South32 for pH and conductivity, therefore lab measurements of these parameters (analysed up to one day later) were used instead. Lab measurements differed by 0- 1.7 pH units and 7-410 µS/cm from field measurements across all other samples.

[b] NV = No ANZG (2018) guideline value available.

[c] Although no guideline value available, Vera et al. (2014) reported a bicarbonate EC10 for 7-d reproduction in the local Australian isolate of *C.* cf. *dubia* of 340 mg/L, and the Office for Environmental Heritage (2012) calculated an interim trigger value to use for bicarbonate of 225 mg/L, based on acute North America freshwater data with an acute to chronic ratio applied.

**Table 6. Summary of water quality measurements taken alongside macrobenthic surveys in 2021**

| | | | Autumn 2021[a] | | | | | | | | | Spring 2021 | | | | | | | | |
|---|---|---|---|---|---|---|---|---|---|---|---|---|---|---|---|---|---|---|---|---|
| | | ANZG (2018) | Reference | | | Discharge monitoring | | | | | | Reference | | | Discharge monitoring | | | | | |
| Analyte | Units | Guideline | GRQ1 | GRUFS | Point 11 | Point 10 | Point 12 | Jutts | Pool 16 | Pool 32 | GRQ18 | GRQ1 | GRUFS | Point 11 | Point 10 | Point 12 | Jutts | Pool 16 | Pool 32 | GRQ18 |
| pH | pH Unit | 6.5-8 | **6.12** | **6.06** | 7.01 | **8.67** | **8.59** | **8.57** | **8.22** | **8.25** | 7.94 | 6.51 | **6.35** | 6.84 | **8.86** | **8.62** | **8.92** | **8.87** | **8.49** | 8 |
| Conductivity | µS/cm | 125-2200 | **116** | **117** | **123** | 951 | 667 | 713 | 431 | 549 | 445 | 192 | 175 | 188 | 1370 | 1030 | 985 | 943 | 802 | 818 |
| Bicarbonate Alkalinity | mg/L | NV[bc] | 4 | 4 | 7 | 500 | 333 | 343 | 191 | 259 | 174 | 8 | 4 | 14 | 559 | 453 | 450 | 420 | 348 | 321 |
| Aluminium | µg/L | 55 | **130** | **130** | **140** | **440** | **310** | **300** | **190** | **270** | **240** | 20 | 10 | **130** | **130** | **90** | **110** | **70** | 50 | 30 |
| Cobalt | µg/L | 1 | <1 | <1 | <1 | <1 | <1 | <1 | <1 | <1 | <1 | <1 | <1 | <1 | <1 | 1 | <1 | <1 | <1 | <1 |
| Copper | µg/L | 1.3 | <1 | <1 | <1 | <1 | <1 | <1 | <1 | 1 | 1 | <1 | <1 | <1 | **4** | **5** | **3** | **2** | **1** | <1 |
| Nickel | µg/L | 11 | <1 | <1 | <1 | 7 | 6 | 7 | 4 | 5 | 5 | 2 | 1 | <1 | **19** | **14** | **14** | **13** | **11** | **12** |
| Zinc | µg/L | 8 | **11** | <5 | **11** | <5 | **41** | **15** | <5 | 8 | **10** | **16** | **14** | **9** | 6 | 5 | **10** | <5 | 6 | 8 |
| Nitrite + Nitrate (NOx) | µg/L | 40 | <10 | <10 | 20 | 280 | 180 | 190 | 110 | 140 | 90 | 10 | 20 | <10 | 30 | 120 | 120 | 50 | <10 | 50 |
| Total Kjeldahl Nitrogen | µg/L | NV | <100 | 200 | 100 | 300 | 400 | 300 | 200 | 300 | 200 | <100 | <100 | 200 | 400 | 200 | 200 | 100 | 200 | <100 |
| Total Nitrogen | µg/L | 500 | <100 | 200 | 100 | **600** | **600** | 500 | 300 | 400 | 300 | <100 | <100 | 200 | 400 | 300 | 300 | 200 | 200 | <100 |

[a] In Autumn 2020, no field data was available from South32 for pH and conductivity, therefore lab measurements of these parameters (analysed up to one day later) were used instead. Lab measurements differed by 0- 1.7 pH units and 7-410 µS/cm from field measurements across all other samples.

[b] NV = No ANZG (2018) guideline value available

[c] Although no guideline value available, Vera et al. (2014) reported a bicarbonate EC10 for 7-d reproduction in the local Australian isolate of *C.* cf. *dubia* of 340 mg/L, and the Office for Environmental Heritage (2012) calculated an interim trigger value to use for bicarbonate of 225 mg/L, based on acute North America freshwater data with an acute to chronic ratio applied.

**Table 7. Summary of water quality measurements taken from LDP40 (end of pipe) in 2021**

| Analyte | Units | ANZG (2018) Guideline | Discharge monitoring at LDP40, 2021 | | | | | | | |
|---|---|---|---|---|---|---|---|---|---|---|
| | | | May | June | July | August | September | October | November | December |
| pH | pH Unit | 6.5-8 | **8.38** | 7.72 | 7.40, **8.15** | **8.10, 8.90, 8.24** | NM[a] | 7.85 | **8.10, 8.5** | **8.43** |
| Conductivity | µS/cm | 125-2200 | 184 | 164 | **97** | 149, 178 | NM | 125 | **122,** 144 | 144 |
| Bicarbonate Alkalinity | mg/L | NV[bc] | 81 | 83 | 64 | 97, 102 | NM | 78 | 70, 81 | 76 |
| Aluminium | µg/L | 55 | NM | <10 | <0.2 | 0.3, 0.4 | NM | 0.6 | <0.2, <10 | 0.6 |
| Cobalt | µg/L | 1 | <0.1 | <1.0 | <0.02, <0.02 | 0.02, <0.02 | NM | <0.02 | <0.02, <1 | <0.02 |
| Copper | µg/L | 1.3 | <0.5 | <1.0 | <0.05, 0.15 | <0.05, <0.05 | NM | <0.05 | <0.05, <1.0 | <0.05 |
| Nickel | µg/L | 11 | NM | <1.0 | 0.8, 0.5 | 0.7, 0.8 | NM | 0.6 | 0.4, <1.0 | 0.4 |
| Zinc | µg/L | 8 | NM | 6.0 | 2.3, 6.4 | 1.2, 0.6 | NM | 0.5 | <0.5, <5 | 1.5 |
| Nitrite + Nitrate (NOx) | µg/L | 40 | 32 | 30 | 42, 40 | 12, 48 | NM | 18 | 28, <0.10 | 14 |
| Total Kjeldahl Nitrogen | µg/L | NV | NM | 400 | NM | NM | NM | NM | 300 | NM |
| Total Nitrogen | µg/L | 500 | 260 | 240, 400 | 310 | 410, 360 | NM | 350 | 230, 300 | 460 |

[a]NM = not measured.

## 3.3 Long term trends in water chemistry (2013-2021)

In this section, we describe the long-term (2013-2021) trends in the key water quality variables: pH, conductivity, aluminium, nickel, zinc and total nitrogen. Across all sites and years (2013 to 2021), the measured parameters of pH, conductivity, aluminium, nickel, zinc and total nitrogen were generally lower at reference sites than at the discharge monitoring sites. Long term trends observed with respect to time and to distance from the discharge source at LDP10 varied for different parameters.

Waters collected from the discharge monitoring sites were consistently higher in pH than those from the reference sites (Figure 12). The reference site GRQ1 and GRUFS have, on occasions been below the ANZG (2018) lower GV for pH while Point 11 has predominantly been within the range of pH GVs (6.2-8) over time. The pH of waters from discharge monitoring sites frequently fell outside the ANZG (2018) GV range of 6.5 – 8. However, the most downstream discharge monitoring site (GRQ18) generally had lower pH values than the other sites in this treatment, and on six (of fifteen) occasions (including the two most recent samplings in 2021) were within the acceptable pH range (6.5-8 GV). The pH of waters in pools at the source of discharge (LDP10) consistently exceeded the upper pH ANZG (2018) GV of 8, and throughout 2016-2018, the pH was greater than 9. Since that time, there has been a slight reduction in pH at Point 10 from 2019 to 2021 (8.7). In general, there was no clear overall decline in pH over time within the discharge monitoring treatment, but certainly pH decreased with increasing distance from Point 10 on each sampling occasion.

In recent years, the conductivity of waters at the discharge monitoring sites (Figure 12) has been within the ANZG (2018) GV range for lowland east coast rivers (125-2,200 µS/cm). However, it was markedly higher in the discharge monitoring sites compared to the reference sites (Figure 13). There was an overall decline in conductivity with increasing distance downstream from Point 10. In addition, conductivity has declined over time in all discharge monitoring sites.

Aluminium concentrations were consistently elevated at all discharge monitoring sites (Figure 14). While measurements varied over time, there have been consistently higher aluminium concentrations in discharge monitoring sites compared with reference sites. The upper discharge monitoring sites (Point 10 and Point 12) had higher concentrations of aluminium than the sites further from the discharge source (GRQ18). While measurements varied over time, concentrations

of aluminium generally declined with downstream distance. On some occasions (e.g., Spring 2021), aluminium exceeded the guideline value in the reference sites (Figure 14).

Cobalt and copper concentrations have declined over time at the discharge monitoring sites. Waters from all sites in the final sampling occasion of Spring 2021, contained concentrations that were at or below GVs. This is in contrast to samples collected in 2013 when concentrations were up to 8 (copper) and 20 (cobalt) fold higher (Figure 15) and (Figure 16). Note that at some sites (Point 10 and Point 12), copper concentrations have been slightly erratic, but the overall trend has still been that of decline over time at each site. Concentrations of these metals also declined with increasing distance from Point 10, and in earlier years (2013 to 2018) were higher than those at reference sites. In Autumn and Spring 2019, waters sampled from the reference sites GRQ1 and GRUFS contained very high concentrations of nickel (Figure 17), but these had dropped in 2020 and 2021 to below GVs. Overall, nickel concentrations declined over time in all discharge monitoring sites.

In general, zinc concentrations have declined over time at discharge monitoring sites but have fluctuated somewhat at reference sites (Figure 18). The highest zinc concentrations at all discharge monitoring sites were observed in 2019 (up to 10-fold above the GV) but have since fallen in 2020 and 2021 to levels sometimes below the GV.

There is a clear difference in total nitrogen concentrations in reference sites and discharge monitoring sites across all years (Figure 19). In recent years (2019-2021), total nitrogen concentrations for all sites were generally below the GV. For the discharge monitoring sites there was a general decline in total nitrogen with distance from the discharge source, with Point 10 generally containing higher concentrations of total nitrogen compared to GRQ18 (8km from Point 10).

There has been some improvement to water quality over time at discharge monitoring sites, with conductivity, and concentrations of copper, cobalt and nickel generally decreasing over time. Indeed, with the exception of nickel, these parameters fell within the acceptable ANZG (2018) GV range in 2021 at several discharge monitoring sites, particularly those furthest from LDP10 and LDP40 discharge points. For pH, and concentrations of aluminium, zinc and nitrogen, however, there were no clear trends with respect to time, and continued exceedances of GVs for these parameters indicate that the combined water quality at the discharge monitoring sites

(particularly those closest to the source) is contaminated and has potential to cause biological and ecological impacts.

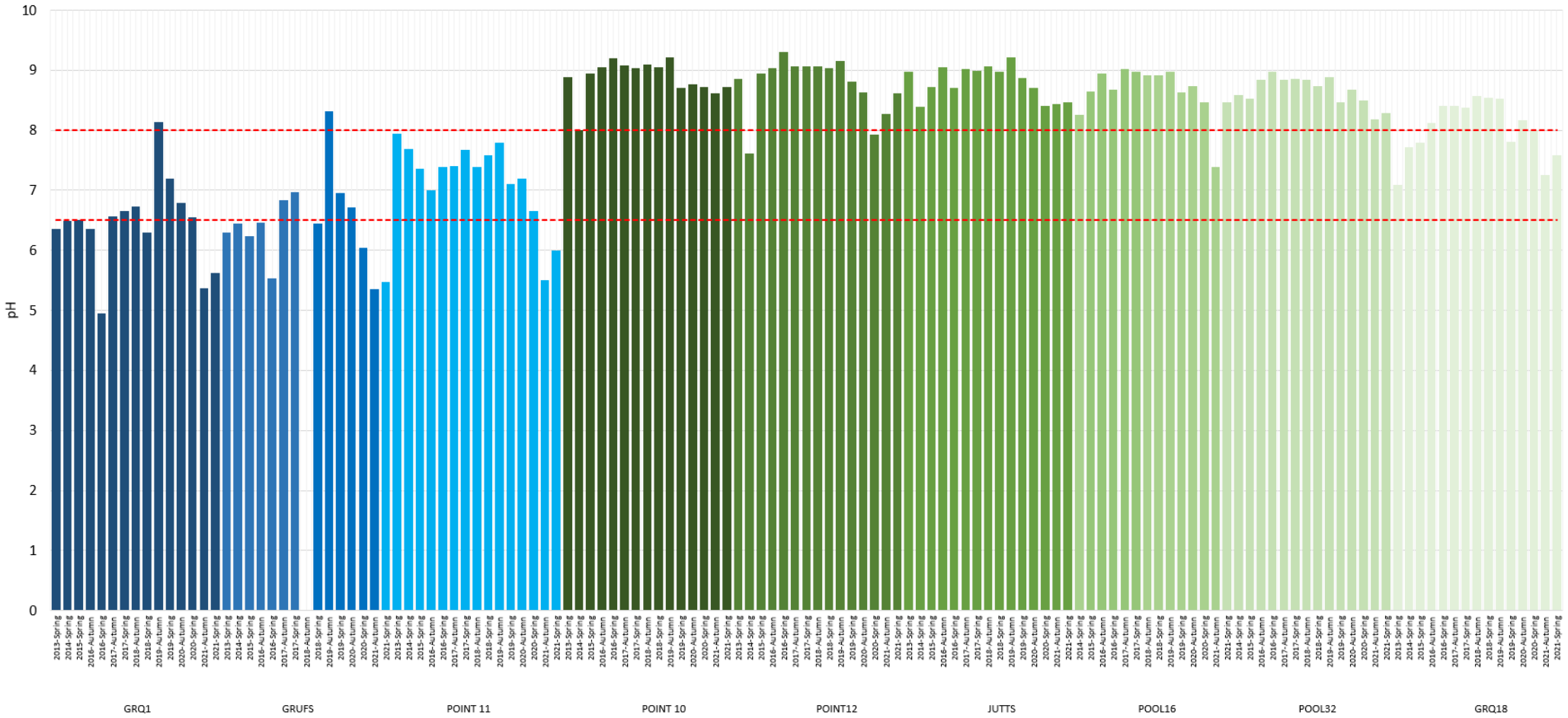


**Figure 12. Long-term trends in pH.**

Reference sites (blue) and discharge monitoring sites (green). Dotted red lines represent the upper and lower ANZG (2018) guideline value for lowland rivers.

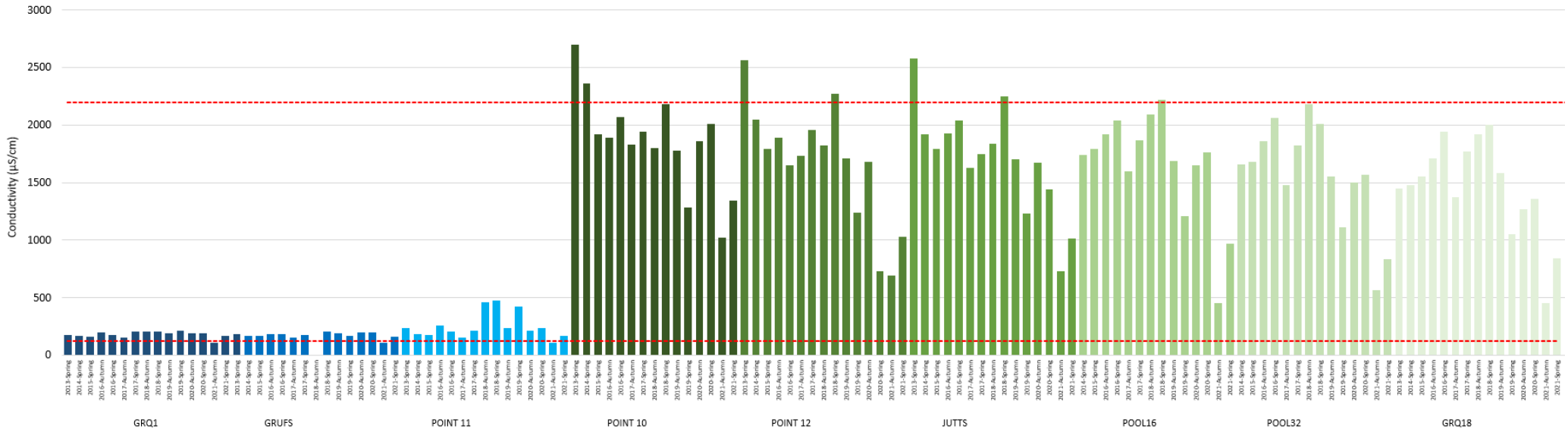


**Figure 13. Long-term trends in conductivity.**

Reference sites (blue) and discharge monitoring sites (green). Dotted red lines represent the upper and lower ANZG (2018) guideline value for conductivity in lowland rivers.

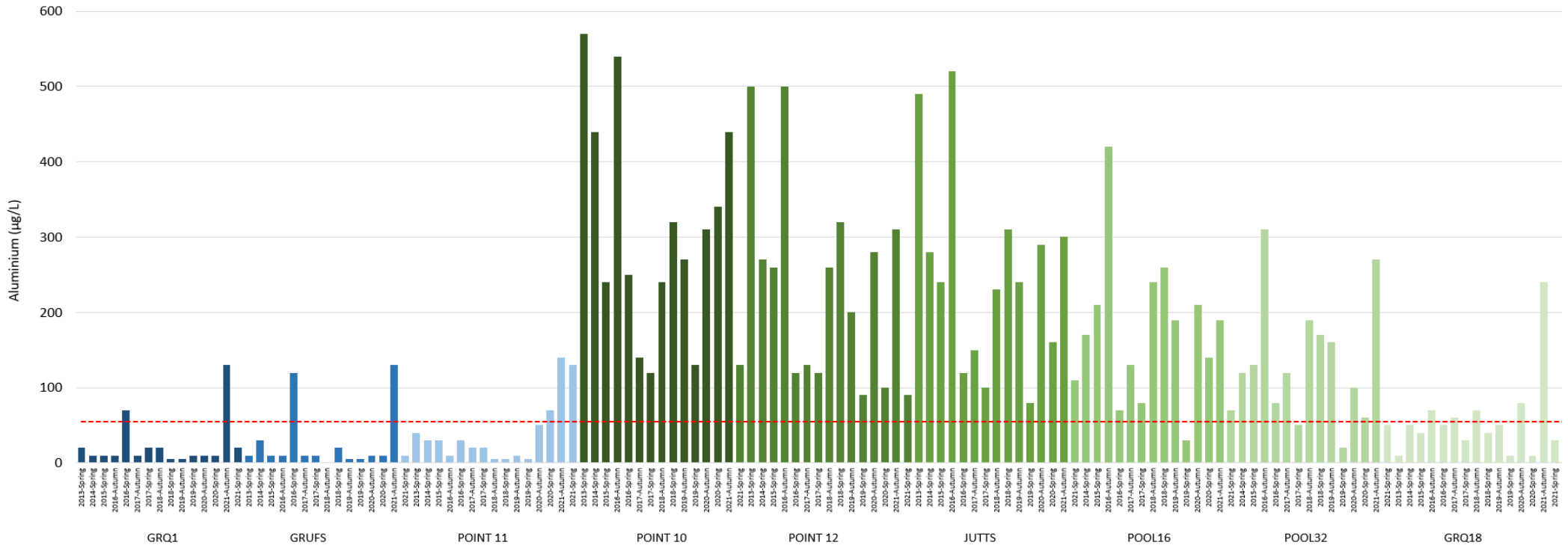


**Figure 14. Long-term trends in aluminium concentrations.**

Reference sites (blue) and discharge monitoring sites (green). Dotted red lines represent the ANZG (2018) guideline value.

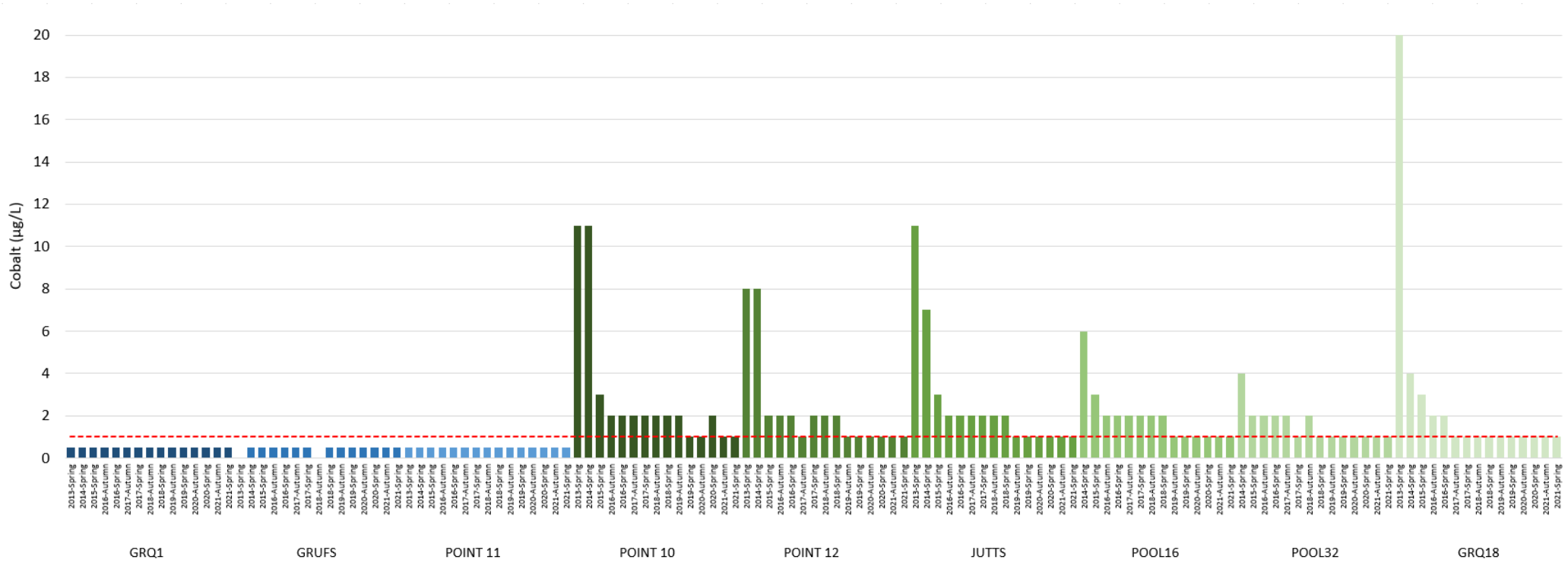


**Figure 15. Long-term trends in cobalt concentrations.**

Reference sites (blue) and discharge monitoring sites (green). Dotted red lines represent the ANZG (2018) guideline value.

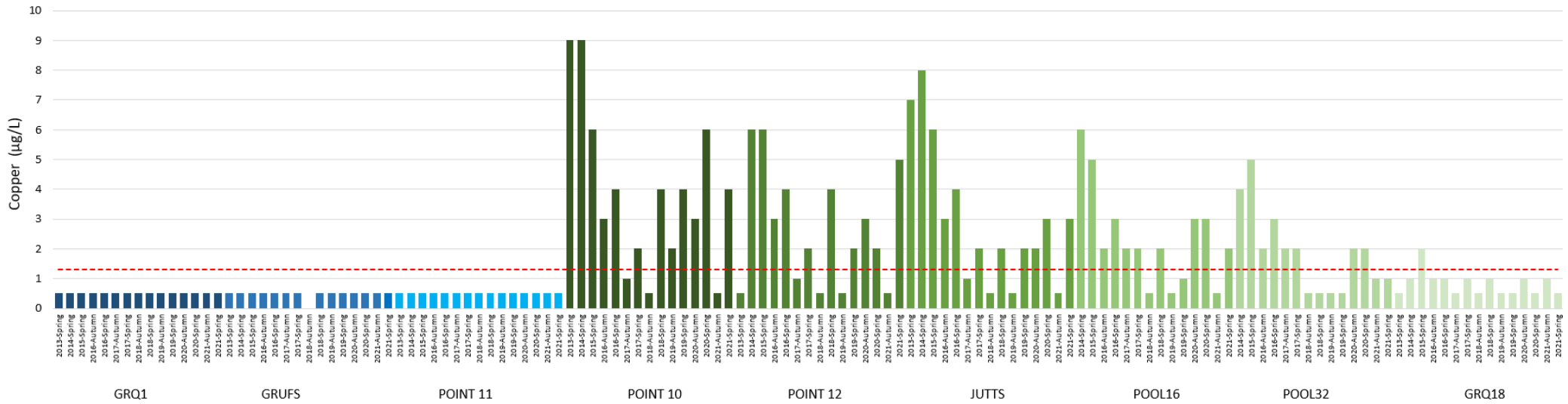


**Figure 16. Long-term trends in copper concentrations.**

Reference sites (blue) and discharge monitoring sites (green). Dotted red lines represent the ANZG (2018) guideline value.

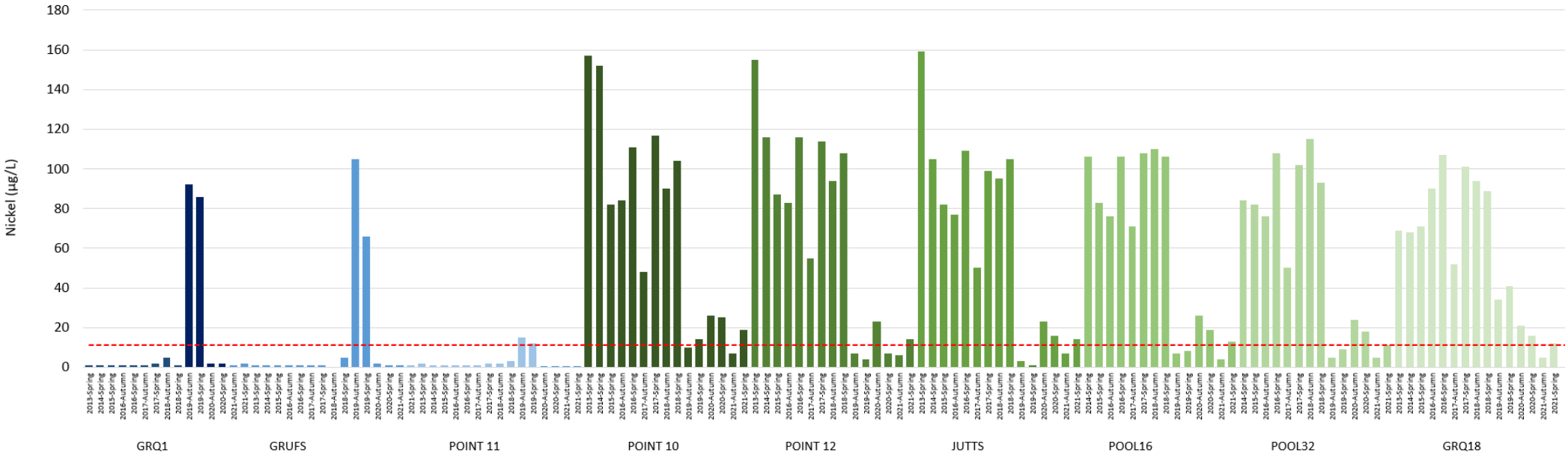


**Figure 17. Long-term trends in nickel concentrations.**

Reference sites (blue) and discharge monitoring sites (green). Dotted red lines represent the ANZG (2018) guideline value.

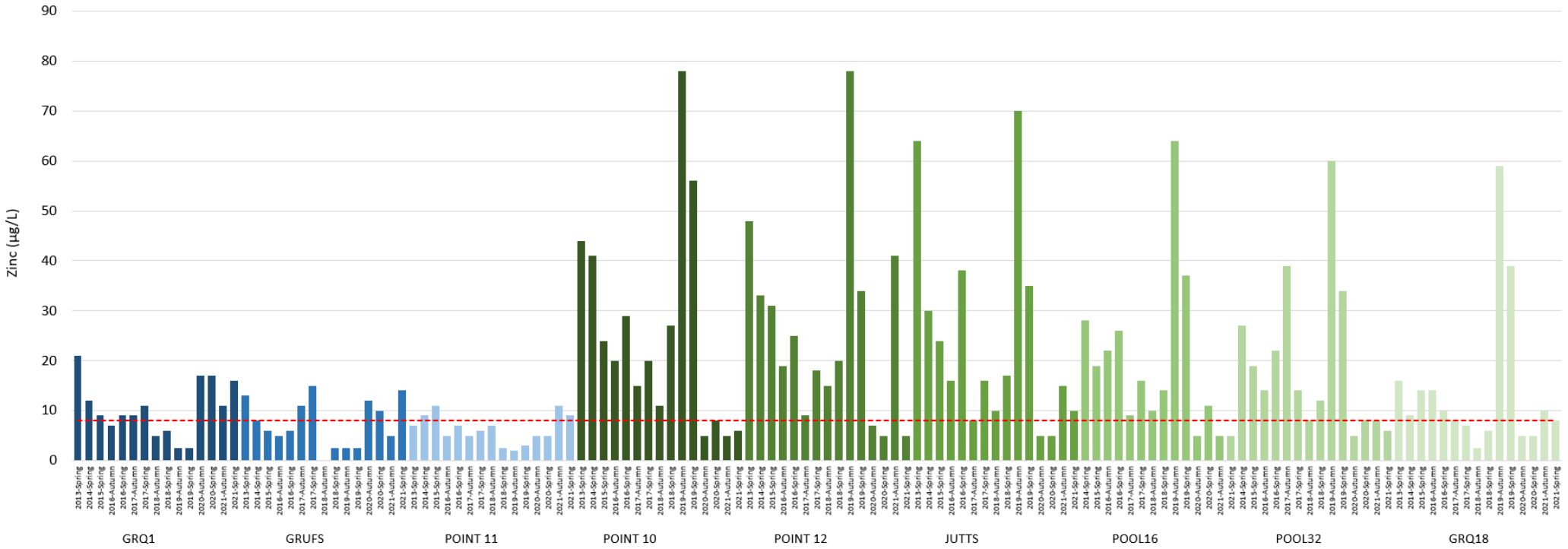


**Figure 18. Long-term trends in zinc concentrations.**

Reference sites (blue) and discharge monitoring sites (green). Dotted red lines represent the ANZG (2018) guideline value.

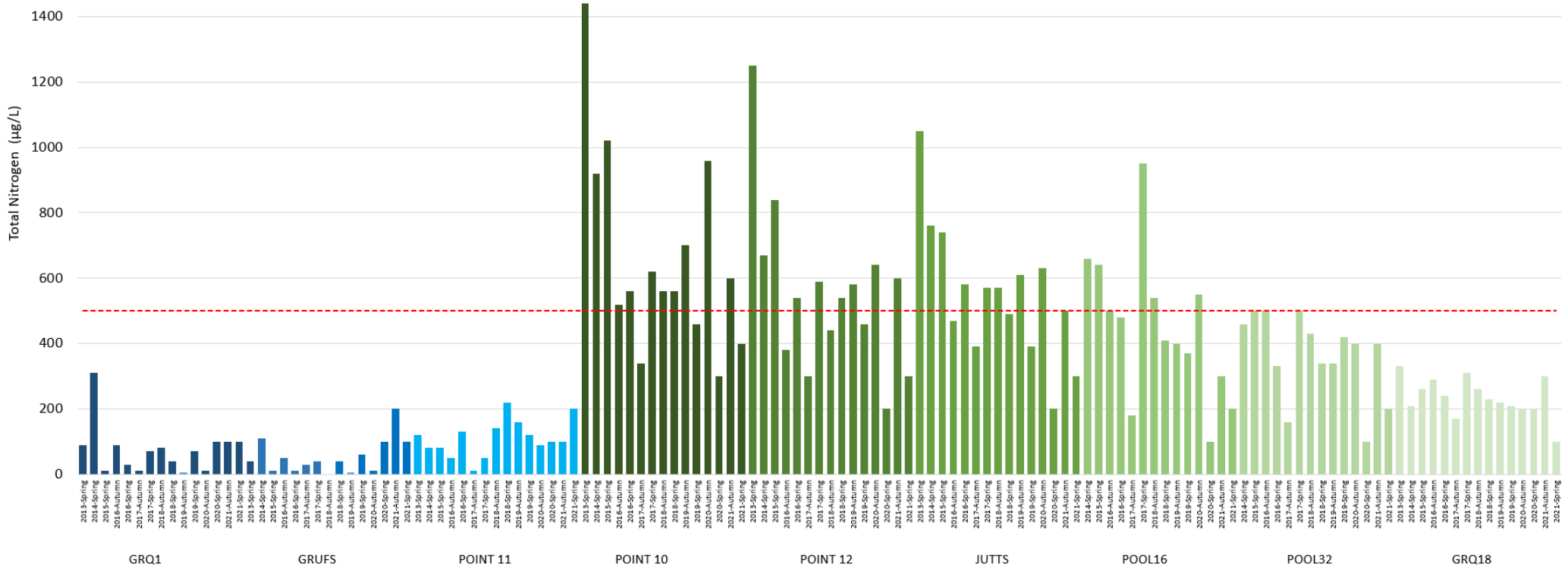


**Figure 19. Long-term trends in total nitrogen concentrations.**

Reference sites (blue) and discharge monitoring sites (green). Dotted red lines represent the ANZG (2018) guideline value.

## 3.4 Ecotoxicity tests for LDP10 and LDP40 (2021)

### 3.4.1 Ecotoxicity tests in 2021

Results of the chronic *Ceriodaphnia dubia* reproduction and 7-d survival tests, and acute 96-h larval imbalance tests with the fish *Melenotaenia splendida* are presented in Table 8 and Appendix A.

Water from LDP10 was not toxic to *C. dubia* reproduction and survival in February 2021 and May 2021 (EC10>100%). It was also not toxic to *M. splendida* larval imbalance in May, August, and November 2021. Acute fish toxicity could not be determined in February because the incorrect fish ecotoxicity test was used (12-d rainbowfish embryo development was used instead of 4-d larval imbalance). No toxicity was observed of LDP10 to the 12-d embryo test. While the 12-d embryo and 4-d larval tests cannot be used interchangeably, given the lack of toxicity observed to the 12-d embryo test, and the lack of toxicity observed also to *C. dubia* (which to date has rarely been less sensitive to LDP10 than the 4-d larval imbalance test), it is likely that the February LDP10 sample would have been non-toxic to the 4-d larval imbalance test, had it been tested.

Toxicity to *C. dubia* reproduction and survival was observed in August and November 2021 with reproduction being the more sensitive (more toxic) endpoint. For each *C. dubia* test endpoint (reproduction and survival), similar toxicity was observed in the August and November 2021 water samples (reproduction EC10 = 48% and 23% respectively, survival EC10 = 61% and 50%, respectively).

Water from LDP40 was not toxic to *M. splendida* larval imbalance over the three samplings following commissioning of the RO WTP at Appin North (May, August, and November EC10 >100%). Toxicity to *C. dubia* was observed in May (reproduction only, EC10 = 68%) and August (reproduction and survival, EC10 = 30% and 36% respectively). No toxicity was observed to *C. dubia* and *M. splendida* in November 2021.

All ecotoxicity tests met their respective quality assurance and quality control criteria. Where samples showed no or low toxicity, concentration-response curves were poor with no or one partial response, resulting in potentially unreliable EC10 values. However, the similar trend in NOECs and EC10 values in this study (Appendix A) provided confidence that the EC10 values quoted here are sufficiently reliable to enable informed water management decisions. In future

testing, modification of ecotoxicity test design (i.e., modifying the concentration series tested) could improve the reliability of the EC10 values.

Toxicity tests with rainbowfish larvae were done without water renewal, based on advice from ESA that this species cannot tolerate excessive handling. There is a concern that without water renewals, that excessive degassing can occur, altering the toxicity of the sample. Degassing would be indicated by an increase in pH of the sample during the test exposure period.

Ecotoxicity tests using *C. dubia* were more sensitive to LDP10 and LDP40 waters than those conducted using fish, with *C. dubia* identifying toxicity in four samples, whereas fish tests did not detect toxicity to any samples tested in 2021. Fish tests were conducted without renewals since the additional handling required for renewing test solution with these larvae would have caused high mortalities in controls (Rick Krassoi, ESA, pers. comm). Renewal of water in toxicity tests prevents degassing of waters, indicated by an increase in sample pH throughout the duration of the toxicity test. CSIRO requested the pH, conductivity, and dissolved oxygen measurements from ESA for each fish test, to check for evidence of degassing. Only one dataset was provided, for samples tested in November 2021. In this dataset, the pH change in *C. dubia* test solutions, which were renewed daily were typically within 0.1 pH unit. In comparison, the fish test solutions, which were not renewed, were also typically within 1 pH unit of that measured at the time of test commencement. This suggests that degassing in these solutions were minimal. Further assessment of the pH data for the other toxicity tests completed in 2021, could help confirm this. It is possible that if methods were improved in future (will require additional ecotox test work to set up methods) to enable renewals to occur that fish tests may become more effective at detecting toxicity. This is because renewal of test solutions (as occurs daily in the *C. dubia* test) minimises degassing and associated pH increases from occurring, which otherwise impact on the bioavailability of some toxicants.

The assessment criteria with respect to ecotoxicity at LDP10 were exceeded on two of the four sampling occasions (August and November) in 2021 with toxicity (EC10<100%) to *C. dubia* observed on each of those occasions. Based on an assessment of key measured water quality parameters, this toxicity was likely due to elevated metals and alkalinity. In comparison, water discharged from the new WTP at LDP40 was toxic to *C. dubia* in May and August, and toxicity was likely due to low conductivity (major ion imbalance). The alignment of sampling for water quality and ecotoxicity in 2021 has been an improvement to the program, compared to previous years,

allowing better cross comparison of key drivers to toxicity. The continuation of this approach will allow for longer term trends to be identified.

Overall, based on the ecotoxicity line of evidence, the discharges from LDP10 and LDP40 had the potential to negatively impact ecosystems in the receiving environment through biological effects on organisms.

**Table 8. Ecotoxicity of waters from LDP40 and LDP10 in 2021**

| Month | Site: | LDP10 | | | LDP40 | | |
|---|---|---|---|---|---|---|---|
| | Species: | *C. dubia* | | *M. splendida* | *C. dubia* | | *M. splendida* |
| | Endpoint: | Reproduction | Survival | Imbalance | Reproduction | Survival | Imbalance |
| **February** | **Toxic** | Not toxic | Not toxic | NT, but not toxic to 12-d embryo test | NT[a] | NT | NT |
| | **EC10 (%)** | >100 | >100 | NT, but EC10>100% to 12-d embryo test | NT | NT | NT |
| **May** | **Toxic** | Not toxic | Not toxic | Not toxic | Toxic | Not toxic | Not toxic |
| | **EC10 (%)** | >100 | >100 | >100 | 68 (57-73)[b] | >100 | >100 |
| **August** | **Toxic** | Toxic | Toxic | Not toxic | Toxic | Toxic | Not toxic |
| | **EC10 (%)** | 48 (10-55) | 61 (50-81) | >100 | 30 (28-33) | 36 (31-50) | >100 |
| **November** | **Toxic** | Toxic | Toxic | Not toxic | Not toxic | Not toxic | Not toxic |
| | **EC10 (%)** | 23 (17-52) | 50 (23-81) | >100 | >100 | >100 | >100 |

[a] NT = Not tested
[a] 95% confidence limits in parentheses

### 3.4.2 Water quality parameters and comparison to ecotoxicity test results (2021)

The water quality parameters measured in the LDP10 and LDP40 water samples used for ecotoxicity testing (and collected from end of pipe) are shown in Table 9 and Appendix A (Table A.1).

The pH of LDP10 water exceeded the ANZG (2018) upper GV for lowland rivers (pH 8) in all four samples by up to 0.8 pH units (pH 8.5 to 8.8). Conductivity was 1460 to 1790 µS/cm, within the ANZG (2018) GV range (125 to 2200 µS/cm). Bicarbonate alkalinity (referred to from here on as alkalinity) was similar on three samplings (730 to 786 mg $CaCO_3$/L) and lower in August (107 mg $CaCO_3$/L). No GVs are provided for alkalinity, however Vera et al. (2014) derived an EC10 for chronic 7-d *C. dubia* (Australian isolate, i.e., same clone used in the current study) reproduction of 340 mg/L and the Office for Environmental Heritage has previously derived a trigger value for alkalinity of 225 mg/L (95% species protection) using acute North America freshwater data with an acute to chronic ratio applied (OEH, 2012). Therefore, the samples collected in February, May and November 2021, had alkalinity levels that were above those deemed to be potentially harmful to freshwater organisms. Concentrations of five metals, as dissolved fractions (0.45 µm filterable) representing the more bioavailable metal concentrations, (rather than particulate metal), exceeded their respective GVs in LDP10 water on at least one occasion. Aluminium concentrations exceeded the GV (55 mg/L) on all four samplings (60 to 883 mg/L). Nickel and zinc concentrations exceeded GVs by about a factor of two in February and May 2021(25 and 17 mg Ni/L), and February (25 mg Zn/L) respectively. Copper concentrations exceeded the GV of 1.3 mg Cu/L on three samplings (up to 3 mg Cu/L) and cobalt concentrations exceeded the GV (1 mg Co/L) on one occasion (2 mg Co/L).

The pH of LDP10 water was lower in May 2021(7.3), and within the ANZG (2018) pH GV range, compared to August and November 2021 samples (pH 8.1) which only just exceeded the upper pH GV range of 8. All LDP40 samples had a lower pH than the LDP10 samples. Conductivity was at least ten times lower in LDP40 samples (118, 115 and 144 µS/cm) compared to LDP10 samples with both the May and August 2021 samples falling below the lower conductivity limit. Alkalinity was also about ten times lower at LDP40 (63, 75 and 81 mg $CaCO_3$/L) compared to LDP10 (730 and 786 mg $CaCO_3$/L), with the exception of the August 2021 sample which had an alkalinity of 107 mg $CaCO_3$/L. Unlike LDP10, none of the five metals (as dissolved concentrations) measured at LDP40 exceeded their respective GVs and were below the limits of detection (except when even lower limits of detection were used in the August sampling). These results indicate that the RO WTP is

removing metals and salts (major ions) from the discharge water resulting in waters at LDP40 with lower pH, lower conductivity, alkalinity and metal concentration well below GVs.

The pH, conductivity, alkalinity and dissolved aluminium concentrations were always higher at LDP10 compared to LDP40 (n = 3). There were no clear trends in toxicity and key water quality parameters (Appendix A, Figure A.1). For example, the sample that had the most key parameters exceeding the GVs, (February 2021 from LDP10), was not toxic to cladocerans and fish. The high aluminium concentrations in the LDP10 August sample may be contributing to toxicity in this sample, however similar toxicity was observed in the November 2021 sample when aluminium concentrations were lower, suggesting that aluminium alone is unlikely to be the only cause of toxicity. Measuring the sensitivity of *C. dubia* reproduction and survival to aluminium would assist to determine if aluminium is contributing to toxicity in these samples. Despite low metal concentrations in LDP40 samples, the May and August 2021 samples were toxic to *C. dubia*. Of note is the low conductivity of these two samples (118 and 115 µS/cm), lower than the lower conductivity GV and also lower than the control water used in the *C. dubia* ecotoxicity test (172 µS/cm). Waters with appropriate conductivity, major ions and their composition, play a crucial role in providing a healthy habitat for aquatic organisms. The RO water entering LDP40 may be lacking in essential major ions and causing stress (toxicity) to *C. dubia*. The conductivity of water in the November sample of 144 µS S/cm was high enough to not cause stress (toxicity) to *C. dubia* reproduction and survival. While the pH of LDP40 waters was commonly higher than the upper GV, they were similar to those in the DMW controls (Table 9) and are therefore unlikely to be the cause of toxicity in this study. However, pH plays an important role in the speciation and therefore bioavailability and resulting toxicity of metals to aquatic organisms.

Based on this study, metal concentrations and alkalinity at LDP10 and low conductivity (major ions) at LDP40 are likely to be contributing to the observed toxicity to *C. dubia*. Ecotoxicity to fish was not observed in any of the samples collected from LDP10 and LDP40.

Table 9. Water quality parameters for LDP10 and LDP40 samples used in ecotoxicity testing in 2021.

| Analyte | Units | Guideline Value [a] | Feb-21 | May-21 | May-21 | Aug-21 | Aug-21 | Nov-21 | Nov-21 | Ecotoxicity Test Control Water |
|---|---|---|---|---|---|---|---|---|---|---|
| | | | LDP10 | LDP10 | LDP40 | LDP10 | LDP40 | LDP10 | LDP40 | DMW [e] |
| pH | pH Unit | 6.5-8 | 8.7 | 8.5 | 7.3 | 8.8 | 8.1 | 8.7 | 8.1 | 8.1-8.2 |
| Conductivity | µS/cm | 125-2200 | 1730 | 1460 | 118 | 1790 | 115 | 1730 | 144 | 172-176 |
| Bicarbonate Alkalinity | mg/L | NV [c] | 786 | 730 | 63 | 107 | 75 | 780 | 81 | NT |
| Aluminium | µg/L | 55 | 60 | 300 | <10 | 883 | 1.3 | 340 | <10 | NT |
| Cobalt | µg/L | 1 | 1 | <1 | <1 | <1 | <0.02 | 2 | <1 | NT |
| Copper | µg/L | 1.3 | 2 | 2 | <1 | <1 | 0.15 | 3 | <1 | NT |
| Nickel | µg/L | 11 | 25 | 17 | <1 | 1 | 0.4 | 2.9 | <1 | NT |
| Zinc | µg/L | 8 | 25 | <5 | <5 | <5 | 1.2 | <5 | <5 | NT |
| Nitrite + Nitrate (NOx) | µg/L | NV | 40 | 310 | 30 | 140 | 0.013 | 40 | <10 | NT |
| Total Kjeldahl Nitrogen | µg/L | NV | 600 | 200 | 100 | 200 | NM[d] | 200 | 300 | NT |
| Total Nitrogen | µg/L | 500 | 600 | 500 | 100 | 300 | 390 | 200 | 300 | NT |
| Toxic to *C. dubia* | | | No | No | Yes | Yes | Yes | Yes | No | No |
| Toxic to *M. splendida* | | | No [b] | No | No | No | No | No | No | No |

Values outside of GV range appear in red.
Metal concentrations are dissolved (0.45 µm filterable).
[a] Water quality guidelines for pH, conductivity and total nitrogen for lowland rivers. Water quality guidelines for metals for 95% species protection for moderately-to-disturbed ecosystems.
[b] 12-d embryo test used instead of 4-d larval imbalance test
[c] No guideline value available in ANZG (2018). However, Vera et al. (2014) reported a bicarbonate EC10 for 7-d *C. dubia* (Australian isolate) of 340 mg/L, and the Office for Environmental Heritage (2012) calculated an interim trigger value for bicarbonate of 225 mg/L, based on acute North America freshwater data with an acute to chronic ratio applied, therefore values above 225 mg/L bicarbonate are likely to be harmful.
[d] NM = not measured.
[e] Dilute mineral water

## 3.5 Long term Ecotoxicology (LDP10 waters collected 2013 – 2021)

The ecotoxicity of LDP10 water has been measured using the chronic *C. dubia* reproduction and survival test and the acute *M. splendida* larval imbalance test from June 2013 to the most recent sampling even in November 2021 (Figure 20), with the exception that fish testing was not carried out during 2019. Also note that testing with other species in previous years are not captured on the graph in Figure 20.

Water from LDP10 was not toxic to rainbowfish larval imbalance in 2021, compared to previous years when of the twelve samples collected across 2013 to 2016, nine were toxic to larval imbalance. Toxicity of LDP10 to *C. dubia* survival and reproduction in 2021 was similar to those observed for previous years, except for two occasions (January 2014 and November 2017), when much higher (up to 6- and 7-fold) toxicity to reproduction was observed. It is not possible to determine whether these events of elevated toxicity were related to any specific toxicant or stress, since water quality parameters were not measured in the same samples collected for ecotoxicity testing, i.e., water quality data for those years were from samples taken at other times

during the year for the macrobenthic analysis. The alignment of sampling for water quality and ecotoxicity in 2021 has been an improvement to the program, allowing better cross comparison of key drivers to toxicity. The continuation of this approach will allow for longer term trends to be identified.

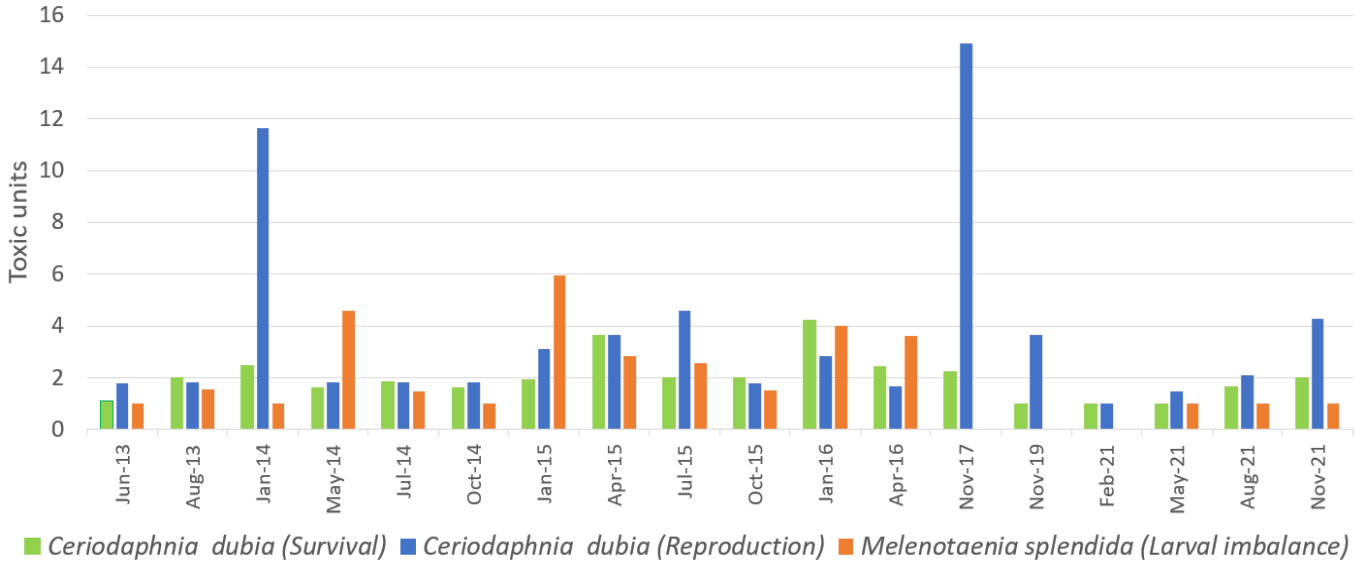


**Figure 20. Ecotoxicity of water from LDP10 to *Ceriodaphnia dubia* survival and reproduction and *Melenotaenia splendida* (Rainbow fish) larval imbalance from June 2013 to November 2021.**

Toxicity is presented as toxic units (100 ÷ EC10 value).

The ecotoxicological tests on the LDP10 discharge waters showed that historically the waters were toxic to *C. dubia* and *M. splendida*, but that there has been a reduction in toxicity to *M. splendida* survival in 2021, compared with previous years. This is likely related to the overall reduction in conductivity and some metal concentrations (Co, Ni, and to some extent Cu and Al) for LDP10 waters over the same period. However, *C. dubia* reproduction is a more sensitive endpoint than survival, based on differing modes of action of toxicants on this endpoint. Therefore, despite the improvements observed in water quality at LDP10- over time, toxicity observed to *C. dubia* reproduction in 2021 is similar to that observed in previous years (albeit lower than the extremes of toxicity observed on two previous occasions).

Collectively, the ecotoxicological tests indicate that the discharge waters from LDP10 may still pose a risk to biota.

## 3.6 Macrobenthic surveys (2020-2021)

In this section, we describe the macrobenthic macroinvertebrate diversity and community structure for the sampling occasions Autumn 2020, Spring 2020, Autumn 2021, and Spring 2021. We also describe the interactions of the macroinvertebrate communities on the sampling occasions with the environmental variables measured.

### 3.6.1 Macrobenthos abundance (2020-2021)

The total abundance for all sites sampled during 2020 and 2021 are illustrated in Figure 21. Broadly, macrobenthic abundance (total number of macroinvertebrates counted per site) was higher in the discharge monitoring sites compared to the reference sites (Figure 21). The mean abundance and standard errors for each treatment for the sampling occasions and One-Way ANOVA results for each treatment for each sampling occasion are presented in Table 10. Total abundance was significantly different for reference and discharge monitoring sites for all sampling seasons except for Spring 2020 (Table 10). Across the sampling period, the mean abundance of the discharge monitoring treatment was greater than that for the reference treatment (Table 10). The exception to this was in Spring 2020, where a nearly significant result was observed ($p=0.053$). It is noted that univariate statistical analysis is limited due to the small sample sizes for the sites. The unbalanced design of only three reference sites and six discharge monitoring sites constrains the use of robust statistical analysis (Chariton & Stephenson 2020).

In Spring 2020, Site GRQ18 recorded the highest abundance (670 individuals) over the sampling period (Figure 21). In contrast, GRUFS had the lowest abundance of all sites and all time points (39 individuals in autumn 2020) (Figure 21). Interestingly flow in autumn 2020 was lower than the 2020 months of February/March where there had been an increase in flows (8ML/day) and then flow reduced (<2ML/day) just before the Autumn 2020 sampling at GRUFS (Figure 6). The Spring 2020 sample Point 11 technical replicate 2 was removed from the analysis due to no macroinvertebrates observed in the replicate sample.

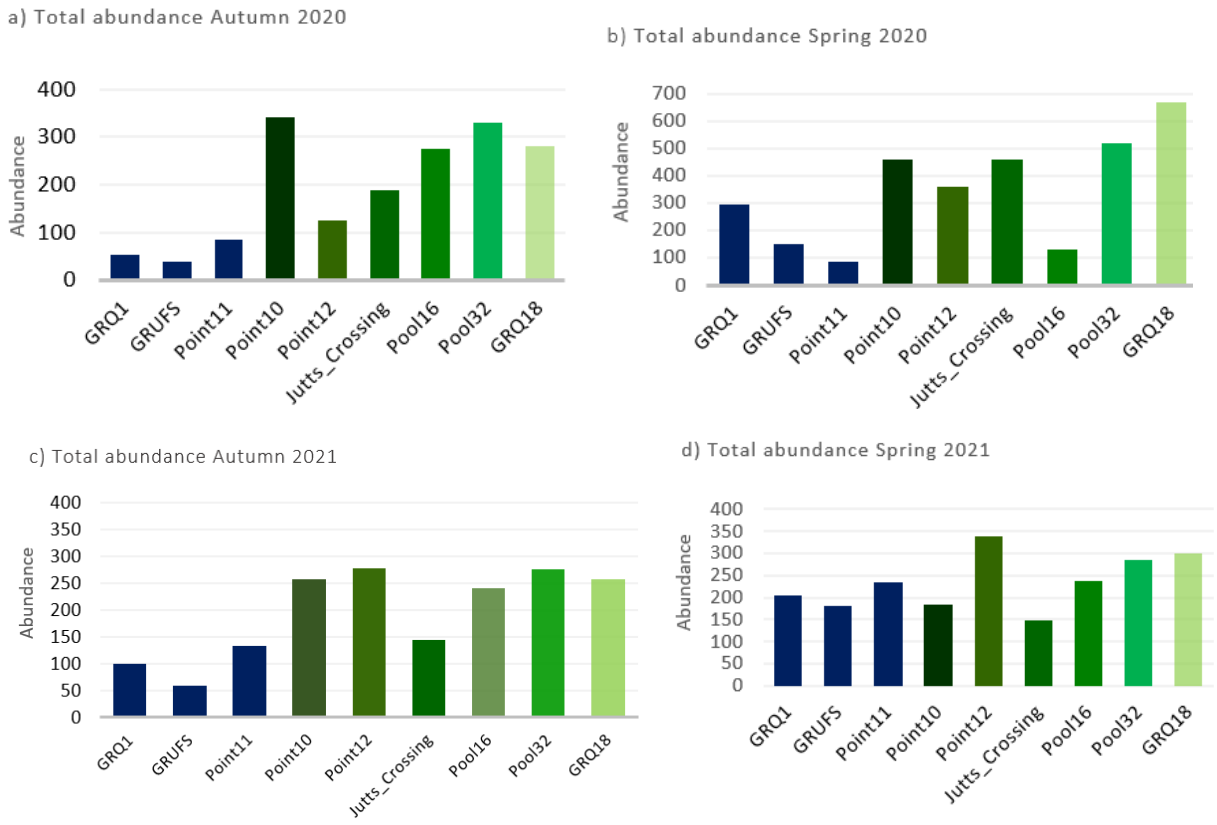


**Figure 21. Abundances of macrobenthic invertebrates (2020-2021).**

Reference sites (blue) and discharge monitoring sites (green). a) Autumn 2020; b) Spring 2020; c) Autumn 2021; and d) Spring 2021.

**Table 10. One-Way ANOVA results on macrobenthic abundance for reference and discharge monitoring sites.**

| **Abundance** | Reference | Reference | Discharge monitoring | Discharge monitoring | One-Way ANOVA | |
|---|---|---|---|---|---|---|
| | mean | ± S.E. | mean | ± S.E. | *F* | *P-value* |
| Autumn 2020 | 13.1 | 2 | 521.6 | 7 | 14 | **<0.05** |
| Spring 2020 | 45.5 | 11 | 87.8 | 14 | 4 | 0.053 |
| Autumn 2021 | 21.3 | 5 | 49 | 6 | 9.6 | **<0.05** |
| Spring 2021 | 104.2 | 20 | 206.4 | 23 | 8.2 | **<0.05** |

Bold values denote significance at $p < 0.05$.

### 3.6.2 Macrobenthos richness (2020-2021)

Richness is a measure of the number of different taxa in a sample or site and does not account for the abundance of the taxa. A summary of family richness from the macrobenthic data collected in 2020 and 2021 is provided in Figure 22. Richness varied across reference and discharge monitoring sites and sampling periods (Figure 22).

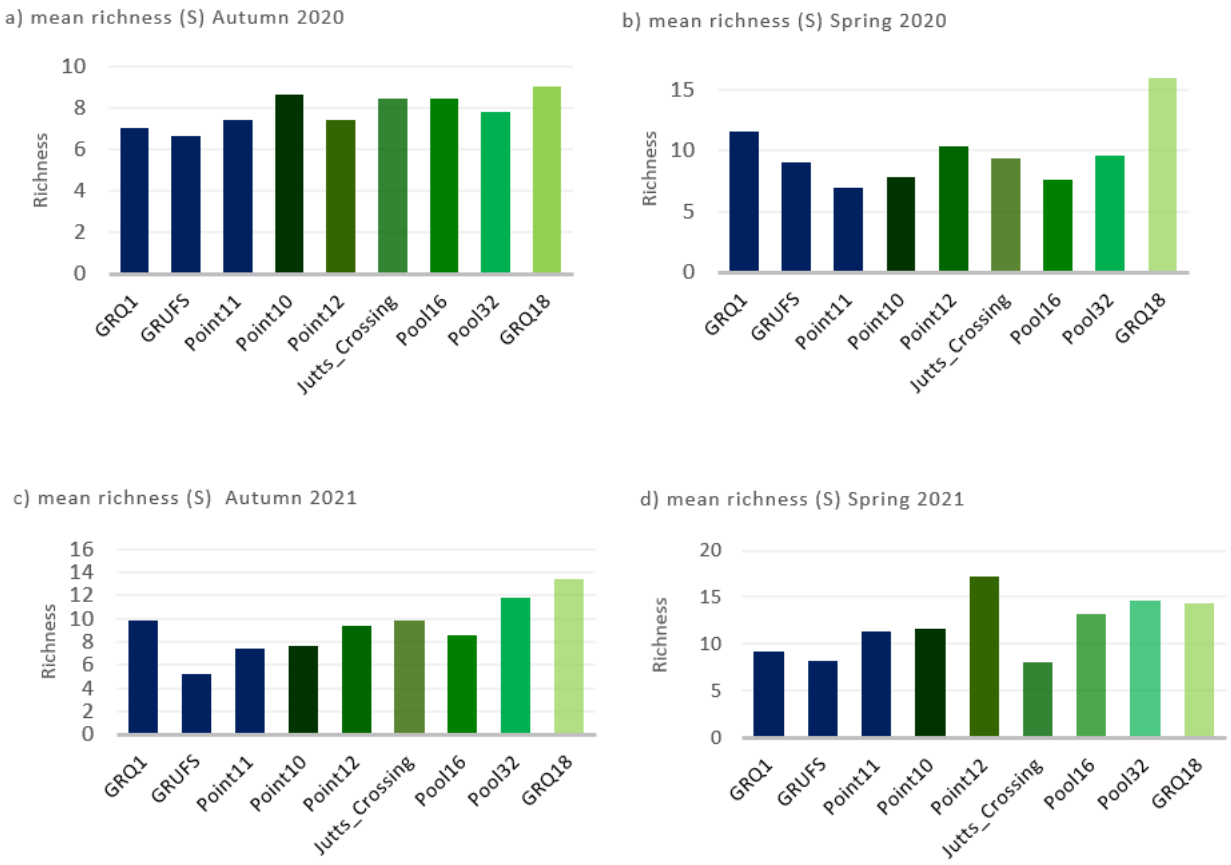


**Figure 22. Mean Family richness of macrobenthic invertebrates (Autumn 2020-2021).**

Reference sites (blue) and discharge monitoring sites (green). a) Autumn 2020; b) Spring 2020; c) Autumn 2020; and d) Spring 2021.

The mean richness and standard errors for each reference and discharge monitoring site and the One-Way ANOVA for richness for each sampling occasion are presented in Table 11. Richness varied across the study sites and sampling times (Figure 22), with no significant difference between reference and discharge monitoring sites for Autumn 2020 and Spring 2020 (Table 11). Richness did vary significantly between reference and discharge monitoring sites in Autumn 2021 and Spring 2021. In Autumn and Spring 2021 mean richness was higher in the discharge monitoring sites compared to the reference sites (Table 11). The One-Way ANOVA for richness (Table 11) detected a significant difference between reference and discharge monitoring sites in Autumn 2021 ($F=6.9$, $p<0.05$) and in Spring 2021 ($F=9.3$, $p<0.05$). Site GRQ18, consistently represented the site with the highest richness for all seasons over 2020 and 2021. Site GRQ18 is the furthest discharge monitoring site from the LDP40 and LDP10 discharge points. Mean richness at Point 10 in Autumn 2020 was higher than the reference sites but richness at Point 10 has since reduced in Spring 2020, Autumn 2021, and Spring 2021 (Figure 22). It is emphasised that these

richness and abundance findings should be taken cautiously given the small sample size, three reference sites and six discharge monitoring sites.

**Table 11. One-Way ANOVA results on macrobenthic richness for reference and discharge monitoring sites.**

| **Richness** | Reference | Reference | Discharge monitoring | Discharge monitoring | One-Way ANOVA | |
|---|---|---|---|---|---|---|
| | mean | ± S.E. | mean | ± S.E. | *F* | *P-value* |
| Autumn 2020 | 7 | 0.6 | 8.3 | 0.4 | 3.0 | 0.09 |
| Spring 2020 | 9.2 | 0.9 | 10.1 | 0.7 | 0.6 | 0.42 |
| Autumn 2021 | 7.5 | 0.7 | 10.1 | 0.6 | 6.9 | **<0.05** |
| Spring 2021 | 9.7 | 0.9 | 13.2 | 0.7 | 9.3 | **<0.05** |

Bold values denote significance at p< 0.05.

It is important to note that abundance and richness independently are regarded as weak measures of environmental stress (Chariton et al., 2015). We suggest removing richness and abundance from the macrobenthic monitoring program for greater emphasis on the SIGNAL and multivariate macrobenthic composition metrics.

### 3.6.3 Macrobenthic composition (2020-2021)

The macrobenthic community structure were investigated to compare reference and discharge monitoring sites. On all sampling occasions, the macrobenthic community structures in reference sites were different to those in the discharge monitoring sites. The similarities/differences between macroinvertebrate assemblages sampled in Autumn and Spring in both 2020 and 2021 are presented in the ordination plots in Figure 23. The ordination plots (Figure 23) show the aggregation of the reference sites in blue and the aggregation of the separate discharge monitoring sites in green. The ordination plots highlight that the discharge monitoring sites were more closely clustered together than the reference sites, indicating that the discharge monitoring macrobenthic communities were more similar to each other. In previous years the macrobenthic composition has shown more of a gradient effect for distance away from the discharge source, however, in 2020 and 2021 two distinct macrobenthic communities for the treatments (reference and discharge monitoring) were clearly separated from each other in the ordinations, most obvious in the Spring seasons. There was less separation of the two treatments in Autumn 2021, which corresponds with the highest rainfall sampling occasion. The 2020/2021 macrobenthic composition shows that Point 11 macroinvertebrate community structure is becoming more similar to the discharge monitoring sites compared to that observed for Point 11 composition in 2019 (Chariton and Stephenson, 2020) and has a unique composition compared to the other reference sites. In the Spring 2020 sampling, one of the five replicates contained no

macroinvertebrates (Point 11 replicate 2) and this sample replicate was removed from Point 11 for further multivariate analysis.

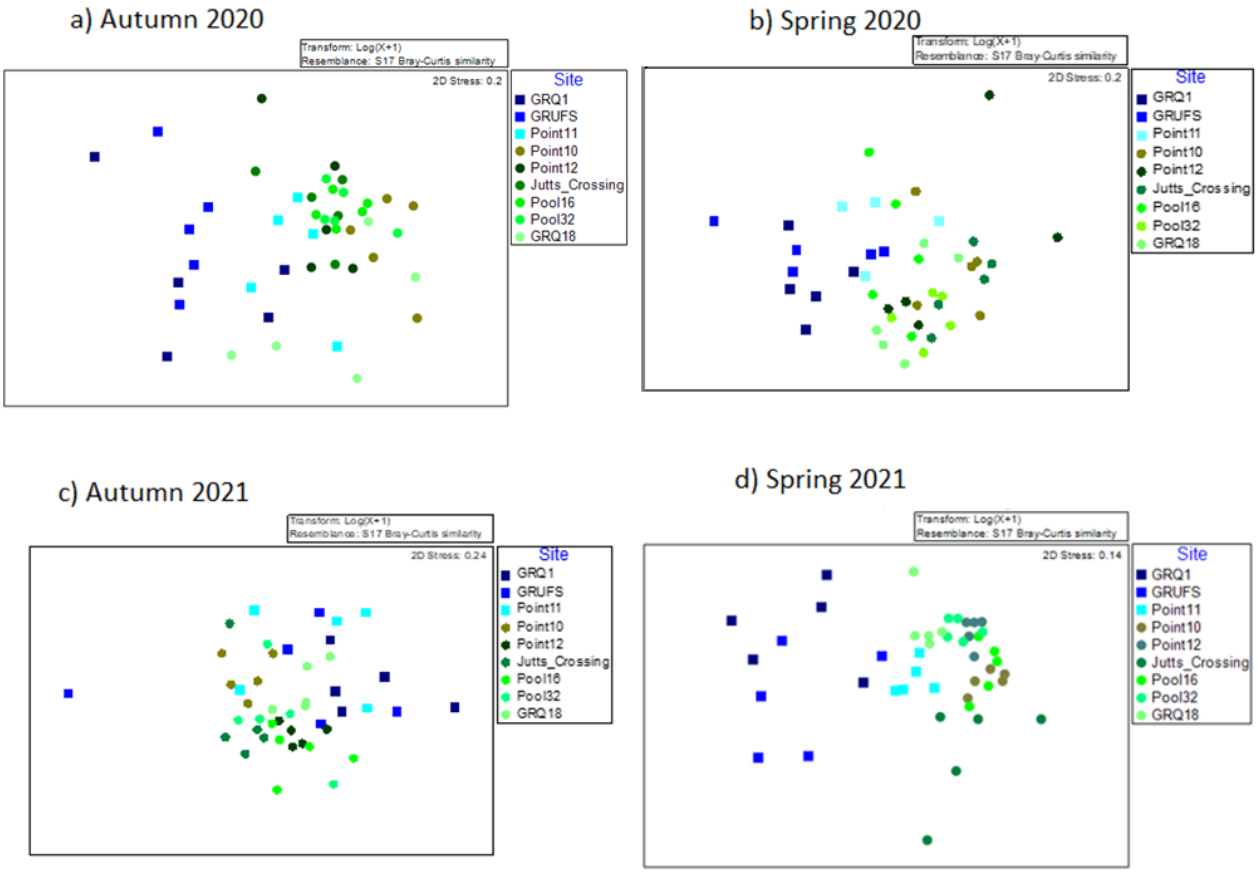


**Figure 23. non-metric Multidimensional Scaling (nMDS) of macrobenthic communities (2020-2021).**

a) Autumn 2020; b) Spring 2020; c) Autumn 2021; and d) Spring 2021.

PERMANOVA tests were undertaken to investigate macrobenthic community structure differences in treatments and time. The results of the PERMANOVAs testing for differences in macroinvertebrate community composition between sampling timepoints (Autumn and Spring 2020 and Autumn and Spring 2021) and treatments for all years are presented in Table 12. On all four occasions, there were significant differences in the composition in macrofauna communities between the reference and discharge monitoring treatments: Autumn 2020 (PERMANOVA: Pseudo-F= 7.7, $p<0.05$); Spring 2020 (PERMANOVA: Pseudo-F= 10.9, $p<0.05$); Autumn 2021 (PERMANOVA: Pseudo-F= 4.8, $p<0.05$); and Spring 2021 (PERMANOVA: Pseudo-F= 14.5, $p<0.05$). Significant differences in community composition were found with respect to time (season/year) (PERMANOVA: Pseudo-F=6.2, $p<0.05$) and treatment (reference or discharge monitoring) (PERMANOVA: Pseudo-F=28.8, $p<0.05$), when tested individually. In addition, there was a

significant interaction between time and treatment (PERMANOVA: Pseudo-F=9.9, p<0.05). The PERMANOVA results confirm that the macrobenthic communities in the reference treatment are different to those in the discharge monitoring treatment and that the communities have changed over time.

**Table 12. Results of PERMANOVA testing for variation in all macrobenthic community composition data (2020 & 2021) between sampling timepoints (season/year), sites (reference vs discharge monitoring).**

| Factor: source of variation | df | MS | Pseudo-F | P(perm) | Unique perms |
|---|---|---|---|---|---|
| **Time (season/year)** | 3 | 12021 | 6.2357 | **0.0001** | 9889 |
| **Reference vs discharge monitoring** | 1 | 51385 | 28.776 | **0.0001** | 9934 |
| **Time*Treatment** | 4 | 15616 | 9.9346 | **0.0001** | 9861 |
| **Res** | 171 | 2.69E+05 | | | |
| **Total** | 178 | 3.67E+05 | | | |

Df: degrees of freedom; MS: mean squares; Pseudo-F: multivariate analogue to Fisher's F test statistic of the null hypothesis; P(perm): probability by permutations; Unique Perms: number of unique permutations.

Bold values denote significance at p< 0.05.

Consistent with previous years, there were marked differences in the macrobenthic community composition between the reference and discharge monitoring treatments in Autumn and Spring 2020 and 2021. Across the sampling times Point 10, Point 12, Jutts and Pool 16 demonstrated similar macrobenthic community compositions while GRQ18 showed unique composition for all years.

The five top taxa which discriminated between the reference and discharge monitoring treatments on each occasion are shown in Table 13**.** In Autumn 2020, key taxa which contributed to the observed differences in compositions in the discharge monitoring treatment were: Caenidae (Ephemeroptera), Tanypodinae (Chironomidae), Chironominae (Chironomidae), and Hydrophilidae (Coleoptera) (Table 13). The taxa Caenidae (Ephemeroptera), Tanypodinae (Chironomidae), Chironominae (Chironomidae), and Hydrophilidae (Coleoptera) were higher in abundance in the discharge monitoring sites and had a positive relationship with discharge monitoring sites. In Spring 2020, the reference treatment had higher abundances of Leptophlebiidae, there was a positive relationship with reference treatments and abundances of Leptophlebiidae in Spring 2020. Tanypodinae, Caenidae, and Chironominae were more abundant in the discharge monitoring sites than the reference sites in Spring 2020. In Autumn 2021, Oligochaeta, Chironominae and Tanypodinae were more abundant in the discharge monitoring sites. In Spring 2021, there was an overall increase in abundances across all identified macroinvertebrates (Table 13) and Leptophlebiidae were characteristic of the reference sites, with relatively higher

abundances of Chironominae, Tanypodinae and Caenidae being indicative of the discharge monitoring treatment. The SIMPER analysis, which explains the dissimilarity between treatment composition, found the reference sites to contain more organisms from the family Leptophlebiidae while the discharge Monitoring sites contained organisms from the families Caenidae, Tanypodinae, and Chironominae which are regarded as tolerant invertebrate taxa (Chessman, 2003; Walsh 2006). Leptophlebiidae have been identified as a potential indicator of health for this system, with this taxon considered to be contamination intolerant (SIGNAL=8) (Chessman, 2003). In general, the discharge monitoring sites had communities composed of more tolerant taxa while those at reference sites included more sensitive taxa. There could be multiple factors explaining the different taxa present in the reference and discharge monitoring sites including differences in habitat, pool depth, turbidity, and substrate type. The differences in composition using SIMPER were not as obvious in 2020 as in 2021. Greater differences in composition in 2021 might be related to weather pattern changes, with greater rainfall especially observed in Autumn 2021 compared to previous sampling in 2018, 2019 and 2020.

**Table 13. SIMPER results illustrating the top 5 taxa which contributed to differences between the reference and discharge monitoring sites (2020-2021)**

| Year | Season | Family | Reference Average abundance | Discharge Monitoring Average abundance | (%) contribution of total dissimilarity |
|---|---|---|---|---|---|
| **2020** | Autumn | Caenidae | 2 | 19 | 27 |
| | | Tanypodinae | 2 | 11 | 17 |
| | | Chironominae | 2 | 5 | 10 |
| | | Hydrophilidae | 2 | 4 | 7 |
| | | Baetidae | 1 | 2 | 5 |
| **2020** | Spring | Tanypodinae | 13 | 27 | 25 |
| | | Caenidae | 2 | 25 | 21 |
| | | Leptophlebiidae | 10 | 1 | 13 |
| | | Chironominae | 4 | 10 | 8 |
| | | Hydrophilidae | 1 | 4 | 7 |
| **2021** | Autumn | Oligochaeta | 2 | 8 | 16 |
| | | Chironominae | 5 | 8 | 16 |
| | | Tanypodinae | 3 | 8 | 13 |
| | | Caenidae | 0.2 | 5 | 6 |
| | | Ecnomidae | 2 | 4 | 6 |
| **2021** | Spring | Chironominae | 34 | 81 | 30 |
| | | Leptophlebiidae | 44 | 7 | 18 |
| | | Caenidae | 1 | 39 | 15 |
| | | Tanypodinae | 8 | 32 | 13 |
| | | Dytiscidae | 0 | 2 | 6 |

### 3.6.4 Relationships between macrobenthic communities and water quality (2020-2021)

Multivariate correlative statistics were undertaken to understand how the macroinvertebrate communities were responding to the water quality variables measured. Correlative patterns were studied to identify which environmental factors were driving the macrobenthic community composition and to identify key relationships between the macroinvertebrate communities and the measured water quality variables. Distance-based linear modelling (DistLM) was used to correlate environmental variables to the composition of the macrobenthic community composition for each sampling occasion and the correlative relationships between the macrobenthic communities and water quality for each sampling are presented in Figure 24 to Figure 27.

**Autumn 2020**

The distance-based analysis of the Autumn 2020 data is presented in Figure 24. The fitted DistLM was visualised using a distance-based redundancy analysis (dbRDA) constrained ordination demonstrating the correlation of significant variables on the Autumn 2020 macrobenthic community. Approximately 77% of the variation of the macrobenthic data sampled in Autumn 2020 could be explained by the measured environmental variables pH, alkalinity, total nitrogen and zinc (Table 14). When examined collectively, pH was the only variable which was significantly correlated ($p<0.05$), explaining approximately 45% of the total variation of the macrobenthic community structure. The dbRDA (Figure 24) shows that axis 1 (dbRDA 1), (which corresponds to pH, alkalinity) is explaining approximately 49% of the total variation and axis 2 (dbRDA 2) (corresponding to total nitrogen) is explaining approximately 12% of the total macrobenthic variation.

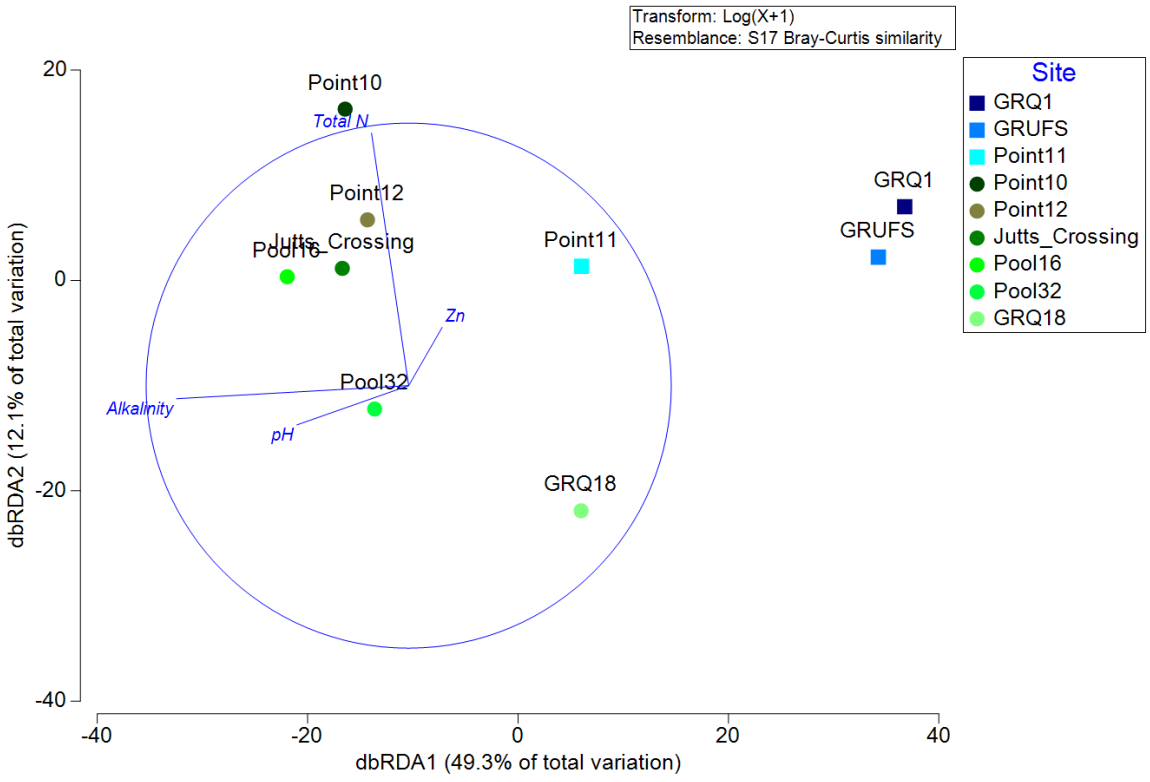


**Figure 24. Ordination plot derived from the distance-based model illustrating the relationships between environmental variables and macrobenthic composition from Autumn 2020**

Table 14. Sequential test results of distance-based linear model (DistLM) Autumn 2020.

| Variable | Adj $R^2$ | SS(trace) | Pseudo-F | P | Prop% | Cumulative contribution | res.df |
|---|---|---|---|---|---|---|---|
| **+pH** | 0.38 | 3697 | 5.82 | **0.0008** | 0.45 | 0.45 | 7 |
| **+Alkalinity** | 0.43 | 993.9 | 1.73 | 0.088 | 0.12 | 0.58 | 6 |
| **+Total nitrogen** | 0.52 | 1023.3 | 2.10 | 0.085 | 0.13 | 0.70 | 5 |
| **+Zinc** | 0.54 | 568.1 | 1.22 | 0.32 | 0.07 | 0.77 | 4 |

SS(trace): sum of squares; Pseudo-F: multivariate analogue to Fisher's F test statistic of the null hypothesis; P: probability; Prop%: the proportion of variation; res.df: residual degrees of freedom.

Bold values denote significance at $p< 0.05$.

### Spring 2020

The distance-based analysis of the Spring 2020 data found that the measured water quality variables of pH, zinc, aluminium, total nitrogen, nickel, conductivity and copper collectively explained 97% of the total variation in the macrobenthic data. When examined collectively, pH (48%) and zinc (14%) were shown to significantly contribute to a proportion of the variation in the data (Table 15). Like autumn 2020, pH was also found to be the most significant variable contributing to the Spring 2020 macrobenthic total variation, explaining approximately 48% of the total variation in the macrobenthic community structure. In Spring 2020, zinc was contributing to the biological variation ($p<0.05$), explaining approximately 14% of the total macrobenthic variation. The fitted DistLM was visualised using a distance-based redundancy analysis (dbRDA) constrained ordination (Figure 25), demonstrating the correlation of significant variables on the Spring 2020 macrobenthic community. The dbRDA (Figure 25) shows that dbRDA 1 (pH, conductivity) is explaining 52% of the total variation and dbRDA 2 is explaining 14% (zinc) of the total variation (Figure 25). The composition of the water quality variables driving Point 10, Point 12, and Jutts differed to those for Point 11, GRUFS and GRQ1. The ordination dbRDA (Figure 25) shows GRQ18, Pool 16 and Pool 32 were separated from the upper discharge sites (Point 10, Point 12, Jutts) in Spring 2020.

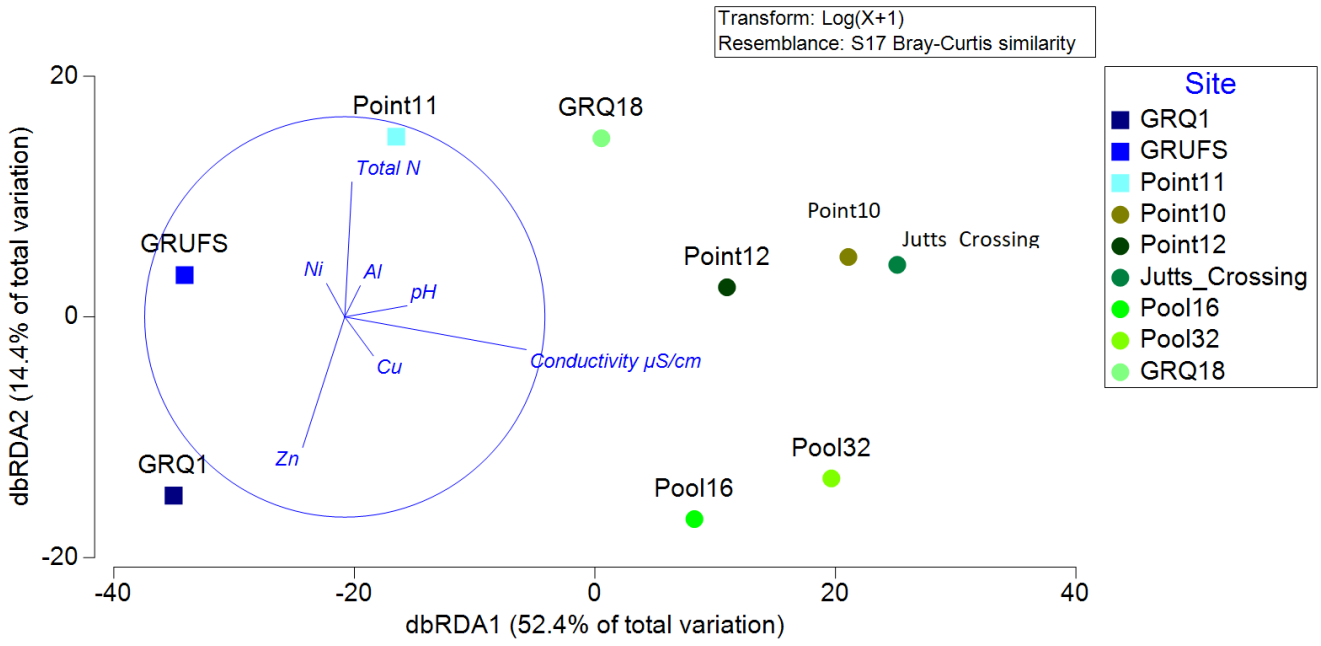


**Figure 25. Ordination plot derived from the distance-based model illustrating the relationships between environmental variables and macrobenthic composition from Spring 2020.**

**Table 15. Sequential test results of distance-based linear model (DistLM) Spring 2020.**

| Variable | Adj $R^2$ | SS(trace) | Pseudo-F | P | Prop%. | Cumulative contribution | res.df |
|---|---|---|---|---|---|---|---|
| **+pH** | 0.41 | 3968.7 | 6.5 | **0.0006** | **0.48** | 0.48 | 7 |
| **+Zinc** | 0.49 | 1131.2 | 2.16 | **0.0153** | **0.14** | 0.62 | 6 |
| **+Aluminium** | 0.57 | 917.6 | 2.06 | 0.0606 | 0.11 | 0.73 | 5 |
| **+Total N** | 0.64 | 757.5 | 2.07 | 0.0922 | 0.092 | 0.82 | 4 |
| **+Nickel** | 0.68 | 485.4 | 1.49 | 0.2537 | 0.059 | 0.88 | 3 |
| **+Conductivity µS/cm** | 0.72 | 404.6 | 1.41 | 0.3249 | 0.049 | 0.93 | 2 |
| **+Copper** | 0.80 | 367.1 | 1.76 | 0.3576 | 0.045 | 0.97 | 1 |

SS(trace): sum of squares; Pseudo-F: multivariate analogue to Fisher's F test statistic of the null hypothesis; P: probability; Prop%: the proportion of variation; res.df: residual degrees of freedom.

Bold values denote significance at $p < 0.05$.

### Autumn 2021

The distance-based analysis of the Autumn 2021 data found the measured variables of pH, conductivity, alkalinity, aluminium, zinc, nickel, and total nitrogen explained 91% of the total variation in macrobenthic community composition. When examined collectively only pH was shown to significantly contribute to a proportion of the variation in the data, explaining approximately 27% of the total variation of the autumn 2021 macrobenthic community structure

(Table 16). pH has been the consistent variable driving the macrobenthic community structure across three sampling periods, from Autumn 2020 to Autumn 2021.

The fitted DistLM was visualised using a distance-based redundancy analysis (dbRDA) constrained ordination (Figure 26), demonstrating the correlation of significant variables on the Autumn 2021 macrobenthic community. pH is driving the discharge monitoring sites to separate from the reference sites. In the dbRDA ordination, dbRDA 1 is explaining 31% of the total variation and dbRDA 2 is explaining 20% of the total macroinvertebrate variation. The dbRDA also highlights that alkalinity may be separating Point 10 communities from the other discharge monitoring sites in Autumn 2021.

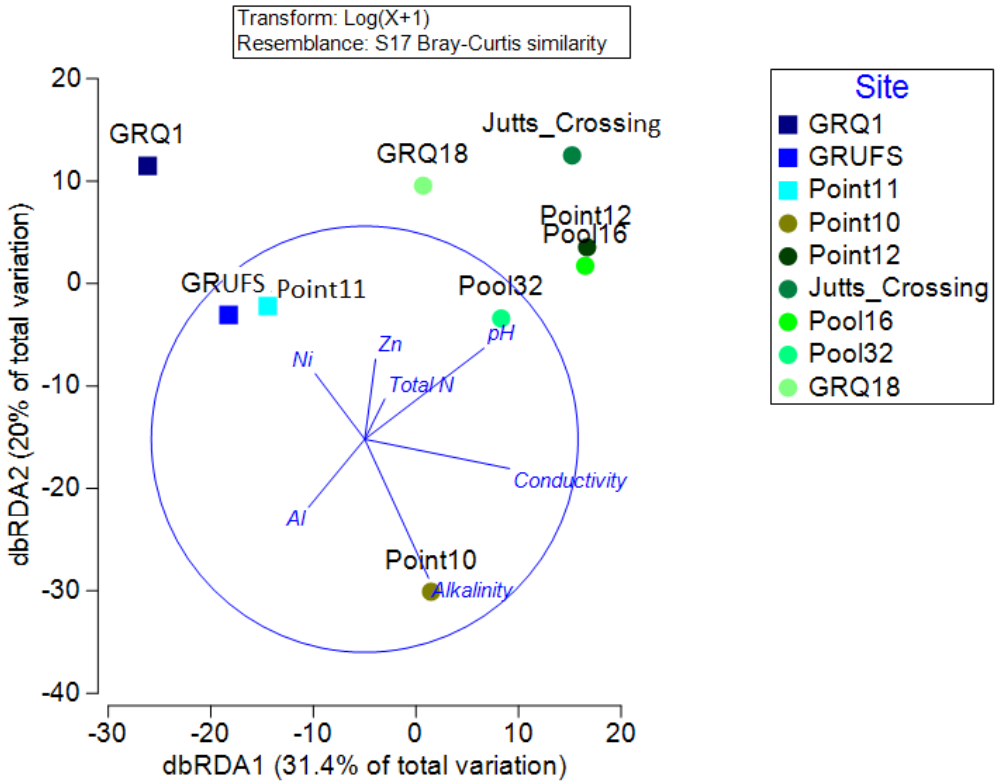


**Figure 26. Ordination plot derived from the distance-based model illustrating the relationships between environmental variables and macrobenthic composition from Autumn 2021**

Table 16. Sequential test results of distance-based linear model (DistLM) Autumn 2021.

| Variable | Adj $R^2$ | SS(trace) | Pseudo-F | P | Prop%. | Cumulative contribution | res.df |
|---|---|---|---|---|---|---|---|
| **+pH** | 0.16 | 1784.5 | 2.58 | **0.003** | 0.27 | 0.27 | 7 |
| **+Conductivity µS/cm** | 0.24 | 1067.3 | 1.70 | 0.073 | 0.16 | 0.43 | 6 |
| **+Alkalinity** | 0.29 | 833.7 | 1.42 | 0.253 | 0.13 | 0.56 | 5 |
| **+Aluminium** | 0.30 | 611 | 1.05 | 0.448 | 0.09 | 0.65 | 4 |
| **+Nickel** | 0.27 | 522 | 0.87 | 0.500 | 0.08 | 0.73 | 3 |
| **+Zinc** | 0.41 | 827.9 | 1.68 | 0.249 | 0.12 | 0.85 | 2 |
| **+Total Nitrogen** | 0.31 | 411 | 0.72 | 0.576 | 0.06 | 0.91 | 1 |

SS(trace): sum of squares; Pseudo-F: multivariate analogue to Fisher's F test statistic of the null hypothesis; P: probability; Prop%: the proportion of variation; res.df: residual degrees of freedom

Bold values denote significance at p< 0.05.

### Spring 2021

The measured variables of zinc, total nitrogen, aluminium, and alkalinity explained 81% of the total variation in Spring 2021 macrobenthic community composition. When examined collectively only zinc was shown to significantly contribute to a proportion of the variation in the data, zinc explaining approximately (56%) of the total variation of the macrobenthic community structure in Spring 2021 (Table 17). The fitted DistLM, dbRDA (Figure 27), demonstrated the correlation of significant variables on the Spring 2021 macrobenthic community. In the dbRDA (Figure 27) dbRDA 1 is explaining approximately 59% of the total macrobenthic variation and dbRDA 2 is explaining approximately 13% of the total variation. The composition of the water quality variables driving Point 11 was separated from the other reference sites (GRQ1 and GRUFS) in Spring 2021. Point 11 composition appears more similar to the discharge monitoring sites than the reference sites GRQ1 and GRUFS in Spring 2021 (Figure 27). Water quality variables contributing to the variation in community composition at Point 10 (alkalinity) and Jutts (zinc and total nitrogen) differed from those variables driving the composition of the other discharge monitoring sites (Figure 27).

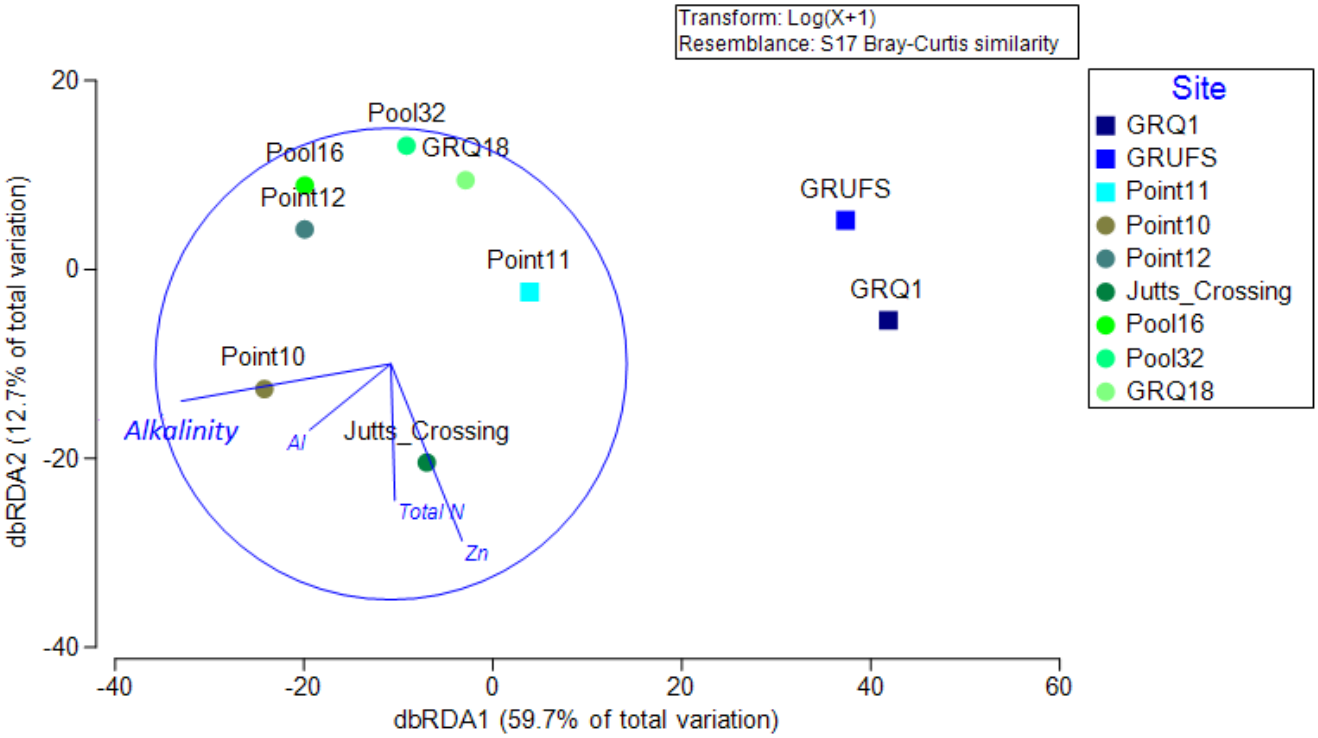


**Figure 27. Ordination plot derived from the distance-based model illustrating the relationships between environmental variables and macrobenthic composition from Spring 2021**

**Table 17. Sequential test results of distance-based linear model (DistLM) Spring 2021.**

| Variable | Adj $R^2$ | SS(trace) | Pseudo-F | P | Prop% | Cumulative contribution | res.df |
|---|---|---|---|---|---|---|---|
| **+Zinc** | 0.49 | 4378.5 | 8.84 | **0.0009** | 0.56 | 0.56 | 7 |
| **+Total Nitrogen** | 0.58 | 1007 | 2.45 | 0.0591 | 0.13 | 0.69 | 6 |
| **+Aluminium** | 0.62 | 590.18 | 1.58 | 0.2158 | 0.08 | 0.76 | 5 |
| **+Alkalinity** | 0.63 | 408.79 | 1.12 | 0.3971 | 0.05 | 0.81 | 4 |

SS(trace): sum of squares; Pseudo-F: multivariate analogue to Fisher's F test statistic of the null hypothesis; P: probability; Prop%: the proportion of variation; res.df: residual degrees of freedom

Bold values denote significance at p< 0.05.

The correlative patterns analysis identified pH as the main driver of the macrobenthic community across all sampling years as well as zinc in 2021. While the statistical analysis suggests pH may be the main driver, we recommend considering the water quality of the metals and pH as a whole interacting with the biology of the system. Given the complexity of the LDP10 discharge waters and the tight relationship between pH, alkalinity and metal bioavailability, we recommend viewing the discharge water quality as whole rather than giving weight to any specific variable.

### 3.6.5 SIGNAL scores (2020-2021)

The SIGNAL scores from the Autumn and Spring macrobenthic surveys performed in 2020 and 2021 are presented in Figure 28. All reference sites had SIGNAL scores below the long-term historical mean (2013-2019) in Autumn and Spring in 2020 and 2021 (Figure 28). Mean SIGNAL scores, standard errors and One-Way ANOVA results for the reference and discharge monitoring treatments are presented in Table 18. Mean SIGNAL scores for the reference treatment in Autumn 2020 (4.2 ± 0.1 S.E.), Autumn 2021 (4.3 ± 0.2 S.E.) and Spring 2021 (4.3± 0.09 S.E.) were significantly greater than those for the discharge monitoring treatment on each sampling occasion (Autumn 2020, 3.6 ± 0.1 S.E.; Autumn 2021, 3.7±0.1 S.E.; Spring 2021, 3.7 ± 0.08 S.E. based on One-Way ANOVA analyses (Autumn 2020: $F=10.3$, $p<0.05$; Autumn 2021: $F= 14.8$, $p<0.05$; Spring 2021: $F= 18.3$, $p<0.05$). For Spring 2020 mean SIGNAL scores for the reference treatment (4.1± 0.3 S.E.) was not significantly different to that for the discharge monitoring treatment (3.8 ± 0.1 S.E.; ANOVA: $F= 0.7$, $p=0.39$).

**Table 18. Table One-Way ANOVA results on macrobenthic SIGNAL values for reference and discharge monitoring treatments.**

| **SIGNAL** | Reference | Reference | Discharge monitoring | Discharge monitoring | One-Way ANOVA | |
|---|---|---|---|---|---|---|
| Sampling time | mean | ± S.E. | mean | ± S.E. | *F* | *P-value* |
| Autumn 2020 | 4.2 | 0.1 | 3.6 | 0.1 | 10.3 | **<0.05** |
| Spring 2020 | 4.1 | 0.3 | 3.8 | 0.1 | 0.7 | 0.39 |
| Autumn 2021 | 4.2 | 0.2 | 3.7 | 0.1 | 14.8 | **<0.05** |
| Spring 2021 | 4.3 | 0.1 | 3.7 | 0.1 | 18.3 | **<0.05** |

Bold values denote significance at p< 0.05.

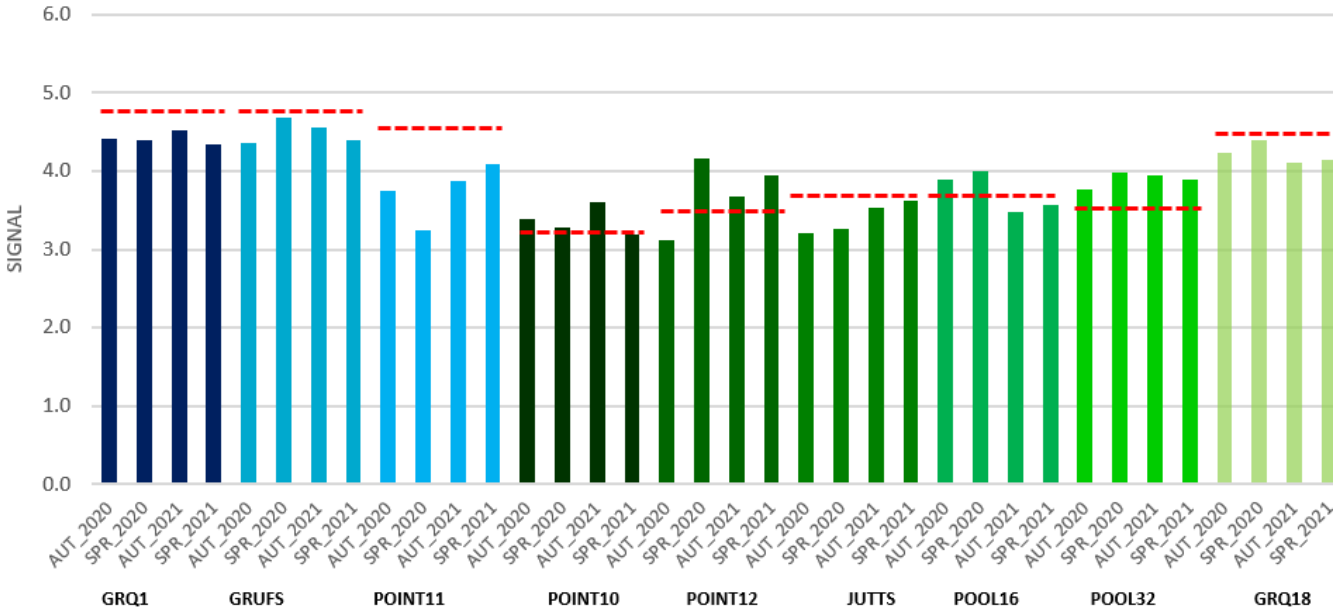


**Figure 28. SIGNAL scores from 2020-2021.**

Reference sites (blue) and discharge monitoring sites (green). Red dashed line indicates mean SIGNAL scores from historical data 2013-2019.

Table 19. SIGNAL scores and rankings for each site (2020-2021).

| Treatment | Year | Season | Site | Potential ranking* | SIGNAL |
|---|---|---|---|---|---|
| Reference | 2020 | Autumn | GRQ1 | Probable moderate contamination | 4.4 |
| | 2020 | Spring | GRQ1 | Probable moderate contamination | 4.4 |
| | 2021 | Autumn | GRQ1 | Probable moderate contamination | 4.5 |
| | 2021 | Spring | GRQ1 | Probable moderate contamination | 4.3 |
| Reference | 2020 | Autumn | GRUFS | Probable moderate contamination | 4.4 |
| | 2020 | Spring | GRUFS | Probable moderate contamination | 4.7 |
| | 2021 | Autumn | GRUFS | Probable moderate contamination | 4.6 |
| | 2021 | Spring | GRUFS | Probable moderate contamination | 4.4 |
| Reference | 2020 | Autumn | Point 11 | Probable severe contamination | 3.8 |
| | 2020 | Spring | Point 11 | Probable severe contamination | 3.2 |
| | 2021 | Autumn | Point 11 | Probable severe contamination | 3.9 |
| | 2021 | Spring | Point 11 | Probable moderate contamination | 4.1 |
| Discharge monitoring | 2020 | Autumn | Point 10 | Probable severe contamination | 3.4 |
| | 2020 | Spring | Point 10 | Probable severe contamination | 3.3 |
| | 2021 | Autumn | Point 10 | Probable severe contamination | 3.6 |
| | 2021 | Spring | Point 10 | Probable severe contamination | 3.2 |
| Discharge monitoring | 2020 | Autumn | Point 12 | Probable severe contamination | 3.1 |
| | 2020 | Spring | Point 12 | Probable moderate contamination | 4.2 |
| | 2021 | Autumn | Point 12 | Probable severe contamination | 3.7 |
| | 2021 | Spring | Point 12 | Probable severe contamination | 3.9 |
| Discharge monitoring | 2020 | Autumn | Jutts | Probable severe contamination | 3.2 |
| | 2020 | Spring | Jutts | Probable severe contamination | 3.3 |
| | 2021 | Autumn | Jutts | Probable severe contamination | 3.5 |
| | 2021 | Spring | Jutts | Probable severe contamination | 3.6 |
| Discharge monitoring | 2020 | Autumn | Pool 16 | Probable severe contamination | 3.9 |
| | 2020 | Spring | Pool 16 | Probable moderate contamination | 4.0 |
| | 2021 | Autumn | Pool 16 | Probable severe contamination | 3.5 |
| | 2021 | Spring | Pool 16 | Probable severe contamination | 3.6 |
| Discharge monitoring | 2020 | Autumn | Pool 32 | Probable severe contamination | 3.8 |
| | 2020 | Spring | Pool 32 | Probable moderate contamination | 4.0 |
| | 2021 | Autumn | Pool 32 | Probable severe contamination | 3.9 |
| | 2021 | Spring | Pool 32 | Probable severe contamination | 3.9 |
| Discharge monitoring | 2020 | Autumn | GRQ18 | Probable moderate contamination | 4.2 |
| | 2020 | Spring | GRQ18 | Probable moderate contamination | 4.4 |
| | 2021 | Autumn | GRQ18 | Probable moderate contamination | 4.1 |
| | 2021 | Spring | GRQ18 | Probable moderate contamination | 4.1 |

*Potential rankings based on Chessman (1995)

The SIGNAL scores overall were low across all sites. SIGNAL is a useful indicator tool for freshwater ecosystem health as it factors in the sensitivity of the invertebrates at a site. In contrast to total abundance and richness, SIGNAL macroinvertebrate metric was designed to focus the analysis on taxa which may be influenced by the ecological condition of the stream. As reported in previous

years (Chariton and Stephenson, 2018 and 2020), the Ephemeropteran, Caenidae, were more abundant at discharge monitoring sites. The family Caenidae is considered moderately insensitive to contaminants (SIGNAL=4) (Chessman, 2003). Leptophlebiidae were more abundant in the reference sites and this taxon considered to be contamination intolerant (SIGNAL=8) (Chessman, 2003).

There have been some slight improvements in the macrobenthic reference site composition likely due to overall increased water flow at the reference sites from increased rainfall in 2021 compared to the previous reporting EIP2 in 2018 – 2019 (Chariton and Stephenson 2020). Higher rainfall and greater water flows through GRUFS has improved the SIGNAL score for GRUFS in 2020 and 2021 at the time of sampling compared with 2018 and 2019 when the system was in drought. It is important to note that the water level at GRUFS has fluctuated over the monitoring period, with low flow observed in Autumn 2020, Spring 2020 and Spring 2021. GRUFS is shallow (0.5m depth) and narrow (2m wide), so the flow and ecological integrity at this site could be related to dynamic weather patterns. The reference site GRUFS has improved SIGNAL scores in 2020 and 2021 compared to 2018 and 2019 with upgrades in classification to 'probable moderate contamination'. This may suggest that water flow and level through the upper reference sites (GRQ1 & GRUFS) is a factor for macrobenthic taxa present and the corresponding SIGNAL score for the sites. The SIGNAL score at Point 11 however has varied over time, suggesting multiple complex inputs at Point 11, in Autumn 2020, Spring 2020 and Autumn 2021; Point 11 was classified as 'probable severe contamination' and only improved to 'probable moderate contamination' in Spring 2021.

The over-arching trend throughout the sampling program is that the composition of macrobenthic invertebrates from the reference sites differ to those from the discharge monitoring sites. It is important to note that habitat and pool substrate is also likely contributing to the observed differences between and within treatments. Observational evidence (pers. obs. David Gregory, South32) also suggests that the structural complexity of the water bodies varies greatly between the reference and discharge monitoring sites, with the former containing more complex habitats, including structures such as log jams. Water discharging from LDP10 remains the dominant flow and water source of the upper sites, consequently, the observed differences between the two treatments is likely due to a combination of the LDP10 discharge waters and invertebrate habitat condition. The higher SIGNAL scores and classification as 'probable moderate contamination' at GRQ18, the most downstream distant site, suggests that the effect of discharge from LDP10 and

LDP40 is lessened by distance downstream, with mixed inputs from additional flows. Confluence creek inputs and other land-based activities in this area of the catchment may be having more influence on the water quality at GRQ18 due to geographical position.

## 3.7 Long term patterns in macrobenthic community attributes

### 3.7.1 Abundance and richness (2013-2021)

The abundance of macroinvertebrates varied greatly between sites and across sampling events Figure 29. The long-term patterns showed a significant difference between the abundance of reference sites compared with the discharge monitoring sites. The long-term patterns of abundance showed that the discharge monitoring sites (101 ± 9.4 S.E.), had a higher mean abundance than the reference sites (50 ± 5.5 S.E.) (ANOVA: $F= 13$, $p<0.05$). It is emphasised that this finding should be taken cautiously given the small sample size, three reference sites and six discharge monitoring.

The mean richness for all sites sampled between 2013 and 2021 is illustrated in Figure 30. Mean family richness was similar in all reference and discharge monitoring sites, with only a slightly significant difference observed (ANOVA: $F= 5.6$, $p=0.05$) detected between the reference (10 ± 0.7 S.E.) and discharge monitoring (12 ± 0.5 S.E.) treatments. No trends were observed in the richness data over the long term.

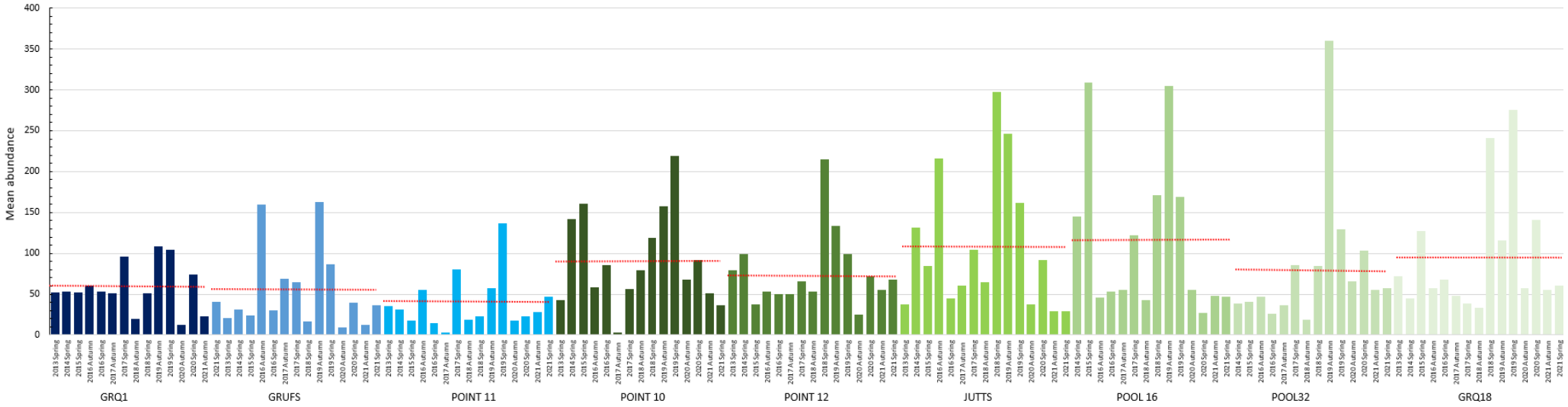


**Figure 29. Long-term abundance patterns in macrobenthos (2013-2021).**

Reference sites (blue) and discharge monitoring sites (green). Dotted red lines represent the mean value for each site. Due to the size of this dataset, not all labels fit on the x-axis. Order of data from left to right for each site is: Spring 2013, Spring 2014, Spring 2015, then for each year thereafter, Autumn data is presented before Spring data

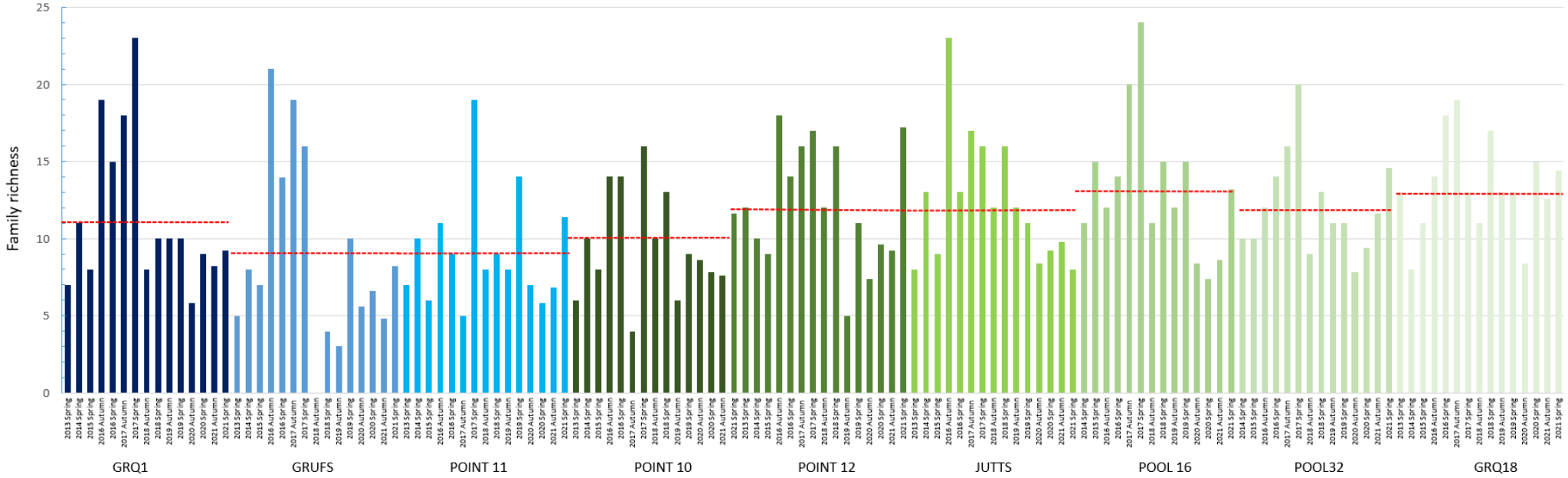


**Figure 30. Long-term Family richness patterns in macrobenthos (2013-2021).**

Reference sites (blue) and discharge monitoring sites (green). Dotted red lines represent the mean value for each site

### 3.7.2 SIGNAL (2013-2021)

Long-term SIGNAL scores for all sites sampled between 2013 and 2021 are illustrated in Figure 31. Based on the classifications for SIGNAL by Chessman (1995) suggests, that on average, at the times of sampling, the reference sites can be considered of 'probable moderate contamination' and the discharge monitoring sites of 'probable severe contamination' (Table 20). The exception being the most distant discharge monitoring site (GRQ18) which was classified as 'probable moderate contamination'. The long-term mean SIGNAL scores for the reference sites (4.5 ± 0.10 S.E.) were greater than the discharge monitoring sites (3.8 ± 0.14 S.E.). The difference between the reference and discharge monitoring long term mean SIGNAL scores was significantly different between the two treatments (ANOVA: $F= 12$, $p<0.05$) (Figure 31).

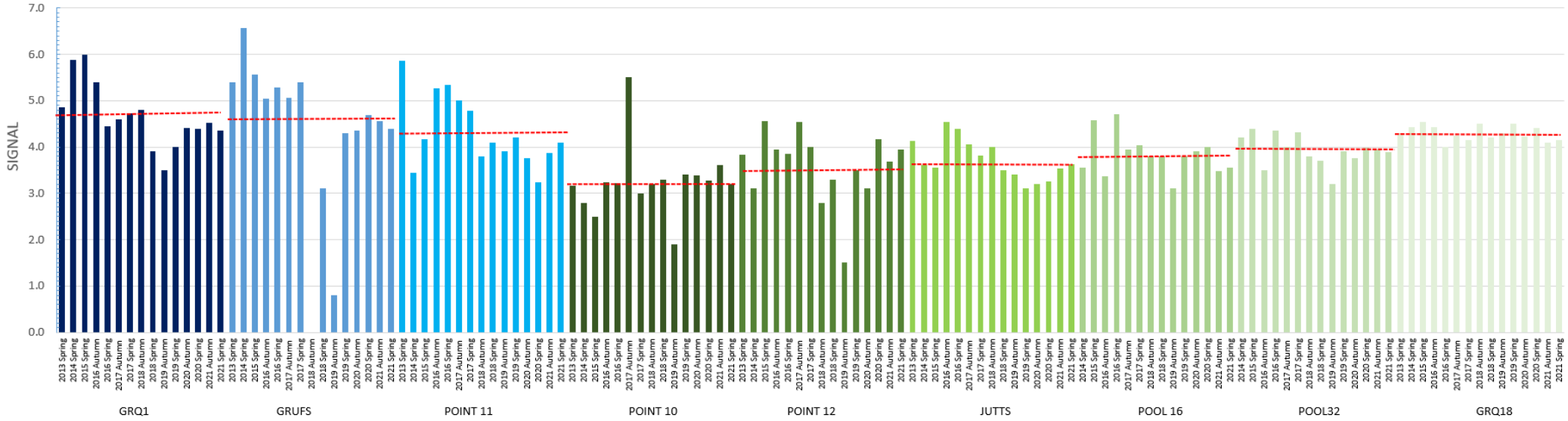


**Figure 31. Long-term SIGNAL scores for sites (2013-2021).**

Reference sites (blue) and discharge monitoring sites (green). Dotted red lines represent the mean value for each site.

Table 20. Mean SIGNAL scores for each site (2013-2021).

| Treatment | Site | Potential ranking* | Mean SIGNAL | Minimum | Maximum |
|---|---|---|---|---|---|
| Reference | GRQ1 | Probable moderate contamination | 4.7 | 3.5 | 6.0 |
| Reference | GRUFS | Probable moderate contamination | 4.6 | 5.1 | 6.6 |
| Reference | Point 11 | Probable moderate contamination | 4.3 | 3.2 | 5.9 |
| Discharge monitoring | Point 10 | Probable severe contamination | 3.2 | 1.9 | 5.5 |
| Discharge monitoring | Point 12 | Probable severe contamination | 3.6 | 1.5 | 4.6 |
| Discharge monitoring | Jutts | Probable severe contamination | 3.7 | 3.1 | 4.5 |
| Discharge monitoring | Pool 16 | Probable severe contamination | 3.8 | 3.1 | 4.7 |
| Discharge monitoring | Pool 32 | Probable severe contamination | 3.9 | 3.2 | 4.4 |
| Discharge monitoring | GRQ18 | Probable moderate contamination | 4.3 | 4.0 | 4.5 |

*Potential rankings based on Chessman (1995).

Some small changes to the SIGNAL scores have occurred over time. When observing the SIGNAL scores from 2013 to 2021 there was a significant difference between the SIGNAL scores for the two treatments. The scores were on average higher in the reference sites. The improved SIGNAL scores also place the reference sites in a better Chessman SIGNAL classification. On average, at the times of sampling, the reference sites can be considered; of 'probable moderate contamination' and the discharge monitoring sites of 'probable severe contamination' the exception being the most distant discharge monitoring site (GRQ18) which was classified as 'probable moderate contamination'. Although we have provided ecological rankings for each site based on their long-term mean SIGNAL scores (Table 20), these scores varied widely within sites. Consequently, these rankings should be limited to emphasising that based on the SIGNAL approach, the reference sites showed better ecological condition than discharge monitoring sites Point 10, Point 12, Jutts, Pool 16 and Pool 32, rather than any specific gradient ranking.

### 3.7.3 Leptophlebiidae genera of interest (2016-2021)

Leptophlebiidae are recognised as sensitive macroinvertebrate taxa (Chessman 1995). The three main Leptophlebiidae taxa of interest; *Atelophlebia* spp*, Ulmerophlebia* spp and *Thraulophlebia* spp abundance for the nine sites from 2016 through to 2021 is presented in Figure 32. As indicated in Figure 32, both the abundance and the occurrence of all three Leptophlebiidae genera were higher in the reference treatment than the discharge monitoring treatment. It should be noted that Leptophlebiidae abundance increased at GRQ1 and GRUFS in Spring 2021. There has been a relative increase in the presence of the indicator species Leptophlebiidae at downstream

sites compared to previous surveys (Niche, 2022). *Ulmerophlebia* spp was most abundant in reference sites GRQ1 and GRUFS across all years. *Ulmerophlebia* spp were rarely observed in the discharge monitoring sites, historically being recorded at Jutts and GRQ18 in 2016. *Atelophlebia* in 2018 – 2021 has been more abundant compared to earlier years 2016-2017 (Figure 32). *Atelophlebia* spp was detected in the discharge monitoring sites Point 12, Jutts and Pool 16 in Spring 2021. GRQ18 contained *Atelophlebia* spp and *Ulmerophlebia* spp and high numbers of *Atelophlebia* spp in Spring 2021 (25 individuals). *Thraulophlebia* spp was predominantly observed in the reference treatment but was also present at downstream site GRQ18.

It has been suggested that specific Leptophlebiidae species are sensitive to conductivity (Cardno, 2010), leading to the recommendation by the Georges River Working Group to examine this group at the species level. The analysis of the 2016-2021 data also showed that *Atelophlebia* spp, *Ulmerophlebia* spp and *Thraulophlebia* spp were observed far more frequently and in higher abundances in the reference sites. The analysis of the 2016-2021 data showed an increase in all Leptophlebiidae in GRQ1 and GRUFS in spring 2021. *Atelophlebia* spp were more abundant at GRQ18 in 2018 and 2019 and again in 2020 and 2021 in GRQ18. A change was observed in that *Atelophlebia* spp was detected in low numbers at the discharge monitoring sites Point 12, Jutts and Pool 16 in Spring 2021. *Atelophlebia* spp remained rare however across all remaining discharge monitoring sites in 2020 and 2021. Leptophlebiidae have been reported to have ecological habitat preferences including riparian vegetation shade cover, low turbidity and flowing water, riffle habitats (Corbin and Goonan 2010). Leptophlebiidae are known to have physical habitat preferences and it is there for important to consider the physical habitat features of the sites, in addition to water flow and water quality where Leptophlebiidae are present rather than water chemistry alone.

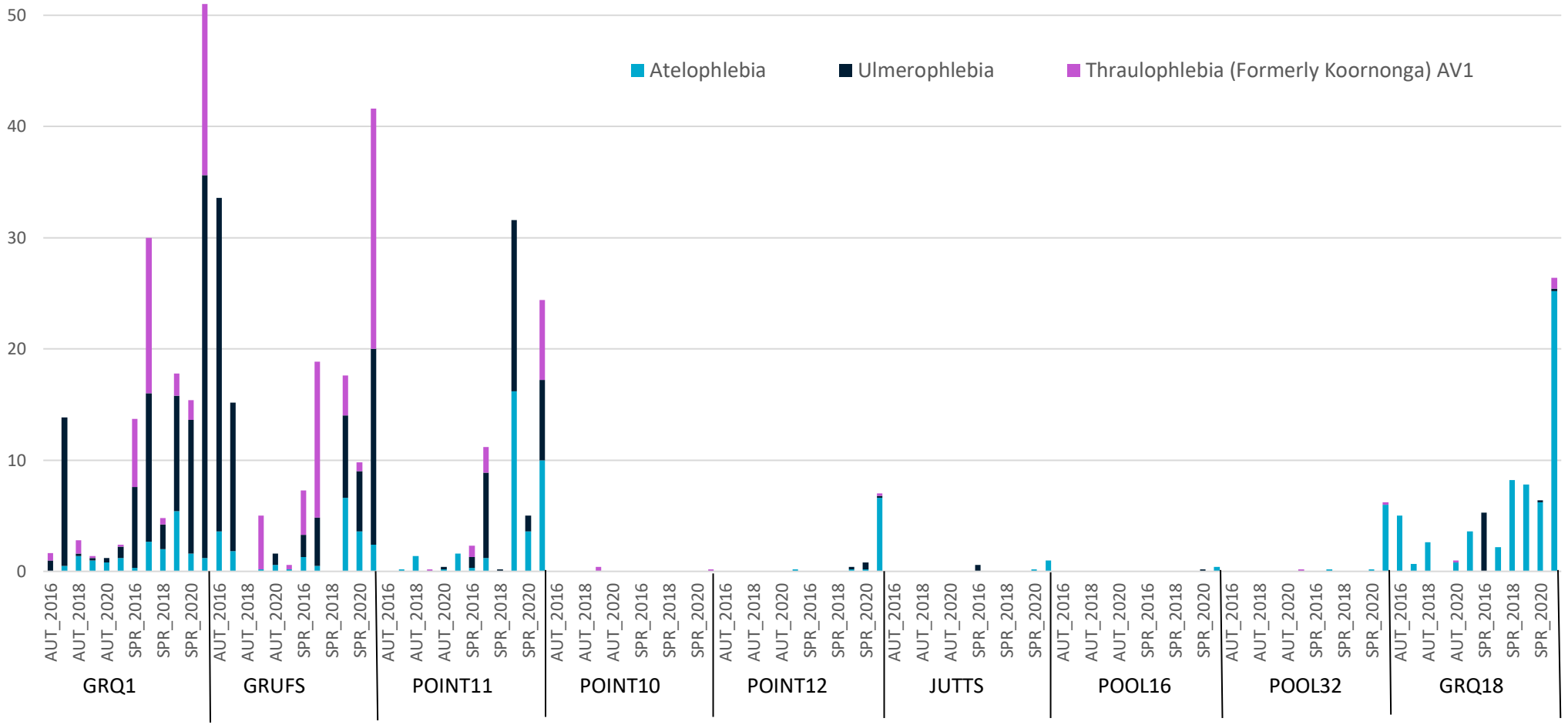


**Figure 32. Abundances of *Atelophlebia* spp., *Ulmerophlebia* spp. and *Thraulophlebia* (formerly *Koornonga*) spp. (2016-2021).**

## 3.8 Metabarcoding survey

This section describes the prokaryote, eukaryote and diatom metabarcoding diversity and community structure for the sampling occasions Spring 2019, Spring 2020 and Spring 2021. The correlative patterns of the metabarcoded OTU communities on the sampling occasions with the water quality variables measured are also presented here. The metabarcoding analysis performed in Spring 2020 and Spring 2021 clearly demonstrated the technique's capacity to capture a diverse range of taxa regardless of the environmental conditions. In contrast to the macrofauna survey, the broad eukaryotes and prokaryotes metabarcoding datasets contained several hundred taxa (OTUs), capturing a wide breadth of prokaryotes and eukaryotes.

### 3.8.1 16S rDNA metabarcoding (prokaryotes)

Across the nine sites surveyed a total of 10,430 OTUs were detected over the years 2019, 2020 and 2021. In 2019, 9622 OTUs were detected, compared with 10,313 OTUs and 10,155 OTUs in 2020 and 2021, respectively. The top 20 most abundant prokaryotic phyla detected at each site for the years 2019 through 2021 are shown in Figure 33 -Figure 35. In general, at the phylum level, prokaryotic community structure was similar across all sites and all years surveyed, with the Proteobacteria and Bacteroidetes being the dominant phyla observed.

At the family taxonomic level, however, some broad trends are apparent across the survey years. The top 20 most abundant families are shown in Figure 36 - Figure 38 as bubble plots and have been ordered by phylum. Prokaryotic families from the phylum Proteobacteria accounted for ten of the top 20 families detected. There are several prokaryotic families that increase in abundance at monitoring sites relative to the reference sites, including the Rhodobacteraceae and Verrucomicrobiaceae. Conversely, there are also families that decrease in relative abundance at the monitoring sites, including the Acidobacteria group 6 and the Bradyrhizobiaceae. These general trends were seen across the survey years. It is interesting to note that taxa from the Rhodobacteracea have been reported to biodegrade xenobiotic organic substrates (Pujalte et al., 2014; Siddavattam et al., 2011; Strnad et al., 2010). The family Verrucomicrobiaceae has had little taxonomic research, in large part because of the problem of uncultivability (Yoon, 2014) but have been identified as methane oxidisers (Guerrero-Cruz et al., 2021). Members of the Acidobacteria family are commonly found in soils and are underexplored again due to difficulties in culturing (Kalam et al., 2020). Comparative genomic analyses of the Acidobacteria revealed that members had metabolic versatility with the capacity to use a diverse collection of carbohydrates, as well as

inorganic and organic nitrogen sources possibly providing advantages in fluctuating nutrient environments (Eichorst et al., 2018). The Bradyrhizobiaceae family contain taxa that are able to use different nitrogen sources in their metabolism to perform fixation and/or other pathways of nitrogen assimilation (Marcondes De Souza et al., 2014). The Bradyrhizobiaceae are thus important components of the biogeochemical nitrogen cycle in various environments and may respond to disturbances in nitrogen levels.


**Figure 33. Bubble plot of the top 20 most abundant prokaryotic Phyla (on average across all sites) for 2019.**

% RA is % relative abundance shown as bubble size.


**Figure 34. Bubble plot of the top 20 most abundant prokaryotic Phyla (on average across all sites) for 2020.**

% RA is % relative abundance shown as bubble size.


**Figure 35. Bubble plot of the top 20 most abundant prokaryotic Phyla (on average across all sites) for 2021.**

% RA is % relative abundance shown as bubble size.

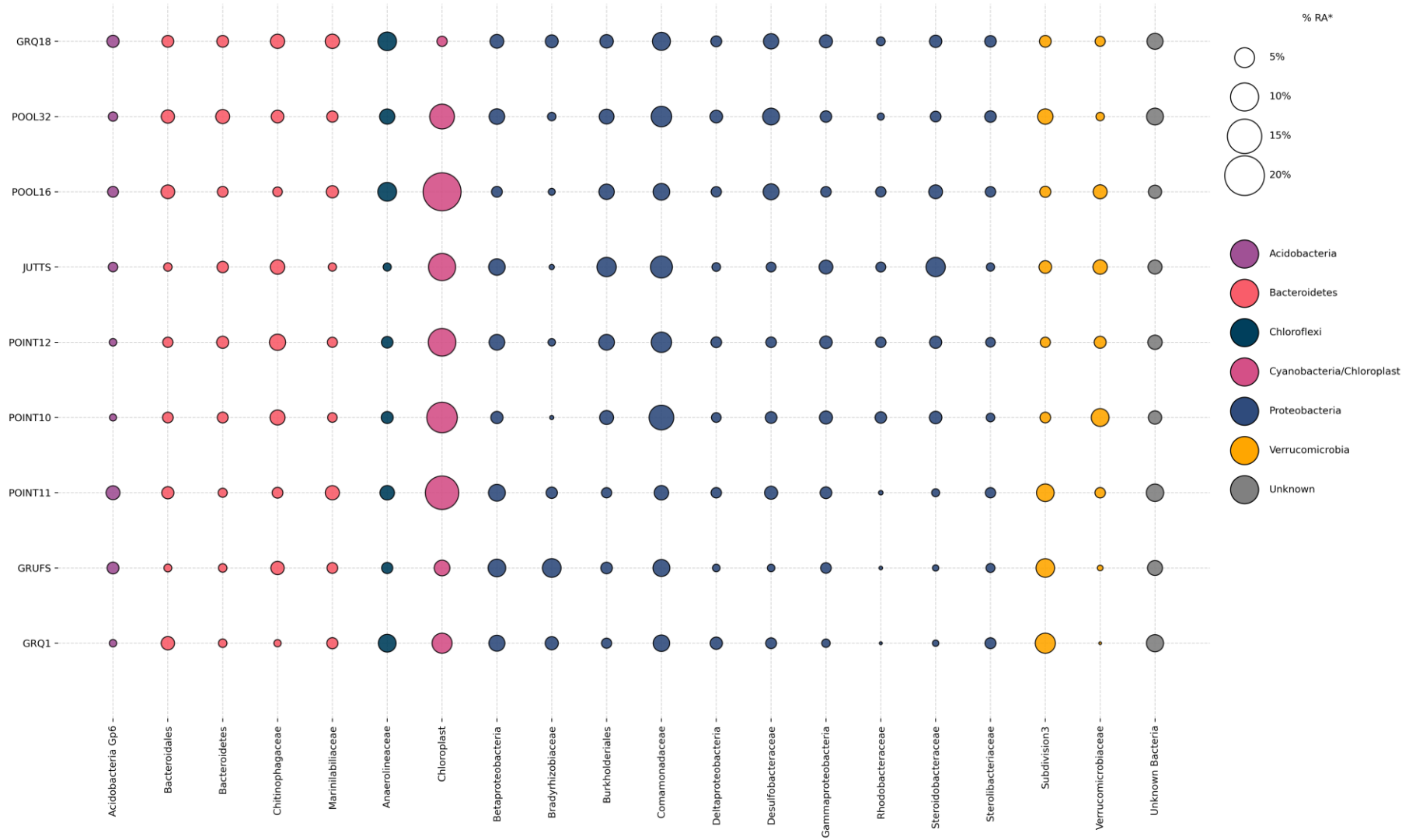


**Figure 36. Bubble plot of the top 20 most abundant prokaryotic Family (on average across all sites) for 2019.**

% RA is % relative abundance shown as bubble size.

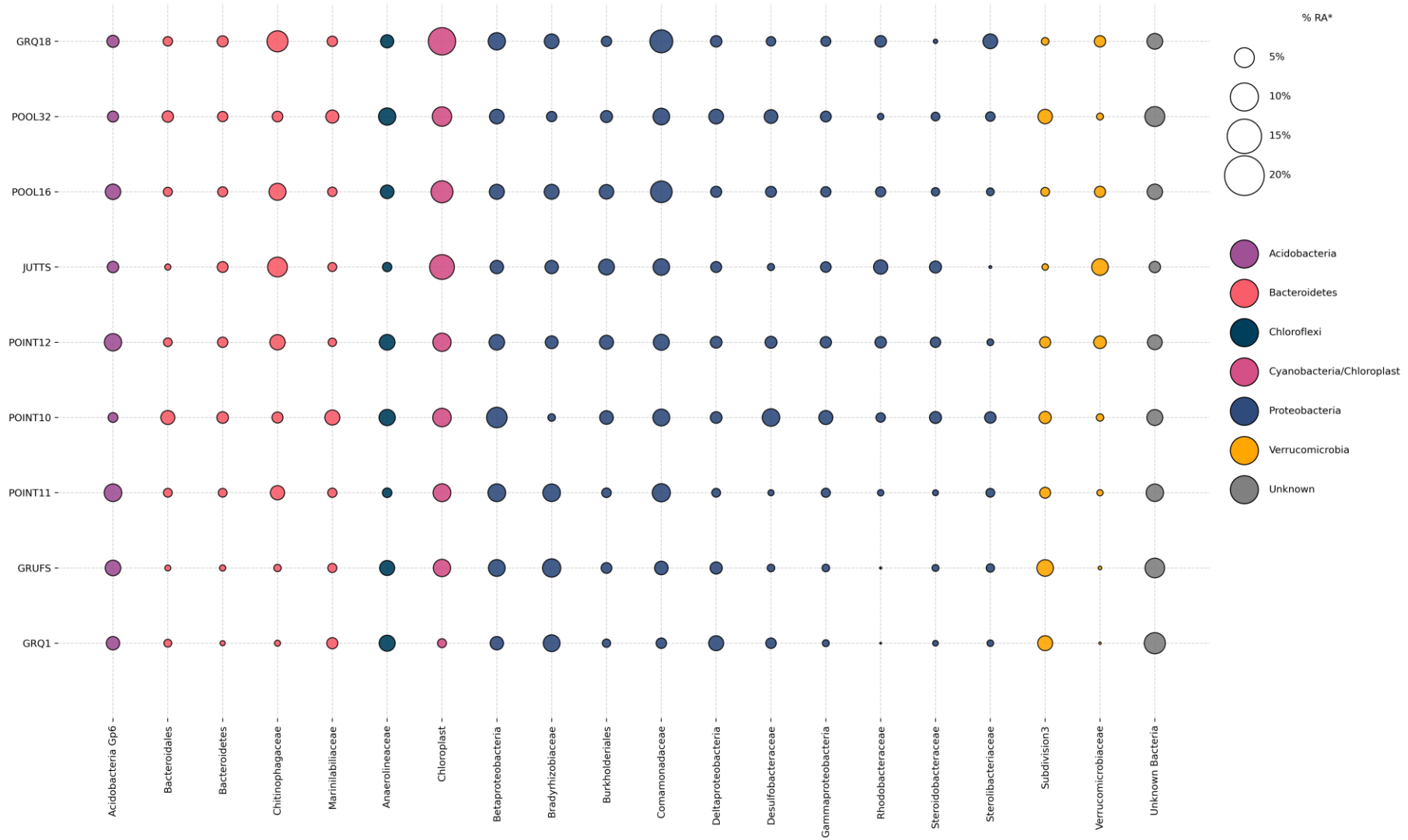


**Figure 37. Bubble plot of the top 20 most abundant prokaryotic Family (on average across all sites) for 2020.**

% RA is % relative abundance shown as bubble size.

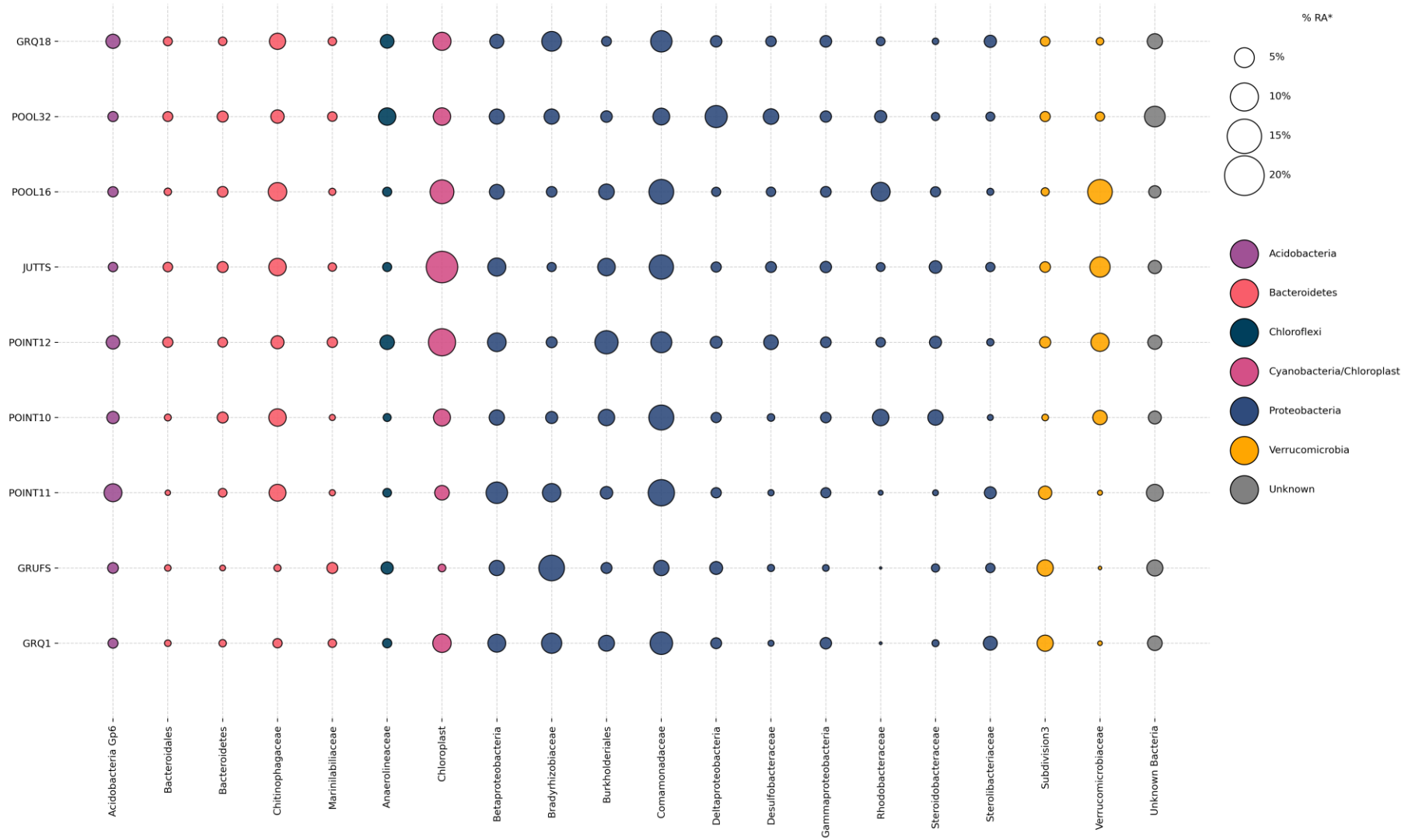


**Figure 38. Bubble plot of the top 20 most abundant prokaryotic Family (on average across all sites) for 2021.**

% RA is % relative abundance shown as bubble size.

### Prokaryote richness

Prokaryote richness for the nine sites over 2019, 2020 and 2021 is presented in Figure 39. Prokaryote richness exhibited a range of values across most sites, treatments, and sampling occasions (Figure 39). Generally, OTU richness was variable across the treatments with no significant difference between treatments in 2020 and 2021 (Table 21). This was in contrast to the Spring 2019 survey were there was significant difference between prokaryotic richness in reference and discharge monitoring treatments (Table 21).

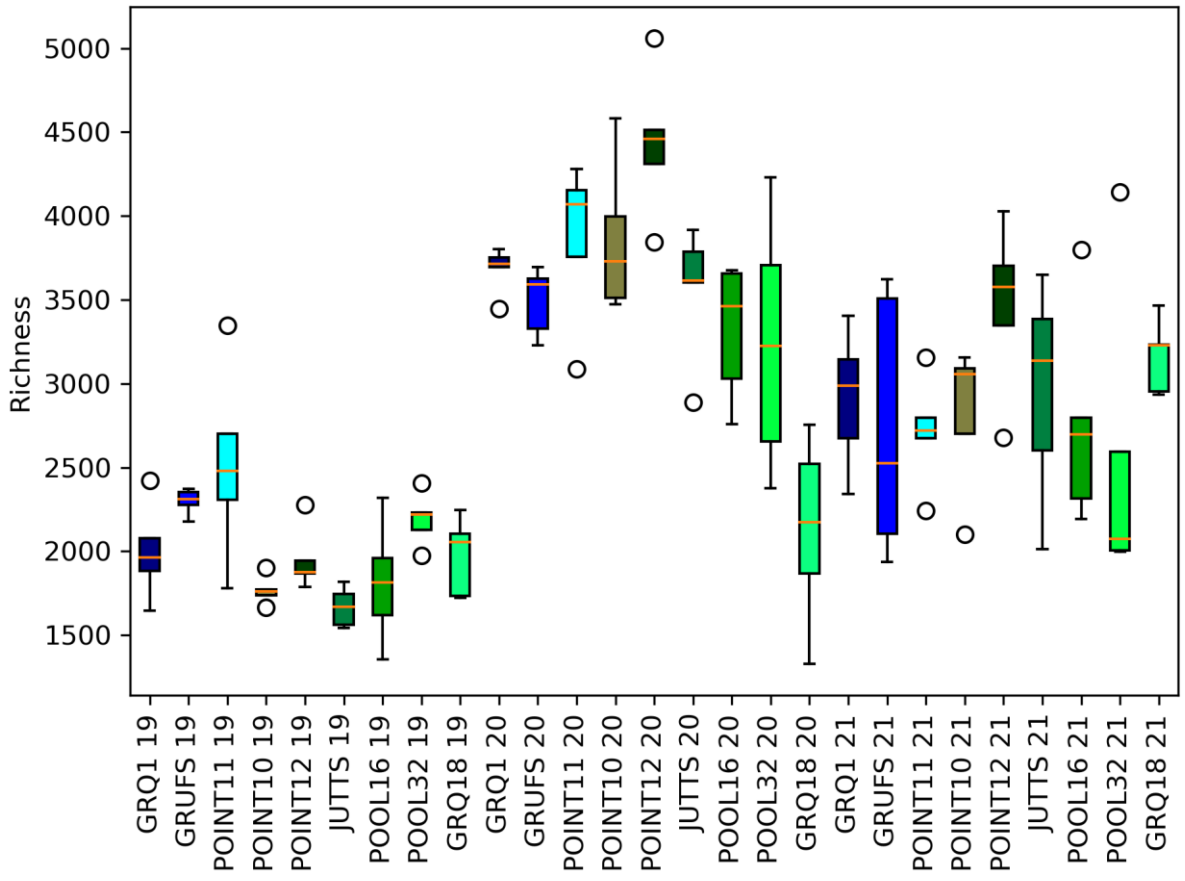


**Figure 39. 16S rDNA bacteria and archaea OTU richness from 2019, 2020 and 2021 OTUs.**

The interquartile range (IQR) between the first and third quartiles (25th and 75th percentiles, respectively) are represented by the boxes and the line inside the box is the median. The whiskers represent the highest and lowest values within 1.5 times the IQR from the first and third quartiles, respectively. outliers exceeding these values are represented as points. Reference sites (blue) and discharge monitoring sites (green).

**Table 21. One-Way ANOVA results on 16S prokaryote richness and read abundance for reference and discharge monitoring treatments.**

| **16S OTU Richness** | Reference | Reference | Discharge monitoring | Discharge monitoring | One-Way ANOVA | |
|---|---|---|---|---|---|---|
| | mean | ± S.E. | mean | ± S.E. | *F* | *p-value* |
| Spring 2019 | 2273 | 106 | 1894 | 47 | 14 | **<0.05** |
| Spring 2020 | 3682 | 85 | 3423 | 156 | 1.3 | 0.27 |
| Spring 2021 | 2789 | 133 | 2955 | 114 | 0.8 | 0.38 |
| **16S OTU read Abundance** | Reference | Reference | Discharge monitoring | Discharge monitoring | One-Way ANOVA | |
| | mean | ± S.E. | mean | ± S.E. | *F* | *p-value* |
| Spring 2019 | 14690 | 887 | 13969 | 431 | 0.68 | 0.4 |
| Spring 2020 | 42130 | 5050 | 37713 | 4149 | 0.41 | 0.5 |
| Spring 2021 | 28860 | 3392 | 30761 | 2740 | 0.17 | 0.7 |

Bold values represent p<0.05

### Prokaryote community composition

The prokaryote community composition, at the OTU level, from the reference sites were markedly different to those from the discharge monitoring sites for 2019, 2020 and 2021. The separation of reference from discharge monitoring site prokaryote communities for 2019, 2020 and 2021 is visualised in the nMDS ordination plots in Figure 40. There was a clear clustering of the reference sites together, separated away from the discharge monitoring sites (Figure 40). The reference sites GRUFS and GRQ1 cluster closer together, across all years, particularly in 2020 and 2021, while Point 11 is more separated. This may indicate the influence of other discharge inputs from Appin East but may also be indicative of geographical differences at Point 11. The prokaryotic communities observed at the discharge monitoring sites are more broadly spread across the nMDS compared to those of the reference sites which appear more tightly clustered (Figure 40). In general, however, the discharge monitoring sites showed a broadly similar prokaryotic composition that was separate from the reference sites.

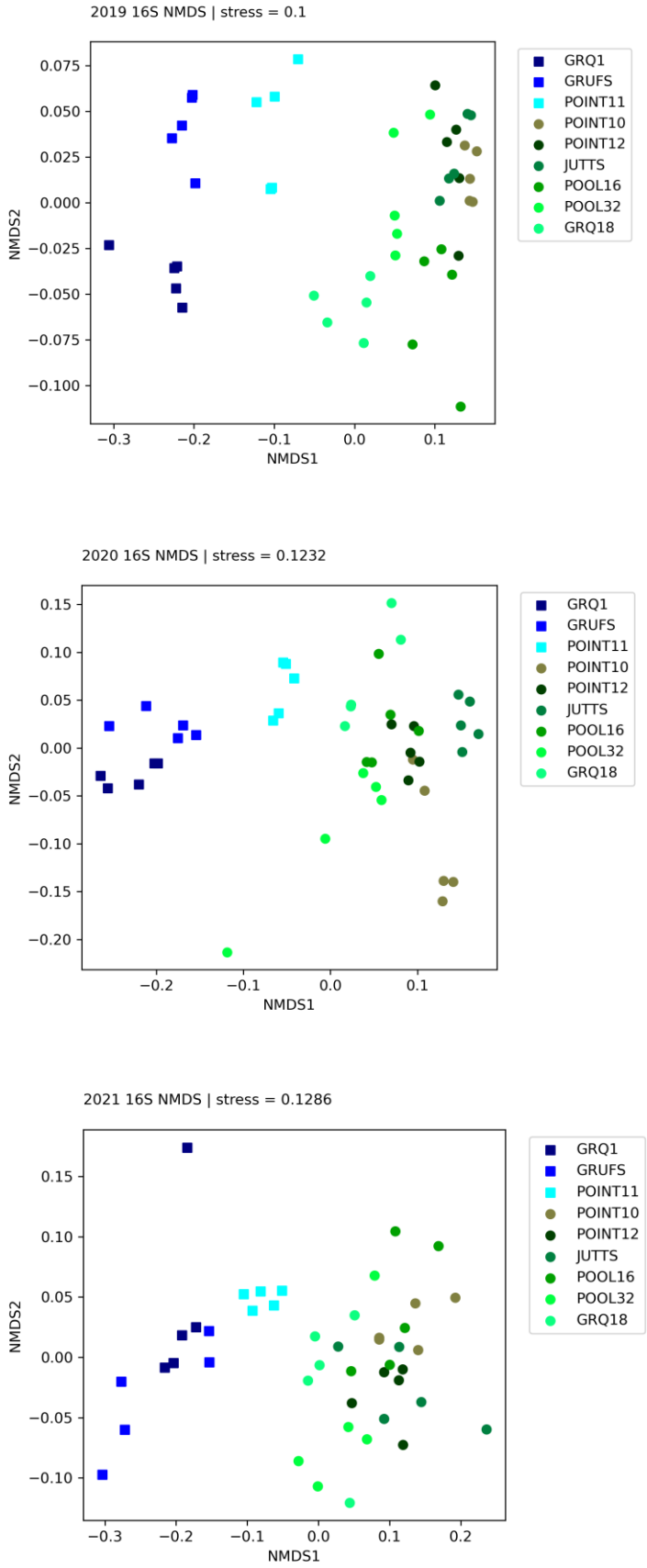


**Figure 40. nMDS of 16S OTU bacteria and archaea communities (2019, 2020 and 2021).**

a) Spring 2019; b) Spring 2020 c) Spring 2021. Analysis is derived from normalised abundance data at the level of Operational Taxonomic Unit (OTU).

PERMANOVA tests were undertaken to investigate 16S rDNA OTU community structure differences in treatments and time. The results of the PERMANOVAs testing for differences in 16SrDNA community composition between sampling timepoints (Spring 2019, 2020 and Spring 2021) and treatments are presented in Table 22. The visual separation of treatments observed in the nMDS (Figure 40) is confirmed by the PERMANOVA which found a significant difference in composition between the two treatments in Spring 2019 (PERMANOVA: F= 21, $p<0.05$), Spring 2020 (PERMANOVA: F= 19 $p<0.05$) and in Spring 2021 (PERMANOVA: F= 18, $p<0.05$). Significant differences in community composition were found with respect to time (season/year) (PERMANOVA: F= 8, $p<0.05$) and treatment (reference or discharge monitoring), when tested individually (Table 22). In addition, there was a significant interaction between time and treatment (PERMANOVA: F= 3, $p<0.05$) (Table 22). PERMANOVA results also revealed significant differences observed at the site level for prokaryotes (Appendix B; Tables B1-B3). In 2019 all sites were significantly different from each other except for Jutts and Point 12, these sites were more similar in prokaryote composition. In 2020 all sites were significantly different from each other. In 2021 most sites were significantly different from each other; the exceptions were Point 12 and Jutts which were not different from each other and Pool 16 and Jutts also had similar prokaryote compositions.

**Table 22. Results of PERMANOVA testing for variation in 16S rDNA community composition (2019, 2020 & 2021) between timepoints (years), and treatments (reference vs discharge monitoring).**

| Factor: source of variation | df | MS | Pseudo-F | P(perm) | Unique perms |
|---|---|---|---|---|---|
| **Treatment (2019)** | 1 | 29079 | 21 | **0.0001** | 9901 |
| **Treatment (2020)** | 1 | 27784 | 19 | **0.0001** | 9892 |
| **Treatment (2021)** | 1 | 20354 | 18 | **0.0001** | 9913 |
| **Time (year)** | 2 | 12921 | 8 | **0.0001** | 9885 |
| **Treatment (2019-2021)** | 1 | 59622 | 41 | **0.0001** | 9915 |
| **Time*Treatment** | 2 | 3932 | 3 | **0.0001** | 9807 |
| **Res** | 129 | 1248 | | | |
| **Total** | 132 | | | | |

Df: degrees of freedom; MS: mean squares; Pseudo-F: multivariate analogue to Fisher's F test statistic of the null hypothesis; P(perm): probability by permutations; Unique Perms: number of unique permutations.

Bold values denote significance at $p< 0.05$.

### 3.8.2 Relationships between prokaryotic community and water quality (2019-2021)

Correlation analysis is presented across all years as well as for each separate year. Prokaryotic community structure and water quality variable correlations were investigated using multivariate statistics including distance linear models (DistLM). The fitted DistLM was visualised using a distance-based redundancy analysis (dbRDA) constrained ordination (Figure 41), demonstrating the correlation of significant variables on the prokaryote community for 2019, 2020 and 2021 datasets combined. The distance-based analysis of the 16S data (2019-2021) found the measured variables including conductivity, alkalinity, nickel, pH, copper, total nitrogen, aluminium, and zinc explained 70% of the total prokaryotic community variation. The distance-based analysis investigating the correlative patterns of the prokaryotic community data with measured environmental variables is shown in Table 23. When examined collectively, the variables which explained a significant proportion ($p<0.05$) of the prokaryotic community structure variation across the period 2019, 2020 and 2021 included conductivity, alkalinity, nickel, pH and copper (Table 23). The variable which explained the most prokaryotic community variation for 2019, 2020 and 2021 was conductivity, explaining 36% of the total variation. The dbRDA (Figure 41) for the prokaryote community shows that axis1 (dbRDA 1) is explaining approximately 41% of the total variation, mostly correlated with conductivity and axis 2 (dbRDA 2), mostly correlated with alkalinity, is explaining approximately 13% of the total prokaryote community composition.

**Table 23. Sequential test results of distance-based linear model (DistLM) for bacteria and archaea OTUs for 2019, 2020 and 2021 data.**

| Variable | Adj $R^2$ | SS(trace) | Pseudo-F | P | Prop%. | Cumulative contribution | res.df |
|---|---|---|---|---|---|---|---|
| **+Conductivity µS/cm** | 0.34 | 11596 | 14.1 | **0.0001** | 0.36 | 0.36 | 25 |
| **+Alkalinity** | 0.44 | 3785.5 | 5.4 | **0.0001** | 0.12 | 0.48 | 24 |
| **+Nickel** | 0.46 | 1486.3 | 2.2 | **0.0061** | 0.05 | 0.53 | 23 |
| **+pH** | 0.49 | 1434.1 | 2.3 | **0.0056** | 0.04 | 0.57 | 22 |
| **+Copper** | 0.52 | 1292.7 | 2.2 | **0.0089** | 0.04 | 0.61 | 21 |
| **+Total Nitrogen** | 0.53 | 890.7 | 1.5 | 0.0733 | 0.03 | 0.64 | 20 |
| **+Aluminium** | 0.54 | 737.6 | 1.3 | 0.1744 | 0.02 | 0.66 | 19 |
| **+Zinc** | 0.55 | 827.7 | 1.5 | 0.1021 | 0.03 | 0.69 | 18 |
| **+Cobalt** | 0.55 | 581.3 | 1.0 | 0.3979 | 0.02 | 0.71 | 17 |

SS(trace): sum of squares; Pseudo-F: multivariate analogue to Fisher's F test statistic of the null hypothesis; P: probability; Prop%: the proportion of variation; res.df: residual degrees of freedom

Bold values denote significance at $p< 0.05$.

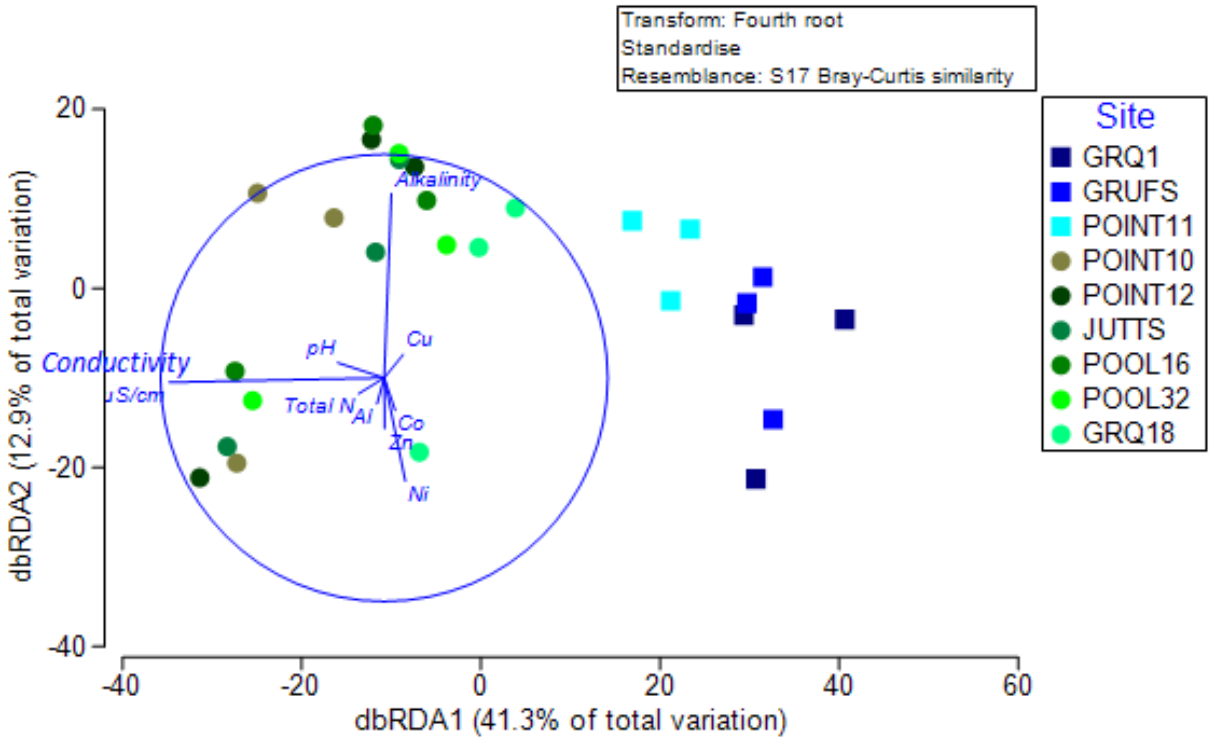


**Figure 41. Ordination plot derived from the distance-based model illustrating the relationships between key environmental variables and metabarcoded prokaryotes composition from Spring 2019 - 2021.**

Reference sites (blue) and discharge monitoring sites (green).

### 2019 prokaryote community relationships with water quality

The fitted DistLM for the 2019 data was visualised using a dbRDA constrained ordination (Figure 42), demonstrating the correlation of significant variables on the prokaryote community for the 2019 sampling occasion. The distance-based analysis investigating the correlative patterns of the prokaryotic community data with measured environmental variables in 2019 is shown in Table 24. The distance-based analysis of the prokaryote data for 2019 found the measured variables including conductivity, pH, nickel, and aluminium explained 84% of the total prokaryotic community variation. When examined collectively, the variables which significantly ($p<0.05$) explained the variation in the prokaryotic community in 2019 were conductivity (57%), pH (12%), and nickel (8%) (Table 24). Figure 42 shows that dbRDA1 is explaining 58% of the total variation and dbRDA2 is explaining 13% of the total biological variation. Figure 42 also shows the discharge monitoring sites at the right of the dbRDA1 correlated with conductivity while a small proportion is contributed by dbRDA2 which is shown to be driven by pH. The dbRDA presents conductivity as the main variable separating the discharge monitoring treatments from the reference treatments in 2019.

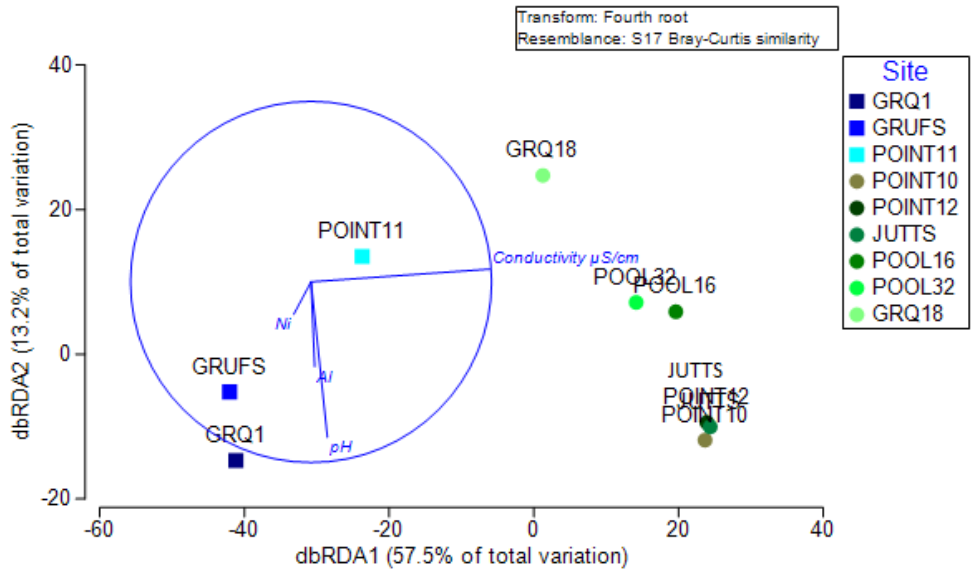


**Figure 42. Ordination plot derived from the distance-based model illustrating the relationships between key environmental variables and metabarcoded prokaryotes composition from Spring 2019.**

**Table 24. Sequential test results of distance-based linear model (DistLM) for prokaryote 2019 data.**

| Variable | Adj $R^2$ | SS(trace) | Pseudo-F | P | Prop%. | Cumulative contribution | res.df |
|---|---|---|---|---|---|---|---|
| **+Conductivity µS/cm** | 0.50 | 6242.5 | 9.1 | **0.0001** | 0.57 | 0.57 | 7 |
| **+pH** | 0.58 | 1308.2 | 2.3 | **0.013** | 0.12 | 0.69 | 6 |
| **+Nickel** | 0.63 | 927.7 | 1.8 | **0.046** | 0.084 | 0.77 | 5 |
| **+Aluminium** | 0.69 | 830.12 | 1.9 | 0.08 | 0.075 | 0.84 | 4 |

SS(trace): sum of squares; Pseudo-F: multivariate analogue to Fisher's F test statistic of the null hypothesis; P: probability; Prop%: the proportion of variation; res.df: residual degrees of freedom

Bold values denote significance at p< 0.05.

### 2020 prokaryotic community relationships with water quality

The 2020 fitted DistLM was visualised using a dbRDA constrained ordination (Figure 43), demonstrating the correlation of significant variables on the prokaryote community for the 2020 sampling occasion. The distance-based analysis of the prokaryotic community data for 2020 found the measured variables including pH, conductivity, copper, and zinc explained 96% of the total variation in prokaryotic community in 2020. The distance-based analysis investigating the correlative patterns of the prokaryotic community data with measured environmental variables in 2020 is shown in Table 25. When examined collectively, the variable which significantly explained the variation in the prokaryotic community in 2020 was pH (46%) (Table 25). Of all variables measured, pH showed the greatest contribution to the prokaryotic community variation in 2020.

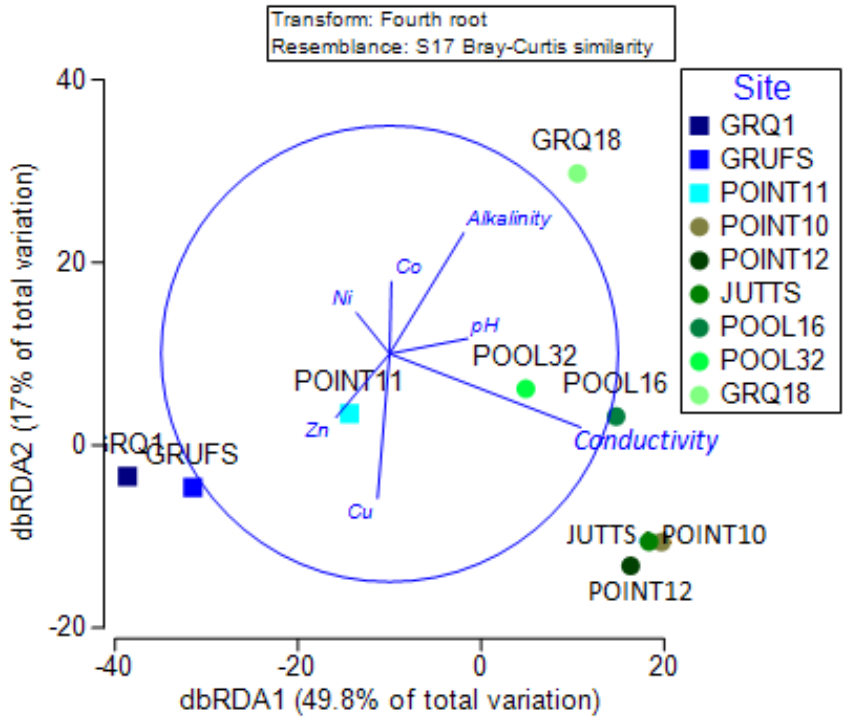


**Figure 43. Ordination plot derived from the distance-based model illustrating the relationships between key environmental variables and metabarcoded prokaryotes composition from Spring 2020.**

**Table 25. Sequential test results of distance-based linear model (DistLM) for prokaryote 2020 data.**

| Variable | Adj $R^2$ | SS(trace) | Pseudo-F | P | Prop%. | Cumulative contribution | res.df |
|---|---|---|---|---|---|---|---|
| **+pH** | 0.38 | 3688.3 | 5.9 | **0.0013** | 0.46 | 0.46 | 7 |
| **+Conductivity µS/cm** | 0.41 | 819 | 1.4 | 0.2154 | 0.10 | 0.56 | 6 |
| **+Copper** | 0.48 | 963.3 | 1.8 | 0.097 | 0.12 | 0.68 | 5 |
| **+Zinc** | 0.52 | 685.4 | 1.4 | 0.2316 | 0.08 | 0.76 | 4 |
| **+Cobalt** | 0.56 | 597.8 | 1.3 | 0.3213 | 0.07 | 0.83 | 3 |
| **+Alkalinity** | 0.57 | 473.6 | 1.1 | 0.4571 | 0.06 | 0.89 | 2 |
| **+Nickel** | 0.66 | 526.6 | 1.6 | 0.3912 | 0.07 | 0.96 | 1 |

SS(trace): sum of squares; Pseudo-F: multivariate analogue to Fisher's F test statistic of the null hypothesis; P: probability; Prop%: the proportion of variation; res.df: residual degrees of freedom

Bold values denote significance at p< 0.05.

**2021 prokaryotic community relationships with water quality**

The fitted DistLM was visualised using a dbRDA constrained ordination (Figure 44), demonstrating the correlations of significant variables on the prokaryote community for the 2021 data. The distance-based analysis of the prokaryotic community data for 2020 found the measured variables including pH, aluminium, total nitrogen, alkalinity, conductivity, copper, and zinc explained 97% of the total 2021 prokaryotic community variation. The distance-based analysis investigating the relationships of the prokaryotic community data with measured environmental variables in 2021, is shown in Table 26. When examined collectively, the variables which significantly explained the variation in the prokaryotic community in 2021 were pH (55%), and total nitrogen (9%). The strongest variable which explained most of the prokaryotic community variation in 2021 was pH again, like in 2020, explaining 55% of the total prokaryotic community variation. In 2020 and in 2021 pH was the dominant driver explaining variation in the prokaryotic community composition.

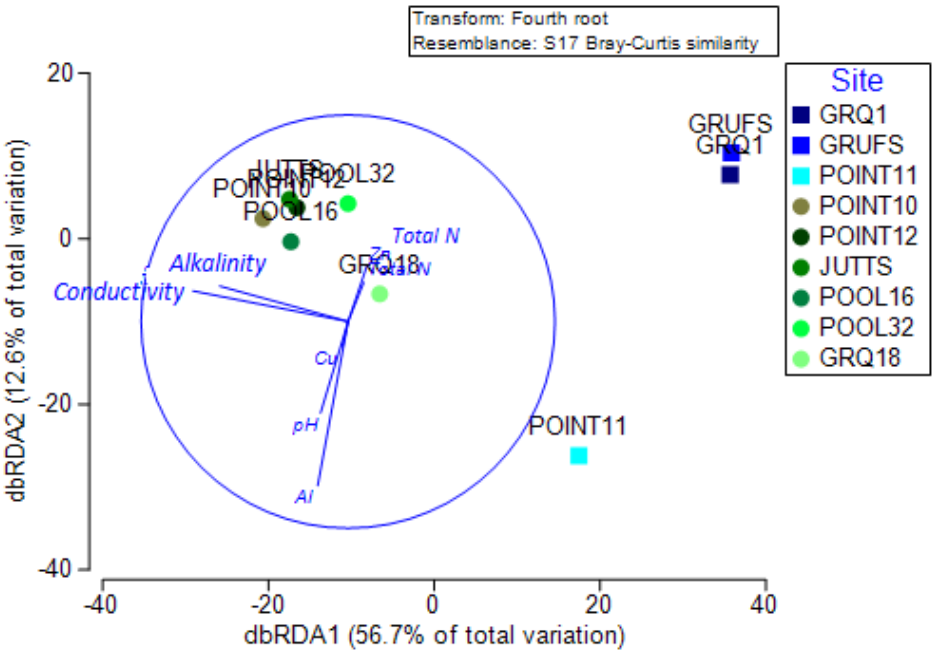


**Figure 44. Ordination plot derived from the distance-based model illustrating the relationships between key environmental variables and metabarcoded prokaryotes composition from Spring 2021.**

**Table 26. Sequential test results of distance-based linear model (DistLM) for prokaryote 2021 data.**

| Variable | Adj $R^2$ | SS(trace) | Pseudo-F | P | Prop%. | Cumulative contribution | res.df |
|---|---|---|---|---|---|---|---|
| **pH** | 0.49 | 4195.0 | 8.6 | **0.0001** | 0.55 | 0.55 | 7 |
| **Aluminium** | 0.54 | 785.1 | 1.8 | 0.055 | 0.10 | 0.65 | 6 |
| **Total Nitrogen** | 0.60 | 746.2 | 2.0 | **0.049** | 0.10 | 0.75 | 5 |
| **Alkalinity** | 0.62 | 457.7 | 1.3 | 0.30 | 0.06 | 0.81 | 4 |
| **Conductivity µS/cm** | 0.65 | 429.0 | 1.3 | 0.32 | 0.06 | 0.87 | 3 |
| **Copper** | 0.68 | 404.8 | 1.3 | 0.33 | 0.053 | 0.92 | 2 |
| **Zinc** | 0.76 | 373.5 | 1.6 | 0.41 | 0.049 | 0.97 | 1 |

SS(trace): sum of squares; Pseudo-F: multivariate analogue to Fisher's F test statistic of the null hypothesis; P: probability; Prop%: the proportion of variation; res.df: residual degrees of freedom

Bold values denote significance at $p< 0.05$.

The key OTUs which contributed to the observed differences in microbial composition between reference and discharge monitoring sites can be seen from the SIMPER analyses (Table 27). SIMPER analysis explains the dissimilarity between treatment and site composition. The top 10 prokaryote taxa which contributed most to the differences between reference and discharge monitoring treatments for the sampling years 2019, 2020 and 2021 are presented in Table 27 and their taxonomic assignments are listed in Table 28. These data are presented relative to the mean of the reference sites, such that a positive value indicates an increase in relative abundance compared to the reference site mean and a negative value indicates a decrease in relative abundance compared to the reference site mean.

Generally, these data indicate that there are a large number of OTUs that are positively affected at all downstream monitoring sites, however, there are also some OTUs that are negatively affected at monitoring sites. Some OTUs have also been identified as drivers of dissimilarity in multiple years. In some instances, probably contamination by pollen from trees, or plant material located on the riverbank have been identified (e.g., OTU_44: *Streptophyta* sp | *Coffea arabica* at Pool 16; OTU_5: *Streptophyta* sp | *Illicium oligandrum* at Jutts in 2020 and 2021; OTU_28: Streptophyta sp | *Chara vulgaris*). It should be noted that some OTUs listed in Table 28 (e.g., OTU_9, OTU_17, OTU_44) have low similarity to the closest species in GenBank (Match %), indicating that these OTUs are likely to be novel organisms.

Of the OTUs that increased in the monitoring sites, OTU_3 and OTU_10 increased in all monitoring sites in 2019 through to 2021. OTU_8 increased in only 2020 and 2021. OTUs 23 and 25 increased in 2020 and 2019, respectively. OTU_3 was identified as the diatom *Phaeodactylum tricornutum*. It should be noted that bacterial 16S rDNA primers also have high affinity for eukaryotic plastid DNA

(Gan et al., 2019). These primers also often co-amplify non-target sequences from chloroplasts and mitochondria (Gan et al., 2019). OTU_3 increased in all years at monitoring sites and this may be due to increased availability of nutrients. OTU_10, is related to *Povalibacter uvarum*, a Gram-negative aerobic chemo-organotroph that is capable of degrading polyvinyl-alcohols (Nogi et. al., 2014) and may be able to access carbon from other complex synthetic polymers. OTU_8 is closely related to *Tabrizicola aquatica*, a Gram-negative bacterium isolated from a potentially disturbed lake near the city of Tabriz, Iran (Tarhriz et al., 2019). This organism has been shown to be able to produce bacteriochlorophyll and is able to grow photosynthetically. OTU_25 is poorly taxonomically resolved, it's closest match being a strain of a recently described species, *Zeimonas arvi* from the family *Burkholderiaceae* (Lin et al., 2021), isolated from soils and shown to harbour xenobiotic-metabolising genes. Other members of the family *Burkholderiaceae* are ecologically significant due to their ability to metabolise aromatic compounds (Hameed et al.2019; Wilhelm et al.2020). OTU_23 is related to a *Desulfobulbus propionicus* (DSM 2032) isolated from a sulfate-reducing fluidised-bed reactor used for treating acidic metal-containing wastewater (Kaksonen et al., 2004). This taxon is known to oxidise elemental sulfur to sulfate and reduce sulfate to sulfide (Lovely and Phillips, 1994) and been implicated in sulfur cycling in aquatic sediments (Pagani et al., 2011). Similarly, OTU_19, a taxon related to *Thiobacillus thioparus* (Boden et al., 2012), may also be involved in sulfur cycling, although it had a variable response across the monitoring sites.

Of the OTUs that decreased in the monitoring sites, there were none that decreased in all three survey years examined here. In all cases where an OTU decreased it did so in only one survey year. In 2019 a marked decrease in OTU_28 (*Chara vulgaris*; a common green macro-algal species) was seen. In 2020 a marked decrease in OTU_6 (*Massilia namucuonensis*) (Kong et al., 2013), and in 2021 decreases in OTUs 9 (*Reticulibacter mediterranei*) (Yabe et al., 2021) and 13 (*Bradyrhizobium lupini*) (Peix et al., 2015) were seen. These OTUs are the only few taxa that respond negatively in a universal way and may potentially be putative indicator taxa for environmental disturbance as they responded negatively at all the monitoring sites.

Several OTUs had variable responses at the monitoring sites, showing both increases and decreases relative to the reference mean. This could indicate that the multiple factors may be contributing to responses. These factors could be geographical, light conditions, vegetation particular to the monitoring site.

**Table 27. SIMPER results illustrating the top 10 prokaryotes that account for most of the dissimilarities between the reference and discharge monitoring sites (2019, 2020 and 2021).**

| | | | Change from Mean Reference | | | | | | |
|---|---|---|---|---|---|---|---|---|---|
| Year | Taxon | Mean Reference | POINT10 | POINT12 | JUTTS | POOL16 | POOL32 | GRQ18 | Comment |
| 2019 | OTU_3 | 0.919 | 3.881 | 4.961 | 5.891 | 6.701 | 3.451 | -0.213 | Mostly increased at monitoring sites |
| | OTU_28 | 4.92 | -4.8375 | -4.91432 | -4.91394 | -4.91181 | -4.8805 | -4.8308 | Decreased at all monitoring sites |
| | OTU_44 | 0.00175 | -0.00175 | 0.02005 | 0.03305 | 8.17825 | 0.00091 | -0.00175 | Probable pollen contamination |
| | OTU_10 | 0.109 | 1.831 | 1.641 | 4.481 | 2.241 | 1.101 | 1.331 | Increased at all monitoring sites |
| | OTU_16 | 0.317 | 4.783 | 2.133 | 0.983 | -0.159 | 0.602 | -0.2369 | Variable response at monitoring sites |
| | OTU_7 | 1.46 | 2.14 | 1.08 | 2.23 | 0.18 | 1.59 | 0.45 | Variable response at monitoring sites |
| | OTU_4 | 0.149 | 1.071 | 1.241 | 1.871 | 1.041 | 0.786 | 0.881 | Increased at all monitoring sites |
| | OTU_17 | 0.00336 | 0.02324 | 0.02954 | 0.65264 | 0.03234 | 0.03424 | 3.68664 | Variable response at monitoring sites |
| | OTU_25 | 0.0046 | 0.8074 | 1.0954 | 1.8654 | 0.8954 | 0.7224 | 0.7114 | Increased at all monitoring sites |
| | OTU_19 | 0.138 | 0.788 | 0.822 | 1.032 | 1.032 | 0.301 | 0.048 | Variable response at monitoring sites |
| 2020 | OTU_3 | 0.81 | 2.09 | 1.61 | -0.004 | 0.36 | 1.6 | 5.73 | Variable response at monitoring sites |
| | OTU_5 | 0.0259 | -0.02302 | 0.0344 | 5.3041 | 3.7841 | -0.0033 | 0.2991 | Variable response at monitoring sites |
| | OTU_6 | 3.15 | -3.1283 | -3.1185 | -3.1341 | -3.0892 | -3.1428 | -3.101 | Decreased at all monitoring sites |
| | OTU_7 | 1.23 | 0.91 | 0.42 | 0.63 | 2.11 | 0.78 | 1.54 | Variable response at monitoring sites |
| | OTU_10 | 0.0387 | 1.6613 | 1.0913 | 1.6313 | 0.6583 | 0.6443 | 0.0365 | Increased at all monitoring sites |
| | OTU_8 | 0.0981 | 0.5439 | 1.0319 | 1.5819 | 0.9119 | 0.2369 | 1.4319 | Increased at all monitoring sites |
| | OTU_19 | 0.371 | 0.859 | 0.217 | -0.158 | 1.969 | 0.132 | -0.001 | Variable response at monitoring sites |
| | OTU_4 | 0.114 | 0.873 | 1.036 | 1.386 | 0.634 | 0.537 | 0.04 | Variable response at monitoring sites |
| | OTU_23 | 0.0335 | 0.3765 | 0.5105 | 1.7565 | 0.0377 | 0.1245 | 0.3135 | Mostly increased at monitoring sites |
| | OTU_14 | 0.438 | 0.572 | -0.112 | -0.383 | 0.02 | 0.252 | 1.452 | Variable response at monitoring sites |
| 2021 | OTU_9 | 4.24 | -4.2074 | -4.23089 | -4.23377 | -4.2296 | -4.2349 | -4.218 | Decreased at all monitoring sites |
| | OTU_7 | 2.54 | 1.77 | 0.55 | 2.16 | 1.76 | -0.76 | 0.75 | Variable response at monitoring sites |
| | OTU_5 | 0.145 | -0.1327 | 0.33 | 6.355 | 0.085 | -0.015 | -0.1092 | Probable pollen contamination |
| | OTU_3 | 0.52 | 1.79 | 3.39 | 1.99 | 0.393 | 0.54 | 1.02 | Increased at all monitoring sites |
| | OTU_17 | 0.0093 | 0.0109 | 0.3537 | 0.0161 | 0.0246 | 0.0162 | 6.8007 | Increased at all monitoring sites |
| | OTU_8 | 0.0864 | 2.5636 | 0.7296 | 0.6146 | 3.1136 | 1.4936 | 0.6346 | Increased at all monitoring sites |
| | OTU_13 | 2.31 | -2.071 | -2.008 | -2.115 | -1.99 | -1.889 | -0.01 | Decreased at all monitoring sites |
| | OTU_12 | 0.00876 | 5.42124 | 0.11424 | 0.00854 | 0.45324 | 0.01604 | 0.08344 | Variable response at monitoring sites |
| | OTU_15 | 0.048 | 0.799 | 1.572 | 1.122 | 3.162 | 0.224 | 0.098 | Variable response at monitoring sites |
| | OTU_10 | 0.034 | 2.736 | 1.576 | 1.566 | 0.966 | 0.578 | 0.196 | Increased at all monitoring sites |

**Table 28. List of OTU, closest taxonomic assignment and match % that account for most of the dissimilarities between the reference and discharge monitoring sites (2019, 2020 and 2021).**

| Taxon | Closest species | Match % |
|---|---|---|
| **OTU_3** | *Bacillariophyta* sp (*Phaeodactylum tricornutum* (EF067920)) | 98.4 |
| **OTU_4** | *Burkholderiales* sp (*Noviherbaspirillum denitrificans* TSA40 (NR 157007)) | 94.5 |
| **OTU_5** | *Streptophyta* sp (*Illicium oligandrum* (EF380354)) | 100 |
| **OTU_6** | *Massilia namucuonensis* 333-1-0411 (NR 118215) | 100 |
| **OTU_7** | *Comamonadaceae* sp (*Azohydromonas riparia* UCM-11 (NR 149203)) | 98.8 |
| **OTU_8** | *Rhodobacteraceae* sp (*Tabrizicola aquatica* RCRI19 (NR 117979)) | 100 |
| **OTU_9** | *Ktedonobacterales* sp (*Reticulibacter mediterranei* 150040 (NR 173686)) | 87.7 |
| **OTU_10** | *Povalibacter* sp (*Povalibacter uvarum* Zumi 37 (NR 126172)) | 96 |
| **OTU_12** | *Cyanobacteria* sp (*Tychonema bourrellyi* CCAP 1459/11B (NR 112123)) | 100 |
| **OTU_13** | *Bradyrhizobium lupini* USDA 3051 (NR 134836) | 100 |
| **OTU_14** | *Georgfuchsia toluolica* G5G6 (NR 115995) | 99.2 |
| **OTU_15** | *Luteolibacter gellanilyticus* CB-286403 (NR 158117) | 98.4 |
| **OTU_16** | *Bacillariophyta* sp (*Phaeodactylum tricornutum* (EF067920)) | 97.6 |
| **OTU_17** | *Cyanobacteria* sp (*Xenococcus spongiosum* TAU-MAC 0615 (NR 172570)) | 91.3 |
| **OTU_19** | *Thiobacillus thioparus* (NR 117560) | 99.6 |
| **OTU_23** | *Desulfobulbus* sp (*Desulfobulbus propionicus* DSM 2032 DSM 2032 (NR 042971)) | 95.3 |
| **OTU_25** | *Burkholderiales* sp (*Zeimonas arvi* CC-CFT501 (NR 173635)) | 94.1 |
| **OTU_28** | *Streptophyta* sp (*Chara vulgaris* (DQ229107)) | 98 |
| **OTU_44** | *Streptophyta* sp (*Coffea arabica* (EF044213)) | 93.7 |

### 3.8.3 18S V7 rDNA metabarcoding (broad eukaryotes)

Sequencing data from 2019 in addition to 2020 and 2021 were included in the 18S V7 rDNA OTU broad eukaryote analysis to make comparisons of OTUs compositions at the study sites and treatments over time. Across the nine sites surveyed, the broad eukaryotes dataset contained 2,026,809 reads encompassing 718 OTUs in 2019, 948 OTUs in 2020 and 915 OTUs in 2021 from 48 phyla and 388 unique families. The 18S V7 rDNA broad eukaryote marker provided comprehensive coverage of eukaryotes for the sampling time points. The top phyla which made up the bulk of the broad eukaryote community across the whole 18S V7 rDNA data set were Bacillariophyta (18%), Arthropoda (18%), Streptophyta (13%) and Annelida (10%). It should be noted that some OTUs

could not be assigned taxonomy to genus or species level from the GenBank reference database, in these cases the higher confident taxonomic level assignment was used to describe OTUs.
The main phyla present in 2019, 2020 and 2021 across sites and the relative read abundances of taxonomic groups for each site are shown in Figure 45, Figure 46 and Figure 47. The bubble plots show the main kingdoms and the main eukaryote phyla on the x-axis of the plot. The bubble plots show, Animalia such as Arthropoda including macroinvertebrates and Annelida (worms) were common across sites for 2019, 2020 and 2021. For all years, the algae, Bacillariophyceae (diatoms) relative abundances were higher at discharge monitoring sites, whereas fungi, such as Ascomycota, were higher in the reference sites than in the discharge monitoring sites for all years. This pattern of fungal taxa reducing at the discharge monitoring sites may be a combined effect of differences in the physical ecosystem, elemental and carbon sources, habitat conditions and water quality. In 2019 Bacillariophyta were higher at Point 10 than other sites. In 2019 Streptophyta were high in the reference sites and at Pool 16.
In 2020 and 2021, Ciliophora relative read abundances were higher in the reference sites compared to the discharge monitoring sites. Cercozoa (free-living amoeba-like protozoa) have higher relative abundances in the reference sites compared to the discharge monitoring sites.
In 2020 fungi and ciliates were more abundant in the reference sites. In 2020 Molluscs and Annelida worms showed higher relative read abundance at Point 10. In 2020 some taxa were consistent in relative read abundance across all sites for example Platyhelminthes (flatworms). Arthropoda read abundance increased at downstream the discharge monitoring sites Pool 16, Pool32 and GRQ18. In 2020 Bacillariophyta diatoms were higher in the discharge monitoring sites. In 2020 Apicomplexa (parasitic micro-eukaryote) relative read abundance was higher in Point12 and Jutts. Arthropoda increased at Pool 16 and Pool32 in Spring 2020 which suggests that there are potential physical habitat features preferential to arthropods at these pools. Streptophyta abundances were variable across sites in 2020. Chlorophyta (green algae) were high at GRQ18 compared to all other sites in 2020.
In 2021, Bacillariophyta were lower in the reference sites and increased in read abundance in the discharge monitoring sites. Ascomycota fungi were more abundant in GRQ1 and GRUFS in 2021. In 2021 Streptophyta microeukaryote relative abundances were higher in the discharge monitoring sites whereas Chaonozoa were present in reference sites and rare in the discharge monitoring sites. In 2021 Annelida, cnidaria and molluscs were more abundant at Point 10 than other sites, suggesting the physical, riparian conditions and water quality features of Point 10 may be more suitable for higher abundances of worms, freshwater cnidaria (hydra) and molluscs.


**Figure 45. Bubble plot of the top 20 most abundant eukaryote Phyla (on average across all sites) for 2019.**

% RA is % relative abundance shown as bubble size.

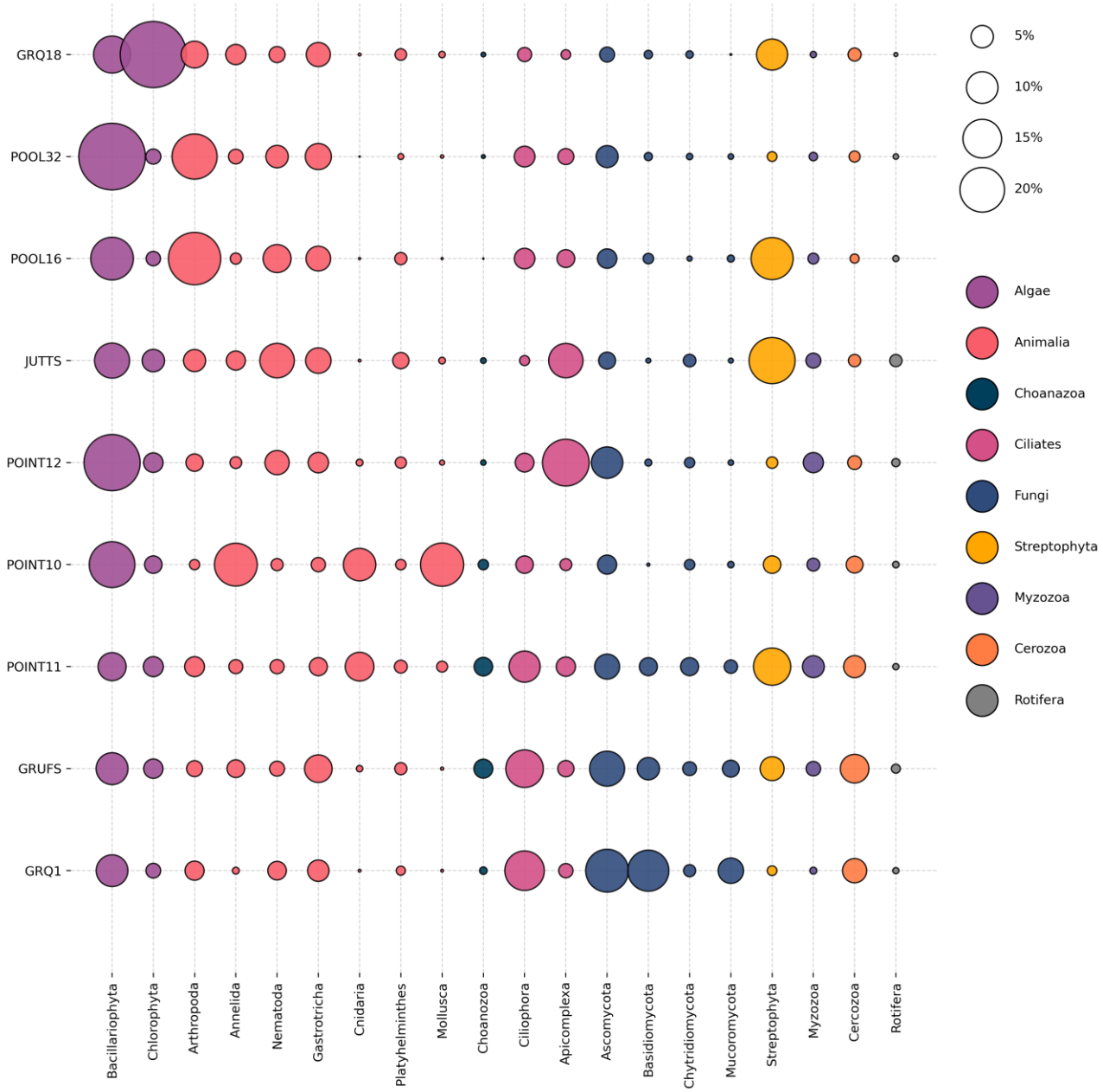


**Figure 46. Bubble plot of the top 20 most abundant eukaryote Phyla (on average across all sites) for 2020.**

% RA is % relative abundance shown as bubble size.

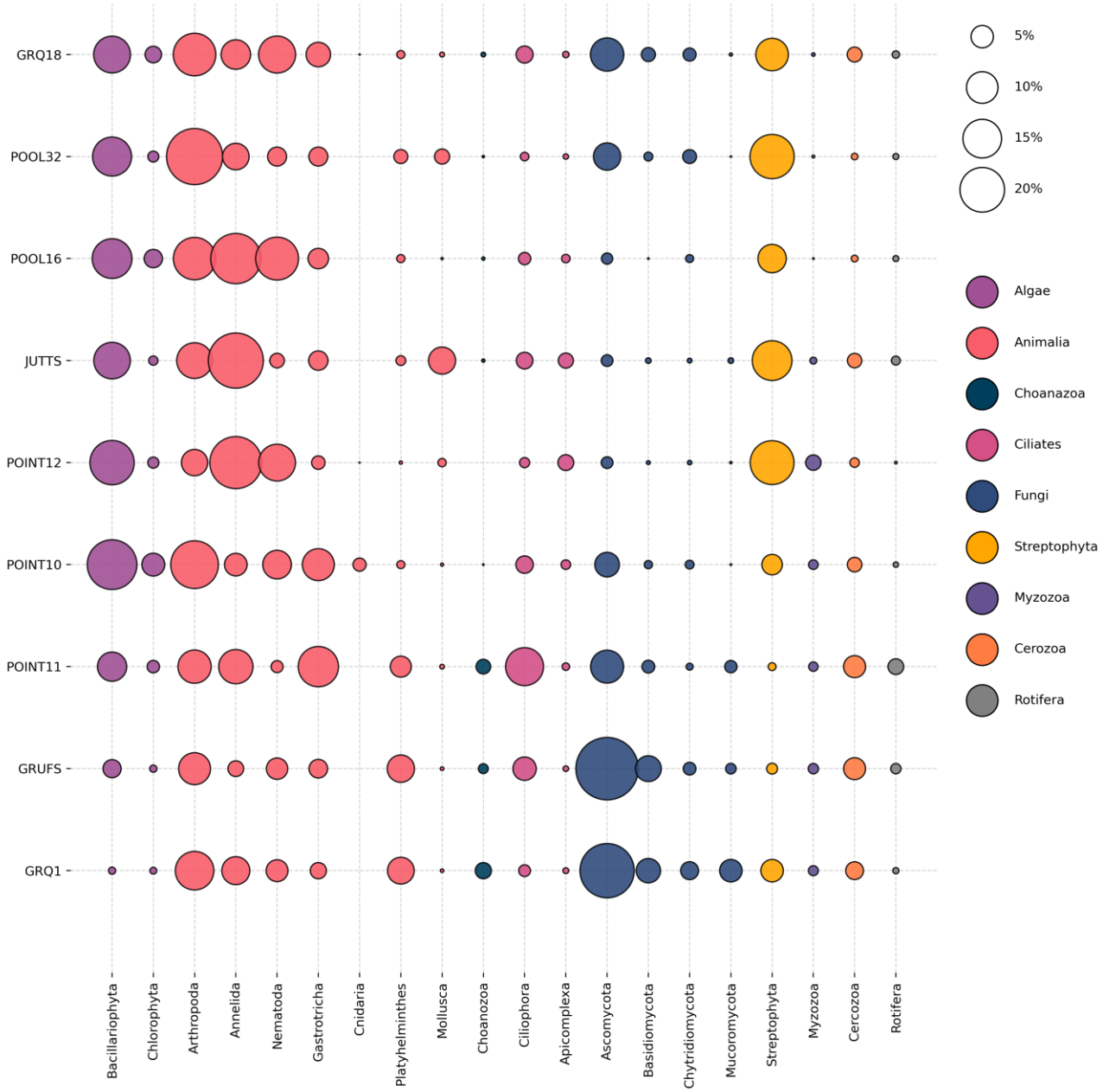


**Figure 47. Bubble plot of the top 20 most abundant eukaryote Phyla (on average across all sites) for 2021.**

% RA is % relative abundance shown as bubble size.

**Eukaryote richness**

The broad eukaryote richness for the nine sites over 2019, 2020 and 2021 is presented in Figure 48. Eukaryote richness exhibited a range of values across most sites, treatments, and sampling times (Figure 48). Generally, OTU richness was higher in the reference treatments compared to the discharge monitoring treatments (Figure 48) but there was only a statistically significant difference in richness between treatments in Spring 2021 (Table 29). Figure 48 shows a general trend of broad eukaryote OTU richness changing with time with an increase in discharge monitoring richness in 2020, then a reduction in discharge monitoring richness in 2021.

The broad eukaryote mean read abundance for the treatments over 2019, 2020 and 2021 is shown in Table 29. Read abundances were significantly different between the two treatments reference and discharge monitoring for all years 2019, 2020 and 2021. The discharge monitoring treatment had higher broad eukaryote read abundances than reference treatment for all years (Table 29) suggesting a high abundance of a lower overall number of eukaryote taxa.

The richest site, with the highest number of OTUs was Point 11 in 2021 (180 OTUs), followed by GRUFS in 2020 (170 OTUs) and the sites with the lowest richness (number of OTUs) were Jutts in 2019 (63 OTUs) and Pool 16 in 2021 (78 OTUs). The most frequently occurring OTU which occurred across the greatest number of samples was OTU_2, Haplotaxida order, Annelida phyla, which was present in 123 of the samples across 2019 to 2021 years. The broad eukaryote OTU which was most abundant (285,483 reads) across the dataset was OTU_2 which had the closest taxonomic match to Haplotaxida order (Annelida phyla). Haplotaxida are an order of freshwater oligochaete worms (Stimpson and Klemm, 1982).

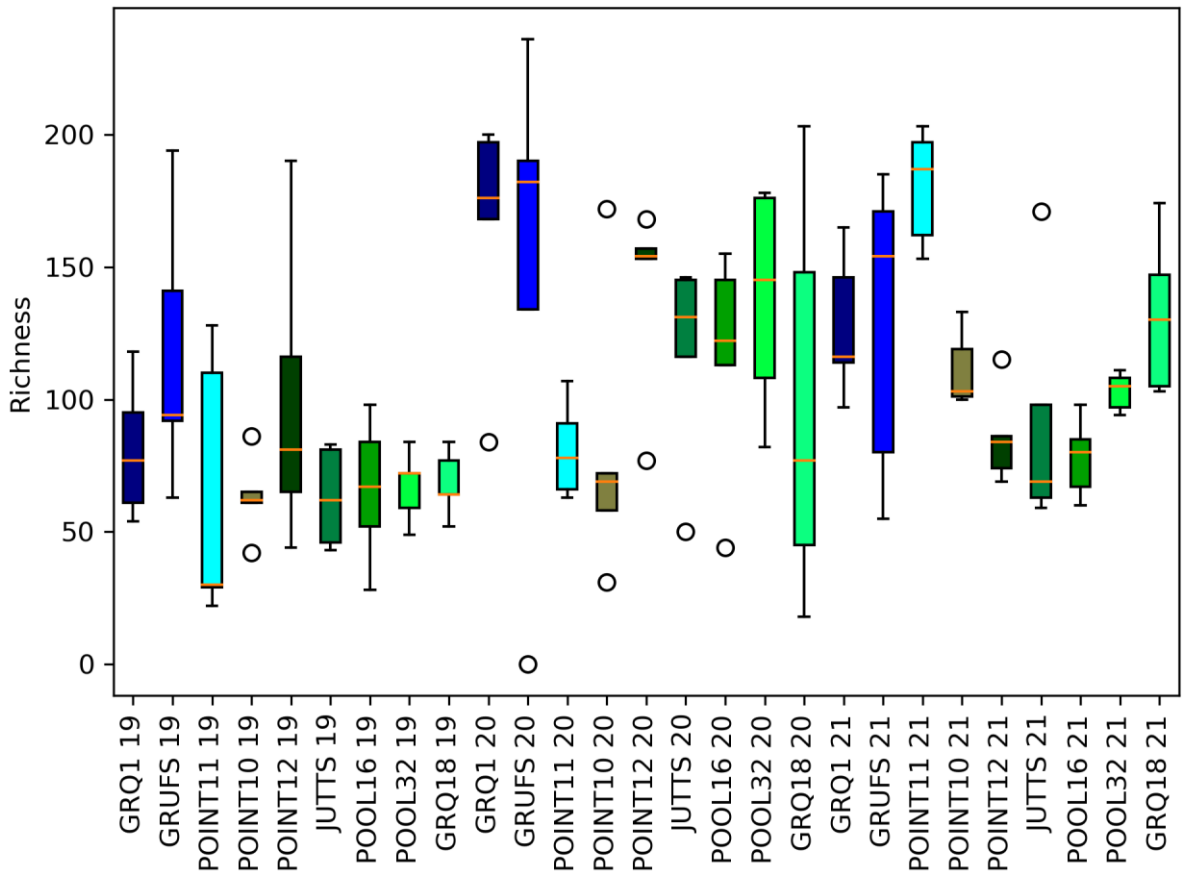


**Figure 48. Broad eukaryote OTU richness from 2019, 2020 and 2021 OTUs.**

Reference sites (blue) and discharge monitoring sites (green).

**Table 29. One-Way ANOVA results on eukaryote richness and read abundance for reference and discharge monitoring treatments.**

| **eukaryote OTU Richness** | Reference | Reference | Discharge monitoring | Discharge monitoring | One-Way ANOVA | |
|---|---|---|---|---|---|---|
| | mean | ± S.E. | mean | ± S.E. | *F* | *P-value* |
| Spring 2019 | 87 | 12.1 | 71 | 5.3 | 2 | 0.16 |
| Spring 2020 | 141 | 15.6 | 115 | 9.4 | 2.2 | 0.15 |
| Spring 2021 | 146 | 11.4 | 100 | 5.4 | 16.9 | **<0.05** |
| **eukaryote OTU read Abundance** | Reference | Reference | Discharge monitoring | Discharge monitoring | One-Way ANOVA | |
| | mean | ± S.E. | mean | ± S.E. | *F* | *P-value* |
| Spring 2019 | 19141 | 2760.6 | 26532 | 1813 | 5.3 | **<0.05** |
| Spring 2020 | 14118 | 3479 | 27175 | 2644.8 | 8.3 | **<0.05** |
| Spring 2021 | 15314 | 1417.7 | 26140 | 2816.6 | 6.9 | **<0.05** |

Bold values denote significance at p< 0.05.

**Eukaryote community composition**

The multivariate analyses of the broad eukaryote metabarcoding data clearly showed that the eukaryote composition at reference sites was markedly different to those at discharge monitoring sites (Figure 49). The eukaryote communities from the reference sites were markedly different to those from the discharge monitoring sites for 2019, 2020 and 2021. The separation of reference from discharge monitoring site eukaryote communities for 2019, 2020 and 2021 were visualised by the nMDS ordination plots in Figure 49. The ordinations in Figure 49, present a clear clustering of the discharge monitoring sites together, which is separating away from the reference sites. PERMANOVA tests were undertaken to investigate eukaryote community structure differences in treatments and time. The results of the PERMANOVAs testing for differences in eukaryote community composition between sampling timepoints (Spring 2019, 2020 and Spring 2021) and treatments are presented in Table 30. The visual separation of treatments is confirmed by the PERMANOVA which found a significant difference in composition between the two treatments in Spring 2019 (PERMANOVA: $F= 11.8$, $p<0.05$), Spring 2020 (PERMANOVA: $F= 8.2$ $p<0.05$) and in Spring 2021 (PERMANOVA: $F= 15.5$, $p<0.05$). Significant differences in community composition were found with respect to time (season/year) (PERMANOVA: $F= 7.5$, $p<0.05$) and treatment (discharge monitoring or reference), when tested individually (Table 30). In addition, there was a significant interaction between time and treatment (PERMANOVA: $F= 3.9$, $p<0.05$) (Table 30). Eukaryote community differences between sites were analysed with a pairwise PERMANOVA (Appendix B, Tables B4 - B6). The PERMANOVA results revealed significant differences observed at the site level for eukaryotes (Appendix B, Tables B4 - B6). In 2019, all sites were significantly different from each other except for GRQ1 and GRUFS reference sites, these sites were more similar in eukaryote composition. In 2020, most sites were significantly different from each other except for GRQ1 and GRUFS which were similar again, Point 11 and GRUFS were similar and finally Pool 16 and Pool 32 had similar eukaryote compositions. In 2021 most sites were significantly different from each other, the exceptions were Point 12, Jutts and Pool 16 were not different from each other these sites had similar eukaryote compositions. In common with the traditional macrobenthic data, the sequenced broad eukaryote communities from the discharge monitoring treatment were more similar than they were for the reference sites.

a) 2019 nMDS

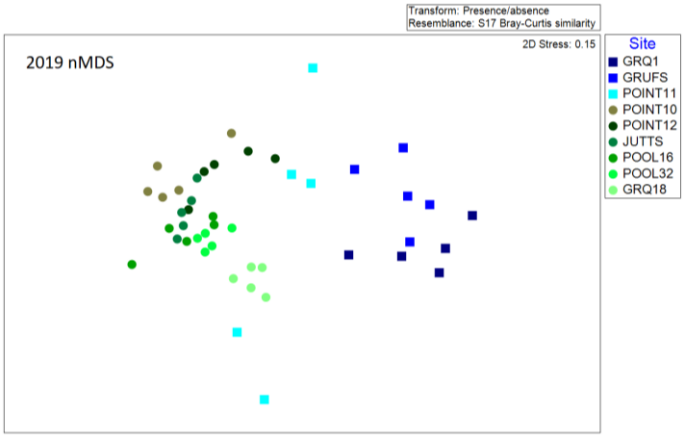


b) 2020 nMDS

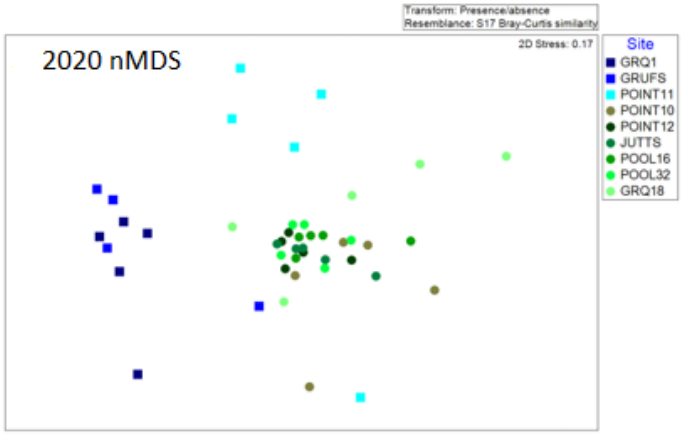


c) 2021 nMDS

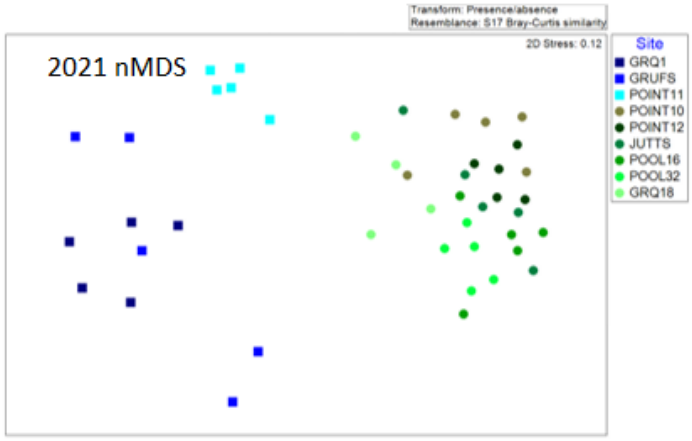


**Figure 49. nMDS of broad eukaryote communities (2019, 2020 and 2021).**

a) Spring 2019; b) Spring 2020 c) Spring 2021. Analysis is derived from presence/absence data at the level of Operational Taxonomic Unit (OTU).

**Table 30. Results of PERMANOVA testing for variation in broad eukaryote community composition (2019, 2020 and 2021) between timepoints (years), and treatments (reference vs discharge monitoring).**

| Factor: source of variation | df | MS | Pseudo-F | P(perm) | Unique perms |
|---|---|---|---|---|---|
| **Treatment (2019)** | 1 | 24978 | 11.8 | **0.0001** | 9903 |
| **Treatment (2020)** | 1 | 16519 | 8.2 | **0.0001** | 9897 |
| **Treatment (2021)** | 1 | 26794 | 15.5 | **0.0001** | 9911 |
| **Time (year)** | 2 | 18268 | 7.5 | **0.0001** | 9849 |
| **Treatment** | 1 | 52830 | 23.1 | **0.0001** | 9897 |
| **Time*Treatment** | 2 | 7673 | 3.9 | **0.0001** | 9813 |
| **Res** | 128 | 1950 | | | |
| **Total** | 133 | | | | |

Df: degrees of freedom; MS: mean squares; Pseudo-F: multivariate analogue to Fisher's F test statistic of the null hypothesis; P(perm): probability by permutations; Unique Perms: number of unique permutations.

Bold values denote significance at p< 0.05.

### 3.8.4 Relationships between broad eukaryotes and water quality (2019-2021)

Broad eukaryote community structure and water quality variable correlations were investigated using multivariate statistics including distance linear models (DistLM). Correlative patterns are presented here using the biological and chemical data for the three years presented on one dbRDA as well as presenting the DistLM and dbRDA results for each separate year. The fitted DistLM was visualised using a dbRDA constrained ordination (Figure 50), demonstrating the correlation of significant variables on the eukaryote community for 2019, 2020 and 2021 data. The distance-based analysis investigating the correlative patterns of the OTU community data with measured environmental variables is shown in Table 31. Approximately 55% of the variation in the 2019, 2020 and 2021 18S broad eukaryote community data could be explained by the environmental variables measured. When examined collectively, the variables which explained significant variation in the broad eukaryote community data included pH, zinc, nickel, conductivity, alkalinity, and copper ($p<0.05$) (Table 31), however the variable which contributed the most to the eukaryote variation was pH (26%). The composition of the water quality variables driving Point 10, Point 12, Jutts, Pool 16 and Pool 32 in 2020 were different to 2021. The discharge monitoring sites also differed to those for GRUFS, GRQ1 and Point 11. The dbRDA (Figure 50) for the eukaryote community shows that dbRDA 1 is explaining approximately 28% of the total variation and dbRDA 2 is explaining approximately 10% of the total eukaryote community composition.

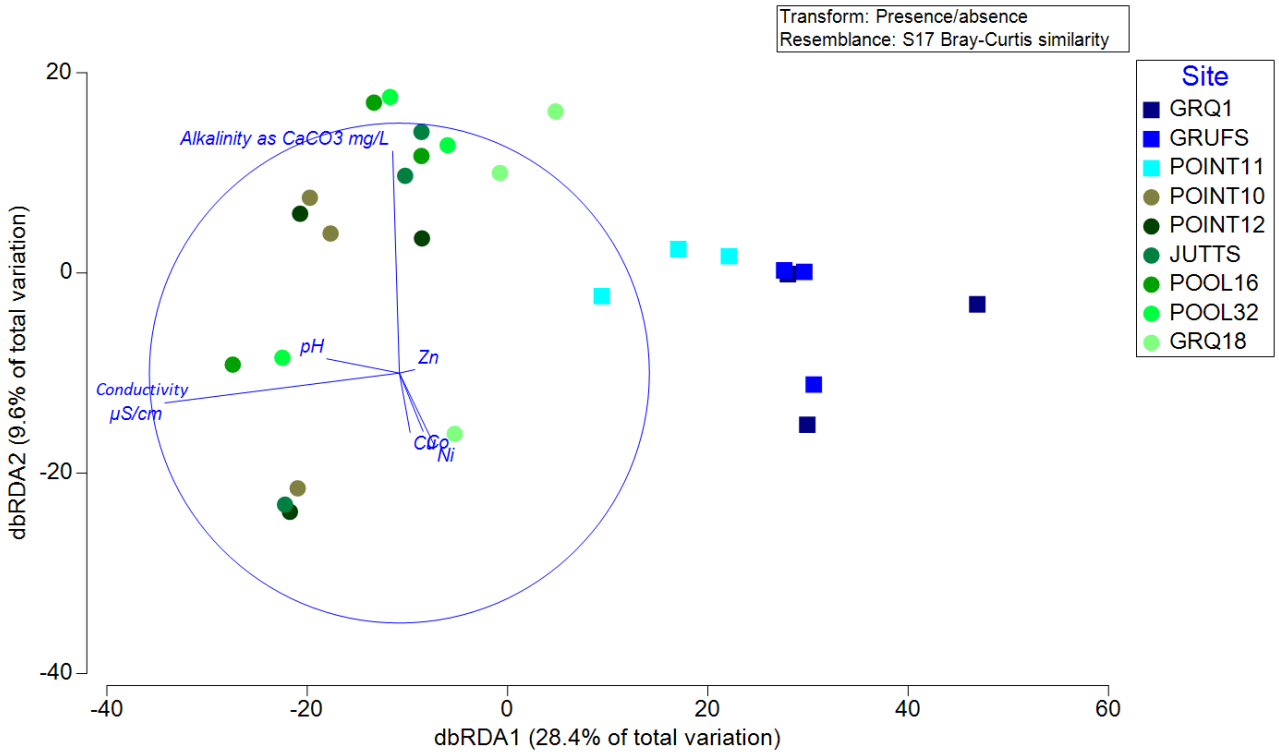


**Figure 50. Ordination plot derived from the distance-based model illustrating the relationships between key environmental variables and metabarcoded 18S broad eukaryotes composition from Spring 2019 - 2021.**

Reference sites (blue) and discharge monitoring sites (green).

**Table 31. Sequential test results of distance-based linear model (DistLM) for broad eukaryotes for 2019, 2020 and 2021 data.**

| Variable | Adj $R^2$ | SS(trace) | Pseudo-F | P | Prop%. | Cumulative contribution | res.df |
|---|---|---|---|---|---|---|---|
| **+pH** | 0.23 | 10805 | 8.7 | **0.0001** | 0.259 | 0.26 | 25 |
| **+Zinc** | 0.28 | 3326.8 | 2.9 | **0.0002** | 0.080 | 0.34 | 24 |
| **+Nickel** | 0.32 | 2513.3 | 2.3 | **0.0016** | 0.060 | 0.40 | 23 |
| **+Conductivity µS/cm** | 0.34 | 1694.2 | 1.6 | **0.041** | 0.041 | 0.44 | 22 |
| **+Alkalinity** | 0.36 | 1697.3 | 1.6 | **0.025** | 0.041 | 0.48 | 21 |
| **+Copper** | 0.38 | 1677 | 1.7 | **0.024** | 0.040 | 0.52 | 20 |
| **+Cobalt** | 0.38 | 1067.7 | 1.1 | 0.36 | 0.026 | 0.55 | 19 |

SS(trace): sum of squares; Pseudo-F: multivariate analogue to Fisher's F test statistic of the null hypothesis; P: probability; Prop%: the proportion of variation; res.df: residual degrees of freedom

Bold values denote significance at $p< 0.05$.

### Spring 2019 broad eukaryotes relationships with water quality

The fitted DistLM was visualised using a dbRDA constrained ordination (Figure 51), demonstrating the influence of significant variables on the eukaryote community for 2019. The correlative patterns of the OTU community data with measured environmental variables in 2019 were analysed by DistLM sequential tests and results are shown in Table 32. Approximately 96% of the variation in the Spring 2019 broad eukaryote community data could be explained by the environmental variables conductivity, aluminium, nickel, pH, zinc, copper, and total nitrogen. When examined collectively, the variables which explained significant variation in the broad eukaryote community data included conductivity and aluminium ($p<0.05$). The variable which explained the most variation was conductivity, which explained 40% of the total variation in the 2019 eukaryote communities, while aluminium explained 15% of the total variation. The dbRDA ordination (Figure 51) shows the discharge monitoring sites positioned to the right of the dbRDA 1 axis, driven by conductivity, while the reference sites GRQ1 and GRUFS remain on the left of the dbRDA1 axis showing a negative relationship with conductivity.

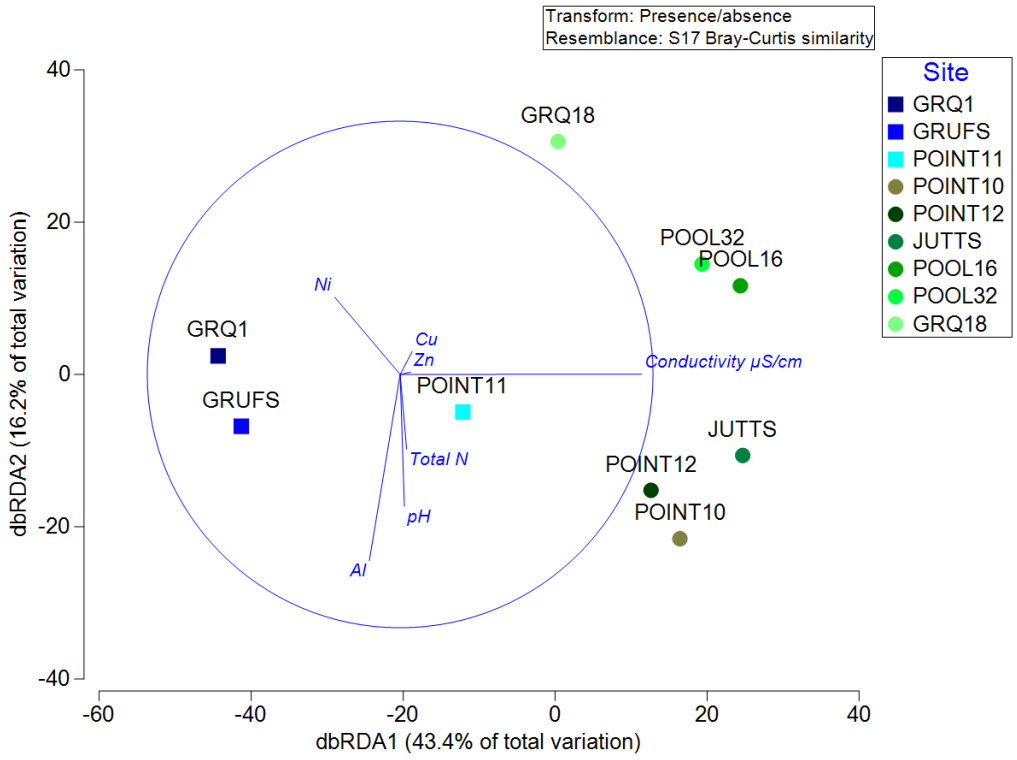


**Figure 51. Ordination plot derived from the distance-based model illustrating the relationships between key environmental variables and metabarcoded 18S broad eukaryotes composition from Spring 2019.**

Reference sites (blue) and discharge monitoring sites (green)

Table 32. Sequential test results of distance-based linear model (DistLM) for broad eukaryotes OTUs for 2019 data.

| Variable | Adj $R^2$ | SS(trace) | Pseudo-F | P | Prop.% | Cumulative contribution | res.df |
|---|---|---|---|---|---|---|---|
| **+Conductivity µS/cm** | 0.32 | 5396.4 | 4.7 | **0.001** | 0.40 | 0.40 | 7 |
| **+Aluminium** | 0.40 | 2033.9 | 2.0 | **0.007** | 0.15 | 0.55 | 6 |
| **+Nickel** | 0.48 | 1624.7 | 1.9 | 0.052 | 0.12 | 0.67 | 5 |
| **+pH** | 0.55 | 1338.2 | 1.8 | 0.11 | 0.10 | 0.77 | 4 |
| **+Zinc** | 0.60 | 1036.8 | 1.6 | 0.22 | 0.08 | 0.85 | 3 |
| **+Copper** | 0.69 | 963.2 | 1.8 | 0.23 | 0.07 | 0.92 | 2 |
| **+Total Nitrogen** | 0.70 | 543.2 | 1.1 | 0.48 | 0.04 | 0.96 | 1 |

SS(trace): sum of squares; Pseudo-F: multivariate analogue to Fisher's F test statistic of the null hypothesis; P: probability; Prop%: the proportion of variation; res.df: residual degrees of freedom

Bold values denote significance at $p< 0.05$.

### Spring 2020 broad eukaryotes relationships with water quality

The fitted DistLM was visualised using a dbRDA constrained ordination (Figure 52), demonstrating the influence of significant variables on the eukaryote community for 2020. Approximately 95% of the variation in the Spring 2020 18S broad eukaryote community data could be explained by the environmental variables pH, zinc, nickel, copper, aluminium, total nitrogen and cobalt. The correlative patterns of the OTU community data with measured environmental variables in 2020 were analysed by DistLM sequential tests and results are shown in Table 33. When examined collectively, the variable which explained significant variation in the broad eukaryote community data once again included pH, explaining 42% of the total eukaryote variation. The ordination (Figure 52), shows pH driving the separation of the green discharge monitoring sites in 2020. discharge monitoring sites positioned to the right of the dbRDA 1 axis, driven by pH, while the reference sites remain on the left of the dbRDA1 axis showing a negative relationship with pH for the reference sites. The composition of the water quality variables driving Point 10, Point 12, Jutts, Pool 16 and Pool 32 in 2020 were different to 2021 and the discharge monitoring sites also differed to those for GRUFS, GRQ1 and Point 11.

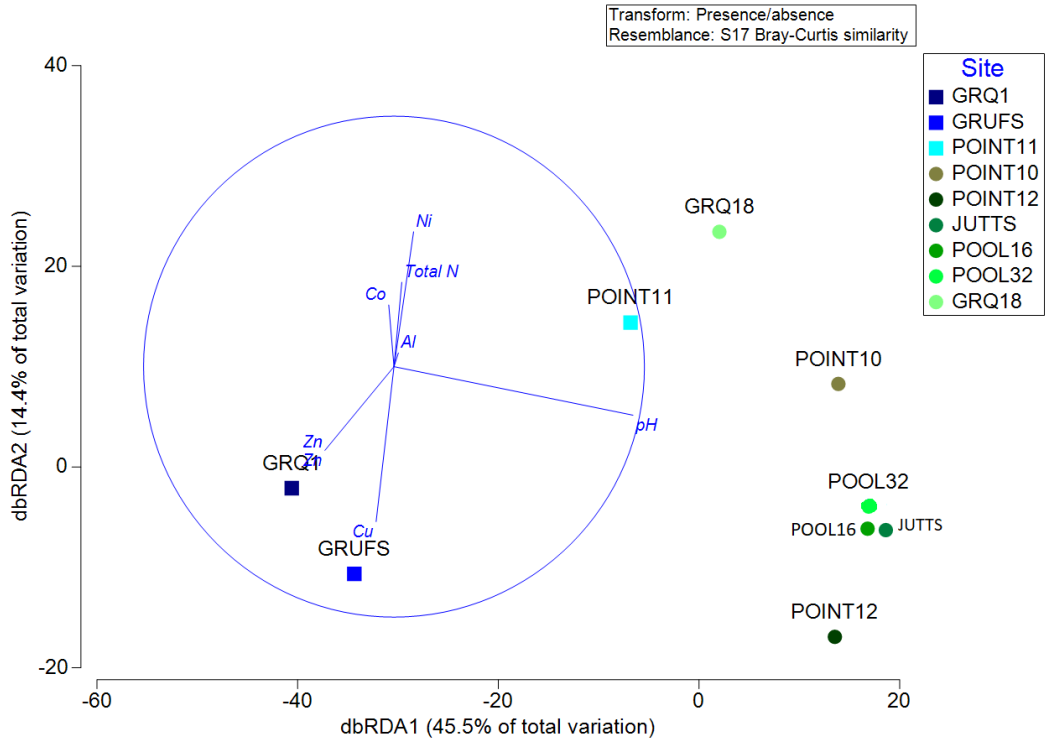


**Figure 52. Ordination plot derived from the distance-based model illustrating the relationships between key environmental variables and metabarcoded 18S broad eukaryotes composition from Spring 2020.**

Reference sites (blue) and discharge monitoring sites (green)

**Table 33. Sequential test results of distance-based linear model (DistLM) for broad eukaryotes OTUs 2020 only.**

| Variable | Adj $R^2$ | SS(trace) | Pseudo-F | P | Prop%. | Cumulative contribution | res.df |
|---|---|---|---|---|---|---|---|
| **+pH** | 0.34 | 3879 | 5.1 | **0.0007** | 0.4 | 0.42 | 7 |
| **+Zinc** | 0.37 | 930 | 1.3 | 0.19 | 0.1 | 0.52 | 6 |
| **+Nickel** | 0.39 | 874 | 1.3 | 0.27 | 0.1 | 0.62 | 5 |
| **+Copper** | 0.44 | 909 | 1.4 | 0.20 | 0.1 | 0.72 | 4 |
| **+Aluminium** | 0.49 | 837 | 1.4 | 0.26 | 0.09 | 0.81 | 3 |
| **+Total Nitrogen** | 0.54 | 681 | 1.3 | 0.36 | 0.07 | 0.88 | 2 |
| **+Cobalt** | 0.6 | 600 | 1.3 | 0.42 | 0.07 | 0.95 | 1 |

SS(trace): sum of squares; Pseudo-F: multivariate analogue to Fisher's F test statistic of the null hypothesis; P: probability; Prop%: the proportion of variation; res.df: residual degrees of freedom

Bold values denote significance at $p< 0.05$.

### Spring 2021 broad eukaryotes relationships with water quality

The fitted DistLM was visualised using a dbRDA constrained ordination (Figure 53), demonstrating the influence of significant variables on the eukaryote community for 2021. The correlative patterns of the eukaryote OTU community data with measured environmental variables in 2021 were analysed by DistLM and results are shown in Table 34. Approximately 83% of the total eukaryote OTU community variation was explained by the measured variables including pH,

aluminium, total nitrogen, nickel, and copper in Spring 2021. When the measured variables were examined collectively, the variables which explained the most eukaryote community variation was again pH (46%) and aluminium which explained a smaller proportion of 12%. The ordination (Figure 53) shows the discharge monitoring sites positioned to the right of the dbRDA 1 axis, driven by pH, while the reference sites remain on the left of the dbRDA1 axis showing a negative relationship with pH for the reference sites.

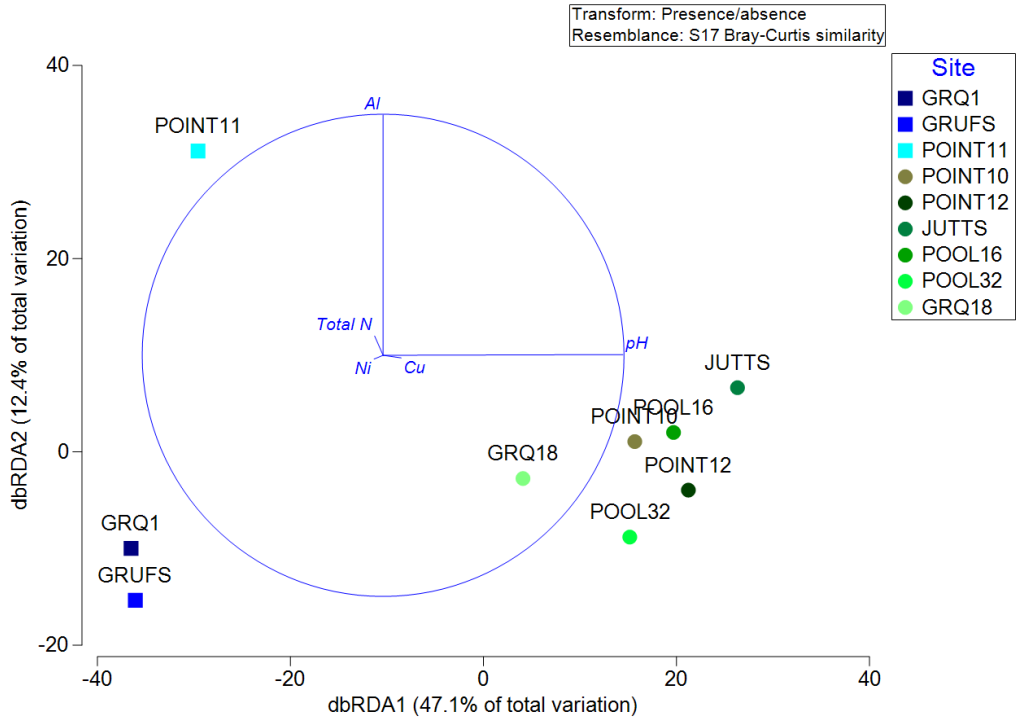


**Figure 53. Ordination plot derived from the distance-based model illustrating the relationships between key environmental variables and metabarcoded 18S broad eukaryotes composition from Spring 2021.**

Reference sites (blue) and discharge monitoring sites (green)

**Table 34. Sequential test results of distance-based linear model (DistLM) for broad eukaryotes OTUs for 2021 data.**

| Variable | Adj $R^2$ | SS(trace) | Pseudo-F | P | Prop%. | Cumulative contribution | res.df |
|---|---|---|---|---|---|---|---|
| **+pH** | 0.39 | 5442 | 6.0 | **0.001** | 0.46 | 0.46 | 7 |
| **+Aluminium** | 0.45 | 1410 | 1.7 | **0.036** | 0.12 | 0.58 | 6 |
| **+Total Nitrogen** | 0.51 | 1281 | 1.8 | 0.059 | 0.11 | 0.69 | 5 |
| **+Nickel** | 0.55 | 937 | 1.4 | 0.221 | 0.08 | 0.77 | 4 |
| **+Copper** | 0.55 | 687 | 1.0 | 0.463 | 0.06 | 0.83 | 3 |

SS(trace): sum of squares; Pseudo-F: multivariate analogue to Fisher's F test statistic of the null hypothesis; P: probability; Prop%: the proportion of variation; res.df: residual degrees of freedom

Bold values denote significance at $p< 0.05$.

The key OTUs which contributed to the observed differences in eukaryote composition between reference and monitoring sites can be seen from the SIMPER analyses (Table 35). The top 10 eukaryote taxa which contributed most to the differences between reference and discharge monitoring treatments for the sampling years 2019, 2020 and 2021 are presented in Table 35 and their taxonomic assignments are listed in Table 36. These data are presented relative to the mean of the reference sites, such that a positive value indicates an increase and a negative value indicates a decrease. It should be noted that some OTUs could not be assigned taxonomy to genus or species level from the GenBank database, in these cases the higher confident taxonomic level assignment was used. Table 35 shows a large number of OTUs which are having variable responses at discharge monitoring sites at the sampling occasions 2019, 2020 and 2021. In 2019 OTU_8, likely a *Navicula sp.* mostly showed a positive response (increased in relative abundance) in the SIMPER analysis for the discharge monitoring sites, with most sites increasing in abundance in relation to the mean reference Table 36. In 2019 OTU_16 assigned as *Mayamaea atomus,* a benthic diatom from family Naviculacae and OTU_17 (*Callistina panda*) an Ephemeroptera invertebrate, from the family Caenidae showed increases at all Discharge Monitoring sites from the mean reference. Ephemeroptera such as Caenidae*,* commonly occur in slow flowing silty freshwater areas typically dwelling in leaf packs, on logs or on macrophytes (Suter et al., 2002). OTU_4 (*Stenocypria sp*) a crustacean ostracod, showed increases at the downstream sites Pool 32 and GRQ18. OTU_7 (*Entomoneis ornate*) benthic diatom taxa, increased at the upper reaches discharge sites (Point 10, 12 and Jutts) and decreased with distance, decreasing at the most distant site GRQ18. The OTU_9 (Cyclopoida, copepod) crustacea, showed the highest change from the mean at Jutts. In 2019 OTU_6 (*Nitella capillaris*) freshwater green macro-algae, decreased at all discharge monitoring sites.

In 2020 OTU_8 (*Navicula*) Naviculacae diatom, increased at all discharge monitoring sites. OTU_14 (*Caespitella pascheri*) green algae species, increased only at site GRQ18. OTU_2 (Haplotaxida) worms, and OTU_12 (*Physella acuta*) an invasive freshwater mollusc, were higher at Point 10 only, relative to the reference mean, in 2020. *Physella acuta* are lunged, breathing freshwater snails and are generally more tolerant of polluted conditions (Spyra et al., 2019). *Physella acuta* are known for metal concentration tolerance and *Physella acuta* have been used to study bioaccumulation of metals in freshwater ecosystems (Adewunmi et al., 1996). Haplotaxida are common annelid, oligochaete worms. In 2020 the SIMPER analysis showed there were no OTUs which reduced at all Discharge Monitoring sites. In 2020 OTU_28 (*Hydra vulgaris*) a freshwater cnidarian and OUT_11 (*Potamogeton crispus*) an aquatic macrophyte, mostly decreased in the discharge monitoring sites but did not decrease for all sites.

In 2021 there were no OTUs which increased at all discharge monitoring sites. OTU_2 (Haplotaxida) and OTU_5 (*Typha angustifolia*), which is an herbaceous wetland plant, did however increase at most discharge monitoring sites. This increase may be due to bank conditions, as well as sediment and benthic structure changes at the discharge monitoring sites. OTU_10 (*Dolerocypris sinensis*) an ostracoda, increased with distance from discharge and was higher in Pool 32. In 2021, OTU_20 (*Pentaphlebia sp* Leptophlebiidae) and OTU_22 (*Reticulascus tulasneorum*) decreased relative to the reference mean at all discharge monitoring sites. *Reticulascus tulasneorum* is an ascomata fungus, known to grow on decaying wood, suggesting the conditions in the reference sites are more suitable for ascomata fungi to cycle carbon from decaying vegetation in the reference sites. The OTUs 20 and 22 were higher in the reference sites than the discharge monitoring sites in 2021.

**Table 35. SIMPER results illustrating the top 10 eukaryote taxa which contributed to differences between the reference and discharge monitoring sites (2019, 2020 and-2021).**

| | | | Change from Mean Reference | | | | | | |
|---|---|---|---|---|---|---|---|---|---|
| | Taxon | Mean Reference | POINT10 | POINT12 | JUTTS | POOL16 | POOL32 | GRQ18 | Comments |
| **2019** | **OTU_4** | 0.0354 | 0.0 | 0.0 | 0.0 | 3.5 | 39.2 | 17.9 | Variable response, increase with distance |
| | **OTU_6** | 24.1 | -24.1 | -23.6 | -24.1 | -24.1 | -24.0 | -24.1 | Decreased at all monitoring sites |
| | **OTU_7** | 0.211 | 31.0 | 13.1 | 7.9 | 1.3 | 1.6 | 0.0 | Mostly increased, decreased with distance |
| | **OTU_2** | 9.49 | -9.1 | -6.3 | -5.5 | -9.3 | -9.2 | 9.1 | Variable response at monitoring sites |
| | **OTU_8** | 0.379 | 17.7 | 2.4 | 14.3 | 2.5 | 4.2 | 8.8 | Mostly increased at monitoring sites |
| | **OTU_9** | 0.0705 | 3.4 | 12.2 | 24.0 | 4.4 | 1.3 | 0.0 | Variable response at monitoring sites |
| | **OTU_10** | 7.11 | -7.1 | -7.0 | -7.1 | -7.1 | 8.0 | -0.6 | Variable response at monitoring sites |
| | **OTU_5** | 0.369 | -0.4 | -0.3 | 5.3 | 13.6 | 3.1 | -0.1 | Variable response at monitoring sites |
| | **OTU_16** | 0.0336 | 3.2 | 1.6 | 4.1 | 10.7 | 3.7 | 0.1 | Increased at all monitoring sites |
| | **OTU_17** | 0.091 | 0.4 | 7.9 | 2.2 | 6.3 | 3.2 | 0.1 | Increased at all monitoring sites |
| **2020** | **OTU_14** | 0.75 | -0.2 | 0.1 | 0.1 | -0.5 | -0.7 | 40.7 | Variable response, increase at GRQ18 |
| | **OTU_8** | 0.627 | 3.9 | 5.3 | 0.9 | 7.1 | 20.5 | 4.7 | Increased at all monitoring sites |
| | **OTU_11** | 2.83 | -2.8 | -2.5 | 16.6 | -2.7 | -2.7 | -0.3 | Mostly decreased at monitoring sites |
| | **OTU_13** | 0.267 | -0.2 | -0.1 | -0.2 | 12.1 | 14.3 | 0.1 | Variable response at monitoring sites |
| | **OTU_2** | 1.66 | 16.7 | -0.4 | -0.7 | -0.5 | 0.4 | 2.2 | Variable response at monitoring sites |
| | **OTU_12** | 0.334 | 18.5 | -0.1 | 0.0 | -0.3 | -0.2 | -0.1 | Variable response, decrease with distance |
| | **OTU_15** | 0.838 | -0.3 | 10.3 | 6.5 | -0.3 | -0.4 | -0.7 | Variable response at monitoring sites |
| | **OTU_28** | 3.12 | 7.5 | -2.6 | -3.0 | -3.1 | -3.1 | -3.0 | Mostly decreased at monitoring sites |
| | **OTU_5** | 1.47 | -1.3 | -1.4 | -1.3 | 5.5 | -1.4 | 5.3 | Variable response at monitoring sites |
| | **OTU_4** | 0.378 | -0.3 | -0.3 | -0.1 | 11.4 | 0.1 | 3.1 | Variable response at monitoring sites |
| **2021** | **OTU_2** | 3.78 | 0.6 | 21.1 | 17.2 | 21.3 | 2.5 | 1.1 | Mostly increased at monitoring sites |
| | **OTU_22** | 12.1 | -9.6 | -11.3 | -11.6 | -11.6 | -7.1 | -7.5 | Decreased at all monitoring sites |
| | **OTU_5** | 0.566 | 0.6 | 15.0 | -0.2 | 2.7 | 1.9 | 4.7 | Mostly increased at monitoring sites |
| | **OTU_19** | 0.148 | 0.6 | 7.1 | 0.5 | 15.0 | 0.4 | 0.2 | Mostly increased at monitoring sites |
| | **OTU_10** | 0.121 | 0.1 | 1.5 | 0.4 | 1.0 | 12.8 | 7.5 | Mostly increased at monitoring sites |
| | **OTU_31** | 2.63 | -2.2 | -2.4 | 5.2 | -2.6 | -2.4 | 0.2 | Variable response at monitoring sites |
| | **OTU_4** | 1.47 | -1.1 | 1.5 | 2.3 | 3.0 | 4.3 | -0.8 | Variable response at monitoring sites |
| | **OTU_692** | 0.0276 | 0.2 | 2.9 | 0.0 | 0.9 | 10.7 | 1.8 | Variable response at monitoring sites |
| | **OTU_11** | 0.159 | -0.2 | 0.3 | 14.3 | -0.1 | 0.0 | 0.0 | Variable response at monitoring sites |
| | **OTU_20** | 4.72 | -4.6 | -4.7 | -4.7 | -4.7 | -4.1 | 0.0 | Decreased at all monitoring sites |

**Table 36. List of OTU, closest eukaryote taxonomic assignment and match % that account for most of the dissimilarities between the reference and discharge monitoring sites (2019, 2020 and 2021).**

| Taxon | Family | Closest species | Match % | NCBI Accession |
|---|---|---|---|---|
| **OTU_2** | Haplotaxida_unknown_family | uncultured eukaryote | 100 | KT072112.1.1802 |
| **OTU_4** | Cyprididae | *Stenocypria sp*. SFH-2011 | 100 | AB674992.1.1763 |
| **OTU_5** | Typhaceae | *Typha angustifolia* | 100 | FJ824758.1.1585 |
| **OTU_6** | Characeae | *Nitella capillaris* | 99.3 | AJ250111.1.1794 |
| **OTU_7** | Entomoneidaceae | *Entomoneis ornata* | 100 | HQ912411.1.1733 |
| **OTU_8** | Naviculaceae | *Navicula cryptocephala* var. veneta | 100 | JQ610162.1.1210 |
| **OTU_9** | Cyclopoida_unknown family | Cyclapoid copepod | 100 | GU070881.1.1745 |
| **OTU_10** | Cyprididae | *Dolerocypris sinensis* | 96.4 | AF220459.1.1769 |
| **OTU_11** | Potamogetonaceae | *Potamogeton crispus* | 99.3 | EF526315.1.1785 |
| **OTU_12** | Physidae | *Physella acuta* | 100 | KP171533.1.1805 |
| **OTU_13** | Corduliidae | *Procordulia jacksoniensis* | 100 | EU055156.1.1787 |
| **OTU_14** | Aphanochaetaceae | *Caespitella pascheri* | 99.3 | LN870284.1.1693 |
| **OTU_15** | Gregarinasina_unknown_family | Heterocapsaceae | 84.2 | EF024723.1.1773 |
| **OTU_16** | Naviculaceae | *Mayamaea atomus* var. atomus | 95.7 | AM501968.1.1737 |
| **OTU_17** | Caenidae | *Callistina panda* | 98.6 | AY749907.1.1830 |
| **OTU_19** | Mermithidae | *Mermis nigrescens* | 95.6 | KF583882.1.1676 |
| **OTU_20** | Leptophlebiidae | *Penaphlebia sp*. EP076 | 100 | AY749858.1.1818 |
| **OTU_22** | Reticulascaceae | *Reticulascus tulasneorum* | 100 | LSAX01000036.22191.23944 |
| **OTU_28** | Hydridae | *Hydra vulgaris* | 100 | ABRM01105037.63.1356 |
| **OTU_31** | Tubificidae | *Bothrioneurum vejdovskyanum* | 100 | AF411908.1.1749 |
| **OTU_692** | Characeae | *Nitella capillaris* | 97.2 | AJ250111.1.1794 |

### 3.8.5 18S V4 rDNA metabarcoding (Bacillariophyceae, diatoms)

Diatom communities were included in the program in 2020 as an additional target DNA based biological community to investigate. The inclusion of meio- and micro-organisms (including bacteria, algae and diatoms) has been demonstrated to be of great benefit, as many of these taxa have been shown to be sensitive indicators of environmental condition (Kennedy and Jacoby, 1999). Due to the trophic position of diatoms (primary producers) and the sensitivity of diatoms to water quality fluxes, diatoms were included as a target group for monitoring changes and community shifts.

After the removal of potentially erroneous sequences, the 18S V4 rDNA Bacillariophyceae (diatom) dataset contained 4,075,496 reads, encompassing 174 unique OTUs in 2020 and 175 OTUs in 2021 from 7 diatom families.

The main diatom taxa present across sites and relative read abundances of taxonomic groups for each site are shown in Figure 54 and Figure 55. Many diatom OTUs relative abundances varied across the survey sites. Diatom OTUs that could not be classified to genus were assigned the

higher taxonomy of Bacillariophyta in the bubble plot. The Raphid-pennate (possess a raphe, also known as Bacillarinneae) coarse taxonomic group of diatoms made up the bulk of the diatom OTUs in all sites of the survey area. Araphid-pennate which do not possess a raphe, (also known as Fragilariineae). diatoms were observed in low abundances in the reference sites and they were higher in the discharge monitoring sites Point 10, 12 and Jutts than other sites in 2020.

The diatoms, *Entomone*is and *Denticula* were low at the reference sites in both 2020 and 2021. *Entomoneis* was observed in highest abundances at the three sites closest to the discharge source, i.e., Point 10, Point12 and Jutts for both years. *Entomenis* benthic diatom species have been associated with cycling nutrients such as nitrogen in benthic aquatic systems (Jauffrais et al., 2016). *Denticula* was present at all discharge monitoring sites in 2021. In 2021, *Entomoneis* was higher in the upper reaches discharge monitoring sites and decreased with distance downstream. *Staurosirella* also had higher relative abundances at the upper discharge monitoring sites for both years. *Staurosirella* relative abundance was highest at the discharge pool Point 10 for both years. *Staurosirella* showed a similar pattern to *Entomoneis* in 2020 with higher abundances in the Point 12 and Jutts. This higher abundance may be associated with the environmental conditions in these sites such as water depth, benthic substrate type, available light, nutrient availability and water quality combined. *Melosira* was only detected in discharge monitoring sites, for both years *Melosira* was absent from the reference treatment sites. In 2020 *Melosira* was only detected in the downstream discharge sites GRQ18 and Pool 16. While in 2021 *Melosira* had high abundances in Pool 16 (20%) and low abundances (<5%) in all other discharge monitoring sites. *Melosira* diatoms are recognised as common freshwater diatoms which are tolerant of aquatic pollution and variable water quality (Lu et al., 2020). *Amphora* diatoms were low in reference sites for both years however abundance increased at discharge source Point 10, Point 12 and Jutts.

The genus *Eunotia* was only present in the reference sites for both 2020 and 2021. *Eunotia's* presence in the upper reference sites could be a result of the low pH observed at these sites. *Eunotia* are known to be acidophilus, oligotrophic diatoms, characteristic of low-alkalinity, naturally slightly-acidic ecosystems (Cantonati and Lange-Bertalot 2011).

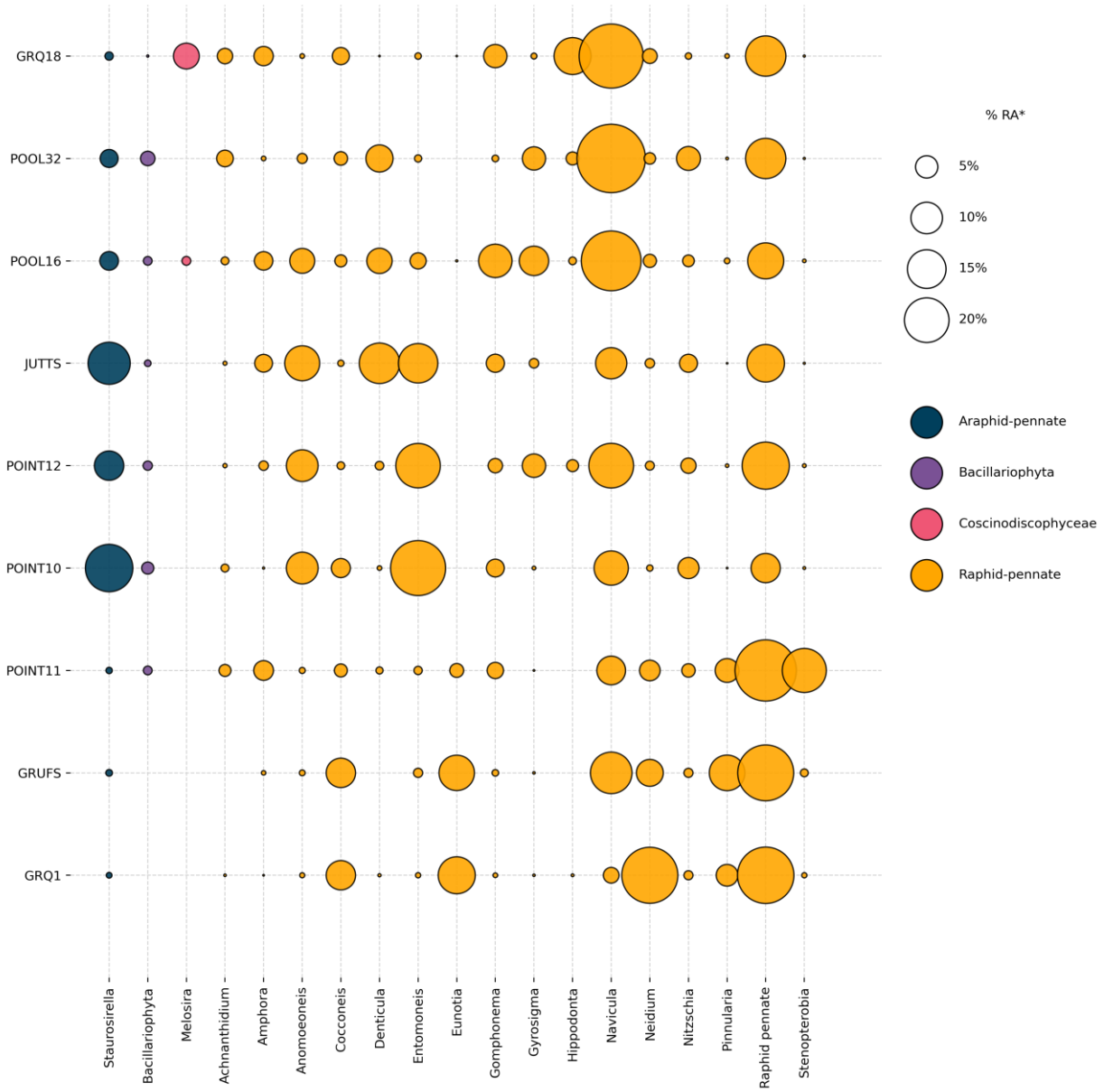


**Figure 54. Bubble plot of the main diatom taxa groups (genus) across all sites in 2020.**

% RA is % relative read abundance shown as bubble size.

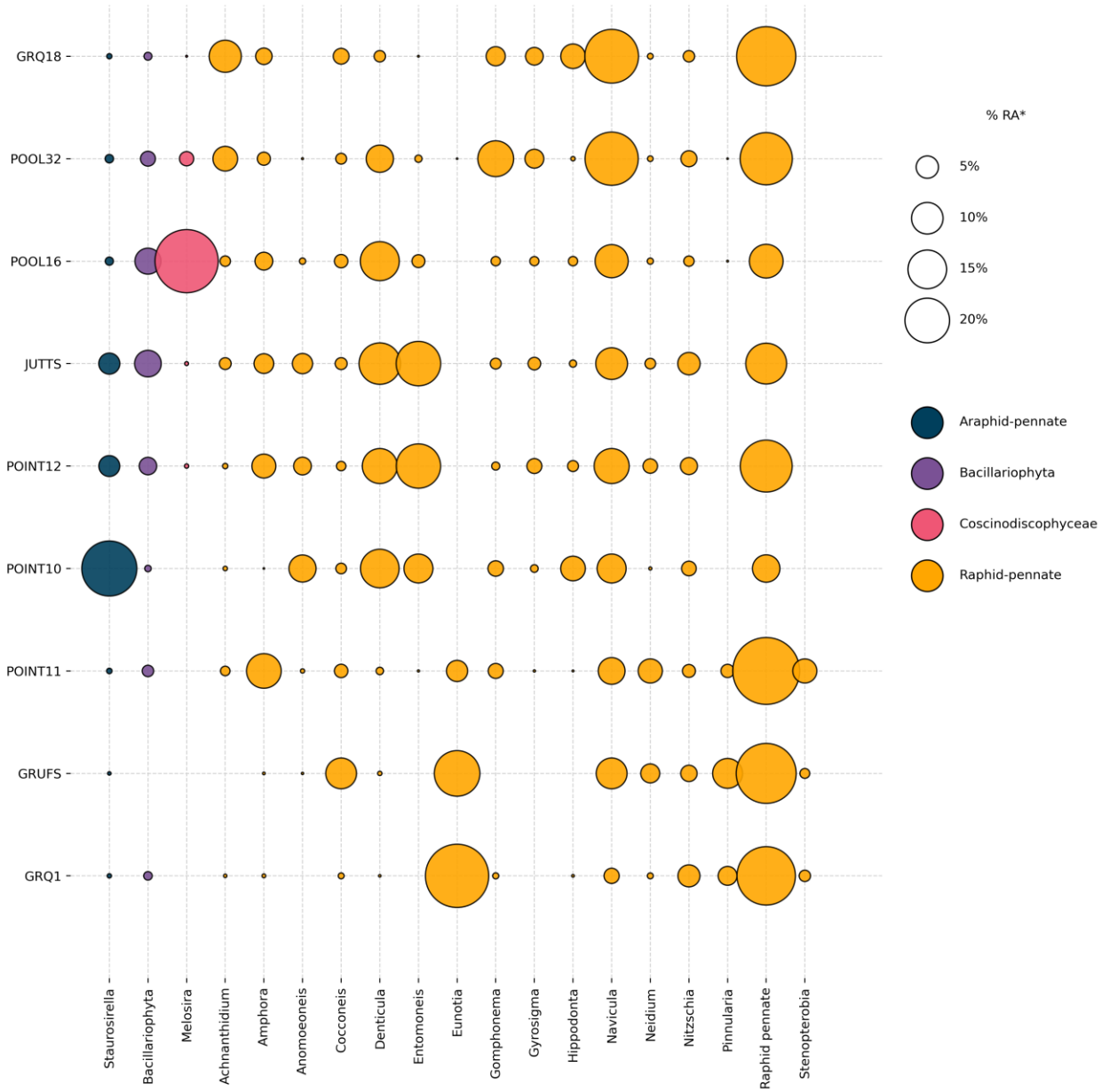


**Figure 55. Bubble plot of the main diatom taxa groups (genus) across all sites in 2021.**

% RA is % relative read abundance shown as bubble size.

**Diatom richness**

A summary of family richness (the number of OTUs) from the diatom data collected in 2020 and 2021 is provided in Figure 56. Overall diatom OTU richness fluctuated over the monitoring period for both treatments. Univariate statistical results including means, standard errors and One-Way ANOVA results for diatom richness and read abundance are presented in Table 37. There were no trends in richness for the diatom OTUs in Spring 2020 or 2021 (Table 37). One-Way ANOVA detected no significant difference between diatom richness for the reference and discharge monitoring treatments for both sampling time points (Table 37). For diatom OTU richness in Spring 2020 was similar for reference (43.8±3.1 S.E.) and discharge monitoring treatments (41.8± 2.2 S.E.) and similar again in Spring 2021 reference (43 ± 2.4 S.E.) and discharge monitoring treatments (40.5± 1.8 S.E.). In 2020 the diatom OTU richness was high in site GRQ18 with a similar richness to the reference sites (Figure 56). Diatom OTU read abundance was higher in the discharge monitoring treatments compared with the reference treatment for both sampling time points (Table 37). The One-Way ANOVA (Table 37) for diatom OTU read abundance detected a significant difference between reference and discharge monitoring treatment read abundances in Spring 2020 ($F=13.1$, $p<0.05$) and in Spring 2021 ($F=17.3$, $p<0.05$).

The diatom OTU, which had the highest read abundance of all the diatom OTUs, was OTU1 *Entomoneis* genus (406,806 reads). The richest site with the highest number of OTUs was Point 11 in 2020 (58 OTUs), followed by Pool 32 in 2020 (55 OTUs) and the site with the lowest OTU richness was Jutts in 2020 (29 OTUs). The most frequently occurring OTU which occurred across the greatest number of samples was OTU 19, *Gomphonema* genus which was present in 80 of the 90 samples across both years. The sample with the highest read abundance was Point 10 replicate D (118,286 reads) in 2020 and the sample with the lowest read abundance was GRQ18 replicate A (821 reads).

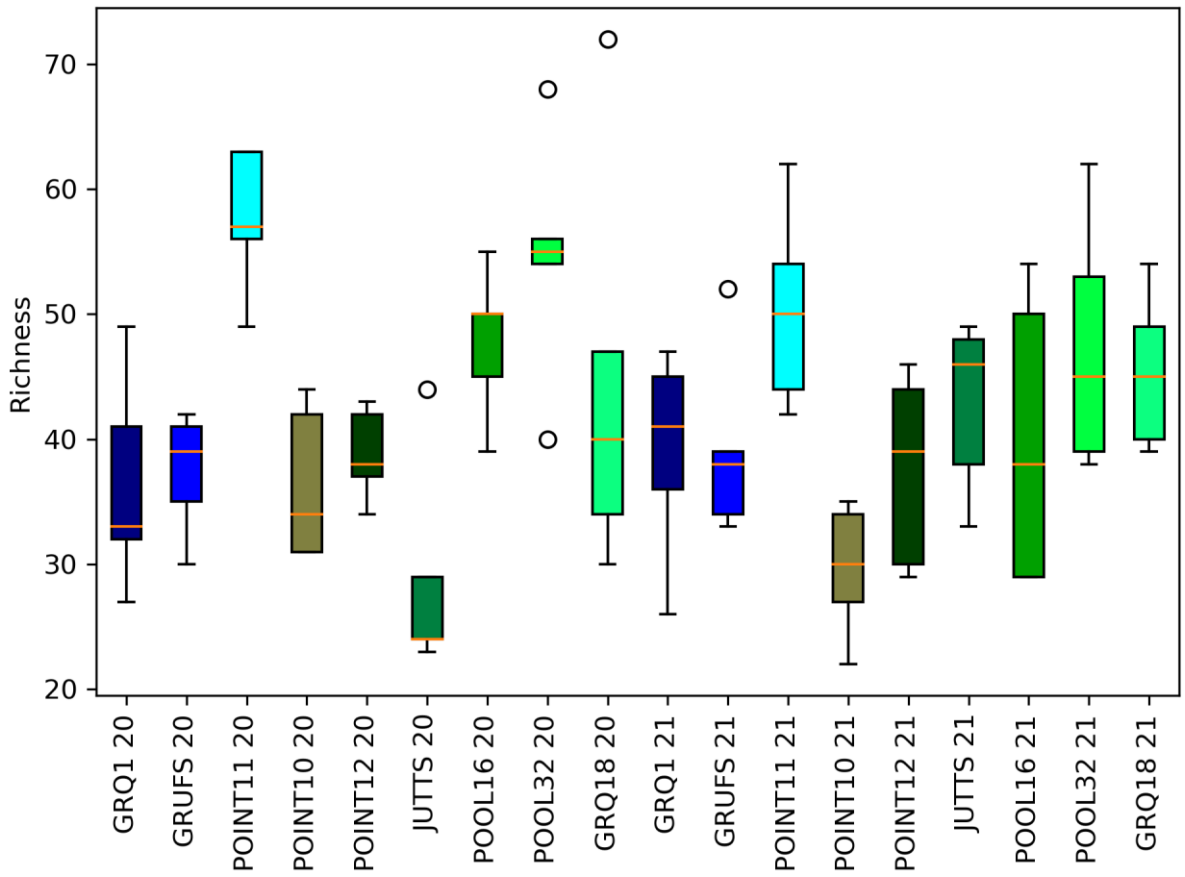


**Figure 56. Diatom OTU richness from 2020 and 2021.**

Reference sites (blue) and discharge monitoring sites (green).

**Table 37. One-Way ANOVA results on diatom richness and read abundance for reference and discharge monitoring treatments.**

| **diatom OTU Richness** | Reference | Reference | Discharge monitoring | Discharge monitoring | One-Way ANOVA | |
|---|---|---|---|---|---|---|
| | mean | ± S.E. | mean | ± S.E. | *F* | *P-value* |
| Spring 2020 | 44 | 3.1 | 42 | 2.2 | 0.5 | 0.61 |
| Spring 2021 | 43 | 2.4 | 41 | 1.8 | 0.6 | 0.43 |

| **diatom OTU read Abundance** | Reference | Reference | Discharge monitoring | Discharge monitoring | One-Way ANOVA | |
|---|---|---|---|---|---|---|
| | mean | ± S.E. | mean | ± S.E. | *F* | *P-value* |
| Spring 2020 | 35001 | 3819.4 | 61871 | 4877.2 | 13.1 | **<0.05** |
| Spring 2021 | 22033 | 2748.3 | 45462 | 3721.8 | 17.3 | **<0.05** |

Bold values represent p<0.05

### Diatom community composition

The diatom community composition similarities and differences are presented in the ordination plot (nMDS) (Figure 57). Figure 57 is showing the similarities/differences between the diatom community structure in Spring 2020 and 2021 for the two treatments. The diatom communities from the reference sites were markedly different to those from the discharge monitoring sites. The diatom ordination plots for 2020 and 2021 also highlight that the diatom communities from the reference sites GRQ1 and GRUFS were markedly different to the Point 11 reference site diatom communities with Point 11 clustering away from the other two reference sites for both years (Figure 57). The sites closest to the discharge (Point 10, Point 12 and Jutts) are separating furthest away from the reference sites in Figure 57. This difference between reference treatments and discharge monitoring treatments is confirmed by the PERMANOVA which found a significant difference in composition between the two treatments in Spring 2020 (PERMANOVA: F= 35.3, $p<0.05$) and in Spring 2021 (PERMANOVA: F= 46.8, $p<0.05$). When looking at the diatom communities over time independently, there was no significant difference between the diatom communities between spring 2020 and 2021 (PERMANOVA: F= 1.91, $p=0.25$). When analysing the contribution of treatment and sampling time to the diatom community, there was a significant difference in diatom treatments (reference and discharge monitoring) with time (2020 compared with 2021) (PERMANOVA: F= 2.1, $p<0.05$). Diatom community differences between sites were analysed with a pairwise PERMANOVA (Appendix B, Tables B7-B8). In 2020 all sites were significantly different from each other except for Pool 16 and Pool 32 which had no significant difference (Appendix B B7-B8). In 2021 all sites were significantly different from each other.

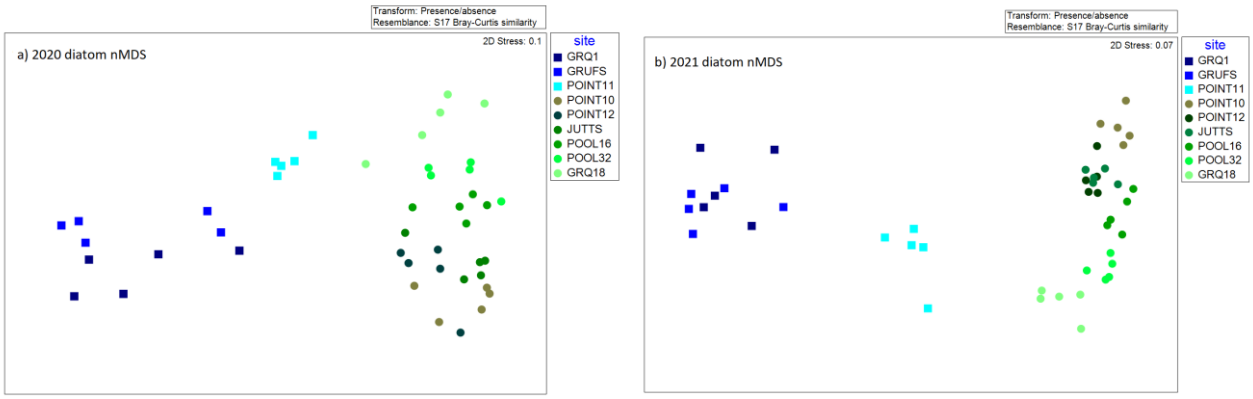


**Figure 57. nMDS of the diatom metabarcoding data 2020 and 2021.**

a) 2020 Diatoms nMDS ordination. b) 2021 Diatoms nMDS ordination. Reference sites (blue) and discharge monitoring sites (green). Analysis is derived from presence/absence data at the level of Operational Taxonomic Unit (OTU).

**Table 38. Results of PERMANOVA testing for variation in diatom community composition (2020 and 2021) between sampling timepoints (years) and treatments (reference vs discharge monitoring).**

| Factor: source of variation | df | MS | Pseudo-F | P(perm) | Unique perms |
|---|---|---|---|---|---|
| **Treatment 2020** | 1 | 45568 | 35.3 | **0.0001** | 9940 |
| **Treatment 2021** | 1 | 31485 | 46.8 | **0.0001** | 9956 |
| **Time (year)** | 1 | 3412 | 1.9095 | 0.248 | 9914 |
| **Treatment (2020&2021)** | 1 | 71591 | 70.726 | **0.0001** | 9945 |
| **Time*Treatment** | 1 | 3289 | 2.0526 | **0.045** | 9937 |
| **Res** | 86 | 951.3 | | | |
| **Total** | 89 | | | | |

Df: degrees of freedom; MS: mean squares; Pseudo-F: multivariate analogue to Fisher's F test statistic of the null hypothesis; P(perm): probability by permutations; Unique Perms: number of unique permutations.

Bold values represent $p<0.05$

### 3.8.6 Relationships between diatom communities and water quality (2020-2021)

The 18S V4 diatom community structure and water quality variable correlations were investigated using multivariate statistics including distance linear models (DistLM). The correlative relationships between the metabarcoded diatom communities and water quality from the Spring 2020 and Spring 2021 sampling events combined is illustrated in Figure 58. Approximately 80% of the variation in the diatom community data could be explained by the environmental variables measured. The ordination plot (Figure 58) suggests that the diatom communities from the discharge monitoring sites are influenced by similar water quality parameters (pH, conductivity and nickel) separating away from the reference sites in the ordination. When examined collectively, the variables which explained significant proportions of the variation in the diatom community data were pH (53%), copper (7%) and nickel (7%). The distance-based analysis investigating the correlative patterns of the diatom OTU community data with measured environmental variables is shown in Table 39. The variable which contributed the most to the diatom variation overall was pH (53%) and the other significant variables copper (7%) and nickel (7%) are contributing a small but significant proportion to the diatom variation. The dbRDA ordination (Figure 58) illustrates the variation explained by the two-distance-based axis, showing axis1 as explaining 58% of the total diatom variation largely driven by conductivity and pH and axis 2 only explaining 9.7% of the total variation driven by the measured metals (nickel and aluminium).

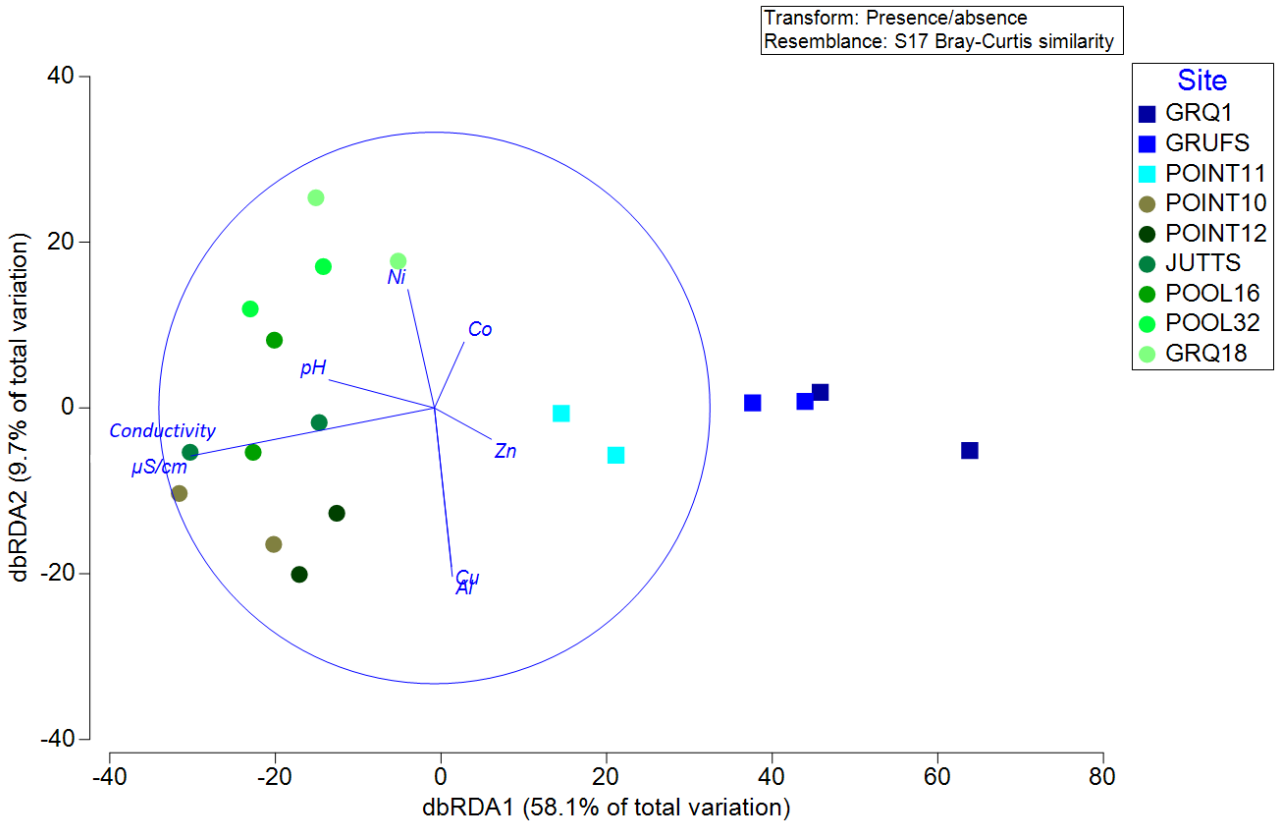


**Figure 58. Ordination plot derived from the distance-based model illustrating the relationships between key environmental variables and metabarcoded diatom composition from Spring 2020 and 2021.**

Reference sites (blue) and discharge monitoring sites (green).

**Table 39. Sequential test results of distance-based linear model (DistLM) for diatom OTUs 2020 and 2021.**

| Variable | Adj $R^2$ | SS(trace) | Pseudo-F | P | Prop.% | Cumulative contribution | res.df |
|---|---|---|---|---|---|---|---|
| **+pH** | 0.51 | 13879 | 18.34 | **0.0001** | 0.53 | 0.53 | 16 |
| **+Copper** | 0.55 | 1810 | 2.64 | **0.0122** | 0.07 | 0.60 | 15 |
| **+Nickel** | 0.60 | 1815 | 3.00 | **0.0072** | 0.07 | 0.67 | 14 |
| **+Zinc** | 0.63 | 1067 | 1.87 | 0.0713 | 0.04 | 0.71 | 13 |
| **+Aluminium** | 0.65 | 908 | 1.67 | 0.0872 | 0.03 | 0.75 | 12 |
| **+Cobalt** | 0.66 | 756 | 1.45 | 0.1742 | 0.03 | 0.78 | 11 |
| **+Conductivity µS/cm** | 0.67 | 685 | 1.35 | 0.2277 | 0.03 | 0.81 | 10 |

SS(trace): sum of squares; Pseudo-F: multivariate analogue to Fisher's F test statistic of the null hypothesis; P: probability(<0.01 significant); Prop%: the proportion of variation; res.df: residual degrees of freedom

Bold values represent p<0.05

### 2020 diatom relationships with water quality

The correlative relationships between the metabarcoded diatom communities and water quality variables from the Spring 2020 sampling are illustrated in Figure 59 and Table 40. The fitted DistLM was visualised using a dbRDA, constrained ordination (Figure 59), demonstrating the correlation of variables on the diatom community for 2020. Approximately 87% of the total diatom variation was explained by the measured variables in Spring 2020 including pH, aluminium, conductivity, copper, and nickel. When examined collectively, the variables which explained significant ($p<0.05$) proportions of the variation in the diatom community data were pH (57%) and conductivity (11%). The ordination shows dbRDA1 is contributing to 62% of the variation which is mostly driven by pH and conductivity and dbRDA2 in contributing 12% of the variation driven by the metals.

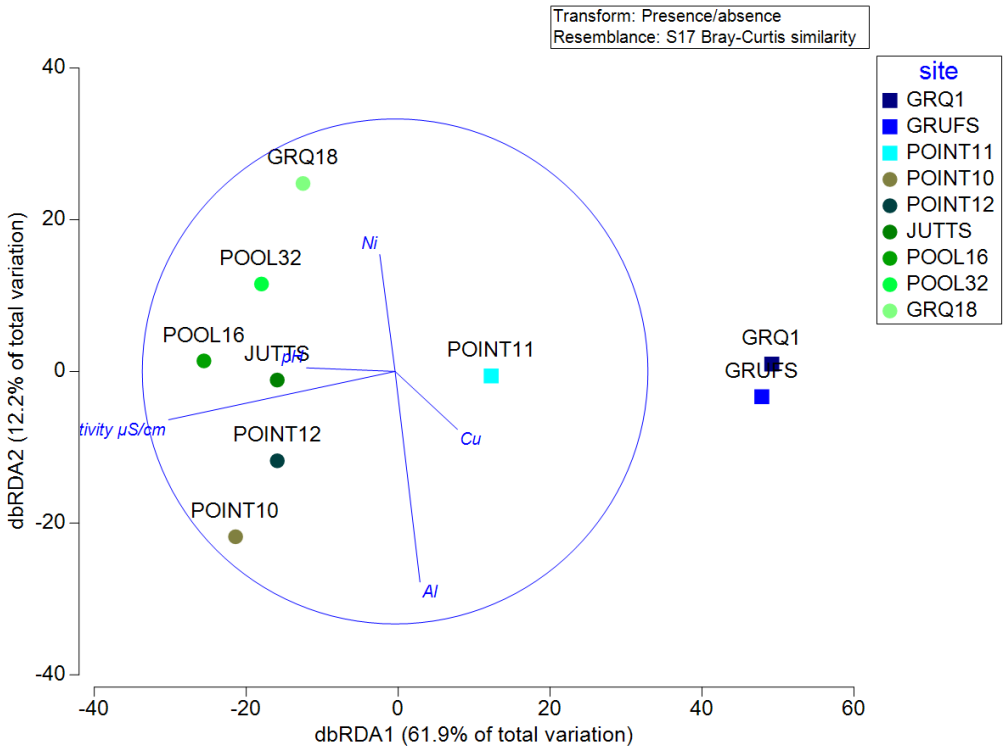


**Figure 59. Ordination plot derived from the distance-based model illustrating the relationships between key environmental variables and metabarcoded diatom composition from Spring 2020.**

Reference sites (blue) and discharge monitoring sites (green).

Table 40. Sequential test results of distance-based linear model (DistLM) for diatom OTUs 2020.

| Variable | Adj $R^2$ | SS(trace) | Pseudo-F | P | Prop%. | Cumulative contribution | res.df |
|---|---|---|---|---|---|---|---|
| **+pH** | 0.50 | 6368.0 | 9.2 | **0.0006** | 0.57 | 0.57 | 7 |
| **+Aluminium** | 0.54 | 970.1 | 1.5 | 0.2019 | 0.09 | 0.65 | 6 |
| **+Conductivity µS/cm** | 0.62 | 1204.6 | 2.2 | **0.0357** | 0.11 | 0.76 | 5 |
| **+Copper** | 0.65 | 723.6 | 1.5 | 0.2240 | 0.06 | 0.82 | 4 |
| **+Nickel** | 0.66 | 559.3 | 1.2 | 0.3624 | 0.05 | 0.87 | 3 |

SS(trace): sum of squares; Pseudo-F: multivariate analogue to Fisher's F test statistic of the null hypothesis; P: probability(<0.01 significant); Prop%: the proportion of variation; res.df: residual degrees of freedom

Bold values represent p<0.05

## 2021 diatom relationships with water quality

The fitted DistLM was visualised using a dbRDA constrained ordination (Figure 60), demonstrating the correlation of variables on the diatom community in Spring 2021. Approximately 98% of the total diatom variation was explained by the measured variables in Spring 2021 including pH, total nitrogen, aluminium, conductivity, zinc, alkalinity, and copper (Table 41). When examined collectively, the variables which explained significant (p<0.05) proportions of the variation in the diatom community data were pH (64%), total nitrogen (11%) and aluminium (12%). In Spring 2021 pH contributed the most to the total diatom variation measured, contributing 64% to the total diatom community variation.

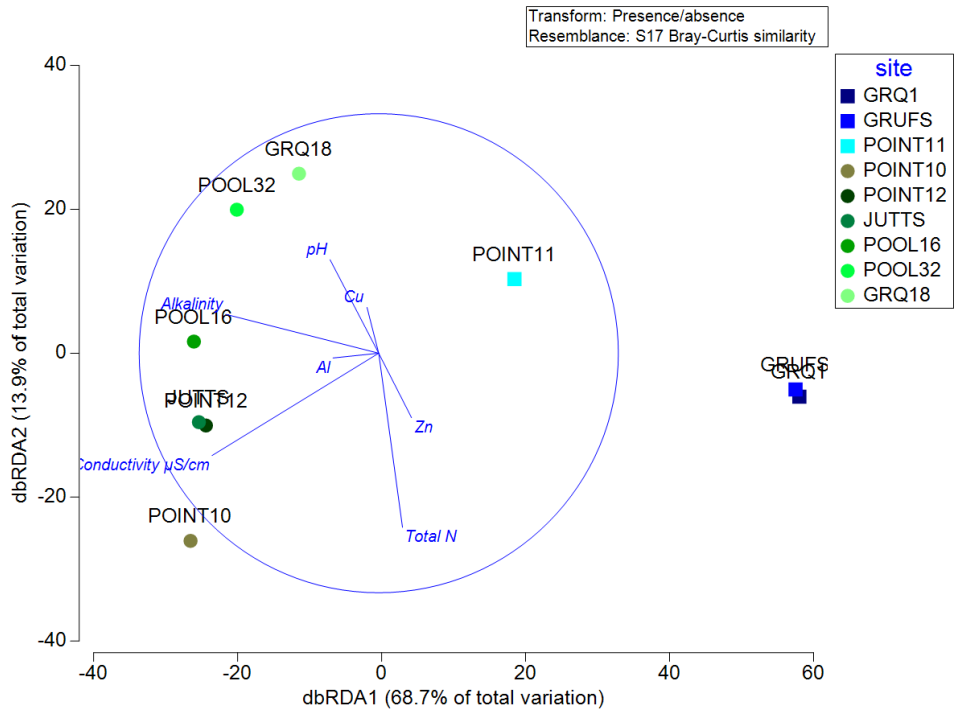


**Figure 60. Ordination plot derived from the distance-based model illustrating the relationships between key environmental variables and metabarcoded diatom composition from Spring 2021.**

Reference sites (blue) and discharge monitoring sites (green).

**Table 41. Sequential test results of distance-based linear model (DistLM) for diatom OTUs in 2021.**

| Variable | Adj $R^2$ | SS(trace) | Pseudo-F | P | Prop%. | Cumulative contribution | res.df |
|---|---|---|---|---|---|---|---|
| **+pH** | 0.59 | 9523.8 | 12.6 | **0.0001** | 0.64 | 0.64 | 7 |
| **+Total Nitrogen** | 0.67 | 1573.4 | 2.5 | **0.0456** | 0.11 | 0.75 | 6 |
| **+Aluminium** | 0.79 | 1725.4 | 4.3 | **0.0197** | 0.12 | 0.87 | 5 |
| **+Conductivity µS/cm** | 0.81 | 550.3 | 1.5 | 0.2055 | 0.04 | 0.90 | 4 |
| **+Zinc** | 0.82 | 451.4 | 1.4 | 0.3051 | 0.03 | 0.93 | 3 |
| **+Alkalinity** | 0.85 | 426.7 | 1.5 | 0.2914 | 0.03 | 0.96 | 2 |
| **+Copper** | 0.90 | 376.8 | 2.1 | 0.3241 | 0.03 | 0.98 | 1 |

SS(trace): sum of squares; Pseudo-F: multivariate analogue to Fisher's F test statistic of the null hypothesis; P: probability(<0.01 significant); Prop%: the proportion of variation; res.df: residual degrees of freedom

Bold values represent p<0.05

The key OTUs which contributed to the observed differences in diatom composition between reference and monitoring sites can be seen from the SIMPER analyses (Table 42). Key diatom taxa which contributed to the observed differences in compositions in the reference treatment were: *Eunotia*, for both 2020 and 2021, also *Neidium* contributed to observed differences in reference treatment in 2020 and *Amphora* in 2021. Key diatom taxa contributing to the observed differences in compositions in the discharge monitoring treatment were: *Navicula* in 2020 and 2021 but also, *Staurosirella* and *Denticula* in 2020 and *Entomoneis, Melosira* and *Gomphonema* were

representative of discharge monitoring in 2021. Raphid-pennate Bacillariophyceae (unknown Genus) diatoms were ubiquitous across both treatments in 2020 and in 2021. The top 10 diatom taxa which contributed most to the differences between reference and discharge monitoring treatments for the sampling years 2020 and 2021 are presented in Table 42 and their taxonomic assignments are listed in Table 43. These data are presented relative to the mean of the reference sites, such that a positive value indicates an increase and a negative value indicates a decrease relative to the reference mean. In 2020 and in 2021, Table 43shows a number of OTUs which had both positive (increases in abundance) and negative (decreases in abundance) responses.

In 2020 OTU_9 (*Anomoeoneis sphaerophora*) and OTU_6 (*Navicula cryptocephala*) mostly increased at the discharge monitoring sites. In 2021 OTU3 (*Navicula gregaria*) increased with distance from the discharge source. In 2020 OTU_2 (*Staurosirella pinnata)* was high at Point 10 and decreased with distance from the discharge point. OTU_18 (*Neidium affine*) and OTU_13 (Raphid-pennate unknown genus) decreased at all discharge monitoring sites.

In 2021 OTU_43 (*Denticula*) increased in all discharge monitoring sites. *Denticula* species presence in freshwater systems have been correlated with increased nutrients (Soeprobowati et al., 2022). OTU_1 (*Entomoneis ornata* ) a common freshwater benthic diatom and OTU_10 (*Amphora libyca* ) mostly increased in the discharge monitoring sites while OTU_5 (*Cocconeis stauroneiformis*) increased at the downstream sites. In 2021 OTU_12 (Raphid-Pennate unknown genus) decreased at all discharge monitoring sites. OTU_112 (*Eunotia* sp) also decreased at all discharge monitoring sites relative to the reference mean. OTU_112 (*Eunotia* sp) diatom was only detected in the reference sites in 2021.

The composition and diversity of the benthic diatom community are affected differently by changes in physico–chemical characteristics of the water (Ács et al., 2004). A number of diatom taxa were identified as indicators from an indicator analysis performed in the 2020 EIP2 report (Chariton and Stephenson 2020). The *Eunotia* diatom continues to be an indicator taxon with higher presence and abundance in the reference sites. SIMPER dissimilarity analysis on diatom OTUs identified *Eunotia* as one of the main taxa distinguishing reference from discharge monitoring treatments. *Eunotia* was also identified as a biological indicator taxa in the 2020 EIP2 report and earlier 2018 monitoring programs (Chariton and Stephenson 2020 and 2018). *Eunotia* are recognised as freshwater diatoms associated with acidic systems (Cantonati and Lange-Bertalot 2011, Luís et al., 2009), *Eunotia* diatoms have also been characterised as sensitive to

elevated metal concentrations (Luís et al., 2016). This makes them a suitable indicator to continue monitoring through the diatom metabarcoding analysis. *Navicula* diatoms were representative of the discharge monitoring sites and had higher average abundances in discharge sites compared to the reference treatment. *Navicula* are common benthic diatoms, commonly found in river benthos. *Navicula* have also been frequently recorded in waters that are nutrient-rich and high in conductivity (Van Dam et al., 1994; Bere and Tundisi 2011).

**Table 42. SIMPER results illustrating the top 10 diatom taxa that account for most of the dissimilarities between the reference and discharge monitoring sites (2019, 2020 and 2021).**

| | | | Change from Mean Reference | | | | | | |
|---|---|---|---|---|---|---|---|---|---|
| | Taxon | Mean Reference | POINT10 | POINT12 | JUTTS | POOL16 | POOL32 | GRQ18 | Comments |
| **2020** | OTU_1 | 0.602 | 29.9 | 19.3 | 15.1 | 2 | -0.1 | -0.2 | Variable response at monitoring sites |
| | OTU_3 | 2.37 | -0.4 | 9.6 | 0.7 | 6.1 | 5.9 | 29.1 | Variable response, increase with distance |
| | OTU_6 | 0.089 | 0.4 | 1.1 | 1.1 | 17.3 | 25.7 | 4.9 | Mostly increase at monitoring sites |
| | OTU_2 | 0.393 | 22.3 | 8.3 | 17.5 | 3.1 | 2.9 | 0.3 | Variable response at monitoring sites |
| | OTU_4 | 0.587 | 0.1 | 16.5 | 9.4 | 5 | 9 | 3.9 | Mostly increase at monitoring sites |
| | OTU_9 | 0.325 | 9.9 | 9.8 | 12.0 | 5.9 | 0.7 | -0.1 | Mostly increase at monitoring sites |
| | OTU_43 | 0.2 | 0 | 0.5 | 16.3 | 6.3 | 7.2 | -0.2 | Variable response at monitoring sites |
| | OTU_18 | 10.4 | -10.3 | -10.4 | -10.4 | -10.3 | -10.4 | -10.1 | Decrease at all monitoring sites |
| | OTU_13 | 8.61 | -8.5 | -8.5 | -8.6 | -8.6 | -8.6 | -8.3 | Decrease at all monitoring sites |
| | OTU_11 | 0.0501 | 0.1 | 5.5 | 0.9 | 8.7 | 5.4 | 0.3 | Variable response at monitoring sites |
| **2021** | OTU_43 | 0.271 | 15 | 12.3 | 17.3 | 15.3 | 7.5 | 1.3 | Increase at all monitoring sites |
| | OTU_8 | 0 | 0 | 0.2 | 0.2 | 40.1 | 2.1 | 0 | Variable response at monitoring sites |
| | OTU_1 | 0.0163 | 8.4 | 19.8 | 19.9 | 1.7 | 0.5 | 0 | Mostly increase at monitoring sites |
| | OTU_5 | 6.73 | 0 | 1 | 5 | 4.7 | 3.1 | 19.9 | Variable response, increase with distance |
| | OTU_2 | 0.203 | 30.5 | 4.4 | 4.5 | 0.7 | 0.7 | 0.3 | Variable response, decrease with distance |
| | OTU_4 | 0.268 | 0.7 | 18.9 | 1.4 | 1.3 | 5.5 | 3.6 | Variable response monitoring sites |
| | OTU_12 | 11.2 | 0 | 0 | 0 | 0 | 0 | 0.2 | Decrease at all monitoring sites |
| | OTU_3 | 2.35 | 1.0 | 3.4 | 3.7 | 3.4 | 9.1 | 13.1 | Variable response, increase with distance |
| | OTU_112 | 9.63 | 0 | 0 | 0 | 0 | 0 | 0 | Decrease at all monitoring sites |
| | OTU_10 | 4.08 | 0.0 | 5.8 | 3.9 | 3.2 | 1.7 | 2.7 | Variable response at monitoring sites |

**Table 43. List of OTU, closest taxonomic assignment and match % that account for most of the dissimilarities between the reference and discharge monitoring sites in diatom dataset (2019, 2020 and 2021).**

| Taxon | Closest Genus | Closest species | Match % | Accession |
|---|---|---|---|---|
| **OTU_43** | Denticula | *Denticula kuetzingii* strain UTEX FD135 | 99.3 | HQ912610.1.162 |
| **OTU_8** | Melosira | *Melosira varians* | 99.3 | KC309539.1.1621 |
| **OTU_1** | Entomoneis | *Entomoneis ornata* strain 14A | 99.3 | HQ912411.1.1733 |
| **OTU_5** | Raphid-pennate | *Cocconeis stauroneiformis* strain s0230 | 93.5 | AB430614.1.1712 |
| **OTU_2** | Staurosirella | *Staurosirella pinnata* strain CCMP330 | 99.7 | HQ912620.1.2328 |
| **OTU_4** | Raphid-pennate | Raphid-pennate X sp. clone I-8-MC812-OTU-59 | 99 | KC771158.1.1787 |
| **OTU_12** | Raphid-pennate | Raphid-pennate X sp. strain MBIC10815 | 91 | AB183645.1.1725 |
| **OTU_3** | Navicula | *Navicula gregaria* strain BA102 | 100 | HM805037.1.1688 |
| **OTU_112** | Eunotia | *Eunotia* sp. strain AT-73Gel02 | 98.6 | AM501963.1.1742 |
| **OTU_10** | Amphora | *Amphora libyca* strain AT-117.10 | 100 | AM501959.1.1736 |
| **OTU_6** | Navicula | *Navicula cryptocephala* strain LCR-S-2-2-1 | 98.3 | JQ610162.1.1206 |
| **OTU_9** | Anomoeoneis | *Anomoeoneis sphaerophora* strain L1222 | 100 | AJ535153.1.1779 |
| **OTU_18** | Neidium | *Neidium affine* strain UTEX FD127 | 96.4 | HQ912583.1.1742 |
| **OTU_13** | Raphid-pennate | Raphid-pennate X sp. clone 6c-H3 | 99.3 | FN690540.1.1679 |
| **OTU_11** | Gyrosigma | *Gyrosigma limosum* | 97.9 | AY485516.1.1623 |

### 3.8.7 Metabarcoding summary

The prokaryote, eukaryote and diatom metabarcoding for the sampling occasions Spring 2019, Spring 2020 and Spring 2021 all showed that at the OTU level, community composition, for prokaryotes (Figure 40), eukaryotes (Figure 49) and diatoms (Figure 57), differed between reference sites and discharge monitoring sites. These observations were supported by statistical analyses (PERMANOVA) for prokaryotes (Table 22), eukaryotes (Table 30) and diatoms (Table 38) which presented statistical evidence of the differences between reference and discharge treatment community structure and correlated with water quality changes. The main driving water quality factors which contributed to the variation in all the metabarcoded communities were pH and conductivity. On some occasions total nitrogen and metals such as aluminium, copper, nickel and zinc were also contributing to the prokaryote, eukaryote and diatom

community variation. For example, for prokaryotes in 2019 conductivity, pH and nickel were statistical key drivers for the community variation while in 2020 only pH was a main driver. In 2021 pH and total nitrogen were the key drivers for prokaryote community composition. For eukaryotes in 2019 conductivity and aluminium were identified as key water quality drivers while in 2020 only pH was identified as a key variable and in 2021 pH and aluminium were key drivers contributing to eukaryote variation. For diatoms in 2020 pH and conductivity were the main drivers of biological variation and in 2021 pH, aluminium and total nitrogen were the main water quality drivers for the diatom communities.

The metabarcoding data also assisted in identifying potential key biological indicators which were representative of the treatments i.e., more abundant in either reference or discharge monitoring sites. The indicator taxa for prokaryotes which were having a negative response, more abundant in reference sites and less abundant in discharge monitoring sites were OTU_6 (*Massilia namucuonensis*), OTUs 9 (*Reticulibacter mediterranei*) and 13 (*Bradyrhizobium lupini*) these may potentially be putative indicator taxa for environmental disturbance as they responded negatively at all the discharge monitoring sites. A large number of prokaryote OTUs were positively affected and increased in abundance at all downstream monitoring sites. Several eukaryote OTUs responded negatively at the discharge monitoring sites including OTU_6 (*Nitella capillaris*) freshwater green macro-algae, OTU_20 (*Pentaphlebia* sp Leptophlebiidae) and OTU_22 *Reticulascus tulasneorum* an Ascomycota fungus. These eukaryote OTUs may potentially be putative indicator taxa for environmental disturbance as they responded negatively at all the discharge monitoring sites. The main indicator which showed a positive change and increased in abundance at discharge monitoring sites was OTU_8 (*Navicula*), Naviculacae diatom, which increased at all discharge monitoring sites. The key indicator taxa for diatoms which were having a negative response, i.e., more abundant in reference sites and less abundant in discharge monitoring sites were OTU_112, *Eunotia* and OTU_12 an unknown Raphid-Pennate diatom. A number of diatom OTUs positively responded at the discharge monitoring sites, i.e., increased in abundance at all downstream monitoring sites, these included OTU_2 *Staurosirella*, OTU_43 *Denticula,* OTU_1 *Entomoneis and* OTU_8 *Melosira.* These key potential indicator taxa can provide evidence of change in the biological composition of the sites and treatments over time and in response to abiotic ecosystem changes.

## 3.9 eDNA detection results: platypus and Macquarie perch

The qPCR assays tested for platypus DNA and Macquarie perch DNA in nine replicate eDNA water filter samples. No platypus or Macquarie perch eDNA were detected at any of the sites analysed in either qPCR assay.

**Table 44. Results of eDNA analysis of water samples for platypus (*Ornithorhynchus anatinus*).**

| Site | Date Sampled | Positive Assays | Test Result |
|---|---|---|---|
| **GRQ1** | 28/09/2021 | 0/9 | Negative |
| **GRUFS** | 28/09/2021 | 0/9 | Negative |
| **POINT 11** | 28/09/2021 | 0/9 | Negative |
| **POINT 10** | 29/09/2021 | 0/9 | Negative |
| **POINT 12** | 28/09/2021 | 0/9 | Negative |
| **JUTTS** | 28/09/2021 | 0/9 | Negative |
| **POOL 16** | 28/09/2021 | 0/9 | Negative |
| **POOL 32** | 28/09/2021 | 0/9 | Negative |
| **GRQ18** | 28/09/2021 | 0/9 | Negative |

**Table 45. Results for eDNA analysis of water samples for Macquarie perch (*Macquaria australasica*)**

| Site | Date Sampled | Positive Assays | Test Result |
|---|---|---|---|
| **GRQ1** | 28/09/2021 | 0/9 | Negative |
| **GRUFS** | 28/09/2021 | 0/9 | Negative |
| **POINT 11** | 28/09/2021 | 0/9 | Negative |
| **POINT 10** | 29/09/2021 | 0/9 | Negative |
| **POINT 12** | 28/09/2021 | 0/9 | Negative |
| **JUTTS** | 28/09/2021 | 0/9 | Negative |
| **POOL 16** | 28/09/2021 | 0/9 | Negative |
| **POOL 32** | 28/09/2021 | 0/9 | Negative |
| **GRQ18** | 28/09/2021 | 0/9 | Negative |

Neither species had been detected in upper reaches of the Georges River in previous surveys, however surveys by Griffiths et al., 2021 had detected Macquarie perch in the middle reaches, downstream of Wedderburn (Griffiths et al., 2021). There are no recent records (<10 years) in the area of either species on the major wildlife databases (Atlas of Living Australia, BioNet).

# 4 Conclusions

- LDP10 continued to be the main water discharged into Brennans Creek in 2020 and 2021. LDP40 discharge is currently contributing a very small proportion of total flows and was only captured in the Spring 2021 sampling.

- Water quality parameters measured at reference treatments were mostly within the ANZG (2018) guideline value (GV) ranges, with some exceptions for one or two sites at each sampling occasion. The pH of waters from Point 10 (7.6-8.9) and all downstream sites were higher than those at reference sites (4.9-7.2). Conductivity, pH, alkalinity, aluminium, copper, and to a lesser extent, nickel, as well as all measures of nitrogen decreased with increasing distance from the discharge source at LDP10 and LDP40.

- Aluminium continues to be a metal with elevated concentrations in sites across the survey. Zinc concentrations were consistent in the reference sites GRUFS and GRQ1 but concentrations were erratic in the discharge monitoring sites, not following a trend.

- While the DISTLM statistics showed pH as a key correlate of the differences in the macrobenthic communities and metabarcoded communities, it seems likely that pH is affecting the bioavailability of metals and resulting in some potential toxicity which could then translate into ecological impacts. In some seasons and years, pH and metals (aluminium, zinc and nickel) were highlighted as potential drivers of biological change. The chemistry of the study area is complex and pH in combination with other water quality variables such as alkalinity, DOC and metal interactions should be considered. Metal bioavailability is influenced by many aspects of water chemistry such as major ions, pH, hardness, alkalinity, and dissolved organic matter. An important characteristic for most metals is pH because many metals will have differing speciation across a pH range, which in turn can lead to differences in toxicity (Price et al., 2021).

- It is acknowledged that GRQ1 and GRUFS are not the optimal reference sites but the only available upstream options with Point11. The reference sites were selected for the EIP2 with knowledge of this limiting effect; however, the project team were unable to find more

suitable reference sites for the GRAHMP in the local area without this limiting experimental design effect.

- Both the macrobenthic and the metabarcoding prokaryote, eukaryote and diatom community structure analysis highlighted the reference treatment biological communities were different to the discharge monitoring biological communities for all years.

- The addition of the diatom specific DNA metabarcoding assay has proved to be insightful in identifying community composition shifts in the lower trophic microeukaryote primary producer component of the Georges River system. The presence of certain diatom taxa can reveal factors about the environment such as nutrient cycling, substrate type water quality and available light for photosynthesis. The diatom survey found diatoms which respond to nutrients such as *Navicula*, *Entomone*is and *Denticula* were more abundant at the discharge monitoring sites while more acidic water tolerant diatoms such as *Eunotia* were only detected in the reference sites.

**Table 46. A summary of multiple lines of evidence obtained between 2013 and 2021.**

| Evidence | Attributes | Evidence | Summary |
|---|---|---|---|
| **Water chemistry** | Conductivity, pH, metals and nutrients | Elevated conductivity, pH, metals and nitrogen at discharge sites, compared to reference sites, and many of these decrease with increasing distance from Point 10. Conductivity and some metals have decreased over time at each site. | Water quality at sites closest to the discharge is still sufficiently contaminated to cause biological impairment. These effects are likely to decrease with increasing distance from the discharge. |
| **Ecotoxicology** | 7 tests (2013-2019), reduced to 2 tests (2020-2021) | Ongoing toxicity observed for LDP10 waters, particularly to *C. dubia* reproduction, however acute toxicity (lethality) has decreased for *C. dubia* and *M. splendida.* | Although there has been a reduction in acute toxicity (lethal endpoints), effects on *C. dubia* survivorship were still observed in 2021, as were effects on *C. dubia* reproduction, indicating ongoing risk of impairment to organisms in the receiving environments. |
| **Macrobenthic communities** | Community structure | Communities from the reference treatment were consistently different to the discharge monitoring treatments. Point 11 has some other water quality/metal inputs (aluminium). | Discharge is altering community structure in the discharge monitoring treatment.<br>The furthest discharge monitoring site GRQ18 is being influenced by other catchment factors. |
| | SIGNAL | SIGNAL scores were slightly higher in the reference sites than the discharge monitoring. | Reference sites have more sensitive taxa suggesting better ecological condition than the discharge monitoring sites. SIGNAL scores declined in 2018/2019 most likely due to drought and SIGNAL scores have started to improve with greater rainfall over 2020/2021. |
| | Leptophlebiidae | This group was more abundant and frequent in reference sites. Abundance increased in Spring 2021 survey. *Thraulophlebia* was predominantly observed in the reference treatment, very | Evidence suggests that this group may be sensitive to the discharge waters. However, most discharge monitoring sites appear to also be unsuitable habitat |

| | | | |
|---|---|---|---|
| | | rarely at the downstream discharge site GRQ18. | for the taxa. Habitat should also be factored into Leptophlebiidae presence. |
| **Metabarcoding** | Metabarcoding | For the eukaryotes, the communities from the reference treatment were consistently different to the discharge monitoring treatments. Point 11 was showing community structure less similar to GRQ1 and GRUFS.<br>Diatom communities are different in the reference treatments compared to the discharge monitoring treatment sites.<br>Similarly, prokaryotic community composition differed between the reference treatments compared to the discharge monitoring treatment sites. | pH, conductivity, alkalinity and some metals (zinc, aluminium, nickel) were contributing to the biological variation in the metabarcoded communities. |

# 5 Recommendations

To investigate the effects of installation of the RO ANWTP to the ecosystem health of the Georges River, we recommend keeping the core lines of evidence consistent for clear detection of water quality changes and observed ecological changes. Consistency in weight of evidence experimental design will assist with identifying correlative patterns between biotic and abiotic factors as the system changes with the implementation of the long-term RO WTP. We have however, identified some guidelines to enhance the current design that we recommend for the ongoing program for 2022 – 2024 sampling and reporting.

**Recommendations**

- Removal of major ions from water, and altering their composition, can also be toxic to aquatic biota. While the RO WTP at LDP40 demonstrated a reduction in metal concentrations compared to LDP10, major ions were also removed, evident by lower conductivity. It is noted that some reference sites also have low concentrations of major ions (conductivity of 100-200 µS/cm), however water from these sites have not been tested for toxicity to *C. dubia*. Target values for conductivity of LDP40 water are required and should be comparable to those in receiving waters to minimise any potential impact to endemic aquatic species and the natural ecosystem. Addition of essential salts may be required to ensure minimal impact from RO-treated water discharge to aquatic biota.

- Consider incorporating total organic carbon and water hardness (as measured by $Ca^{2+}$ and $Mg^{2+}$) in the key parameters measured in the water samples. Revised ANZG GVs for copper, nickel and potentially zinc will be based on modifying factors depending on pH, water hardness and total organic carbon. These revised ANZG GVs can be applied to the GRAHMP water chemistry metal analysis if total organic carbon and water hardness measurements are collected and analysed. Potential to investigate site specific water quality guidelines as the ANZG GVs are updated.

- Modification of ecotoxicity test design (i.e., changing/expanding the concentration series tested) could improve the reliability of the EC10 values.

- Inclusion of field blanks for chemical analysis is recommended to enable identification of any possible contamination sources during sampling, particularly in light of the erratic zinc concentrations reported for 2020/2021 in both reference and discharge monitoring sites.

- Consider optimal ways of visualising the long term chemistry data. Potentially starting long term chemistry data at Autumn 2016 data point for consistency of seasonal Autumn and Spring sampling data. For 2013-2015 only Spring chemistry data is available.

- Optimise water level measurement data collection so it can be normalised and compared between sites as a variable for multivariate statistics. For example, including water depth data in addition to the nail reading water level measurements.

- Remove richness and abundance metrics from macrobenthic analysis. Abundance on its own provides little information about the ecosystem health of the sites as it doesn't consider which taxa (sensitive or tolerant) were present. Community composition using Bray-Curtis similarities and dissimilarities is a much stronger analysis.

- We recommend continuing the diatom target DNA metabarcoding assay for comparisons of diatom community shifts post implementation of the ANWTP 2022.

- We suggest running small metabarcoding microcosm experiments using subsampled, environmental water from the reference sites and discharge monitoring sites. This is a suggestion to isolate the effect of water quality in a controlled system and could involve analysing the eukaryote and prokaryote community composition from the water samples taken from the study sites that were placed into small microcosms (e.g. 250ml beakers). The DNA could then be analysed from the microcosm samples exposed to the site water.

# References

Ács, É., Szabó, K., Tóth, B., and Kiss, K.T. (2004) Investigation of benthic algal communities, especially diatoms of some Hungarian streams in connection with reference conditions of the water framework directives. Acta Botanica Hungarica, 46(3–4): 255–277.

Adewunmi, C.O., Becker, W., Kuehnast, O., Oluwole, F. and Dörfle, G. (1996) Accumulation of copper, lead and cadmium in freshwater snails in southwest Nigeria. Science of the Total Environment., 193, pp. 69-73

Ali, A.E., Sloane, D.R. and Strezov, V. (2018). Assessment of impacts of coal mining in the region of Sydney, Australia on the aquatic environment using macroinvertebrates and chlorophyll as indicators. International Journal of Environmental Research and Public Health, 15, 1–15. https://doi.org/10.3390/ijerph15071556

ANZECC/ARMCANZ (2000) Australian and New Zealand Guidelines for Freshwater and Marine Water Quality Vol.1. Australian and New Zealand Environment and Conservation Council and Agriculture and Resource Management Council of Australia and New Zealand, Canberra.

ANZG (2018). Australian and New Zealand Guidelines for Fresh and Marine Water Quality. Australian and New Zealand Governments and Australian state and territory governments, Canberra ACT, Australia.

Bailey, H.C., Krassoi, R., Elphick, J.R., Mulhall, A., Hunt, P., Tedmanson, L. and Lovell, A. (2000) Application of *Ceriodaphnia* cf. *dubia* for whole effluent toxicity tests in the Hawkesbury-Nepean watershed, New South Wales, Australia: method development and validation. Environmental Toxicology and Chemistry 19, 88-93.

Barbour M.T. and Stribling B. (1991). Use of habitat assessment in evaluating the biological integrity of stream communities. Pages 25–38 in Biological criteria: Research and regulation. U.S. Environmental Protection Agency, Office of Water Report No. EPA-440/5-91/00 5., Washington D.C.

Batley, G.E., van Dam, R.A., Warne, M.St.J., Chapman, J.C., Fox, D.R., Hickey, C.W. and Stauber, J.L. (2018). Technical rationale for changes to the Method for Deriving Australian and New Zealand

Water Quality Guideline Values for Toxicants. Prepared for the revision of the Australian and New Zealand Guidelines for Fresh and Marine Water Quality. Australian and New Zealand Governments and Australian state and territory governments, Canberra, ACT, 49 pp.

Batley, G.E., van Dam, R.A., Warne, M.St.J., Chapman, J.C., Fox, D.R., Hickey C.W. and Stauber, J.L. (2018). Technical rationale for changes to the method for deriving Australian and New Zealand water quality guideline values for toxicants– update of 2014 version. Prepared for the revision of the Australian and New Zealand Guidelines for Fresh and Marine Water Quality. Australian and New Zealand Governments and Australian state and territory governments, Canberra, 43 pp.

Bere, T., and Tundisi, J.G. (2011). Influence of ionic strength and conductivity on benthic diatom communities in a tropical river (Monjolinho), São Carlos-SP, Brazil. Hydrobiologia, 661, 261–276.

Boden, R., Cleland, D., Green, P.N., Katayama, Y., Uchino, Y., Murrell, J.C. and Kelly, D.P., (2012). Phylogenetic assessment of culture collection strains of Thiobacillus thioparus, and definitive 16S rRNA gene sequences for T. thioparus, T. denitrificans, and Halothiobacillus neapolitanus. Archives of Microbiology. 194, 187–195. https://doi.org/10.1007/s00203-011-0747-0

Cantonati, M. and Lange-Bertalot, H. (2011). Diatom Monitors of Close-to-Pristine, Very-Low Alkalinity Habitats: Three New Eunotia Species from Springs in Nature Parks of the South-Eastern Alps. Journal of Limnology 70 (2):209-21. https://doi.org/10.4081/jlimnol.2011.209.

Caporaso, J.G., Lauber, C.L., Walters, W.A., Berg-Lyons, D., Huntley, J., Fierer, N., Owens, S.M., Betley, J., Fraser, L., Bauer, M., Gormley, N., Gilbert, J.A, Smith, G. and Knight, R. (2012). Ultra-high-throughput microbial community analysis on the Illumina HiSeq and MiSeq platforms. International Society for Microbial Ecology, 6, 1621-1624

Cardno Ecology Lab Pty Ltd (2010) ACARP C1506 – Effects of Mine Water Salinity on Freshwater Biota, Investigations of Coal Mine Water Discharge in NSW.

Chariton A.A., Stephenson S., Morgan M., Steven A., Colloff, M., Court L. and Hardy, C. (2015). Metabarcoding of benthic eukaryote communities predicts the ecological condition of estuaries. Environmental Pollution 203, 165-174

Chariton, A.A., and Stephenson, S. CSIRO (2020). Georges River Environment Improvement Program (EIP2). Prepared for Illawarra Coal/South32. CSIRO Oceans and Atmosphere Report No. EP201808 Lucas Heights, NSW

Chariton A.A., and Stephenson S. CSIRO (2018). Georges River Environment Improvement Program (EIP2). Report Prepared for Illawarra Coal. CSIRO Oceans and Atmosphere Report, Lucas Heights, NSW.

Chariton A.A., and Stephenson S. CSIRO (2016). Aquatic Monitoring Program for the Upper Georges River/Brennans Creek: Metabarcoding of the benthic eukaryotic assemblages. Prepared for South 32. Lucas Heights, NSW.

Chariton A.A., and Stephenson S. CSIRO (2014). Aquatic Monitoring Program for the Upper Georges River: Metabarcoding of the benthic eukaryotic assemblages. CSIRO Oceans and Atmosphere Report prepared for BHP Billiton/Illawara Coal.

Chariton A.A., Baird D.J. and Pettigrove, V. (2016). Chapter 7: Ecological Assessment. In Handbook for Sediment Quality Assessment, 2nd Edition edited by S.L. Simpson and G.E. Batley. CSIRO Publishing, Clayton, Vic, pp. 151-189

Chessman, B.C. (1995). Rapid assessment of rivers using macroinvertebrates: A procedure based on habitat-specific sampling, Family level identification and a biotic index. Australian Journal of Ecology, 20, 122-129.

Chessman, B.C. (2003). New sensitivity grades for Australian river macroinvertebrates. Marine and Freshwater Research, 54, 95-103.

Corbin, T.A., and Goonan, P.M., (2010). Habitat and Water Quality Preferences of Mayflies and Stoneflies from South Australian Streams, Transactions of the Royal Society of South Australia, 134:1, 5-18, DOI: 10.1080/3721426.2010.10887129

Cole J. R., Wang Q., Fish J. A., Chai B., McGarrell D.M., Sun Y., Brown C.T., Porras-Alfaro A., Kuske C. R. and Tiedje J.M. (2014). Ribosomal Database Project: data and tools for high throughput rRNA analysis. Nucleic Acids Research 42, D633-D642

Driscoll, C. and Postek, K. (1996). The chemistry of aluminium in surface waters., in: Sposito, G. (Ed.), The Environmental Chemistry of Aluminium. Lewis Publishers, New York, pp. 363–418.

Edgar R.C. (2013) UPARSE: Highly accurate OTU sequences from microbial amplicon reads, Nature Methods 10, 996-998.

Egge E., Bittner L., Andersen T., Audic S., de Vargas C. and Edvardsen, B. (2013). 454 Pyrosequencing to describe microbial eukaryotic community composition, diversity and relative abundance: a test for marine haptophytes. PLoS ONE 8, e74371

Eichorst, S.A., Trojan, D., Roux, S., Herbold, C., Rattei, T. and Woebken, D. (2018). Genomic insights into the Acidobacteria reveal strategies for their success in terrestrial environments. Environmental Microbiology. 20, 1041–1063. https://doi.org/10.1111/1462-2920.14043

ESA (2016a) ESA SOP 102 –Acute Toxicity Test Using *Ceriodaphnia dubia*. Issue No 11. Ecotox Services Australasia, Sydney, NSW.

ESA (2016b) SOP 117 –Freshwater and Marine Fish Imbalance Test. Issue No 12. Ecotox Services Australasia, Sydney, NSW

Gan, H.M., Szegedi, E., Fersi, R., Chebil, S., Kovács, L., Kawaguchi, A., Hudson, A.O., Burr, T.J. and Savka, M.A. (2019). Insight into the microbial co-occurrence and diversity of 73 grapevine (Vitis vinifera) crown galls collected across the northern hemisphere. Frontiers Microbiology. 10, 1–14. https://doi.org/10.3389/fmicb.2019.01896

Greenfield, P. (2017) Greenfield Hybrid Analysis Pipeline (GHAP). v1. CSIRO. Software Collection. https://doi.org/10.4225/08/59f98560eba25

Griffith, S J., Impey, R. and Weeks, A. (2021). *Platypus Pals: understanding local platypus populations through citizen science and eDNA*. EnviroDNA, Parkville, VIC.

Griffiths, J., Impey ,R., and Licul ,S. (2021) Detecting occurrence of platypus and Macquarie perch in the Georges River. EnviroDNA, Parkville, VIC.

Guerrero-Cruz, S., Vaksmaa, A., Horn, M. A., Niemann, H., Pijuan, M., and Ho, A. (2021). Methanotrophs: Discoveries, Environmental Relevance, and a Perspective on Current and Future Applications. Frontiers in Microbiology 12. https://doi.org/10.1099/ijs.0.000082

Guillou, L., Bachar, D., Audic, S., Bass, D., Berney, C., Bittner, L., Boutte, C., Burgaud, G., de Vargas, C., Decelle, J., del Campo, J., Dolan, J. R., Dunthorn, M., Edvardsen, B., Holzmann, M., Kooistra, W. H. C. F., Lara, E., Le Bescot, N., Logares, R., Christen, R. (2013). The Protist Ribosomal Reference database (PR2): a catalog of unicellular eukaryote Small Sub-Unit rRNA sequences with curated taxonomy. Nucleic Acids Research, 41(D1), D597–D604. https://doi.org/10.1093/nar/gks1160

Hameed, A., Shahina, M., Young, L. Sen, Lai, W.A., Sridhar, K.R., and Young, C.C. (2019). Bacteriostatic stimulus of meropenem on allelochemical-metabolizing Burkholderia sp. LS-044 mitigates ferulic acid autotoxicity in rice (Oryza sativa ssp. japonica cv. Tainung 71). Plant and Soil 443, 73–86. https://doi.org/10.1007/s11104-019-04195-7

Hardy C.M., Krull E.S., Hartley D.M. and Oliver R.L. (2010) Carbon source accounting for fish using combined DNA and stable isotope analyses in a regulated lowland river weir pool. Molecular Ecology. 2010 Jan;19(1):197-212. doi: 10.1111/j.1365-294X.2009.

Holland, A., Duivenvoorden, L.J., Kinnear, S.H.W. (2012). Naturally acidic waterways: Conceptual food webs for better management and understanding of ecological functioning. Aquat. Conserv. Marine Freshwater Ecosystems 22, 836–847. https://doi.org/10.1002/aqc.2267

Jauffrais, T., Jesus, B., Méléder, V., Turpin, V., Russo, A. D. P. G., Raimbault, P., and Jézéquel, V. M. (2016). Physiological and photophysiological responses of the benthic diatom Entomoneis paludosa (Bacillariophyceae) to dissolved inorganic and organic nitrogen in culture. Marine Biology, 163(5), 115. https://doi.org/10.1007/s00227-016-2888-9

Kaksonen, A.H., Plumb, J.J., Robertson, W.J., Franzmann, P.D., Gibson, J.A.E. and Puhakka, J.A., (2004). Culturable Diversity and Community Fatty Acid Profiling of Sulfate-Reducing Fluidized-Bed Reactors Treating Acidic, Metal-Containing Wastewater. Geomicrobiology Journal. 21, 469–480. https://doi.org/10.1080/01490450490505455

Kalam, S., Basu, A., Ahmad, I., Sayyed, R.Z., El-Enshasy, H.A., Dailin, D.J., and Suriani, N.L., (2020). Recent Understanding of Soil Acidobacteria and Their Ecological Significance: A Critical Review. Frontiers in Microbiology. 11. https://doi.org/10.3389/fmicb.2020.580024

Kennedy, A.D., and Jacoby, C.A. (1999) Biological indicators of marine environmental health: Meiofauna - A neglected benthic component? Environmental Monitoring and Assessment 54, 47-68. https://doi.org/10.1023/A:1005854731889

Kociolek, J.P., Blanco, S., Coste, M., Ector, L.; Liu, Y., Karthick, B., Kulikovskiy, M., Lundholm, N., Ludwig, T., Potapova, M., Rimet, F.; Sabbe, K., Sala, S., Sar, E., Taylor, J., Van de Vijver, B., Wetzel, C.E., Williams, D.M., Witkowski, A. and Witkowski, J. (2022). DiatomBase. Accessed at https://www.diatombase.org on 2022-03-15. doi:10.14284/504

Kong, B.H., Li, Y.H., Liu, M., Liu, Y., Li, C.L., Liu, L., Yang, Z.W. and Yu, R., (2013). Massilia namucuonensis sp. nov., isolated from a soil sample. International Journal of Systematic and Evolutionary Microbiology 63, 352–357. https://doi.org/10.1099/ijs.0.039255-0

Legendre P. and Anderson M.J. (1999) Distance-based redundancy analysis: testing multispecies responses in multifactorial ecological experiments. Ecological Monographs 69, 1-24

Lin, S.Y., Hameed, A., Tsai, C.F. and Young, C.C. (2021). Zeimonas arvi gen. nov., sp. nov., of the family Burkholderiaceae, harboring biphenyl- and phenolic acid-metabolizing genes, isolated from a long-term ecological research field. Antonie van Leeuwenhoek, International Journal of General and Molecular Microbiology, 114, 2101–2111. https://doi.org/10.1007/s10482-021-01664-x

Lovley, D.R. and Phillips, E.J.P. (1994.) Novel processes for anaerobic sulfate production from elemental sulfur by sulfate-reducing bacteria. Applied Environmental Microbiology 60, 2394–2399. https://doi.org/10.1128/aem.60.7.2394-2399.1994

Lu, X., Liu, Y., & Fan, Y. (2020). Diatom Taxonomic Composition as a Biological Indicator of the Ecological Health and Status of a River Basin under Agricultural Influence. Water, *12*(7) 2067 https://doi.org/10.3390/w12072067

Luís, A.T., Teixeira, P., Almeida, S.F.P. (2009) Impact of Acid Mine Drainage (AMD) on Water Quality, Stream Sediments and Periphytic Diatom Communities in the Surrounding Streams of Aljustrel Mining Area (Portugal). Water Air Soil Pollution 200, 147–167 (2009). https://doi.org/10.1007/s11270-008-9900-z

Luís, A.T., Durães, N., de Almeida, S.F.P., and da Silva, E.F. (2016). Integrating geochemical (surface waters, stream sediments) and biological (diatoms) approaches to assess AMD environmental impact in a pyritic mining area: Aljustrel (Alentejo, Portugal). Journal of Environmental Sciences, 42, 215–226. https://doi.org/https://doi.org/10.1016/j.jes.2015.07.008

Lugg, W.H., Griffiths, J., van Rooyen, A.R., Weeks, A.R., and Tingley, R. (2018). Optimal survey designs for environmental DNA sampling. Methods in Ecology and Evolution, 9(4), 1049–1059. https://doi.org/https://doi.org/10.1111/2041-210X.12951

Marcondes De Souza, J.A., Carrareto Alves, L.M., De Mello Varani, A., De Macedo Lemos, E.G., (2014). The Family Bradyrhizobiaceae. The Prokaryotes: Alphaproteobacteria and Betaproteobacteria, edition 4, 135–154. https://doi.org/10.1007/978-3-642-30197-1_253

Niche (2022). Appin North – South 32 Aquatic Health Monitoring Report 2021 data.

Niche (2016). Appin North – South 32 Pollution Reduction Program 20 – Aquatic Health Monitoring Report 2015.

Niche (2014). Westcliff Colliery – BHP Illawarra Coal: Aquatic monitoring report 2013

Nogi, Y., Yoshizumi, M., Hamana, K., Miyazaki, M. and Horikoshi, K., (2014). Povalibacter uvarum gen. nov., sp. nov., a polyvinyl-alcohol-degrading bacterium isolated from grapes. International Journal of Systematic Evolutionary Microbiology 64, 2712–2717. https://doi.org/10.1099/IJS.0.062620-0

NSW DPE (2022) Georges River Catchment. NSW Department of Planning Environment. https://www.planning.nsw.gov.au/Policy-and-Legislation/Georges-River-Catchments

Pagani, I., Lapidus, A., Nolan, M., Lucas, S., Hammon, N., Deshpande, S., Cheng, J.F., Chertkov, O., Davenport, K., Tapia, R., Han, C., Goodwin, L., Pitluck, S., Liolios, K., Mavromatis, K., Ivanova, N., Mikhailova, N., Pati, A., Chen, A., Palaniappan, K., Land, M., Hauser, L., Chang, Y.J., Jeffries, C.D., Detter, J.C., Brambilla, E., Kannan, K.P., Djao, O.D.N., Rohde, M., Pukall, R., Spring, S., Göker, M., Sikorski, J., Woyke, T., Bristow, J., Eisen, J., Markowwitz, V., Hugenholtz, P., Kyrpides, N.C., and Klenk, H.P. (2011). Complete genome sequence of Desulfobulbus propionicus type strain (1pr3T). Standards in Genomic Sciences, *4*(1), 100–110. https://doi.org/10.4056/sigs.1613929

Peix, A., Ramírez-Bahena, M. H., Flores-Félix, J. D., de la Vega, P., Rivas, R., Mateos, P. F., Igual, J. M., Martínez-Molina, E., Trujillo, M. E., and Velázquez, E. (2015). Revision of the taxonomic status of the species Rhizobium lupini and reclassification as Bradyrhizobium lupini comb. nov. International Journal of Systematic and Evolutionary Microbiology, 65(Pt 4), 1213–1219. https://doi.org/https://doi.org/10.1099/ijs.0.000082

Price, G. A. V, Stauber, J. L., Holland, A., Koppel, D. J., Van Genderen, E. J., Ryan, A. C., & Jolley, D. F. (2021). The Influence of pH on Zinc Lability and Toxicity to a Tropical Freshwater Microalga.

Environmental Toxicology and Chemistry, *40*(10), 2836–2845. https://doi.org/https://doi.org/10.1002/etc.5177

Pujalte, M.J., Lucena, T., Ruvira, M.A., Arahal, D.R., and Macián, M.C., (2014). The family Rhodobacteraceae, in: The Prokaryotes: Alphaproteobacteria and Betaproteobacteria. Springer, Berlin, Heidelberg, 4, pp. 439–512. https://doi.org/10.1007/978-3-642-30197-1_377

QIAGEN (2016) Quick-Start Protocol DNeasy® PowerMax® Kit. Germany. June 2016.

https://www.qiagen.com/us/resources/resourcedetail?id=8ba278a1-2b94-4d79-942b-19310489f09f&lang=en

Quast, C., Pruesse, E., Yilmaz, P., Gerken, J., Schweer, T., Yarza, P., Peplies, J. and Glöckner F.O. (2013) The SILVA ribosomal RNA gene database project: improved data processing and web-based tools. Nucleic Acids Research 41, D590–D596.

Siddavattam, D., Karegoudar, T.B., Mudde, S.K., Kumar, N., Baddam, R., Avasthi, T.S., and Ahmed, N. (2011). Genome of a Novel Isolate of Paracoccus denitrificans Capable of Degrading N,N-Dimethylformamide. Journal of Bacteriology, 193, 5598. https://doi.org/10.1128/JB.05667-11

Soeprobowati, T. R., Purnaweni, H., Jumari, J., and Sari, K. (2022). The Relationship of Water Quality to Epipelic Diatom Assemblages in Cebong Lake, Dieng Indonesia. Polish Journal of Environmental Studies, 31(1), 281–295. https://doi.org/10.15244/pjoes/137084

South32 (2017). Georges River Environmental Improvement Program. Appin, NSW.

South32 (2021). Georges River Aquatic Health Monitoring Program. Appin, NSW.

Spyra, A., Cieplok, A., Strzelec, M., and Babczyńska, A. (2019). Freshwater alien species Physella acuta (Draparnaud, 1805) - A possible model for bioaccumulation of heavy metals. Ecotoxicology and Environmental Safety, 185, 109703. https://doi.org/https://doi.org/10.1016/j.ecoenv.2019.109703

Stimpson, K.S., and Klemm, D.J. (1982). A guide to the freshwater Tubificidae (Annelida: Clitellata: Oligochaeta) of North America. U.S. Environmental Protection Agency. 61 pp.

Stoeck, T., Frühe, L., Forster D., Cordier, T., Martins, C. and Pawlowski, J. (2018). Environmental DNA metabarcoding of benthic bacterial communities indicates the benthic footprint of salmon aquaculture. Marine Pollution Bulletin, 127, 139-149

Strnad, H., Lapidus, A., Paces, J., Ulbrich, P., Vlcek, C., Paces, V., and Haselkorn, R. (2010). Complete Genome Sequence of the Photosynthetic Purple Nonsulfur Bacterium Rhodobacter capsulatus SB 1003. Journal of Bacteriology 192, 3545. https://doi.org/10.1128/JB.00366-10

Sutcliffe, B., Hose, G.C., Harford, A.J., Midgley, D.J, Greenfield, P., Paulsen, I. and Chariton, A.A. (2019). Microbial communities are sensitive indicators for freshwater sediment copper contamination. Environmental Pollution. 247:1028-1038. https://doi.org/10.1016/j.envpol.2019.01.104

Sutter, P. J., Conrick , D., Choy, S. and Cockyane, B. (2002) Habitat profiles of Queensland Mayflies, Families Baetidae, Caenidae and Prosopistomtidae. Identification Keys No.41. The Murray-Darling Freshwater Research Centre, La Trobe University Press. Albury, NSW.

Tarhriz, V., Hirose, S., Fukushima, S. I., Hejazi, M.A., Imhoff, J.F., Thiel, V., Hejazi, M.S., (2019) Emended description of the genus Tabrizicola and the species Tabrizicola aquatica as aerobic anoxygenic phototrophic bacteria. Antonie van Leeuwenhoek, International Journal of General. Molecular Microbiology, 112, 1169–1175. https://doi.org/10.1007/s10482-019-01249-9

USEPA (2000) Method guidance and recommendations for whole effluent toxicity (WET) testing (40 CFR Part 136). U.S. Environmental Protection Agency, Office of Water Report No. EPA/821/B - 00/004, Washington, D.C.

USEPA (2002a) Short-term Methods for Estimating the Chronic Toxicity of Effluents and Receiving Waters to Freshwater Organisms.4thEd. United States Environmental Protection Agency, Office of Water, Washington DC.

USEPA (2002b) Methods for measuring the acute toxicity of effluents and receiving waters to freshwater and marine organisms. Fifth edition EPA-821-R-02-012. United States Environmental Protection Agency, Office of Research and Development, Washington DC, USA

Van Dam, H., Mertens, A. and Sinkeldam, J. (1994). A coded checklist and ecological indicator values of freshwater diatoms from the Netherlands. Netherlands Journal of Aquatic Ecology, 28, 117–133.

Walsh, C. J. (2006). Biological indicators of stream health using macroinvertebrate assemblage composition: a comparison of sensitivity to an urban gradient. Marine and Freshwater Research, *57*(1), 37–47. https://doi.org/10.1071/MF05041

Warne, M.St.J., Batley, G.E., van Dam, R.A., Chapman, J.C., Fox, D.R., Hickey C.W. and Stauber, J.L. (2018). Revised Method for Deriving Australian and New Zealand Water Quality Guideline Values for Toxicants – update of 2015 version. Prepared for the revision of the Australian and New Zealand Guidelines for Fresh and Marine Water Quality. Australian and New Zealand Governments and Australian state and territory governments, Canberra, 48 pp.

Wilhelm, R.C., DeRito, C.M., Shapleigh, J.P., Madsen, E.L. and Buckley, D.H., (2021). Phenolic acid-degrading Paraburkholderia prime decomposition in forest soil. ISME Communications. 1, 1–12. https://doi.org/10.1038/s43705-021-00009-z

Wright, I.A., Belmer, N., Davies, P.J., (2017). Coal Mine Water Pollution and Ecological Impairment of One of Australia's Most 'Protected' High Conservation-Value Rivers. Water Air Soil Pollution. 228. https://doi.org/10.1007/s11270-017-3278-8

Yabe, S., Zheng, Y., Wang, C.M., Sakai, Y., Abe, K., Yokota, A., Donadio, S., Cavaletti, L., Monciardini, P. (2021). Reticulibacter mediterranei gen. Nov., sp. nov., within the new family reticulibacteraceae fam. nov., and ktedonospora formicarum gen. nov., sp. nov., ktedonobacter robiniae sp. nov., dictyobacter formicarum sp. nov. and dictyobacter arantiisoli sp. nov., belonging to the class ktedonobacteria. International Journal of Systematic and Evolutionary Microbiology. 71. https://doi.org/10.1099/ijsem.0.004883

Yoon, J., (2014). The family verrucomicrobiaceae, in: The Prokaryotes: Other Major Lineages of Bacteria and The Archaea. Springer, Berlin, Heidelberg, 4, pp. 1017–1018. https://doi.org/10.1007/978-3-642-38954-2_145

Zimmermann J., Jahn R., Gemeinholzer B. (2011) Barcoding diatoms: evaluation of the V4 subregion on the 18S rRNA gene, including new primers and protocols. Organisms Diversity and Evolution 11**,** 173 (2011). https://doi.org/10.1007/s13127-011-0050-6

**As Australia's national science agency and innovation catalyst, CSIRO is solving the greatest challenges through innovative science and technology.**

CSIRO. Unlocking a better future for everyone.


**Contact us**

1300 363 400
+61 3 9545 2176
csiroenquiries@csiro.au
www.csiro.au

**For further information**

**Oceans and Atmosphere**
Sarah Stephenson
+61 2 9710 6889
**Sarah.stephenson@csiro.au**
**csiro.au/oceans and atmosphere**

# Appendix A – Ecotoxicity Results

**Table A1. Ecotoxicity results for LDP10 and LDP40 samples tested in 2021**

| | | Feb-21 | | | May-21 | | |
|---|---|---|---|---|---|---|---|
| **LDP10** | **Test** | **EC50** | **EC10** | **NOEC** | **EC50** | **EC10** | **NOEC** |
| | *Ceriodaphnia dubia*- survival | >100% | >100% | 100% | >100% | >100% | 100% |
| | *Ceriodaphnia dubia*- reproduction | >100% | >100% | 100% | >100% | >100% | 100% |
| | *M. splendida* fish imbalance over 96h | ND[a] | ND | ND | >100% | >100% | 100% |
| **LDP40** | **Test** | **EC50** | **EC10** | **NOEC** | **EC50** | **EC10** | **NOEC** |
| | *Ceriodaphnia dubia*- survival | NA[b] | NA | NA | >100% | >100% | 100% |
| | *Ceriodaphnia dubia* - reproduction | NA | NA | NA | >100% | 68% | 50% |
| | *M. splendida* fish imbalance over 96h | NA | NA | NA | >100% | >100% | 100% |

| | | Aug-21 | | | Nov-21 | | |
|---|---|---|---|---|---|---|---|
| **LDP10** | **Test** | **EC50** | **EC10** | **NOEC** | **EC50** | **EC10** | **NOEC** |
| | *Ceriodaphnia dubia*- survival | 78% | 61% | 50% | 77% | 50% | 50% |
| | *Ceriodaphnia dubia*- reproduction | 77% | 48% | 25% | 70% | 23% | 50% |
| | *M. splendida* fish imbalance over 96h | >100% | >100% | 100% | >100% | >100% | 100% |
| **LDP40** | **Test** | **EC50** | **EC10** | **NOEC** | **EC50** | **EC10** | **NOEC** |
| | *Ceriodaphnia dubia*- survival | 54% | 36% | 50% | >100% | >100% | 100% |
| | *Ceriodaphnia dubia* - reproduction | 52% | 30% | 25% | >100% | >100% | 100% |
| | *M. splendida* fish imbalance over 96h | >100% | >100% | 100% | >100% | >100% | 100% |

[a] Not applicable, WTP was not yet installed

[b] Not determined. Incorrect fish endpoint of 7-d embryo development used. EC50 and EC10 were >100%, NOEC was 100%

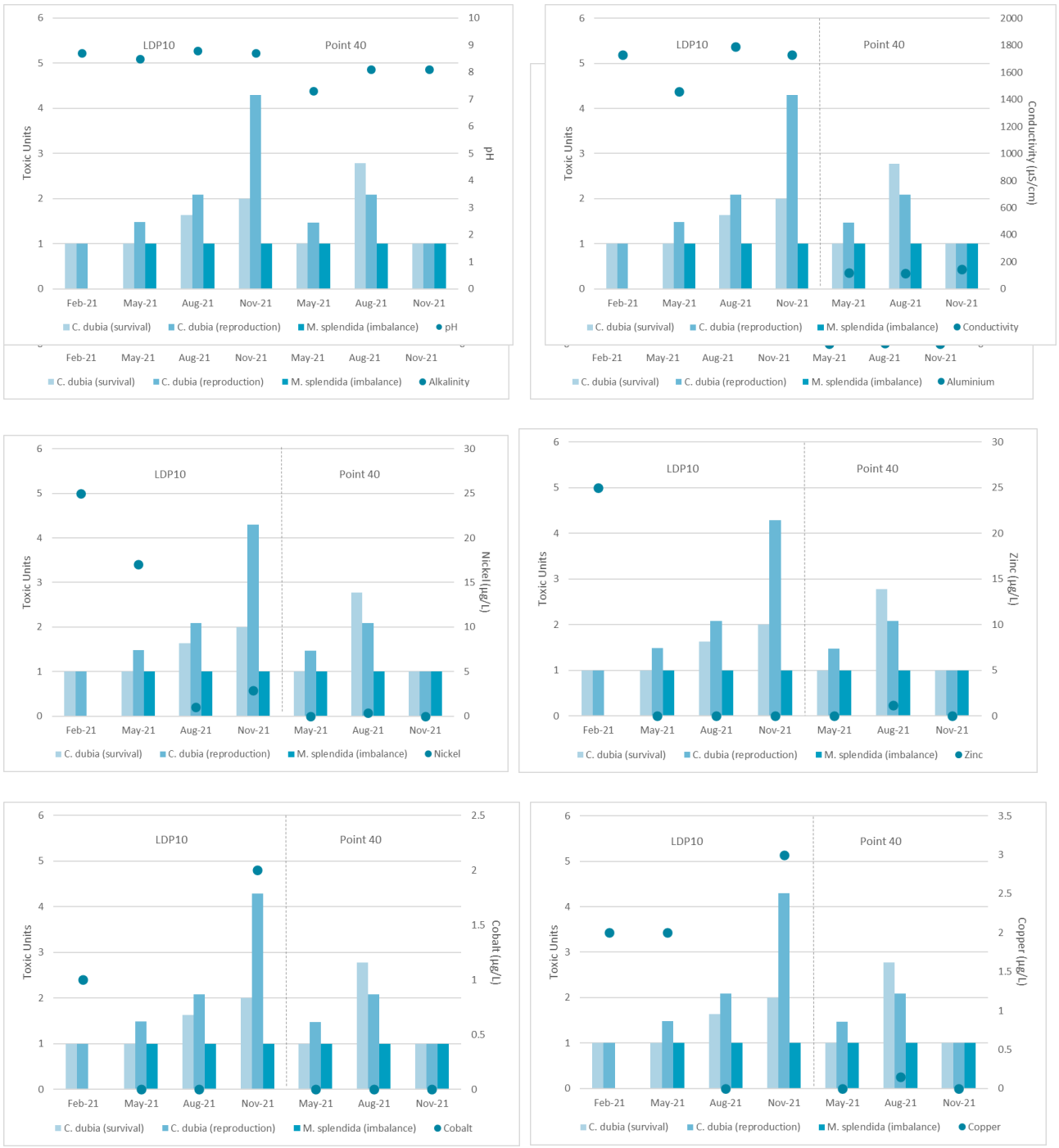


**Figure A.1 Comparison of LDP10 and LDP40 toxicity with measured water quality parameters.**

# Appendix B – Metabarcoding sites pairwise PERMANOVA

### Table B1 16S OTU 2019 pairwise PERMANOVA analysis for site.

| | 2019_GRQ1 | 2019_GRUFS | 2019_POINT11 | 2019_POINT10 | 2019_POINT12 | 2019_JUTTS | 2019_POOL16 | 2019_POOL32 | 2019_GRQ18 |
|---|---|---|---|---|---|---|---|---|---|
| 2019_GRQ1 | | 0.0072 | 0.008 | 0.009 | 0.0063 | 0.0064 | 0.0075 | 0.0082 | 0.0086 |
| 2019_GRUFS | 0.0072 | | 0.007 | 0.0101 | 0.007 | 0.0075 | 0.0091 | 0.0074 | 0.0075 |
| 2019_POINT11 | 0.008 | 0.007 | | 0.0077 | 0.0079 | 0.0075 | 0.0083 | 0.0086 | 0.0075 |
| 2019_POINT10 | 0.009 | 0.0101 | 0.0077 | | 0.0099 | 0.0084 | 0.0094 | 0.0086 | 0.0095 |
| 2019_POINT12 | 0.0063 | 0.007 | 0.0079 | 0.0099 | | 0.1113 | 0.0079 | 0.0163 | 0.0073 |
| 2019_JUTTS | 0.0064 | 0.0075 | 0.0075 | 0.0084 | 0.1113 | | 0.0072 | 0.0073 | 0.0086 |
| 2019_POOL16 | 0.0075 | 0.0091 | 0.0083 | 0.0094 | 0.0079 | 0.0072 | | 0.009 | 0.0053 |
| 2019_POOL32 | 0.0082 | 0.0074 | 0.0086 | 0.0086 | 0.0163 | 0.0073 | 0.009 | | 0.0076 |
| 2019_GRQ18 | 0.0086 | 0.0075 | 0.0075 | 0.0095 | 0.0073 | 0.0086 | 0.0053 | 0.0076 | |

Highlighted pink cells indicate significant difference at level p<0.05.

### Table B2 16S OTU 2020 pairwise PERMANOVA analysis for site.

| | 2020_GRQ1 | 2020_GRUFS | 2020_POINT11 | 2020_POINT10 | 2020_POINT12 | 2020_JUTTS | 2020_POOL16 | 2020_POOL32 | 2020_GRQ18 |
|---|---|---|---|---|---|---|---|---|---|
| 2020_GRQ1 | | 0.0072 | 0.008 | 0.009 | 0.0063 | 0.0064 | 0.0075 | 0.0082 | 0.0086 |
| 2020_GRUFS | 0.0072 | | 0.007 | 0.0101 | 0.007 | 0.0075 | 0.0091 | 0.0074 | 0.0075 |
| 2020_POINT11 | 0.008 | 0.007 | | 0.0077 | 0.0079 | 0.0075 | 0.0083 | 0.0086 | 0.0075 |
| 2020_POINT10 | 0.009 | 0.0101 | 0.0077 | | 0.0176 | 0.0084 | 0.0094 | 0.0179 | 0.0095 |
| 2020_POINT12 | 0.0063 | 0.007 | 0.0079 | 0.0176 | | 0.008 | 0.0079 | 0.0075 | 0.0073 |
| 2020_JUTTS | 0.0064 | 0.0075 | 0.0075 | 0.0084 | 0.008 | | 0.0072 | 0.0073 | 0.0086 |
| 2020_POOL16 | 0.0075 | 0.0091 | 0.0083 | 0.0094 | 0.0079 | 0.0072 | | 0.009 | 0.0053 |
| 2020_POOL32 | 0.0082 | 0.0074 | 0.0086 | 0.0179 | 0.0075 | 0.0073 | 0.009 | | 0.0076 |
| 2020_GRQ18 | 0.0086 | 0.0075 | 0.0075 | 0.0095 | 0.0073 | 0.0086 | 0.0053 | 0.0076 | |

Highlighted pink cells indicate significant difference at level p<0.05.

### Table B3 16S OTU 2021 pairwise PERMANOVA analysis for site.

| | 2021_GRQ1 | 2021_GRUFS | 2021_POINT11 | 2021_POINT10 | 2021_POINT12 | 2021_JUTTS | 2021_POOL16 | 2021_POOL32 | 2021_GRQ18 |
|---|---|---|---|---|---|---|---|---|---|
| 2021_GRQ1 | | 0.0831 | 0.008 | 0.009 | 0.0063 | 0.0064 | 0.0075 | 0.0082 | 0.0086 |
| 2021_GRUFS | 0.0831 | | 0.007 | 0.0101 | 0.007 | 0.0075 | 0.0091 | 0.0074 | 0.0075 |
| 2021_POINT11 | 0.008 | 0.007 | | 0.0077 | 0.0079 | 0.0075 | 0.0083 | 0.0086 | 0.0075 |
| 2021_POINT10 | 0.009 | 0.0101 | 0.0077 | | 0.0099 | 0.0084 | 0.0162 | 0.0086 | 0.0095 |
| 2021_POINT12 | 0.0063 | 0.007 | 0.0079 | 0.0099 | | 0.2091 | 0.0161 | 0.0075 | 0.0073 |
| 2021_JUTTS | 0.0064 | 0.0075 | 0.0075 | 0.0084 | 0.2091 | | 0.0753 | 0.0073 | 0.0086 |
| 2021_POOL16 | 0.0075 | 0.0091 | 0.0083 | 0.0162 | 0.0161 | 0.0753 | | 0.0184 | 0.0053 |
| 2021_POOL32 | 0.0082 | 0.0074 | 0.0086 | 0.0086 | 0.0075 | 0.0073 | 0.0184 | | 0.0076 |
| 2021_GRQ18 | 0.0086 | 0.0075 | 0.0075 | 0.0095 | 0.0073 | 0.0086 | 0.0053 | 0.0076 | |

Highlighted pink cells indicate significant difference at level p<0.05.

## Table B4 18S 2019 pairwise PERMANOVA analysis for site.

| | 2019_GRQ1 | 2019_GRUFS | 2019_POINT11 | 2019_POINT10 | 2019_POINT12 | 2019_JUTTS | 2019_POOL16 | 2019_POOL32 | 2019_GRQ18 |
|---|---|---|---|---|---|---|---|---|---|
| 2019_GRQ1 | | 0.1106 | 0.037 | 0.009 | 0.0063 | 0.0064 | 0.0075 | 0.0082 | 0.0086 |
| 2019_GRUFS | 0.1106 | | 0.007 | 0.0101 | 0.007 | 0.0075 | 0.0091 | 0.0074 | 0.0075 |
| 2019_POINT11 | 0.037 | 0.007 | | 0.0077 | 0.0079 | 0.0075 | 0.0083 | 0.0086 | 0.0137 |
| 2019_POINT10 | 0.009 | 0.0101 | 0.0077 | | 0.0099 | 0.0084 | 0.0094 | 0.0086 | 0.0095 |
| 2019_POINT12 | 0.0063 | 0.007 | 0.0079 | 0.0099 | | 0.008 | 0.0079 | 0.0075 | 0.0073 |
| 2019_JUTTS | 0.0064 | 0.0075 | 0.0075 | 0.0084 | 0.008 | | 0.0072 | 0.0073 | 0.0086 |
| 2019_POOL16 | 0.0075 | 0.0091 | 0.0083 | 0.0094 | 0.0079 | 0.0072 | | 0.009 | 0.0053 |
| 2019_POOL32 | 0.0082 | 0.0074 | 0.0086 | 0.0086 | 0.0075 | 0.0073 | 0.009 | | 0.0335 |
| 2019_GRQ18 | 0.0086 | 0.0075 | 0.0137 | 0.0095 | 0.0073 | 0.0086 | 0.0053 | 0.0335 | |

Highlighted pink cells indicate significant difference at level p<0.05.

## Table B5 18S OTU 2020 pairwise PERMANOVA analysis for site.

| | 2020_GRQ1 | 2020_GRUFS | 2020_POINT11 | 2020_POINT10 | 2020_POINT12 | 2020_JUTTS | 2020_POOL16 | 2020_POOL32 | 2020_GRQ18 |
|---|---|---|---|---|---|---|---|---|---|
| 2020_GRQ1 | | 0.0517 | 0.0072 | 0.0074 | 0.0087 | 0.0081 | 0.0086 | 0.0068 | 0.0056 |
| 2020_GRUFS | 0.0517 | | 0.0817 | 0.023 | 0.0069 | 0.0172 | 0.0087 | 0.0077 | 0.0073 |
| 2020_POINT11 | 0.0072 | 0.0817 | | 0.0382 | 0.009 | 0.0419 | 0.0085 | 0.0084 | 0.008 |
| 2020_POINT10 | 0.0074 | 0.023 | 0.0382 | | 0.0228 | 0.0189 | 0.0078 | 0.0191 | 0.0094 |
| 2020_POINT12 | 0.0087 | 0.0069 | 0.009 | 0.0228 | | 0.0168 | 0.0171 | 0.0093 | 0.0086 |
| 2020_JUTTS | 0.0081 | 0.0172 | 0.0419 | 0.0189 | 0.0168 | | 0.0067 | 0.0076 | 0.0081 |
| 2020_POOL16 | 0.0086 | 0.0087 | 0.0085 | 0.0078 | 0.0171 | 0.0067 | | 0.084 | 0.0242 |
| 2020_POOL32 | 0.0068 | 0.0077 | 0.0084 | 0.0191 | 0.0093 | 0.0076 | 0.084 | | 0.0089 |
| 2020_GRQ18 | 0.0056 | 0.0073 | 0.008 | 0.0094 | 0.0086 | 0.0081 | 0.0242 | 0.0089 | |

Highlighted pink cells indicate significant difference at level p<0.05.

## Table B6 18S OTU 2021 pairwise PERMANOVA analysis for site.

| | 2021_GRQ1 | 2021_GRUFS | 2021_POINT11 | 2021_POINT10 | 2021_POINT12 | 2021_JUTTS | 2021_POOL16 | 2021_POOL32 | 2021_GRQ18 |
|---|---|---|---|---|---|---|---|---|---|
| 2021_GRQ1 | | 0.0072 | 0.008 | 0.009 | 0.0063 | 0.0064 | 0.0075 | 0.0082 | 0.0086 |
| 2021_GRUFS | 0.0072 | | 0.007 | 0.0101 | 0.007 | 0.0075 | 0.0091 | 0.0074 | 0.0075 |
| 2021_POINT11 | 0.008 | 0.007 | | 0.0077 | 0.0079 | 0.0075 | 0.0083 | 0.0086 | 0.0075 |
| 2021_POINT10 | 0.009 | 0.0101 | 0.0077 | | 0.0099 | 0.0084 | 0.0094 | 0.0086 | 0.0095 |
| 2021_POINT12 | 0.0063 | 0.007 | 0.0079 | 0.0099 | | 0.1719 | 0.1182 | 0.0075 | 0.0073 |
| 2021_JUTTS | 0.0064 | 0.0075 | 0.0075 | 0.0084 | 0.1719 | | 0.0963 | 0.0073 | 0.0086 |
| 2021_POOL16 | 0.0075 | 0.0091 | 0.0083 | 0.0094 | 0.1182 | 0.0963 | | 0.009 | 0.0053 |
| 2021_POOL32 | 0.0082 | 0.0074 | 0.0086 | 0.0086 | 0.0075 | 0.0073 | 0.009 | | 0.0076 |
| 2021_GRQ18 | 0.0086 | 0.0075 | 0.0075 | 0.0095 | 0.0073 | 0.0086 | 0.0053 | 0.0076 | |

Highlighted pink cells indicate significant difference at level p<0.05.

**Table B7 Diatoms 2020 pairwise PERMANOVA analysis for site. Highlighted pink cells indicate significant difference at level <0.05.**

| | 2020_GRQ1 | 2020_GRUFS | 2020_POINT11 | 2020_POINT10 | 2020_POINT12 | 2020_JUTTS | 2020_POOL16 | 2020_POOL32 | 2020_GRQ18 |
|---|---|---|---|---|---|---|---|---|---|
| 2020_GRQ1 | | 0.0072 | 0.008 | 0.009 | 0.0063 | 0.0064 | 0.0075 | 0.0082 | 0.0086 |
| 2020_GRUFS | 0.0072 | | 0.007 | 0.0101 | 0.007 | 0.0075 | 0.0091 | 0.0074 | 0.0075 |
| 2020_POINT11 | 0.008 | 0.007 | | 0.0077 | 0.0079 | 0.0075 | 0.0083 | 0.0086 | 0.0075 |
| 2020_POINT10 | 0.009 | 0.0101 | 0.0077 | | 0.0099 | 0.0084 | 0.0094 | 0.0086 | 0.0095 |
| 2020_POINT12 | 0.0063 | 0.007 | 0.0079 | 0.0099 | | 0.0238 | 0.0079 | 0.0075 | 0.0073 |
| 2020_JUTTS | 0.0064 | 0.0075 | 0.0075 | 0.0084 | 0.0238 | | 0.0072 | 0.0073 | 0.0086 |
| 2020_POOL16 | 0.0075 | 0.0091 | 0.0083 | 0.0094 | 0.0079 | 0.0072 | | 0.1449 | 0.0053 |
| 2020_POOL32 | 0.0082 | 0.0074 | 0.0086 | 0.0086 | 0.0075 | 0.0073 | 0.1449 | | 0.0076 |
| 2020_GRQ18 | 0.0086 | 0.0075 | 0.0075 | 0.0095 | 0.0073 | 0.0086 | 0.0053 | 0.0076 | |

Highlighted pink cells indicate significant difference at level p<0.05.

**Table B8 Diatoms 2021 pairwise PERMANOVA analysis for site. Highlighted pink cells indicate significant difference at level <0.05.**

| | 2021_GRQ1 | 2021_GRUFS | 2021_POINT11 | 2021_POINT10 | 2021_POINT12 | 2021_JUTTS | 2021_POOL16 | 2021_POOL32 | 2021_GRQ18 |
|---|---|---|---|---|---|---|---|---|---|
| 2021_GRQ1 | | 0.0138 | 0.008 | 0.009 | 0.0063 | 0.0064 | 0.0075 | 0.0082 | 0.0086 |
| 2021_GRUFS | 0.0138 | | 0.007 | 0.0101 | 0.007 | 0.0075 | 0.0091 | 0.0074 | 0.0075 |
| 2021_POINT11 | 0.008 | 0.007 | | 0.0077 | 0.0079 | 0.0075 | 0.0083 | 0.0086 | 0.0075 |
| 2021_POINT10 | 0.009 | 0.0101 | 0.0077 | | 0.0099 | 0.0084 | 0.0094 | 0.0086 | 0.0095 |
| 2021_POINT12 | 0.0063 | 0.007 | 0.0079 | 0.0099 | | 0.0163 | 0.0079 | 0.0075 | 0.0073 |
| 2021_JUTTS | 0.0064 | 0.0075 | 0.0075 | 0.0084 | 0.0163 | | 0.0072 | 0.0073 | 0.0086 |
| 2021_POOL16 | 0.0075 | 0.0091 | 0.0083 | 0.0094 | 0.0079 | 0.0072 | | 0.009 | 0.0053 |
| 2021_POOL32 | 0.0082 | 0.0074 | 0.0086 | 0.0086 | 0.0075 | 0.0073 | 0.009 | | 0.0076 |
| 2021_GRQ18 | 0.0086 | 0.0075 | 0.0075 | 0.0095 | 0.0073 | 0.0086 | 0.0053 | 0.0076 | |

Highlighted pink cells indicate significant difference at level p<0.05.